

Silanes, Silicon(II), and Germanium(II) Anions Bearing Nitrogen Heterocycles

Stepping Stones towards Novel Ligands for Base Metals

Witte man, Léon

Silanes, Silicon(II), and Germanium(II) Anions Bearing Nitrogen Heterocycles
Stepping Stones towards Novel Ligands for Base Metals

ISBN: 978-90-393-6955-5

The work described in this PhD thesis was carried out at:
Organic Chemistry and Catalysis, Debye Institute for Nanomaterials Science, Faculty
of Science, Utrecht University, Utrecht, The Netherlands

Silanes, Silicon(II), and Germanium(II) Anions Bearing Nitrogen Heterocycles

Stepping Stones towards Novel Ligands for Base Metals

**Stikstof Heterocycli Dragende Silanen, Silicium(II) en
Germanium(II) Anionen**

Een Weg naar Nieuwe Liganden voor
Onedele Metalen

(met een samenvatting in het Nederlands)

Proefschrift

ter verkrijging van de graad van doctor aan de Universiteit Utrecht op gezag van de rector magnificus, prof.dr. G.J. van der Zwaan, ingevolge het besluit van het college voor promoties in het openbaar te verdedigen op woensdag 18 april 2018 des middags te 2.30 uur

door

Léon Witteman

geboren op 9 november 1989 te Nieuwegein.

Promotor: Prof.dr. R.J.M. Klein Gebbink

Copromotor: Dr. M.-E. Moret

Contents

Chapter 1	9
The Evolution of Low-Valent Silicon(II) Compounds as Ligands for Transition Metals	
Chapter 2	25
Hydrosilylation in Aryliminopyrrolide Substituted Silanes	
Chapter 3	49
Synthesis of N-heterocycle Substituted Silyl Ligands Within the Coordination Sphere of Iron	
Chapter 4	67
A Free Silanide from Nucleophilic Substitution at Silicon(II)	
Chapter 5	81
Synthesis and Complexation of a Free Germanide bearing a tridentate N-heterocyclic substituent	
Appendix	96
Summary and Outlook	99
Samenvatting en Vooruitblik	105
Dankwoord	111
Curriculum Vitae	114
List of Publications	115

1

The Evolution of Low-Valent Silicon(II) Compounds as Ligands for Transition Metals

Low-valent Si(II) compounds have recently emerged as a promising class of strong donor ligands for transition metals, with potential applications in homogeneous catalysis. The two main structural types in Si(II) chemistry are silylenes ($R_2Si:$, $R_2Si=M$), which can be additionally stabilized by coordination of a Lewis-Base to Si, and silyl anions or silanides (R_3Si^- , R_3Si-M). In particular, silylenes have been developed as ancillary ligands for several catalytic transformations. Through time, several challenges regarding the relatively low stability of Si(II) species have been overcome, allowing for the isolation of two-coordinate silylenes, base stabilized silylenes and free anionic silanides.

Introduction

The impact and versatility of homogeneous catalysis largely derives from the ability to tailor catalysts for their intended use by tuning the electronic and steric properties of the ligands. Two classes of ligands that have found numerous uses in this field are phosphines and N-heterocyclic carbenes (NHCs).^{1–3} In phosphines, substituents directly bound to the metal-coordinating phosphorus atom have a strong influence on the steric and electronic properties of the ligand. For example, grafting more electron-withdrawing substituents on the phosphorus atom stabilizes the lone pair on phosphorus and results in a less σ -donating phosphine. Concomitantly, electron-withdrawing substituents lower the energy of the R–P σ^* -orbitals and increases their coefficient on P, enhancing π -backbonding.

NHCs consist of a C(II) centre featuring at least one α -nitrogen substituent. The nitrogen atom(s) provide a two-fold stabilization of the carbene (Chart 1.1A). First, the carbon-centered lone-pair is stabilized inductively by withdrawing electron-density along the polar C–N σ -bond. Second, the N-centered lone pair(s) overlap with the empty p-orbital of the C(II) center, resulting in mesomeric stabilization. The primary determinant of the NHCs electronic properties is the architecture of the (most often) five-membered ring encompassing the C(II) centre (Chart 1.1). The steric demand of the NHC can often be modified in a straightforward manner through the substituents in the vicinity of the carbene. The directed steric bulk provides kinetic shielding of the C(II) centre, which is of significant importance in the stability of the NHC.^{4–8}

More recently, low-valent Si(II) compounds have attracted attention as a new class of ligands. As a heavier analogue of carbon, silicon is able to form geometrically similar ligands to NHCs, N-heterocyclic silylenes (NHSi's) (Chart 1.2, left), albeit with generally higher σ -donor and π -acceptor strength.^{9–13} Because of the higher Lewis-acidity of the central Si atom, silylenes can often be additionally stabilized by a donor moiety engaging in a Lewis complex (Chart 1.2, middle). As a last class of stable Si(II) compounds, silanides (R_3Si^-) are formally isoelectronic to phosphines but can be expected to be considerably stronger donors because of the anionic charge. In this chapter, first the evolution of silylene synthesis is described, followed by the use of their transition metal complexes in catalysis. Further, the synthesis and properties silyl ligands ($\text{R}_3\text{Si(III)}^-$) are covered, culminating in the synthesis of free silanides ($\text{R}_3\text{Si(II)}^-$) and their direct complexation.

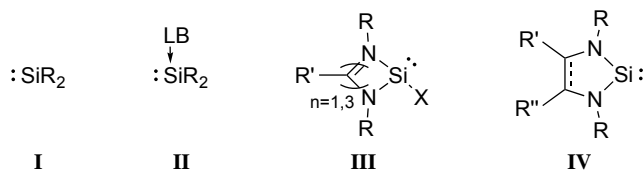
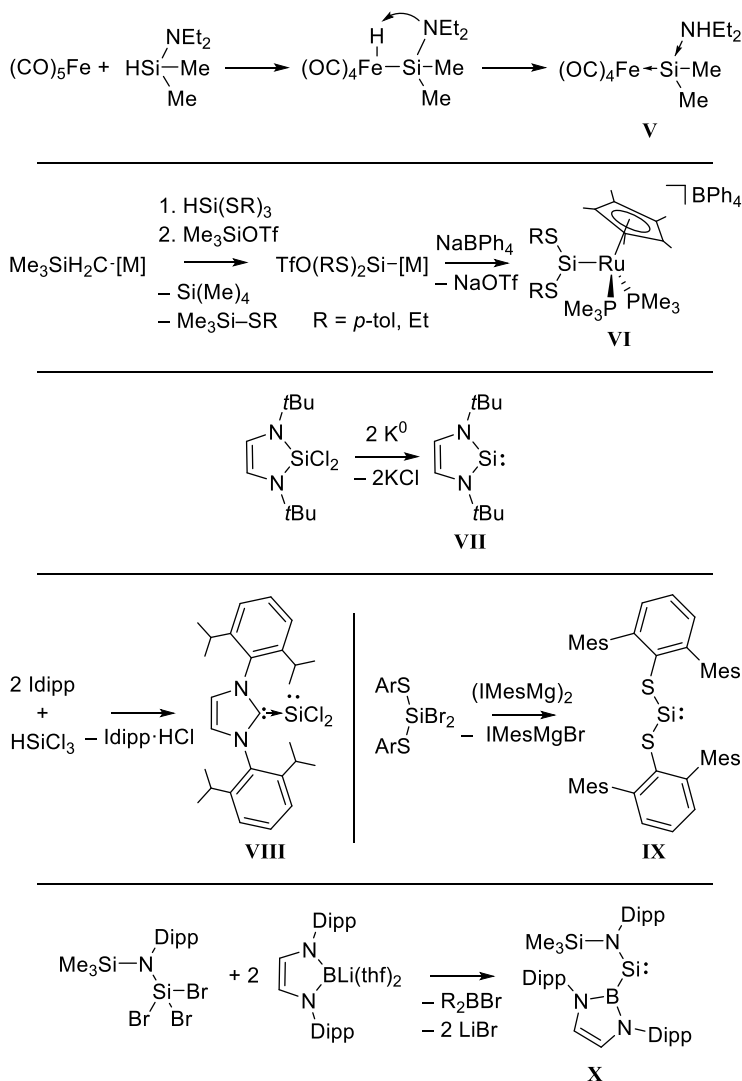


Chart 1.3 General classification of silylenes. **I**) divalent Si(II), **II**) base-stabilized silylene, **III**) intramolecular base-stabilized NHSi, **IV**) base-free NHSi.

Early reports of silylenes exploited base-stabilization and complexation to a metal centre to isolate these reactive species. The first isolated silylene was $\text{Fe}(\text{CO})_4$ -bound dimethylsilylene stabilized by diethylamine, reported in 1977 (Scheme 1.1, **V**). The complex was synthesised by oxidative addition of $\text{HSiMe}_2\text{N}(\text{Et})_2$ to $\text{Fe}(\text{CO})_5$ to initially form an iron(II) silyl hydride complex which underwent a 1,3-proton shift to form the amine stabilized silylene complex.²⁶ Later, the necessity of Lewis-base stabilization was circumvented by grafting the silylene on an electron-rich transition metal fragment. Triflate abstraction from a $\text{TfO}(\text{RS})_2\text{Si-}$ silyl ligand ($\text{R} = p\text{-tol, Et}$) bound to ruthenium resulted in the isolation of the first complexes of base-free silylenes as bisthiolato silylene in $\text{Cp}^*(\text{PMe}_3)_2\text{RuSi}(\text{SR})_2\text{BPh}_4$ complexes in 1990 (Scheme 1.1, **VI**).²⁷ The first metal-, and base-free silylene was synthesized by Denk *et al.* in 1994 through reductive cleavage of the Si-Cl bonds in the corresponding dichlorosilane. This N-heterocyclic silylene employed the chelate effect, directed steric bulk, and N-Si hyperconjugation for stabilization of the Si(II) centre (Chart 1.3, **IV**, Scheme 1.1, **VII**).²⁸ Following this report, a large number of metal-free Si(II) compounds have been isolated.^{29–32} In particular, Lewis-base stabilisation allowed for isolation of a stable complex of $\text{Si}(\text{II})\text{Cl}_2$ in 2009 (Scheme 1.1, **VIII**). It was synthesised from HSiCl_3 and 2 equivalents of the NHC Idipp (1,3-bis(2,6-diisopropylphenyl)imidazol-2-ylidene), which acts as both Brønsted base – abstracting HCl – and stabilising Lewis Base.³³ In the base-free monomeric form, SiCl_2 is only stable as a gas at temperatures above 1000 °C and disproportionates or polymerizes upon cooling down.³⁴ Very recently, the first base-free acyclic silylenes were isolated in the form of the bulky bisthiatosilylene and boryl(amino)silylene (Chart 1.3, **I**; Scheme 1.1, **IX**, **X**).^{35,36} Silylene **IX** was synthesised by reductive cleavage of the Si-Br bonds in the corresponding dibromosilane. Silylene **X** was synthesised from the corresponding amino tribromosilane and 2 equivalents boryllithium. Remarkably, the boryl reagent has two distinct roles in this transformation: reduction of the silane and bromide substitution.

Boryl(amino)silylene **X** also displays remarkable reactivity, being the first example of a silylene capable of dihydrogen activation forming the corresponding dihydrosilane, which until recently was almost exclusively the realm of transition metals.³⁶ This illustrates the general ability of silylenes to activate small molecules, owing to their rather high-lying lone-pair (HOMO) and low-lying vacant orbital (LUMO).³⁷ In silylene **X**, the singlet-triplet gap – which correlates almost linearly with the HOMO-LUMO

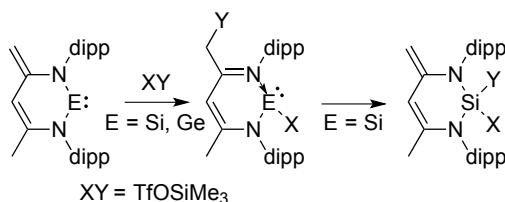
gap³⁷ – is particularly small to allow for the activation of H₂. Earlier, silylenes have been shown to also activate other bonds like E–H, E–X, E–O and E–E (E = group 14–16 elements).³⁸



Scheme 1.1 Seminal examples of the synthesis of silylenes: base-stabilized (**V**) and base-free (**VI**) metal-bound, cyclic base-free (**VII**), base-stabilised dihalosilylene (**VIII**) and acyclic base-free (**IX**, **X**)., Idipp = 1,3-bis(dipp)imidazol-2-ylidene, Mes = 2,4,6-methylphenyl, IMes = 1,3-bis(mes)imidazol-2-ylidene.

Strikingly, even though the first free acyclic silylenes were synthesised only in 2012, free, acyclic germylenes $[[(\text{Me}_3\text{Si})_2\text{N}]_2\text{Ge}]$ were synthesised as early as 1974.³⁹ The silicon(II) analogue of the latter decomposes rapidly above 0 °C, illustrating the intrinsic higher stability of the Ge(II) state.⁴⁰ Another illustrative example of this

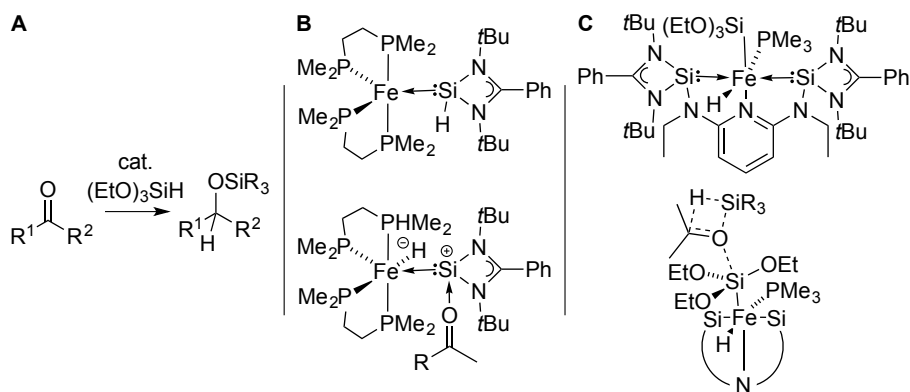
stability is the addition of small molecules to the β -diketiminato silylene and germylene (Scheme 1.2). Despite their intriguing structural resemblance, the silylene showed a thermodynamic preference for 1,1-addition and formal oxidation of Si(II) to Si(IV), whereas in the germylenes 1,4-addition was preferred, transforming the diamido-germylene centre in a base-stabilised amido(triflate)germylene.^{23,38,41} Ge(II) is more stable compared to Si(II) because of increasing energy separation of the central atom's s- and p-orbital, descending down group 14.²²



Scheme 1.2 Distinct reactivity of Si(II) and Ge(II) in small molecule activation. Dipp = 2,6-diisopropylphenyl^{23,38,41}

The isolation of the free NHSi **VII** sparked intense research into the properties and reactivity of NHSis, including complexation to transition metals. Metal complexes bearing NHSi's are now most often synthesized by coordination of the corresponding free silylene to the metal precursor, often substituting a labile ligand.^{14,15,19} The next logical step in the chemistry of NHSis was their application as supporting ligands in catalysis. Despite a slow start – the first two examples were reported 7 years apart (2001–2008)^{42,43} – the number of catalytic examples using silylene ligands is now sufficient to substantiate the unique properties of these ligands, *e.g.* strong σ -donor/ π -acceptor properties and its ability of substrate activation (Scheme 1.3).^{18,44,45} The NHSi TM-complexes found to be active in catalysis, are often based on three silylene motifs;^{18,44–49} the 4-membered amidinato silylene (**III**, $n = 1$), the (un)saturated 5-membered NHSi **VII**, and the 6-membered zwitterionic silylene **III**, which remarkably all took the same time (7 years) from their first synthesis until their first use in catalysis. Silylene ligands have been employed in a wide variety of catalytic reactions, *e.g.* ketone (Fe) and olefin (Pt) hydrosilylation, amide reduction (Rh, Ir), alkyne cyclotrimerisation (Co), arene borylation (Co), aryl halide amination (Ni), and hydroformylation (Rh).^{44,46–53} Additionally, catalytic C–C cross-coupling reactions are well-represented with examples of Pd-catalysed Suzuki and Heck, and Ni-catalysed Kumada, Negishi, and Sonogashira reactions.^{42,43,54–56} Recent applications in iron-catalyzed ketone hydrosilylation illustrate the potential of Si(II) ligands in catalysis, not only as strongly donating supporting ligands, but also as versatile cooperative ligands. An iron(0) complex of a monodentate amidinatosilylene (Scheme 1.3B) was found to be active in the hydrosilylation of ketones.⁵¹ There, the Si(II) ligand was found to participate in catalysis by acting as a Lewis acid to activate the substrate. A related substrate activation by a Si(II) ligand was also observed by Metsänen *et al.*,⁵⁰ who reported an iron-pincer complex featuring an additional

triethoxysilyl ligand active in ketone hydrosilylation (Scheme 1.3C). A catalytic mechanism was proposed on the basis of labelling, cross-over and competition experiments, as well as DFT computations. The unconventional peripheral mechanism involves turnover at the silyl ligand, without participation of the metal centre. The calculations suggest that the activation barriers of more conventional metal-centred inner ($E_{\text{act}} = 34.9$ kcal/mol) and outer sphere ($E_{\text{act}} = 33.7$ kcal/mol) mechanisms are higher in energy by approximately 20 kcal/mol ($E_{\text{act, peripheral}} = 14.3$ kcal/mol). In the peripheral mechanism, the triethoxysilyl ligand is solely involved in activation of the ketone to allow for the subsequent outer-sphere σ -bond metathesis and release of the newly formed silyl ether. Remarkably, none of the substrates bind to the iron centre during catalysis; they bind to the Lewis acidic triethoxysilyl ligand exclusively.



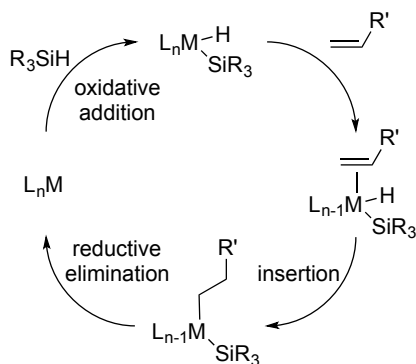
Scheme 1.3 Generic ketone hydrosilylation reaction (A). Catalytically active species in ketone hydrosilylation (B, C top) and their key intermediates (B, C bottom).

Occasionally, Ge(II) ligands are also being used in catalysis. However, this field is underexplored.⁵⁷ Mostly, these ligands serve to compare catalytic activity with the analogous Si(II) ligand.^{44,53,56,58} Benedek and Szilvási performed a theoretical side-by-side comparison of 81 Si(II) and Si(0), and 144 Ge(II) and Ge(0) ligands with benchmark NHCs and phosphines to assess the relative σ -donor and π -acceptor ability, ligand-to-metal charge transfer, and steric parameters. They showed that several low-valent silicon ligands can compete or even outperform classic NHC and phosphine ligands. This collection of computed parameters was presented as a convenient way to select a ligand possessing the desired properties.^{9,57}

In general, silylenes are regarded as “certainly more than simple isoelectronic replacements for more traditional ligands”¹⁸ and “advanced tunable steering ligands”⁴⁵ and hence are promising alternatives to widely used classical ligands, such as phosphines or N-heterocyclic carbenes.

Complexes of Silanides

Another group of low-valent Si(II) compounds has received considerably less attention for their potential use as supporting ligands: silanides (R_3Si^-), the heavier congeners of carbanions. Transition-metal complexes of silanides have mostly been studied because of their role as intermediates in catalytic hydrosilylation. The widely-accepted Chalk-Harrod mechanism⁵⁹ for this transformation involves oxidative addition of a hydrosilane to a metal complex with subsequent coordination of an olefin, insertion into the M-H bond followed by reductive elimination of, generally, an anti-Markovnikov product (Scheme 1.4). Mimicking the silane-activation step, TM-silyl species are most commonly accessed synthetically by oxidative addition of an H-Si bond to a reduced metal fragment.^{60,61}



Scheme 1.4 Catalytic cycle of the Chalk-Harrod mechanism.

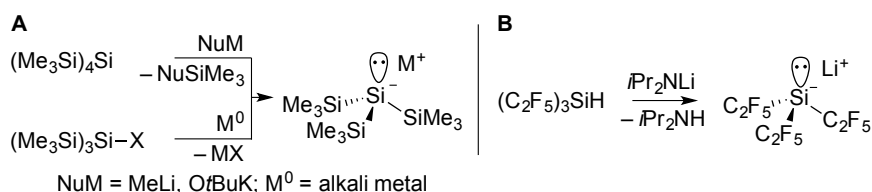
Because silanides are formally isoelectronic to phosphines and base-stabilized silylenes (Chart 1.2), the former being widely applied as monodentate ligands in homogeneous catalysis, one could expect to find a similar application of monodentate silyl ligands. However, studies on reactive silyl-metal intermediates show that the cleavage of the Si-M bond is usually facile through reductive elimination, nucleophilic attack at the silicon atom, insertion, and σ -bond metathesis.^{62,63} This broad reactivity spectrum is a likely reason why monodentate ancillary silyl ligands are not widely used. Interestingly, the strong σ -donor character of silyl ligands⁶⁴ has lead researchers to incorporate a silyl moiety into multidentate ligands,^{62,65} which diminishes the propensity of Si-M bond cleavage, resulting in an “almost uncountable number of bidentate silicon-based ligand systems and their metal complexes”⁶⁵ as well as tri- and tetradentate silyl ligands.^{62,65–67} This makes for electron-rich metal centres facilitating, *e.g.*, oxidative addition of a substrate or dissociation of a co-ligand. A second distinctive feature of silyl ligands is a strong trans-effect.^{62,65} Using this effect, the group of Peters was able to develop a series of iron complexes of a tetradentate trisphosphinosilyl ($[\text{Si}(\text{o-C}_6\text{H}_4\text{PR}_2)_3]^-$) ligand, which are capable of binding N_2 and putative intermediates of the

reduction cascade to NH_3 .⁶⁸ In general, the strong *trans* influence posed by the silyl moiety creates a labile coordination-site, facilitating turn-over during catalysis.

Free Silanides and Direct Complexation

In analogy with the field of silylenes, where TM-complexes are generally accessed by complexation of a free silylene to a TM-fragment, it would be of interest to development synthetic routes towards free silanides and subsequent metal coordination.

In principle, silanides are expected to be stronger reducing agents than silylenes on account of their charge, and hence more reactive, which hampers their isolation. The isolation of the silanides benefits from taming their reducing power, which can be achieved by kinetic stabilisation by steric bulk and/or electronic stabilization by electron withdrawing groups (EWGs) bound to the anionic centre. The former approach has been fruitfully applied with the most widely studied members of this group, that is the super- and hypersilyl anion ($t\text{Bu}_3\text{Si}^-$ and $(\text{Me}_3\text{Si})_3\text{Si}^-$, resp.) and derivatives thereof.^{10,69–75} In recent years also the related oligosilyl anions attracted much attention.^{64,76–81} These silanides are most often synthesised by nucleophilic cleavage of a Si–Si bond with MeLi ⁸² or $\text{KO}t\text{Bu}$,⁷⁶ or by reduction of the halosilane by an alkali metal [Scheme 1.5A].^{10,70} Interestingly, they can form TM–silicon bonds by direct complexation, as first described by Tilley and co-workers in 1987.^{83,84} The large steric demand also provides kinetic stabilization to the corresponding transition-metal complexes. Exploiting this, the low-coordinate iron complexes Hyp_2FeL (Hyp = hypersilyl, L = THF, Et_2O) were synthesised.^{84,85} Related low-coordinate complexes $[(\text{Me}_3\text{Si})_2\text{FeL}]$ (L = THF, Cl^-) have been shown to be highly reactive and are capable of catalytic reductive silylation of nitrogen to form $(\text{Me}_3\text{Si})_3\text{N}$ from N_2 , Na^0 and Me_3SiCl .⁸⁶ Electronically, the hypersilyl ligands are characterized by strong σ -donor and weak π -acceptor capabilities.^{10,70,73,87,88}

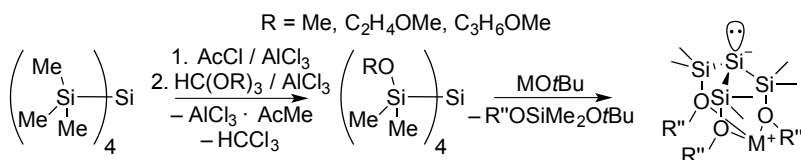


Scheme 1.5 Synthesis of free silanides $(\text{Me}_3\text{Si})_3\text{Si}^-$ (hypersilanide) and $(\text{C}_2\text{F}_5)_3\text{Si}^-$.

Further stabilization of the anion, by installing electron withdrawing groups, may allow for significantly less bulky free silanides. This approach has allowed for the isolation of free silanides bearing aromatic^{69,81,89–93} and more recently pentafluoroethyl^{94,95} moieties (Scheme 1.5B). Moreover, the use of EWGs makes deprotonation of an Si–H bond a viable synthesis route to silanides as was shown by the isolation of $(\text{C}_2\text{F}_5)_3\text{Si}^-$.

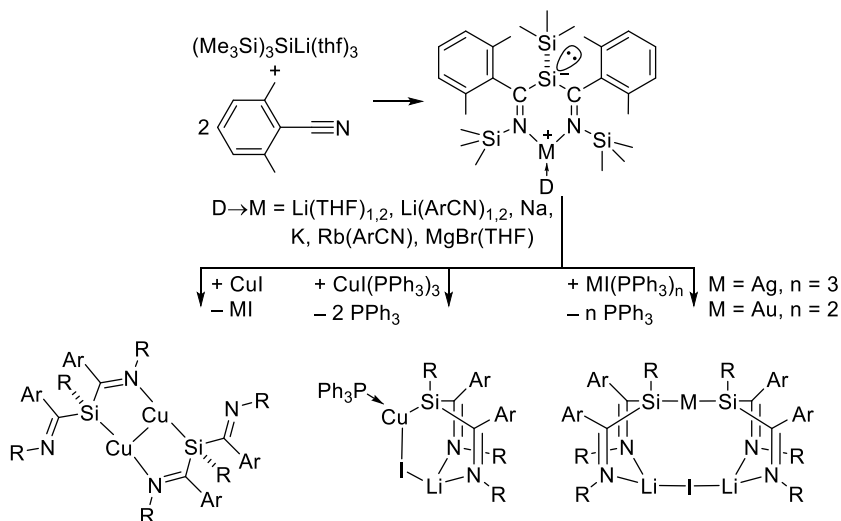
Zwitterionic Silanides

Most silanide anions are stabilized to some extent by interaction with a counterion, most often an alkali-metal. In recent years, a new strategy has emerged to isolate truly free silanides devoid of stabilization by coordination: additional donor groups are incorporated in the structure to encapsulate the counterion away from the Si⁻ center. The group of Krempner developed a series of silanides incorporating additional Lewis-Base functionalities on the hypersilanide scaffold [(Me₃Si)₃Si⁻]. Formal substitution of one of the methyl groups for residues featuring ether or pyrazole moieties on each Me₃Si terminus of (Me₃Si)₄Si afforded donor functionalized silanes (Scheme 1.6). Nucleophilic cleavage of one of the Si–Si bonds in these donor-functionalized silanes with MOtBu (M = Li, Na, K) affords the corresponding zwitterionic silanides. Using the same method, these authors also report the carbanion (synthesized by deprotonation of R₃CH) and germanide homologues. The availability of the naked Si anion for complex formation was demonstrated by its complexation to a range of Lewis acids: BPh₃, B(C₅F₆)₃, W(CO)₅, AlMe₃, and ZnR₂ (R = Cl, I, Me).^{74,75,96–101}

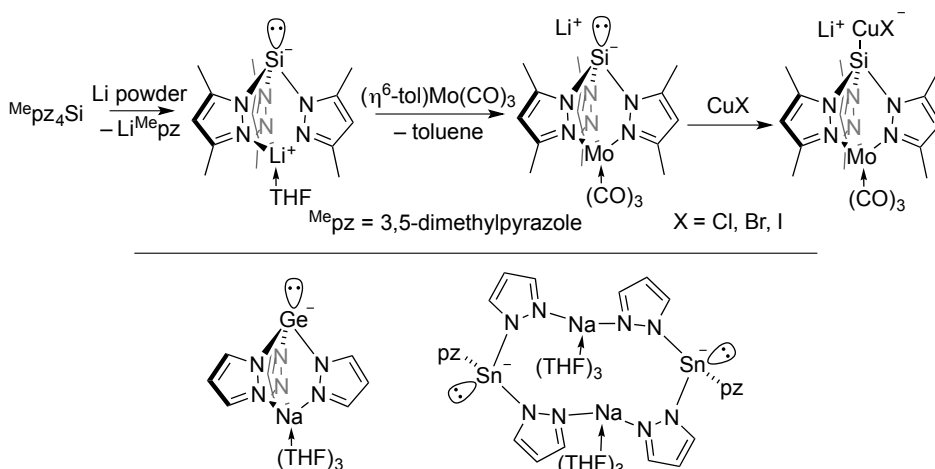


Scheme 1.6 Synthesis of ether-functionalised zwitterionic silanides.

Using a similar approach toward free silanides, the group of Lappert^{102–106} developed the zwitterionic silanide 3-sila- β -diketiminato in which the silicon anion is stabilized by conjugation (Scheme 1.7). The imine functionalities are installed by formal insertion of an aryl nitrile into Si–SiMe₃ bonds of LiSi(SiMe₃)₃, whereby Li⁺ is ligated by the imine nitrogens. The additional imine functionalities flanking the Si⁻ anion give rise to interesting coordination chemistry. Coinage metal complexes bearing this ligand were accessed by reaction of the zwitterion with CuI and Ml(PPh₃)₃, (M = Cu, Ag, Au; Scheme 1.7). Interestingly, liberation of LiI was only observed in the absence of PPh₃ resulting in a neutral copper dimer with the ligands bound in a Si,N-bidentate fashion. However, in the presence of PPh₃ a monomeric metallabicyclo[2.2.2]octane complex was formed, consisting of a Si–[C=N]₂–Li ring and a Si–Cu–I–Li half-ring, in which one PPh₃ is still bound to Cu. Complexation of the zwitterion to silver- and gold iodide yields isostructural complexes in which the linearly coordinated metal ion bears two silyl ligands with a bridging iodide bound to the Li-ions. Complexation to mercury chloride results in a linear, neutral, bis-silyl mercury complex and concomitant liberation of LiCl.



Scheme 1.7 Synthesis and complexation to coinage metal salts of imine-functionalised zwitterionic silanides.



Scheme 1.8 Synthesis of pyrazole-functionalised zwitterionic silanides and direct complexation thereof (top). Trispyrazolylgermanide and stannide (bottom).

The group of Breher combined the remote donor-functionality needed for zwitterionic silanides with the electron withdrawing nature of N-heterocycles, allowing for an inductive stabilising effect through the Si-N σ -bond similar to that in NHSis and NHCs (*vide supra*). They synthesised zwitterionic trispyrazolyl silanides by reductive cleavage of an N-Si bond in $\text{Si}(\text{Me}_4\text{pz})_4$ with Li-powder [Scheme 1.8].¹⁰⁷ Structurally analogous zwitterionic germanides were synthesised by Steiner et al. [Scheme 1.8].¹⁰⁸ However, attempted synthesis of the tin derivative resulted in a cyclic dimer. The zwitterionic silanide was transformed in an anionic ligand by replacement of Li^+ with $\text{Mo}(\text{CO})_3$ [Scheme 1.8].¹⁰⁹ The Si lone pair was shown to be

available for coordination by complexation of the ligand to CuCl, CuBr, and CuI, yielding the corresponding linear silyl halocuprates. The pyrazolyl groups in these silanides are significantly less sterically encumbering than the $-\text{SiMe}_3$ groups in the hypersilyl analogues and are more electron-withdrawing, which lowers the Lewis basicity of the Si-centre.

Outlook

The strong σ -donor capabilities of silanides could potentially prove beneficial in catalysis for facilitating substrate activation or creating labile coordination sites. In view of the contemporary incentive to replace precious metals by base metals, silanides may offer interesting perspectives. In high-spin, first row transition metal complexes, some of the unpaired electrons often occupy the M–L π^* -orbitals, weakening the M–L bond. The additional electrostatic bonding between the silyl ligand and the metal centre, which is expected not to be strongly affected by the high-spin state, is envisaged to enhance the M–L bond strength in comparison with neutral phosphine analogues. In addition, silanides are capable of stabilizing low-coordinate metal species (*vide supra*).¹⁰ In this respect, they are likely to be effective ligands for a range of catalytic reactions including, for example, C–C cross couplings catalysed by first-row transition metals, which often proceed *via* high-spin organometallic intermediates.^{110,111}

This Work

Building on the existing knowledge presented in the previous paragraphs, the synthesis of stable silyl ligands based on pyrrole and related heterocycles as electron-withdrawing substituents is investigated in this work. Pyrrole was previously identified by Moloy et al. and Hübler et al. to be strongly electron-withdrawing – in the pyr_3Si^- and pyr_3P ligands – which was ascribed to the involvement of the N lone pair in the aromatic system.^{112,113} The larger coefficient on Si of the R–Si σ^* -orbitals, caused by electron-withdrawing R groups (R = Me < OH < Cl < F), was shown to lead to a higher Si–M bond order due to increasing π -back-bonding from the metal.¹¹⁴ Besides simple monodentate heterocycles, bidentate 2-[N-aryliminomethyl]pyrrole [ArIMP^{H}] derivatives as well as the tridentate tris[3-methylindol-2-yl]methane (tmim) scaffolds as shown in Chart 1.5 are investigated in this work.

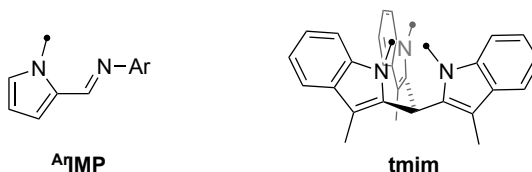


Chart 1.5 Substituents used; 2-[N-aryliminomethyl]pyrrole (left) and tri[3-methylindol-2-yl]methane (right).

Hydrosilanes bearing the 2-[N-(2,6-diisopropylphenyl)iminomethyl]pyrrolide (^{dipp}IMP) substituent are studied as potential precursors for silanides. Somewhat unexpectedly, these silanes undergo an intra-molecular hydrosilylation reaction of the imine, hampering their use as a silyl precursor. This unusual hydrosilylation reaction is studied in **Chapter 2**, where details of the reaction pathway are investigated, and substitution patterns that favour or hamper this reaction are identified. Next, as described in **Chapter 3**, heterocycle-substituted silyl ligands were prepared within the coordination sphere of iron as a way to circumvent the intermediacy of hydrosilanes. Namely, nucleophilic substitution of Cl^- on the Cl_3Si -ligand bound to the Fe(II) fragment $\text{CpFe}(\text{CO})_2$ or to the Fe(0) fragment $\text{LFe}(\text{CO})_4^-$ for anionic heterocycles (Het⁻) gives access to heterocycle-based silyl ligands. In **Chapter 4**, a novel synthesis method for free silanides is introduced: nucleophilic substitution of Cl^- for tmim^{3-} on the NHC-stabilized Si(II) precursor $\text{Idipp} \rightarrow \text{SiCl}_2$ ($\text{Idipp} = \{1,3\text{-bis}[2,6\text{-diisopropylphenyl}]\text{imidazol-2-ylidene}\}$, Scheme 1.1, **VIII**). This method circumvents the use of intermediate tetrahedral silicon species, which are more strained than the target silanide as indicated by DFT calculations. Coordination of this ligand to CuCl and FeCl_2 demonstrates its potential as a supporting ligand. Analogous to the Si(II) anion, the synthesis of a germyl anion from tmim^{3-} and $\text{GeCl}_2\cdot\text{dioxane}$ is described in **Chapter 5**. Coordination to CuCl and $\text{Fe}(\text{CO})_4$ affords the corresponding complexes. Interestingly, only weak coordination to Fe(II)Cl_2 is observed, whereas the Si(II) anion forms the silyl dichloro ferrate upon complexation. The Ge(II) ligand is shown to exhibit intermediate donor strength, relative to the Si and P analogues. The findings described in this thesis contribute to the understanding of low-valent heavier group 14 ligands and their complexes. The knowledge acquired is anticipated to assist in the further development of this promising class of ligands.

References

- [1] Leyssens, T.; Peeters, D.; Orpen, A. G.; Harvey, J. N. *Organometallics* **2007**, *26*, 2637–2645.
- [2] Comas-Vives, A.; Harvey, J. N. *Eur. J. Inorg. Chem.* **2011**, *2011*, 5025–5035.
- [3] Crabtree, R. H. In *The Organometallic Chemistry of the Transition Metals*; 2009; pp 99–104.
- [4] Hopkinson, M. N.; Richter, C.; Schedler, M.; Glorius, F. *Nature* **2014**, *510*, 485–496.
- [5] Díez-González, S.; Marion, N.; Nolan, S. P. *Chem. Rev.* **2009**, *109*, 3612–3676.
- [6] Boehme, C.; Frenking, G. *J. Am. Chem. Soc.* **1996**, *118*, 2039–2046.
- [7] Arduengo, A. J.; Harlow, R. L.; Kline, M. *J. Am. Chem. Soc.* **1991**, *113*, 361–363.
- [8] Nelson, D. J.; Nolan, S. P. *Chem. Soc. Rev.* **2013**, *42*, 6723–6753.

- [9] Benedek, Z.; Szilvási, T. *RSC Adv.* **2015**, *5*, 5077–5086.
- [10] Lerner, H. *Coord. Chem. Rev.* **2005**, *249*, 781–798.
- [11] Li, J.; Merkel, S.; Henn, J.; Meindl, K.; Döring, A.; Roesky, H. W.; Ghadwal, R. S.; Stalke, D. *Inorg. Chem.* **2010**, *49*, 775–777.
- [12] Su, B.-Y.; Li, L.; Wang, J.-X.; Li, X.-Y. *Acta Crystallogr. Sect. E Struct. Reports Online* **2012**, *68* (Pt 10), o2888.
- [13] Álvarez-Rodríguez, L.; Cabeza, J. A.; García-Álvarez, P.; Polo, D. *Coord. Chem. Rev.* **2015**, *300*, 1–28.
- [14] Blom, B.; Stoelzel, M.; Driess, M. *Chem. Eur. J.* **2013**, *19*, 40–62.
- [15] Asay, M.; Jones, C.; Driess, M. *Chem. Rev.* **2011**, *111*, 354–396.
- [16] Sen, S. S.; Khan, S.; Samuel, P. P.; Roesky, H. W. *Chem. Sci.* **2012**, *3*, 659–682.
- [17] Bag, P.; Ahmad, S. U.; Inoue, S. *Bull. Chem. Soc. Jpn.* **2017**, *90*, 255–271.
- [18] Blom, B.; Gallego, D.; Driess, M. *Inorg. Chem. Front.* **2014**, *1*, 134–148.
- [19] Blom, B.; Pohl, M.; Tan, G.; Gallego, D.; Driess, M. *Organometallics* **2014**, *33*, 5272–5282.
- [20] Mandal, S. K.; Roesky, H. W. *Chem. Commun.* **2010**, *46*, 6016.
- [21] Haaf, M.; Schmedake, T. A.; West, R. *Acc. Chem. Res.* **2000**, *33*, 704–714.
- [22] Mizuhata, Y.; Sasamori, T.; Tokitoh, N. *Chem. Rev.* **2009**, *109*, 3479–3511.
- [23] Driess, M.; Yao, S.; Brym, M.; van Wüllen, C.; Lentz, D. *J. Am. Chem. Soc.* **2006**, *128*, 9628–9629.
- [24] Heinicke, J.; Oprea, A.; Kindermann, M. K.; Karpati, T.; Nyulászi, L.; Veszprémi, T. *Chem. Eur. J.* **1998**, *4*, 541–545.
- [25] Jutzi, P.; Leszczyńska, K.; Neumann, B.; Schoeller, W. W.; Stammer, H.-G. *Angew. Chemie Int. Ed.* **2009**, *48*, 2596–2599.
- [26] Schmid, G.; Welz, E. *Angew. Chemie Int. Ed.* **1977**, *16*, 785–786.
- [27] Straus, D. A.; Grumbine, S. D.; Tilley, T. D. *J. Am. Chem. Soc.* **1990**, *112*, 7801–7802.
- [28] Denk, M.; Lennon, R.; Hayashi, R.; West, R.; Belyakov, A. V.; Verne, H. P.; Haaland, A.; Wagner, M.; Metzler, N. J. *Am. Chem. Soc.* **1994**, *116*, 2691–2692.
- [29] Redies, K. M.; Fallon, T.; Oestreich, M. *Organometallics* **2014**, *33*, 3235–3238.
- [30] Kosai, T.; Ishida, S.; Iwamoto, T. *Angew. Chemie Int. Ed.* **2016**, *55*, 15554–15558.
- [31] Dong, Z.; Reinhold, C. R. W.; Schmidtman, M.; Müller, T. *J. Am. Chem. Soc.* **2017**, *139*, 7117–7123.
- [32] Alvarado-Beltran, I.; Baceiredo, A.; Saffon-Merceron, N.; Branchadell, V.; Kato, T. *Angew. Chemie Int. Ed.* **2016**, *55*, 16141–16144.
- [33] Ghadwal, R. S.; Roesky, H. W.; Merkel, S.; Henn, J.; Stalke, D. *Angew. Chemie Int. Ed.* **2009**, *48*, 5683–5686.
- [34] Uhlemann, F.; Köppe, R.; Schnepf, A. *Zeitschrift für Anorg. und Allg. Chemie* **2014**, *640*, 1658–1664.
- [35] Rekken, B. D.; Brown, T. M.; Fetting, J. C.; Tuononen, H. M.; Power, P. P. *J. Am. Chem. Soc.* **2012**, *134*, 6504–6507.
- [36] Protchenko, A. V.; Birj Kumar, K. H.; Dange, D.; Schwarz, A. D.; Vidovic, D.; Jones, C.; Kaltsoyannis, N.; Mountford, P.; Aldridge, S. J. *Am. Chem. Soc.* **2012**, *134*, 6500–6503.
- [37] Wang, Y.; Ma, J. *J. Organomet. Chem.* **2009**, *694*, 2567–2575.
- [38] Yao, S.; Xiong, Y.; Driess, M. *Organometallics* **2011**, *30*, 1748–1767.
- [39] Harris, D. H.; Lappert, M. F. *J. Chem. Soc., Chem. Commun.* **1974**, No. 21, 895–896.
- [40] Lee, G.; West, R.; Mu, T. *J. Am. Chem. Soc. Commun.* **2003**, *125*, 8114–8115.
- [41] Meltzer, A.; Inoue, S.; Präsaang, C.; Driess, M. *J. Am. Chem. Soc.* **2010**, *132*, 3038–3046.
- [42] Fürstner, A.; Krause, H.; Lehmann, C. W. *Chem. Commun.* **2001**, *80*, 2372–2373.
- [43] Zhang, M.; Liu, X.; Shi, C.; Ren, C.; Ding, Y.; Roesky, H. W. *Zeitschrift für Anorg. und Allg. Chemie* **2008**, *634*, 1755–1758.
- [44] Schmidt, M.; Blom, B.; Szilvási, T.; Schomäcker, R.; Driess, M. *Eur. J. Inorg. Chem.* **2017**, *2017*, 1284–1291.
- [45] Rao-fmoghaddam, S.; Zhou, Y. P.; Wang, Y.; Driess, M. *J. Organomet. Chem.* **2016**, *829*, 2–10.
- [46] Imura, T.; Akasaka, N.; Iwamoto, T. *Organometallics* **2016**, *35*, 4071–4076.
- [47] Imura, T.; Akasaka, N.; Kosai, T.; Iwamoto, T.; Bertrand, G.; Saffon-Merceron, N.; Branchadell, V.; Kato, T. *Dalton Trans.* **2017**, *46*, 8868–8874.

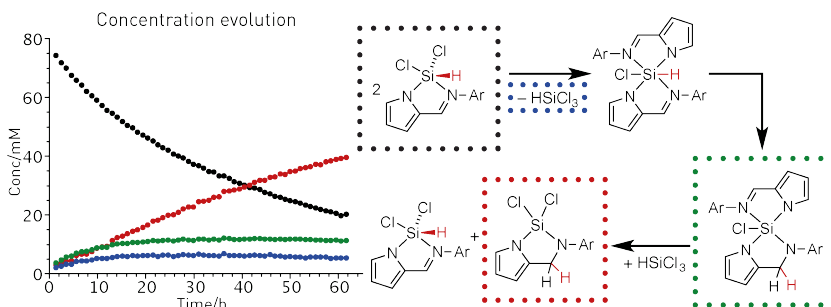
- [48] Zhou, Y.-P.; Raoufmoghaddam, S.; Szilvási, T.; Driess, M. *Angew. Chemie Int. Ed.* **2016**, *55*, 12868–12872.
- [49] Ren, H.; Zhou, Y.-P.; Bai, Y.; Cui, C.; Driess, M. *Chem. Eur. J.* **2017**, *23*, 5663–5667.
- [50] Metsänen, T. T.; Gallego, D.; Szilvási, T.; Driess, M.; Oestreich, M. *Chem. Sci.* **2015**, *6*, 7143–7149.
- [51] Blom, B.; Enthaler, S.; Inoue, S.; Irran, E.; Driess, M. *J. Am. Chem. Soc.* **2013**, *135*, 6703–6713.
- [52] Stoelzel, M.; Präsang, C.; Blom, B.; Driess, M. *Aust. J. Chem.* **2013**, *66*, 1163–1170.
- [53] Wang, W.; Inoue, S.; Enthaler, S.; Driess, M. *Angew. Chemie Int. Ed.* **2012**, *51*, 6167–6171.
- [54] Tan, G.; Enthaler, S.; Inoue, S.; Blom, B.; Driess, M. *Angew. Chemie Int. Ed.* **2015**, *54*, 2214–2218.
- [55] Wang, W.; Inoue, S.; Yao, S.; Driess, M. *J. Am. Chem. Soc.* **2010**, *132*, 15890–15892.
- [56] Gallego, D.; Brück, A.; Irran, E.; Meier, F.; Kaupp, M.; Driess, M.; Hartwig, J. F. *J. Am. Chem. Soc.* **2013**, *135*, 15617–15626.
- [57] Benedek, Z.; Szilvási, T. *Organometallics* **2017**, *36*, 1591–1600.
- [58] Brück, A.; Gallego, D.; Wang, W.; Irran, E.; Driess, M.; Hartwig, J. F. *Angew. Chemie Int. Ed.* **2012**, *51*, 11478–11482.
- [59] Chalk, A. J.; Harrod, J. F. *J. Am. Chem. Soc.* **1965**, *87*, 16–21.
- [60] Corey, J. Y. *Chem. Rev.* **2016**, *116*, 11291–11435.
- [61] Hofmann, R.; Vlatković, M.; Wiesbrock, F. *Polymers (Basel)*. **2017**, *9*, 534.
- [62] Okazaki, M.; Ohshitanai, S.; Iwata, M.; Tobita, H.; Ogino, H. *Coord. Chem. Rev.* **2002**, *226*, 167–178.
- [63] Tilley, T. D. In *The Chemistry of Organic Silicon Compounds*; Patai, S., Rappoport, Z., Eds.; John Wiley & Sons, Ltd: Chichester, UK, 1989; pp 1415–1477.
- [64] Zitz, R.; Hlina, J.; Aghazadeh Meshgi, M.; Krenn, H.; Marschner, C.; Szilvási, T.; Baumgartner, J. *Inorg. Chem.* **2017**, *56*, 5328–5341.
- [65] Simon, M.; Breher, F. *Dalton Trans.* **2017**, *46*, 7976–7997.
- [66] Balakrishna, M. S.; Chandrasekaran, P.; George, P. P. *Coord. Chem. Rev.* **2003**, *241*, 87–117.
- [67] Shimada, S.; Tanaka, M. *Coord. Chem. Rev.* **2006**, *250*, 991–1011.
- [68] Lee, Y.; Mankad, N. P.; Peters, J. C. *Nat. Chem.* **2010**, *2*, 558–565.
- [69] Brown, J. L.; Montgomery, A. C.; Samaan, C. A.; Janicke, M. T.; Scott, B. L.; Gaunt, A. J. *Dalton Trans.* **2016**, *45*, 9841–9852.
- [70] Wiberg, N. *Coord. Chem. Rev.* **1997**, *163*, 217–252.
- [71] Klinkhammer, K. W. *Chem. Eur. J.* **1997**, *3*, 1418–1431.
- [72] Aghazadeh Meshgi, M.; Baumgartner, J.; Marschner, C. *Organometallics* **2015**, *34*, 3721–3731.
- [73] Klink, R.; Schrenk, C.; Schnepf, A. *Dalton Trans.* **2014**, *43*, 16097–16104.
- [74] Thalangaarachchige, V. D.; Li, H.; Cordes, D. B.; Unruh, D. K.; Krempner, C. *Inorg. Chem.* **2017**, *56*, 9869–9879.
- [75] Thalangaarachchige, V. D.; Unruh, D. K.; Cordes, D. B.; Krempner, C. *Inorg. Chem.* **2015**, *54*, 4189–4191.
- [76] Marschner, C. *Organometallics* **2006**, *25*, 2110–2125.
- [77] Hlina, J.; Stella, F.; Meshgi, M. A.; Marschner, C.; Baumgartner, J. *Molecules* **2016**, *21*, 1079.
- [78] Stueger, H.; Hasken, B.; Gross, U.; Fischer, R.; Torvisco Gomez, A. *Organometallics* **2013**, *32*, 4490–4500.
- [79] Marro, E. A.; Press, E. M.; Purkait, T. K.; Jimenez, D.; Siegler, M. A.; Klausen, R. S. *Chem. Eur. J.* **2017**, *23*, 15633–15637.
- [80] Zitz, R.; Gatterer, K.; Reinhold, C. R. W.; Müller, T.; Baumgartner, J.; Marschner, C. *Organometallics* **2015**, *34*, 1419–1430.
- [81] Präsang, C.; Scheschewitz, D. In *Structure and Bonding*; 2013; Vol. 156, pp 1–47.
- [82] Gutekunst, G.; G. Brook, A. J. *Organomet. Chem.* **1982**, *225*, 1–3.
- [83] Campion, B. K.; Falk, J.; Tilley, T. D. *J. Am. Chem. Soc.* **1987**, *109*, 2049–2056.
- [84] Roddick, D. M.; Tilley, T. D.; Rheingold, A. L.; Geib, S. J. *J. Am. Chem. Soc.* **1987**, *109*, 945–946.
- [85] Heyn, R. H.; Tilley, T. D. *Inorg. Chim. Acta* **2002**, *341*, 91–98.
- [86] Yuki, M.; Tanaka, H.; Sasaki, K.; Miyake, Y.; Yoshizawa, K.; Nishibayashi, Y. *Nat. Commun.* **2012**, *3*, 1254.

- [87] Jenkins, D. M.; Teng, W.; Englich, U.; Stone, D.; Ruhlandt-Senge, K. *Organometallics* **2001**, *20*, 4600–4606.
- [88] Nakamoto, M.; Fukawa, T.; Lee, V. Y.; Sekiguchi, A. *J. Am. Chem. Soc.* **2002**, *124*, 15160–15161.
- [89] Sekiguchi, A.; Lee, V. Y.; Nanjo, M. *Coord. Chem. Rev.* **2000**, *210*, 11–45.
- [90] Tamao, K.; Kawachi, A. *Adv. Organomet. Chem.* **1995**, *38*, 1–58.
- [91] Lickiss, P. D.; Smith, C. M. *Coord. Chem. Rev.* **1995**, *145*, 75–124.
- [92] Kleeberg, C.; Cascarano, G.; Giacomazzo, C.; Guagliardi, A.; Nudelman, A.; Stoltz, B. M.; Bercaw, J. E.; Goldberg, K. I. *Dalton Trans.* **2013**, *42*, 8276–8287.
- [93] Mashin, E.; Kratish, Y.; Kaushansky, A.; Bravo-Zhivotovskii, D.; Apeloig, Y. *Struct. Chem.* **2017**, *28*, 537–544.
- [94] Schwarze, N.; Steinhauer, S.; Neumann, B.; Stammeler, H.-G.; Hoge, B. *Angew. Chemie Int. Ed.* **2016**, *55*, 16156–16160.
- [95] Schwarze, N.; Steinhauer, S.; Neumann, B.; Stammeler, H.-G.; Hoge, B. *Angew. Chemie Int. Ed.* **2016**, *55*, 16161–16164.
- [96] Li, H.; Aquino, A. J. A.; Cordes, D. B.; Hase, W. L.; Krempner, C. *Chem. Sci.* **2017**, *8*, 1316–1328.
- [97] Krempner, C.; Chisholm, M. H.; Gallucci, J. *Angew. Chemie Int. Ed.* **2008**, *47*, 410–413.
- [98] McNerney, B.; Whittlesey, B.; Krempner, C. *Eur. J. Inorg. Chem.* **2011**, *2011*, 1699–1702.
- [99] Carlson, B.; Aquino, A. J. A.; Hope-Weeks, L. J.; Whittlesey, B.; McNerney, B.; Hase, W. L.; Krempner, C. *Chem. Commun.* **2011**, *47*, 11089.
- [100] Li, H.; Hope-Weeks, L. J.; Krempner, C. *Chem. Commun.* **2011**, *47*, 4117–4119.
- [101] Li, H.; Hung-Low, F.; Krempner, C. *Organometallics* **2012**, *31*, 7117–7124.
- [102] Hitchcock, P. B.; Lappert, M. F.; Layh, M. *Chem. Commun.* **1998**, 2179–2180.
- [103] Farwell, J. D.; Fernandes, M. A.; Hitchcock, P. B.; Lappert, M. F.; Layh, M.; Omondi, B. *Dalton Trans.* **2003**, *102*, 1719–1729.
- [104] Farwell, J. D.; Hitchcock, P. B.; Lappert, M. F.; Protchenko, A. V. *Chem. Commun.* **2005**, No. 17, 2271–2273.
- [105] Farwell, J. D.; Hitchcock, P. B.; Lappert, M. F.; Protchenko, A. V. *J. Organomet. Chem.* **2007**, *692*, 4953–4961.
- [106] Farwell, J. D.; Hitchcock, P. B.; Lappert, M. F. *Chem. Commun.* **2002**, No. 5, 456–457.
- [107] Armbruster, F.; Fernández, I.; Breher, F. *Dalton Trans.* **2009**, *29*, 5612.
- [108] Steiner, A.; Stalke, D. *J. Chem. Soc., Chem. Commun.* **1993**, No. 22, 1702–1704.
- [109] Styra, S.; González-Gallardo, S.; Armbruster, F.; Oña-Burgos, P.; Moos, E.; Vonderach, M.; Weis, P.; Hampe, O.; Grün, A.; Schmitt, Y.; Gerhards, M.; Menges, F.; Gaffga, M.; Niedner-Schatteburg, G.; Breher, F. *Chem. Eur. J.* **2013**, *19*, 8436–8446.
- [110] Bedford, R. B. *Acc. Chem. Res.* **2015**, *48*, 1485–1493.
- [111] Bauer, I.; Knölker, H. *Chem. Rev.* **2015**, *115*, 3170–3387.
- [112] Moloy, K. G.; Petersen, J. L. *J. Am. Chem. Soc.* **1995**, *117*, 7696–7710.
- [113] Hübler, K.; Roper, W. R.; Wright, L. J. *Organometallics* **1997**, *16*, 2730–2735.
- [114] Hübler, K.; Hunt, P. A.; Maddock, S. M.; Rickard, C. E. F.; Roper, W. R.; Salter, D. M.; Schwerdtfeger, P.; Wright, L. J. *Organometallics* **1997**, *16*, 5076–5083.

2

Hydrosilylation in Aryliminopyrrolide Substituted Silanes

A range of silanes was synthesized by the reaction of HSiCl_3 with iminopyrrole derivatives in the presence of NEt_3 . In certain cases, intramolecular hydrosilylation converts the imine substituent into an amino substituent. This reaction is inhibited by factors such as electron-donating substitution on Si and steric bulk. The monosubstituted $[\text{DippIMP}]\text{SiHMeCl}$ ($\text{DippIMP} = 2\text{-[N-(2,6-diisopropylphenyl)imino-methyl]pyrrolide}$), is stable towards hydrosilylation, but slow hydrosilylation is observed for $[\text{DippIMP}]\text{SiHCl}_2$. Reaction of 2 equiv $[\text{DippIMP}]\text{PH}$ with HSiCl_3 results in the hydrosilylation product $[\text{DippAMP}][\text{DippIMP}]\text{SiCl}$ ($\text{DippAMP} = 2\text{-[N-(2,6-diisopropylphenyl)aminomethylene]pyrrolide}$), but the trisubstituted $[\text{DippIMP}]_3\text{SiH}$ is stable. Monitoring the hydrosilylation reaction of $[\text{DippIMP}]\text{SiHCl}_2$ reveals a reactive pathway involving substituent redistribution reactions to form the disubstituted $[\text{DippAMP}][\text{DippIMP}]\text{SiCl}$ as an intermediate. The reaction is strongly accelerated by the presence of chloride anions.



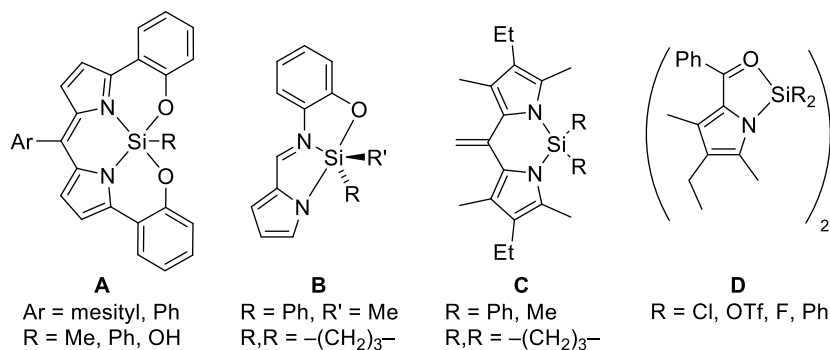
This work has been published as: Witteman, L.; Evers, T.; Shu, Z.; Lutz, M.; Klein Gebbink, R. J. M.; Moret, M.-E. *Chem. Eur. J.* **2016**, 22, 6087–6099.

Introduction

Silicon(II) compounds supported by nitrogen substituents are attracting a renewed interest because of their use as strongly donating, high-field ligands.¹⁻³ The first stable silylene was developed using a chelating di-anionic N-donor substituent that forms a 5-membered ring with silicon(II),⁴ in an analogous fashion to Arduengo's N-heterocyclic carbene.⁵ In recent years, stable silylenes have also been isolated with a range of monoanionic, bidentate N-donor substituents such as (bis)amidinato, (bis)guanidinato,⁶⁻¹² and β -diketiminato.¹³⁻¹⁶ In addition, a free silicon(II) anion has recently been afforded by cleavage of one pyrazolyl off of a tetrapyrazolyl silane,¹⁷ which has been coordinated to transition metals such as Pd, Pt, and Cu,^{18,19} demonstrating the use of electron-withdrawing heterocyclic substituents to stabilize novel low-valent silicon chemistry.

In this context, the coordination chemistry of pyrrolyl-substituted silicon(II) ligands is underdeveloped. In one isolated example, tri-*N*-pyrrolylsilane has been shown by Hübler, Roper and Wright¹ to undergo Si-H oxidative addition to Ru and Os complexes to form the tri-*N*-pyrrolylsilyl ligand, which is strongly π -accepting due to the electron withdrawing character of the pyrrolyl substituents. Nevertheless, a range of pyrrolyl-substituted silanes is known. The better part of the existing compounds with an *N*-pyrrolylsilyl substructure is being studied in the form of 1) phthalocyanines,²⁰ porphyrins,²¹ and analogs thereof, 2) silyl-protected pyrroles²² (mainly R_3SiPyr where R = alkyl or aryl) or 3) chemical vapor deposition (CVD) precursors ($Pyr_nSiH_{(4-n)}$ (n = 1-3)).²³ In addition, three research groups have specifically studied the structure and reactivity of pyrrolylsilane derivatives (Chart 2.1): the dihydroxyphenol dipyrin **A** by Sakamoto *et al.*,²⁴ the (NNO) pyrrolehydroxyphenol carbaldimine **B** by Gerlach *et al.*,^{25,26} and dipyrins **C** and acylpyrroles **D** by Kämpfe *et al.*²⁷⁻²⁹ Interestingly, the latter comment that the acyl moiety in **D** does not undergo hydrosilylation; the acylpyrrolide hydrosilanes involved during preparation of **D** preferentially liberate H₂ upon reaction with the second substituent.

Aryliminopyrrolides (related to **B**, albeit with a non-coordinating aryl function) have found broad usage as bidentate, monoanionic ligands for transition metals and f-block elements.³⁰ However, the use of these groups in main group chemistry is less developed. The most widely studied main-group aryliminopyrrolide complexes are based on aluminum.³¹⁻³⁵ In particular, these Al-complexes find usage as catalysts in lactide ring opening polymerization (ROP)³⁶⁻³⁸ and guanylation.³⁹ Anderson *et al.* have prepared a range of aryliminopyrrolide phosphines as P,N-chelating ligands on Rh, Pd, and Ni complexes for olefin oligomerization⁴⁰ and Vránová *et al.* synthesized aryliminopyrrolyl antimony chloride.^{40b} In addition, 2-[*N*-(2,6-diisopropylphenyl)iminomethyl]-5-*tert*-butylpyrrolide has recently been shown to afford a series of stable Ge(II) compounds by Yang *et al.*³⁵

Chart 2.1 Pyrrolyl silanes in literature.^{24–29}

The aimed development of new silicon(II) ligands for transition-metal chemistry was a lead to study the silicon chemistry of the aryliminopyrrolide substituent 2-[N-(2,6-diisopropylphenyl)iminomethyl]pyrrolide (^{Dipp}IMP, Scheme 2.1). Here, the reactions of ^{Dipp}IMPH with hydrosilanes are reported. In some cases, the tethered imine functionality in the ^{Dipp}IMP substituent is found to undergo intramolecular 1,2-hydrosilylation. In related iminohydrosilanes a hydrosilylation reaction of the tethered imine functionality was also observed.^{41–43} In addition, 1,4-hydrosilylation has been observed in a phenanthroline hydrosilane by Fester *et al.*⁴⁴ To contribute to a better understanding and control of this generally undesired reaction, the factors controlling the hydrosilylation process are investigated. In particular, this reaction was found to be catalyzed by the chloride anion and can be sterically inhibited.

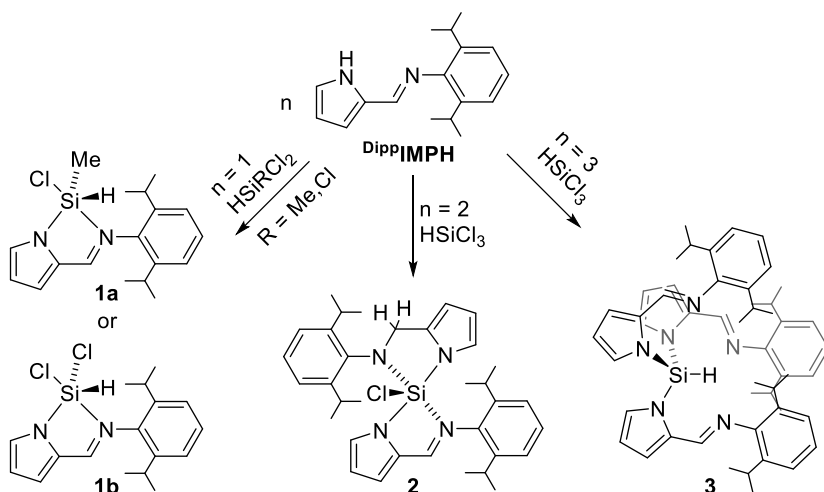
Results and Discussion

Synthesis of monosubstituted aryliminopyrrolide silanes

The iminopyrrole ^{Dipp}IMPH was conveniently obtained in one step from 2-formylpyrrole and 2,6-diisopropylaniline according to the procedure of Li, Li, and Li.⁴⁵ In a first experiment, analogous to the reported procedure for tri-pyrrolylsilane,¹ ^{Dipp}IMPH was treated with dichloromethylsilane (1 equiv) at $-78\text{ }^{\circ}\text{C}$ in the presence of triethylamine (NEt_3) to yield the monosubstituted compound **1a** (Scheme 2.1). A single ^{29}Si NMR signal at -64.9 ppm indicates a pentacoordinate geometry around silicon resulting from the coordination of the imine moiety. The Si–H bond in **1a** is intact, as evidenced by a ^1H NMR signal at 6.16 ppm with ^{29}Si satellites ($^1J(\text{Si},\text{H}) = 312\text{ Hz}$), the doublet of quartets splitting pattern of the ^{29}Si resonance ($^1J(\text{Si},\text{H}) = 312\text{ Hz}$, $^2J(\text{Si},\text{H}) = 8.5\text{ Hz}$), and an IR absorption at 2211 cm^{-1} . In addition, the HH-COSY spectrum of **1a** displays a diagnostic cross peak between the Si–H (6.16 ppm) and Si–CH₃ (0.64 ppm) resonances with a coupling constant of ca. 1.7 Hz , confirming the existence of the H–Si–Me fragment. The ^1H NMR signals corresponding to the isopropyl groups of **1a** appear broad at room temperature, which may be indicative of a fluxional process. Indeed, VT NMR measurements (Figure 2.2) show that the two

isopropyl groups are inequivalent at low temperature ($< -20\text{ }^{\circ}\text{C}$) but rapidly exchange at high temperature ($> 60\text{ }^{\circ}\text{C}$), with a coalescence temperature of $28\text{ }^{\circ}\text{C}$, corresponding to a free enthalpy of activation of $\Delta G^{\ddagger}_{301\text{ K}} = 14.1\text{ kcal/mol}$.⁴⁶ This fluxional process is assigned to the hindered rotation around the single $\text{C}_{\text{aryl}}\text{--N}_{\text{imine}}$ bond, presumably *via* reversible dissociation of the $\text{N}_{\text{imine}}\text{--Si}$ coordination bond. This interpretation is additionally supported by a relaxed potential energy surface (PES) scan of this rotation calculated at the B3LYP/6-31G(d,p) level of theory, from which an activation energy ($\Delta E_{\text{electronic}}$) of 12.8 kcal/mol can be estimated, in good agreement with the experimental ΔG^{\ddagger} value of 14.1 kcal/mol . The PES scan shows an increase in distance between the silicon and imine nitrogen from 2.33 \AA in the stable configuration to a maximum of 3.15 \AA for the highest energy configuration. Because of the extended conformational space associated with the “crossing” of two flexible, bulky substituents, the optimization of a single transition state was not attempted for this process.

The pentacoordinate structure inferred from the ^{29}Si NMR chemical shift was confirmed by an X-ray crystal structure determination (Figure 2.1). The structure exhibits a distorted trigonal bipyramidal (TBP) geometry ($\tau = 0.83$)⁴⁷ with the imine nitrogen atom and the chloride substituent found in apical positions. This geometry can be rationalized by the fact that the apical positions in a hypervalent TBP geometry are usually occupied by the most electron-withdrawing substituents (apicophilic) that engage in a three-center-four-electron (3c4e) bond with a pair of electrons delocalized over the substituents.⁴⁸



Scheme 2.1 Silylation of DippIMPH to form compounds **1a**, **1b**, **2**, and **3**.

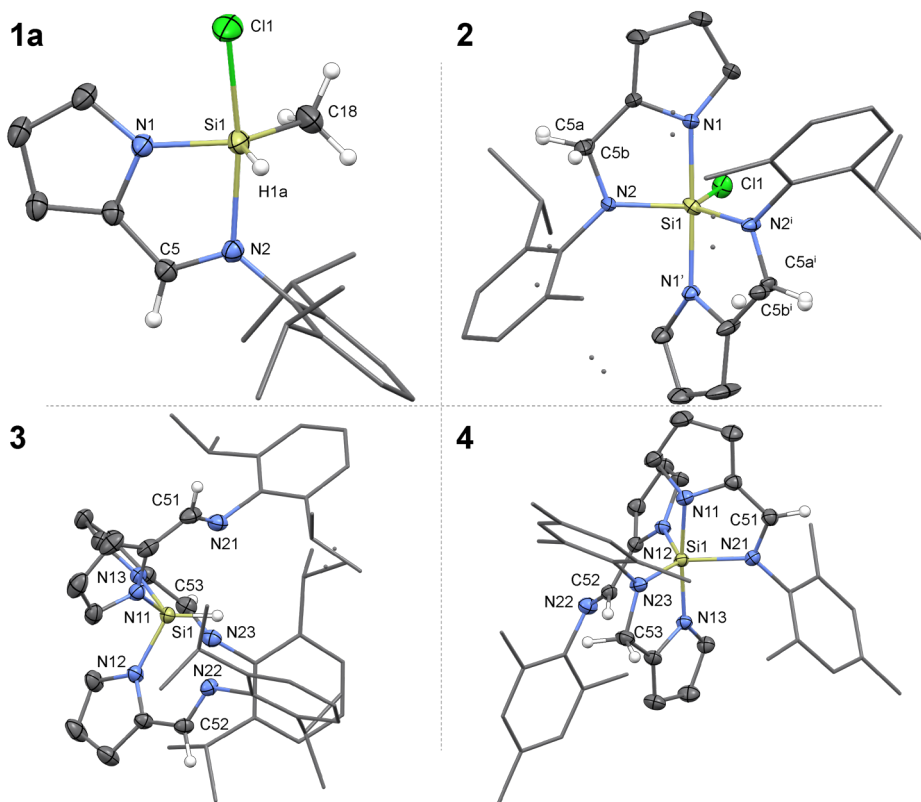


Figure 2.1 Molecular structure of **1a**, **2**, **3**, and **4** in the crystal. Displacement ellipsoids are drawn at the 50% probability level. Hydrogen atoms other than CH_3 , SiH , $\text{N}=\text{CH}$, and $\text{N}-\text{CH}_2$ are omitted and aryl group displayed as wireframe for clarity. In **2**, the disordered atoms $\text{C5a}/\text{C5b}$ were refined with 50% occupancy, respectively. Symmetry code i : $1-x, y, 0.5-z$. Selected bond distances (\AA) and angles ($^\circ$): compound **1a**: $\text{Si1}-\text{N1}$ 1.7884(9), $\text{Si1}-\text{N2}$ 2.0663(9), $\text{Si1}-\text{C18}$ 1.8568(14), $\text{Si1}-\text{Cl1}$ 2.2330(4), $\text{N1}-\text{Si1}-\text{N2}$ 81.10(4), $\text{N1}-\text{Si1}-\text{C18}$ 120.89(6), $\text{N1}-\text{Si1}-\text{Cl1}$ 92.02(3), $\text{N2}-\text{Si1}-\text{Cl1}$ 170.67(3). Compound **2**: $\text{Cl1}-\text{Si1}$ 2.0994(5), $\text{Si1}-\text{N1}$ 1.8589(7), $\text{Si1}-\text{N2}$ 1.7987(7), $\text{Cl1}-\text{Si1}-\text{N1}$ 92.20(3), $\text{Cl1}-\text{Si1}-\text{N2}$ 118.09(3), $\text{N1}-\text{Si1}-\text{N2}$ 85.09(3), $\text{N1}-\text{Si1}-\text{N1'}$ 175.60(5), $\text{N2}-\text{Si1}-\text{N2'}$ 123.81(6), $\text{N1}-\text{Si1}-\text{N2'}$ 92.83(3). Compound **3**: $\text{N11}-\text{Si1}$ 1.7760(11), $\text{N12}-\text{Si1}$ 1.7660(10), $\text{N13}-\text{Si1}$ 1.7738(11), $\text{N21}-\text{Si1}$ 2.868(1), $\text{N22}-\text{Si1}$ 2.783(1), $\text{N23}-\text{Si1}$ 2.822(1), $\text{N21}-\text{C51}$ 1.271(2), $\text{N22}-\text{C52}$ 1.272(2), $\text{N23}-\text{C53}$ 1.275(2), $\text{N11}-\text{Si1}-\text{N12}$ 101.47(5), $\text{N11}-\text{Si1}-\text{N13}$ 100.84(5), $\text{N12}-\text{Si1}-\text{N13}$ 101.99(5). Compound **4**: $\text{N21}-\text{C51}$ 1.3244(15), $\text{N22}-\text{C52}$ 1.2775(15), $\text{N23}-\text{C53}$ 1.4647(15), $\text{N12}-\text{Si1}-\text{N21}$ 110.59(4).

The analogous reaction of DippIMPH with HSiCl_3 and NEt_3 yielded a more complex mixture of products (*vide infra*) that contained the monosubstituted compound **1b** as a major component (Scheme 2.1), but this mixture was found to be difficult to separate. Using a different synthesis circumvented this problem: the iminopyrrole was first deprotonated with $n\text{BuLi}$, and the obtained salt DippIMPLi was treated with HSiCl_3 at -78°C to yield analytically pure **1b** after recrystallization from hexanes. The intact $\text{Si}-\text{H}$ bond in **1b** is evidenced by the corresponding IR absorption (2208 cm^{-1}), a doublet signal for $\text{Si}-\text{H}$ in ^1H NMR (6.57 ppm, $^4J(\text{H},\text{H}) = 1.8\text{ Hz}$) flanked by ^{29}Si satellites, and a doublet ^{29}Si NMR signal (-92.7 ppm , $^1J(\text{Si},\text{H}) = 385\text{ Hz}$). The doublet

signal in the ^1H NMR spectrum arises from a 4J -coupling between Si- H and N=C- H , as confirmed by HH-COSY. The ^{29}Si NMR chemical shift is consistent with a 5-coordinate geometry analogous to that of **1a**, which is to be expected due to the stronger Lewis acidity expected after formal replacement of a methyl group in **1a** by a more electron withdrawing chloro-substituent in **1b**.

Fluxional processes in compound **1b**

In contrast to what is observed for **1a**, the two isopropyl groups in **1b** are equivalent on the ^1H NMR timescale at room temperature and down to -80°C as evidenced by a single septet at 2.83 ppm (Figure 2.2). The methyl groups appear as two doublets that coalesce at 60°C , corresponding to a free enthalpy of activation of $\Delta G^\ddagger_{333\text{ K}} = 15.6\text{ kcal/mol}$ at this temperature. This process is assigned to rotation around the $\text{C}_{\text{aryl}}\text{-N}_{\text{imine}}$ bond, similar to **1a**, as this has an activation barrier of $\Delta G^\ddagger_{301\text{ K}} = 14.1\text{ kcal/mol}$ for **1a** and would be expected to have a similar activation barrier for **1b** on the basis of steric hindrance. At first sight, the two equivalent isopropyl groups (a single resonance for both C- H) might be seen as suggesting a C_s symmetrical geometry in which the Si- H bond would occupy an apical position, which however should be unfavorable on electronic grounds. An alternative explanation would be that the ground state geometry is unsymmetrical – in analogy with that of **1a** – and that the two isopropyl groups are exchanged by a rapid fluxional process.

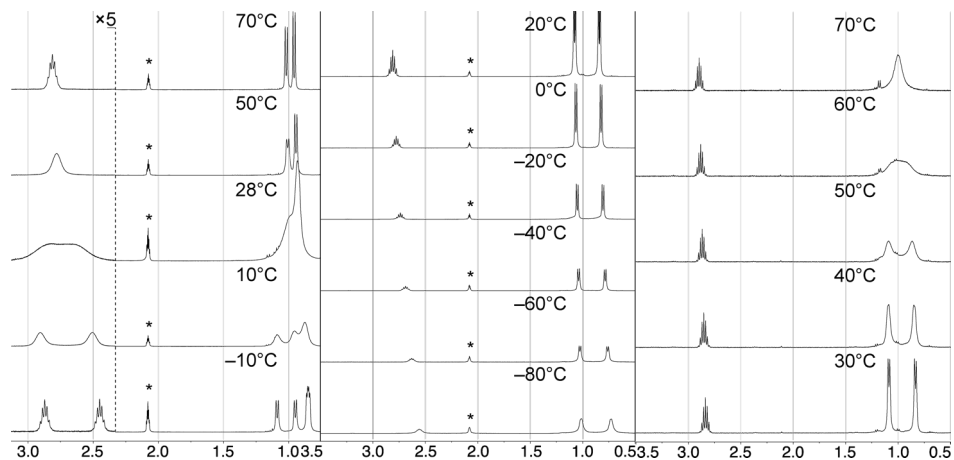


Figure 2.2 VT-NMR of **1a** in C_7D_8 (left, $-10^\circ\text{C} < T < 70^\circ\text{C}$), **1b** in C_7D_8 (centre, $-80^\circ\text{C} < T < 20^\circ\text{C}$) and **1b** in C_6D_6 (right, $30^\circ\text{C} < T < 70^\circ\text{C}$). * denotes residual $\text{C}_7\text{D}_7\text{H}$ signal.

Having identified the rotation around the $\text{C}_{\text{aryl}}\text{-N}_{\text{imine}}$ bond to occur only above 60°C on NMR timescale a different process must be in play. This process can be envisioned to be a facile Berry pseudorotation-type mechanism⁴⁹ around the 5-coordinate silicon atom. Reported activation energies for conformer interconversion in both pentacoordinate silanes and silicates vary from 8 to 15 kcal/mol.^{50–53} In

structurally similar dibromo phenyl κ^2 -2-[[dimethylamino)methyl]phenyl tin studied by van Koten *et al.* also a low energy barrier for conformer interconversion has been observed [coalescence temperature ~ -90 °C].⁵⁴ Comparable with observations made in this study the energy barrier is significantly higher in the bromo methyl phenyl analog [coalescence temperature > 123 °C].⁵⁵

More light on fluxional processes in **1b** was shed by DFT calculations (Figure 2.3). The lowest energy structure was found to be the TBP structure **I**¹ with the imine nitrogen atom and a chloride substituent in the axial positions, analogous to the crystal structure of **1a**. Two low-energy pathways were identified that would exchange the two isopropyl groups, *i.e.* swap the two faces of the iminopyrrole plane and epimerize the Si center. The first one proceeds through a single transition state (**TS**¹) in which rotation around the N_{pyrrole}–Si bond is coupled to decooordination of the imine moiety (Si–N_{imine}: 3.23 Å) and which is associated with a free enthalpy of activation of $\Delta G^\ddagger_{298\text{ K}} = 4.9$ kcal/mol. The second exchange pathway, with an overall barrier of $\Delta G^\ddagger_{298\text{ K}} = 9.1$ kcal/mol, starts with a Berry pseudorotation^{56,57} with the hydrogen atom as the pivot to form the TBP intermediate **I**², followed by a second Berry-like step bringing the Si–H bond in axial position in the symmetrical intermediate **I**³, which lies 3.5 kcal/mol above the ground state structure **I**¹. The Si–N_{imine} bond in **I**³ is considerably elongated (2.96 Å), which is likely due to the low apicophilicity of hydrogen, this structure can be best described as tetrahedral with only a weak Si–N_{imine} interaction.

The predicted existence of multiple low-energy pathways for the epimerization of the Si center is consistent with the observation of a single C–H resonance for the isopropyl groups. The two methyl groups on a single isopropyl residue are diastereotopic and are not exchanged by the epimerization of the Si center only, but by an additional rotation around the C_{aryl}–N_{imine} bond. The activation energy for this process was estimated by a relaxed PES scan, which yielded an activation energy ($\Delta E_{\text{electronic}}$) of 15.3 kcal/mol, in good agreement with the measured free enthalpy of activation $\Delta G^\ddagger_{333\text{ K}} = 15.6$ kcal/mol for the exchange of the methyl groups. Like for **1a**, because of the extended conformational space associated with the “crossing” of two flexible, bulky substituents, the optimization of a single transition state was not attempted for this process.

The two Si-epimerization pathways in **1b** can be loosely described as an overall 360° rotation around the N_{pyrrole}–Si bond with decooordination of the N_{imine} in the symmetrical intermediate **I**³ and transition state **TS**¹ (Figure 2.3). Hence, they would not epimerize a Si center with five different substituents, as the chiral information would not be lost in the tetrahedral structures **TS**¹ and **I**³. This explains why two distinct isopropyl moieties are observed in the ¹H NMR spectrum of the Me-substituted analogue **1a** up to the temperature where C_{aryl}–N_{imine} bond rotation becomes fast on the ¹H NMR timescale.

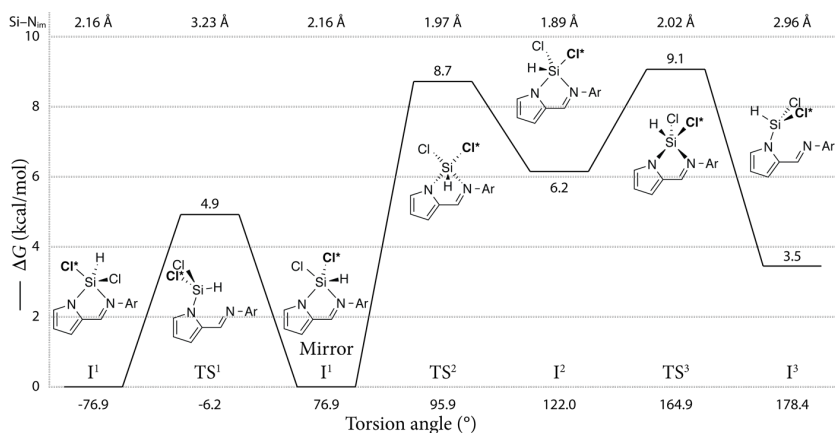


Figure 2.3 Calculated mechanism of epimerization at silicon in **1b**. Method used: B3LYP/6-31G(d,p). Torsion angle pyrC2-N-Si-H is given on the horizontal axis, the Si-N_{im} distance is given on top, ΔG calculated at 298.15 K.

Compounds **1a** and **1b** are new members of the family of pentacoordinate silanes with bidentate N,N substituents. Only two other compounds in this family bear bidentate monoanionic N,N substituents that form a 5-membered ring with silicon, viz. the trimethyl- and trichloro aminotroponimine silanes by Dias *et al.*⁵⁸ In contrast to those, silanes **1a** and **1b** bear both a hydrogen and chloride substituent, which are known to be easily abstracted with an alkali metal non-coordinating base to yield silylenes in other monoanionic, N,N bidentate chloro hydrosilanes, e.g. chloro bis amidinato hydro silane.⁵⁹

Higher degree of substitution

With the synthesis and characterization of the monosubstituted compounds **1a,b** at hand, we sought to increase the number of iminopyrrolide substituents on silicon. The reaction of 2 equiv ^{Dipp}IMPH with HSiCl₃ and NEt₃ at -78 °C yielded compound **2**, whose crude formula corresponds to the substitution of two chlorides by iminopyrrolide substituents (Scheme 2.1). It was isolated in analytically pure form by recrystallization from acetonitrile at -35 °C. The ¹H NMR spectrum of **2** shows a total of 8 separate doublets and 4 septets for respectively the isopropyl CH₃ and CH protons, indicating disubstitution, bidentate coordination of both substituents, and a low symmetry structure. Surprisingly, no signal corresponding to a silicon-bound H-atom was found, and H coupled ²⁹Si NMR displays a singlet at -116.2 ppm, indicating pentacoordination around silicon and the absence of a Si-H moiety. Instead, two mutually coupled doublets appear at δ = 4.49 and 4.32 ppm, respectively, of which the coupling constant of ²J(H,H) = 13.9 Hz is typical for geminal coupling between diastereotopic methylene protons. Hence, an intramolecular hydrosilylation (1,3-hydride shift) has taken place to form the amino-substituted compound **2** (Scheme 2.1). In line with this interpretation, the signal from the remaining imine methine

proton ($\delta = 7.39$ ppm) accounts for only one proton. The structure of **2** was confirmed by an X-ray crystal structure determination (Figure 2.1), showing again a distorted TBP structure ($\tau = 0.86$)⁴⁷ in which the apical positions are occupied by the pyrrole moieties. This contrasts with the geometry observed for the monosubstituted compounds **1a,b**, which can be explained by the steric influence of the dipp moieties, which minimize their repulsion with each other and with the pyrrole groups in this geometry. The electron withdrawing nature of the pyrrole groups¹ likely allows them to engage in a 3c4e bond.^{25,26,60} In the crystal structure the molecule is located on an exact, crystallographic twofold rotation axis. Consequently, the imine CH group and the aminomethylene CH₂ group resulting from hydrosilylation are equivalent by symmetry. A disorder model in a 1:1 ratio was used to resolve this issue.

Trisubstitution at silicon was achieved by reacting 3 equiv of DippIMPH with HSiCl₃ in the presence of triethylamine to yield silane **3**. The presence of a Si–H bond is evidenced by an IR absorption at 2355 cm⁻¹ and by a doublet in ²⁹Si NMR at $\delta = -60.5$ ppm [¹J(Si,H) = 417 Hz]. The position of this chemical shift indicates tetracoordination around silicon; hence, all substituents are bound in a monodentate fashion. In the ¹H NMR spectrum, the Si–H resonance ($\delta = 7.63$ ppm) has been identified from its ²⁹Si satellites [¹J(Si,H) = 417 Hz] and integrates to 1/3 with respect to the N=CH and pyrrole–H signals, confirming trisubstitution. Additionally, the limited number of signals indicates that this structure is highly symmetric. For instance, only one signal arising from the N=CH is observed, and the combined pyrrole protons give rise to 3 signals, i.e. all substituents are equivalent in solution. This can be explained by a C₃ rotation axis through the Si–H bond. Interestingly, broad signals were observed for the *i*Pr CH and for half of the *i*Pr–CH₃ groups. VT NMR measurements show that the two isopropyl groups are inequivalent at low temperature (< -60 °C) but rapidly exchange at high temperature (> 80 °C), indicating hindered rotation around the C_{aryl}–N_{imine} bond at moderate temperatures. This hindering is tentatively ascribed to steric effects between the bulky aromatic groups of the different substituents.

This hypothesis is substantiated by the solid-state structure in which the steric congestion between the aryl groups is clearly visible (Figure 2.1). The structure contains an approximate, non-crystallographic three-fold rotation axis through the Si–H bond. It is of interest to compare **3** and tri-pyrrolyl silane (Pyr₃SiH), which is the only other structurally characterized pyrrolyl-substituted hydrosilane. The N–Si–N angles in **3** (100.84[5]°, 101.47[5]°, and 101.99[5]°) are considerably smaller than those in Pyr₃SiH (106.8[2]°, 107.3[2]°, and 112.8[2]°) and the N–Si bonds in **3** are slightly longer (1.7660(10) Å, 1.7738(11) Å, and 1.7760(11) Å vs 1.711(4) Å, 1.735(4) Å, 1.740(4) Å), which can be explained by the steric repulsion between the aryl groups being mechanically transmitted through the rigid iminopyrrolide plane. This difference in geometry appears to strongly impact the properties of the Si–H bond: the corresponding infrared absorption shifts by ca. 120 cm⁻¹, from 2233 cm⁻¹ in

Pyr₃SiH to 2355 cm⁻¹ in **3**, and the ¹H coupling constant ¹J(Si,H) increases from 285 Hz in Pyr₃SiH to 417 Hz in **3**. These differences can be attributed to an increased *s*-character of the bonding σ (Si–H) orbital in **3** originating from the more acute N–Si–N angles that increases the *p*-character of the hybrid orbitals involved in Si–N bonding. In agreement with this interpretation, the geometry around silicon in **3** resembles more that of the silyl ligand derived from Pyr₃SiH in the osmium complex Os(SiPyr₃)(H)(CO)₂(PPh₃)₂, which displays N–Si–N angles of 99.5(3)°, 100.3(3)°, and 101.1(3)° and N–Si bond lengths of 1.770(7) Å, 1.787(7) Å, and 1.788(7) Å (Table 2.1).

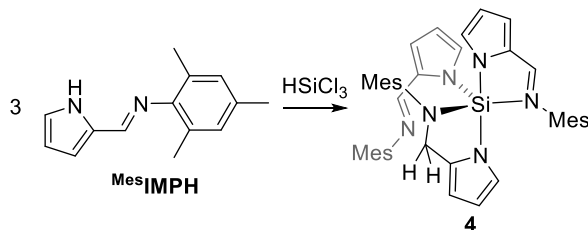
Table 2.1 Bond distances and angles in the crystal structures of **3**, Pyr₃SiH and a Pyr₃Si[−] osmium complex.

	3	Pyr ₃ SiH ¹	(PPh ₃) ₂ (CO) ₂ Os(H)Si(Pyr) ₃ ¹
Si–N (Å)	1.7660(10)	1.711(4)	1.770(7)
	1.7738(11)	1.735(4)	1.787(7)
	1.7760(11)	1.740(4)	1.788(7)
N–Si–N (°)	100.84(5)	106.8(2)	99.5(3)
	101.47(5)	107.3(2)	100.3(3)
	101.99(5)	112.8(2)	101.1(3)

The small N–Si–N angles suggest higher *s*-character, with concomitant higher acidity of H, in the Si–H bond, obeying Bent's rule. This interpretation was confirmed *in silico* by DFT calculations at the B3LYP/6-31G(d,p) level of theory. The calculated average angles of 103° and 109° for **3** and Pyr₃SiH, respectively, reproduce the experimental trend accurately. At the same time, the Si–H bond length decreases from 1.472 Å in Pyr₃SiH to 1.443 Å in **3**. Natural Bonding Orbital analysis⁶¹ of these compounds shows an increase in *p*-character for the Si-centered Natural Hybrid Orbital (NHO) involved in Si–N bonding from sp^{3.31} in Pyr₃SiH to sp^{3.76} in **3**. In line with this, the *p*-character in the Si hybrid orbital involved in Si–H bonding decreases (sp^{2.11} in Pyr₃SiH; sp^{1.59} in **3**). Consequently, the hydrogen acquires more H⁺ character in **3**, as shown by the natural charges on hydrogen (NC): −0.204 in Pyr₃SiH and −0.154 in **3**. This accumulation of positive charge on the hydrogen might facilitate subsequent deprotonation.

The trisubstituted hydrosilane **3** is thermally stable, and no sign of hydrosilylation was observed even after heating a sample at 100 °C for 70.5 h. This is likely due to steric congestion preventing imine coordination (N–Si distances of ca. 2.82 Å in the solid state) and access to the Si–H bond. To test this hypothesis, analogous chemistry with the iminopyrrole compound ^{Mes}IMPH was investigated, in which the diisopropylphenyl is replaced by the less sterically demanding mesityl group. Exposing three equiv of ^{Mes}IMPH to HSiCl₃ in the presence of NEt₃ resulted in the formation of the trisubstituted silane **4**, in which one of the imine functionalities has been hydrosilylated (Scheme 2.2). The X-ray crystal structure of **4** (Figure 2.1) reveals a pentacoordinated compound with a distorted TBP geometry ($\tau = 0.79$)⁴⁷, in which one of the imine moieties is not coordinated to the Si center. The apical positions are occupied by two pyrrole substituents, as was also observed for compound **2**. The

structure of compound **4**, however, does not suffer from the same disorder as that of **2** and the hydrosilylation site is clearly identified by a C–N bond length of 1.4647(15) Å, typical for a single bond,⁶² and the presence of a CH₂ and two CH groups, with all the hydrogens located in difference Fourier maps. The coordinated C=N bond (1.3244(15) Å) is slightly longer than the non-coordinated one (1.2775(15) Å), indicating a somewhat weaker bond.



Scheme 2.2 Silylation reaction of MesIMPH to compound **4**.

In ¹H NMR on crystalline material of **4**, 9 different pyrrole-*H* resonances were observed, indicating three different substituents around silicon. In addition, a double doublet signal, which accounts for 2 H's, was observed at a chemical shift of 3.96 ppm. As seen in compound **2** this double doublet signal is characteristic for a hydrosilylated imine (CH₂–N) with diastereotopic hydrogens. Moreover, a singlet resonance was observed in proton coupled ²⁹Si NMR at δ = –120.4 ppm. In ¹³C NMR two resonances for imine carbons were observed at δ = 156.0 and 160.4 ppm and one resonance for CH₂ at δ = 48.0 ppm. From the HMQC spectrum, the resonances for the two imine CH's in ¹H NMR could be deduced; δ = 6.55 and 6.67 ppm. Interestingly, in ¹H NMR all resonances for the pyrrole and methyl hydrogens appear slightly broad due to fluxional processes on the NMR timescale. In a low temperature measurement at –25 °C the resonances appear sharp, whereas at 70 °C the signals coalesce into fewer, broad signals. Most notably the CH₂ resonance broadens, hence the two hydrogens are no longer diastereotopic. This means that the process makes the two non-hydrosilylated substituents equivalent and is therefore likely to consist of reversible detachment of the bound imine.

From ¹H NMR it was obvious that a second, minor species was present; 0.16 ppm downfield of the major CH₂ signal a second double doublet signal appeared with an intensity of 32% relative to the major CH₂ signal at 25 °C. This minor species is in equilibrium with **4** in solution as substantiated by EXSY NMR at –10 °C, which shows cross peaks for protons that mutually exchange (see Appendix Figure 1). For **4** and the minor species it shows exchange between the CH₂ signals at δ = 3.96 (**4**, major) and 4.23 (minor) ppm and between the imine signals mutually. Following from the proposed reversible detachment of the non-hydrosilylated substituents, for the minor compound an imine-detached tetrahedral structure was proposed, which has not been identified due to the low equilibrium concentration.

Compound **4** shows the propensity of $(^{\text{Ar}}\text{IMP})_3\text{SiH}$ to undergo the intramolecular hydrosilylation process, which was previously observed in silane **2**, but not in silane **3**. In that respect, the occurrence of hydrosilylation in compound **4** shows that indeed not electronics, but steric interactions inhibit this process in the more bulky compound **3**. Compound **4** is an unusual all-N pentacoordinate silane, preceded only by azasilatranes, which consist of a tetradentate, tri-anionic substituent and a second monodentate N-substituent (NCS^- or N_3^-) bound to silicon.⁶³

Hydrosilylation reaction in monosubstituted silanes and identification of a hexacoordinate intermediate species

Intramolecular hydrosilylation processes related to those described above have been reported recently by Lippe *et al.*⁴¹ and Novák *et al.*⁴² In view of the growing interest in N-bound silanes as precursors for silicon(II) compounds, it is of interest to understand the factors controlling this – generally undesired – reactivity. Hence, this process was further investigated. First, a 95 mM solution of the monosubstituted compound **1a** with mesitylene as an internal standard was heated to 70 °C in a closed J-Young NMR-tube and the hydrosilylation reaction was monitored by ^1H NMR. Over a period of 260 h very slow conversion was found to a hydrosilylated species (~5%), this species showed two strongly mutually coupled doublets at $\delta = 4.17$ ppm and 4.38 ppm for the methylene protons, but could not be identified otherwise. Concomitantly, the low boiling HSiCl_2Me was formed, as evidenced by a characteristic quartet for Si-H at $\delta = 5.21$ ppm and doublet for Si- CH_3 at $\delta = 0.18$ ppm ($^3J(\text{H},\text{H}) = 2.3$ Hz). Because of the low conversion over a long time for **1a**, compound **1b** was subjected to the same conditions; the hydrosilylation reaction in an 80 mM C_6D_6 solution of **1b** was monitored by ^1H NMR. Over a period of 60 h, the concentration of **1b** decreased to ca. 20 mM with concomitant appearance of three new species (Scheme 2.3). The two minor products were straightforwardly assigned: the imino/amino compound **2** (ca. 12 mM) was identified by comparison with an isolated sample and HSiCl_3 (ca. 6 mM) by a signal at 5.53 ppm in ^1H NMR with ^{29}Si satellites ($^1J(\text{Si},\text{H}) = 372$ Hz). The lower concentration of the latter can be ascribed to loss to the headspace ($T_b = 32$ °C). The major product (40 mM) is assigned as the aminopyrrolide compound **5** (Scheme 2.3), formed by intramolecular hydrosilylation from **1b**, on the basis of NMR data. In particular, a diagnostic ^1H NMR resonance at $\delta = 4.20$ ppm shows the presence of the N- CH_2 moiety, and a singlet ^{29}Si NMR resonance at $\delta = -36.5$ ppm indicates a tetracoordinate environment around silicon and the absence of an Si-H bond. In agreement with this assignment, DFT calculations predict a chemical shift of $\delta = -31.2$ ppm for **5**.

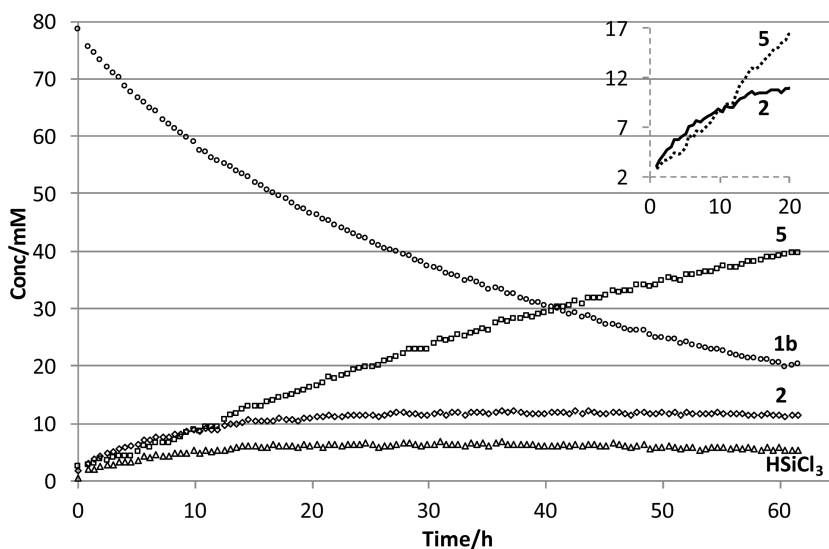
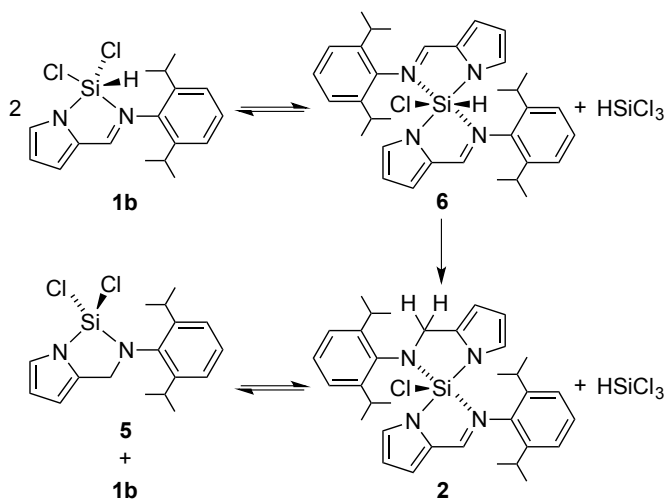


Figure 2.4 Reaction composition of the hydrosilylation of **1b** determined through internal standard (mesitylene) at 70 °C; average integral of the isolated resonances relative to IS. Inset shows a zoom of the early stages of the reaction ($t = 0\text{--}20$ h).



Scheme 2.3 Proposed pathway for the hydrosilylation in **1b**.

This reaction was monitored by ^1H NMR and the evolution of the concentration for different compounds is plotted in Figure 2.4. The concentration of **1b** decreases throughout the reaction while that of **5** increases steadily. In contrast, the concentrations of both **2** and HSiCl_3 increase more rapidly than **5** at early stages (inset in Figure 2.4) but reach a plateau after ca. 20 h, suggesting that these may be intermediates in the overall process. To account for this reaction profile, the reaction pathway shown in Scheme 2.3 was proposed. First, a substituent redistribution

process disproportionates two equiv of compound **1b** into both HSiCl_3 and the disubstituted compound **6**, which then undergoes an intramolecular hydrosilylation reaction to form compound **2**. A subsequent substituent redistribution process then finally releases one equiv of the product **5** and one equiv of **1b** from **2** and HSiCl_3 . On basis of the data, alternative intermolecular attack of the Si–H on another molecules C=N bond cannot be fully excluded.

The individual steps in this proposed reaction scheme were investigated in a series of stoichiometric experiments. First, the feasibility of the product-releasing step was demonstrated by addition of a substoichiometric amount of HSiCl_3 to a solution of **2**; after 2.5 h at 70 °C this yielded both **1b** and **5**, along with remaining **2** in a 21%:36%:43% ratio (**1b**:**5**:**2**), in which [**5**] increased over time to reach a ratio of 2%:66%:32% after 20.5 h at 70 °C. Then, we sought to observe the postulated disubstituted hydrosilane **6**, which was not detected under the reaction conditions. This was achieved by reacting **1b** with a slight excess of DippIMPLi in a mixture of $[\text{D}_8]\text{toluene}$ and $[\text{D}_8]\text{THF}$ at room temperature, affording a solution containing a mixture of **6** and the trisubstituted **3** after filtration. These conditions were chosen so that the main byproduct in solution is the highly symmetrical **3**, limiting peak overlap. The ^{29}Si NMR spectrum of **6** at –60 °C exhibits a doublet at $\delta = -168.4$ ppm ($^1J(\text{Si},\text{H}) = 287$ Hz), indicating a hexacoordinate structure containing a Si–H bond. The ^1H NMR spectrum of **6** is very broad at room temperature, indicating the presence of fluxional processes that may involve reversible detachment of an imine moiety, but a sharp spectrum can be obtained at –60 °C (see Appendix Figure 2). It shows that the compound has low symmetry, as evidenced by four individual signals for the inequivalent *iPr* CH groups, two signals for imine moieties, and one for the Si–H bond ($\delta = 5.83$ ppm), identified by flanking ^{29}Si satellites and a correlation with the silicon resonance in Si,H HSQC. Compound **6** partially converts into compound **2** when the mixture is heated to 70 °C over a period of 16 h. However, if the reaction is conducted with an excess of silane instead of DippIMPLi , the hydrosilylation process is faster. Compound **6** could also be synthesized by adding HSiCl_3 to two equiv of DippIMPLi at –78 °C in THF, but it could not be isolated from the mixtures containing **1b** and **3**.

The low symmetry found in low temperature ^1H NMR was a lead to investigate the conformation of **6** by density functional theory calculations including NMR shifts, *J*-coupling values, and free energy calculations. These were conducted on three relevant low symmetry structures as well as one higher symmetry structure; 1) *cis-all* (Chart 2.2, left) featuring the pyrroles, imines, and H and Cl mutually *cis* to each other. 2) *trans-im* (Chart 2.2, middle-left) having mutual *cis* pyrrole, and mutual *trans* imine groups, 3) *trans-pyr* (Chart 2.2, middle-right) having mutual *cis* for imine, and mutual *trans* for pyrrole, and 4) the C_2 symmetric *trans-all* (Chart 2.2, right). These calculations, summarized in Table 2.2, show that only *trans-pyr* is consistent with the experimental NMR data: only half of the number of signals for the substituents can be expected in *trans-all*, the $^1J(\text{Si},\text{H})$ coupling calculated for

trans-im deviates significantly from the one observed and the *cis-all* conformer cannot be optimized as a hexacoordinate structure. Additionally, a hexacoordinate structure can be imagined with the H and Cl substituent trans with respect to each other and the imine and pyrrole groups mutually cis. This structure cannot be optimized because both dipp groups point towards each other in such a structure and experience too much steric repulsion. The calculated energy differences between the three optimized hexacoordinated conformers are $\Delta\Delta G_{213\text{ K}} = 1.8$ kcal/mol for *trans-im* and $\Delta\Delta G_{213\text{ K}} = 3.6$ kcal/mol for *trans-pyr* compared to the lowest energy structure *trans-all*. The fact that the structure calculated to have the lowest energy (*trans-all*) is not the observed one (*trans-pyr*) is ascribed to the error in energy calculations.

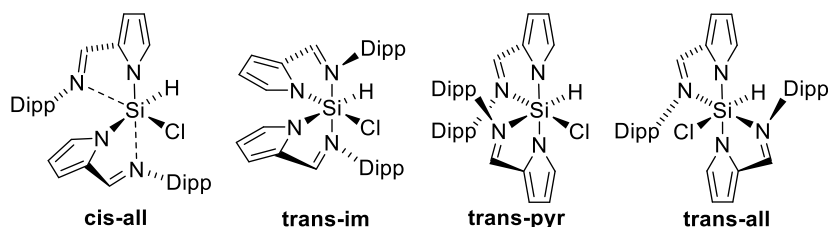


Chart 2.2 Calculated isomers of hexacoordinate **6**.

Table 2.2 Calculated versus observed ^{29}Si chemical shift and $^1J(\text{Si},\text{H})$ coupling for **6**.

	δ ppm vs TMS	Deviation ppm	$^1J(\text{Si},\text{H})$ Hz	Deviation Hz
Observed	-168	-	288 ^[a]	-
Cis-all	-52	116	-419	131
Trans-im	-169	-1	-361	72
Trans-pyr	-163	5	-307	19
Trans-all	-176	-8	-309	21

^[a] Absolute value observed for J -coupling.

The intramolecular hydrosilylation reaction of **1b** to **5**, taking place over more than 60 h at 70 °C, should in principle not have hampered the isolation of **1b**. Nevertheless, analysis of the reaction mixture obtained after the reaction of 1 equiv of $^{\text{Dipp}}\text{IMPH}$ with HSiCl_3 in the presence of NEt_3 at room temperature (*vide supra*) revealed the presence of both **2** and **5**, suggesting that this hydrosilylation process may be catalyzed by one of the components of the reaction mixture. In addition, monitoring in solution a sample of **1b** that had been obtained from the reaction of $^{\text{Dipp}}\text{IMPLi}$ with HSiCl_3 without thorough purification by crystallization (ca. 98% purity by ^1H NMR) revealed significantly faster hydrosilylation; conversion of 35% versus 3% in 73 h at room temperature and 80% versus 37% in 17 h at 70 °C. The lower reaction rate of the pure sample suggests the influence of a catalytically competent species in the crude product. Catalytic entities potentially present in the non-purified compound are trace amounts of chloride (NEt_3HCl , LiCl) or base (NEt_3 , $^{\text{Dipp}}\text{IMP}$). To

investigate the influence of the chloride anion, ca. 5 mol% tetrabutylammonium chloride (Bu_4NCl) was added to a C_6D_6 solution of isolated **1b**. This resulted in a drastic increase in reaction rate, viz. 23% conversion in 5.5 h at room temperature compared to no measurable conversion for a sample of purified **1b**. Conversely, addition of 1 equiv NEt_3 seems to inhibit the reaction so that only minute conversion is observed after 16 h at 70 °C. These results indicate that the chloride anion is an efficient catalyst for the described hydrosilylation process in **1b**. In contrast, Bu_4NCl did not induce hydrosilylation in silanes **1a** and **3** upon heating to 70 °C for 23 h.

The mode of action of the chloride anion was not investigated in detail. It is plausible that transient chloride coordination to silicon [e.g. substituting an imine substituent in intermediate **6**] increases the nucleophilicity of the Si–H bond, in line with the observation by Yamamura et al. that catalytic amounts of F^- facilitate the intramolecular hydrosilylation of an azobenzene derivative.⁶⁴ Alternatively, it seems likely that some of the required substituent exchange steps would be susceptible to nucleophilic catalysis.^{53,65,66}

Conclusions

During the attempts in this work to synthesize iminopyrrolyl hydrosilanes, hydrosilylation was found to occur in several cases. The pentacoordinated silane $[\text{Dipp}]\text{IMP}\text{SiHCl}_2$ [$\text{Dipp}]\text{IMP} = 2\text{-[N-(2,6-diisopropylphenyl)iminomethyl]pyrrolide}$] proved to undergo intramolecular hydrosilylation. This reaction is catalyzed by the chloride anion and involves hexa- (**6**) and pentacoordinated (**2**) disubstituted silanes formed by substituent redistribution as intermediates. In contrast, the pentacoordinated monosubstituted chloromethyl silane was much more reluctant to undergo this process. Hence, the hydrosilylation reaction can be influenced by tuning the electron density on silicon. This process can also be influenced by steric effects, which was shown with the tetracoordinated trisubstituted silane $[\text{Dipp}]\text{IMP}_3\text{SiH}$ **3** in which hydrosilylation is completely inhibited. Reducing the size of the aryl groups from 2,6-diisopropylphenyl to mesityl restored hydrosilylation reactivity and yielded the pentacoordinated trisubstituted all-N silane **4**, indicating that trisubstituted silanes are also susceptible to hydrosilylation.

The obtained knowledge of the conditions favoring and disfavoring the imine hydrosilylation reaction complements existing approaches in which the imine moiety is passivated by incorporation in a conjugated π -system, i.e. aromatic heterocycles⁶⁷⁻⁷² and amidinate/guanidinate compounds.^{59,73-76} This is anticipated to aid in the controlled synthesis of N substituted silicon compounds as precursors for silicon(II) ligands.

Experimental Section

All reactions involving silicon-containing compounds were conducted under an N₂ atmosphere using standard glovebox or Schlenk techniques. Diethyl ether, n-hexane, toluene, and acetonitrile were dried by an MBRAUN MB SPS-79 system, degassed by bubbling with N₂ for 30 min, and stored over molecular sieves in a glovebox. THF was distilled from benzophenone/Na, degassed by bubbling with N₂ for 30 min and stored over molecular sieves in a glovebox. All chemicals were obtained commercially and used as received unless stated otherwise. Dichloromethylsilane was purchased from Fluka; pyrrole-2-carboxaldehyde (99%), n-butyllithium (1.6 M in hexanes), and triethylamine (99%) were purchased from Acros; trichlorosilane (99%), 2,4,6-trimethylaniline (98%), tetrabutylammonium chloride (≥ 97%, anhydrous), and 2,6-diisopropylaniline (92%) were purchased from Sigma-Aldrich. Both silanes were transferred into and stored in a Teflon stoppered Schlenk upon arrival. Triethylamine was degassed by bubbling with N₂ for 30 min and stored over molecular sieves. All NMR chemical shifts are reported relative to TMS using the residual solvent signal as internal standard.⁷⁷ All NMR experiments involving silicon-containing compounds were conducted in J-Young NMR tubes under an N₂ atmosphere. For compound **5** Cr(acac)₃ was used as a paramagnetic relaxation agent for ²⁹Si NMR. Elemental analysis was conducted by the Mikroanalytisches Laboratorium Kolbe. The substituents ^{Dipp}IMPH,⁴⁵ ^{Dipp}IMPLi,⁷⁸ and ^{Mes}IMPH⁷⁹ were prepared according to literature procedures.

Computational methods

All DFT calculations were performed using Gaussian09.⁸⁰ Geometry optimizations were performed using the B3LYP functional with 6-31G(d,p) as the basis set on all atoms. A frequency calculation was performed on all converged geometries to verify that they were minima. For transition state calculation one imaginary frequency was obtained. NMR calculations at the B3LYP/IGLO-III level were performed after a single point calculation at the B3LYP/6-31G(d,p) level, for coupling constants using the “spinspin” option. For NBO calculations, the NBO6 program up to the NLMO basis set was used.⁶¹

X-ray crystal structure determinations

X-ray reflections were measured on a Bruker Kappa ApexII diffractometer with sealed tube and Triumph monochromator ($\lambda = 0.71073$ Å). The intensities were integrated with the Eval15 software.⁸¹ Multiscan absorption correction and scaling was performed with SADABS.⁸² The structures were solved by Patterson superposition methods using SHELXT.⁸³ Least-squares refinement was performed with SHELXL-2013 or SHELXL-2014⁸⁴ against F² of all reflections. Non-hydrogen atoms were refined freely with anisotropic displacement parameters. Hydrogen atoms were located in difference Fourier maps (compounds **1a** and **4**) or introduced in calculated positions (compounds **2** and **3**). Geometry calculations and checking for higher symmetry was performed with the PLATON program.⁸⁵ CCDC 1436231-1436234 contain the supplementary crystallographic data for this paper. These data can be obtained free of charge from The Cambridge Crystallographic Data Centre via www.ccdc.cam.ac.uk/data_request/cif.

Silane synthesis

Chloromethyl(^{Dipp}IMP)silane (1a). ^{Dipp}IMPH (1.83 g, 7.19 mmol) and NEt₃ (1.5 mL, 10.76 mmol) were dissolved in THF (25 mL) and cooled to -78 °C. HSiMeCl₂ (0.9 mL, 8.78 mmol) was added rapidly. The mixture was stirred for one hour at -78 °C, during which the clear solution became turbid. Subsequently, the mixture was stirred 16 h at room temperature. n-Hexane (75 mL) was added, the solids were filtered off and extracted with n-hexane (2 x 10 mL). The filtrate was combined with the n-hexane extracts and freed of solvent *in vacuo* to yield **1a** as an off-white powder pure enough for further use (2.2 g, 6.6 mmol, 92%). Crystals suitable for X-ray analysis were grown by vapor diffusion of n-hexane into a diethylether solution of **1a**. ¹H NMR (400 MHz, C₆D₆, 25 °C): δ = 8.19 (ddd, ⁴J(H,H) = 0.9 Hz, ⁴J(H,H) = 1.3 Hz, ³J(H,H) = 2.6 Hz, 1H, pyrrole-H3), 7.46 (t, ⁴J(H,H) = 0.9 Hz, ⁴J(H,H) = 0.9 Hz, 1H, N=C-H), 7.07, 7.00 (AB₂ pattern, J_{AB} = 7.9 Hz, 3H, Ar-H), 6.56 (dd, ⁴J(H,H) = 1.3 Hz,

$^3J(\text{H,H}) = 3.6$ Hz, 1H, pyrrole-*H5*), 6.30 (dd, 1H, $^3J(\text{H,H}) = 2.6$ Hz, $^3J(\text{H,H}) = 3.6$ Hz, pyrrole-*H4*), 6.16 (br s, 1H, $^1J(\text{Si,H}) = 312$ Hz, Si-*H*), 2.92 (br, 1H, *iPr CH*), 2.56 (br, 1H, *iPr CH*), 0.99 (br, 12H, *iPr-CH₃*), 0.64 ppm (d, 3H, $^3J(\text{H,H}) = 1.7$ Hz, $^2J(\text{Si,H}) = 8.5$ Hz, Si-*CH₃*); ^{13}C NMR (100 MHz, C_6D_6 , 25 °C): $\delta = 154.8$, 140.6, 137.7, 134.2, 127.6, 124.4, 119.7, 115.2, 28.7 (br), 26.5 (br), 25.4 (br), 24.1 (br), 22.9 (br), 6.11 ppm (Si-*C*, $^1J(\text{Si,C}) = 84.6$ Hz); ^{29}Si NMR (79 MHz, C_6D_6 , 25 °C): $\delta = -64.9$ ppm (dq, $^1J(\text{Si,H}) = 313$ Hz, $^2J(\text{Si,H}) = 8$ Hz); IR (ATR): $\tilde{\nu} = 2211$ (Si-*H*), 1648 cm^{-1} (C=N); Elemental analysis calcd (%) for $\text{C}_{18}\text{H}_{25}\text{N}_2\text{SiCl}$: C 64.93, H 7.57, N 8.41; found: C 65.12, H 8.33, N 7.97; X-ray: $\text{C}_{18}\text{H}_{25}\text{ClN}_2\text{Si}$, Fw = 332.94, colorless block, $0.43 \times 0.41 \times 0.31$ mm³, monoclinic, $P2_1/n$ (no. 14), $a = 14.2957(6)$, $b = 9.4401(2)$, $c = 15.2753(3)$ Å, $\beta = 115.112(1)^\circ$, $V = 1866.59(9)$ Å³, $Z = 4$, $D_x = 1.185$ g/cm³, $\mu = 0.27$ mm⁻¹. 31830 Reflections were measured at a temperature of 150(2) K up to a resolution of $[\sin \theta/\lambda]_{\text{max}} = 0.65$ Å⁻¹. 4286 Reflections were unique ($R_{\text{int}} = 0.014$), of which 4026 were observed [$I > 2\sigma(I)$]. The Si-H hydrogen atom was refined freely with an isotropic displacement parameter. All other H-atoms were refined with a riding model. 208 Parameters were refined with no restraints. $R1/wR2$ [$I > 2\sigma(I)$]: 0.0304 / 0.0811. $R1/wR2$ [all refl.]: 0.0319 / 0.0821. $S = 1.036$. Residual electron density between -0.29 and 0.36 e/Å³.

Dichloro(^{Dipp}IMP)silane (1b). ^{Dipp}IMPLi (0.841 g, 1.97 mmol, 39 mass% Et₂O by ¹H NMR) was dissolved in THF (25 mL) and cooled to -78 °C. HSiCl₃ (0.300 mL, 2.97 mmol) was added rapidly. The mixture was stirred for 45 min and allowed to warm up to 0 °C, after which it was freed of solvent *in vacuo*. The solid residue was extracted in toluene (10 mL) and freed of solvent *in vacuo*. This operation was repeated with toluene (12 mL) yielding an orange powder in 97% yield, containing 15% of hydrosilylated products (**2** and **5**), which presumably formed during the evaporation of toluene. The solid was stored in a glovebox at -35 °C. Pure samples were freshly prepared by crystallization from a saturated n-hexane solution at -35 °C prior to following experiments to yield spectroscopically pure **1b** as cloudy crystals. ¹H NMR (400 MHz, C_6D_6 , 25 °C): $\delta = 8.06$ (ddd, $^4J(\text{H,H}) = 1.0$ Hz, $^3J(\text{H,H}) = 2.7$ Hz, $^4J(\text{H,H}) = 1.2$ Hz, 1H, pyrrole-*H3*), 7.30 (dd, $^4J(\text{H,H}) = 1.0$ Hz, $^4J(\text{H,H}) = 1.8$ Hz, 1H, N=C-*H*), 7.08, 6.99 [AB₂ pattern, $J_{\text{AB}} = 7.9$ Hz, 3H, Ar-*H*], 6.57 (d, $^4J(\text{H,H}) = 1.8$ Hz, $^1J(\text{Si,H}) = 385$ Hz, 1H, Si-*H*), 6.44 (dd, $^3J(\text{H,H}) = 3.6$ Hz, $^3J(\text{H,H}) = 1.2$ Hz, 1H, pyrrole-*H5*), 6.16 (dd, $^3J(\text{H,H}) = 2.7$ Hz, $^3J(\text{H,H}) = 3.6$ Hz, 1H, pyrrole-*H4*), 2.83 (sept, $^3J(\text{H,H}) = 6.8$ Hz, 2H, *iPr CH*), 1.09 (d, $^3J(\text{H,H}) = 6.8$ Hz, 6H, *iPr-CH₃*), 0.83 ppm (d, $^3J(\text{H,H}) = 6.9$ Hz, 3H, *iPr-CH₃*); ^{13}C NMR (100 MHz, C_6D_6 , 25 °C): $\delta = 154.9$, 143.6, 139.2, 137.7, 132.9, 128.6, 124.6, 121.3, 116.7, 29.1, 26.3, 23.4 ppm; ^{29}Si NMR (79 MHz, C_6D_6 , 25 °C): $\delta = -92.7$ ppm [$^1J(\text{Si,H}) = 385$ Hz]; IR (ATR): $\tilde{\nu} = 2209$ (Si-*H*), 1650 cm^{-1} (C=N); Elemental analysis calcd (%) for $\text{C}_{17}\text{H}_{22}\text{Cl}_2\text{N}_2\text{Si}$: C 57.78%, H 6.28%, N 7.93%; found: C 57.99%, H 5.91%, N 7.85%.

Alternative synthesis of dichloro(^{Dipp}IMP)silane (1b) without crystallization. ^{Dipp}IMPLi (528 mg, 1.24 mmol, 39 mass% Et₂O by ¹H NMR) was dissolved in THF (25 mL) and cooled to -78 °C. HSiCl₃ (0.300 mL, 2.97 mmol) was added swiftly. The mixture was stirred for 45 min and allowed to slowly warm up to -30 °C in a beaker containing the cold acetone from the dry-ice bath. The cooling was removed and the mixture was allowed to warm to 0 °C, after which it was freed of solvent *in vacuo*. The solid was extracted with C_6D_6 , the solution contained **1b** with only about 2% of hydrosilylated products (**2** and **5**). This sample was used without further purification to monitor hydrosilylation.

Chloro(^{Dipp}IMP (=L))(^{Dipp}AMP (=L')) silane (2). To a solution of NEt₃ (1.0 mL, 7.18 mmol) and ^{Dipp}IMPH (1.2744 g, 5.05 mmol) in THF (50 mL) at -78 °C HSiCl₃ (0.28 mL, 2.8 mmol) was added. This was stirred at -78 °C for 45 min, yielding a cloudy, white mixture, which was stirred for 16 h at room temperature. The resulting yellow suspension was filtered and the solvent was evaporated *in vacuo* to yield a yellow foam. The solid residue (1.60 g) was extracted with acetonitrile (10 x 7.5 mL), which dissolved 1.01 g. The combined extracts (75 mL) were stored at -35 °C. After 3 days, orange needle-shaped crystals of **2** (0.473 g, 0.828 mmol, 33%) had formed, which were suitable for XRD crystallography. ¹H NMR (400 MHz, C_6D_6 , 25 °C): $\delta = 7.37$ (dd, $^4J(\text{H,H}) = 1.2$ Hz, $^5J(\text{H,H}) = 0.5$ Hz, 1H, N=C-*H*), 7.15-6.85 (m, 6H, Ar-*H*), 6.39 (t, $^3J(\text{H,H}) = 4.0$ Hz, $^4J(\text{H,H}) = 0.9$ Hz, 1H, L'-pyrrole-*H5*), 6.31 (br s, 1H, L'-pyrrole-*H3*), 6.25 (m, 1H, L'-pyrrole-*H5*), 6.14 (t, $^3J(\text{H,H}) = 2.8$ Hz, 1H, L'-pyrrole-*H4*), 5.94 (m, 1H, L'-pyrrole-*H3*), 5.79 (ddd, $^3J(\text{H,H}) = 4.0$ Hz, $^3J(\text{H,H}) = 2.0$ Hz, $^5J(\text{H,H}) = 0.5$ Hz, 1H, pyrrole-*H4*), 4.49 (d, $^2J(\text{H,H}) = 14.0$ Hz, 1H, N-*CH₂*), 4.32 (d, $^2J(\text{H,H}) = 14.0$ Hz, 1H, N-*CH₂*), 3.69 (sept, $^3J(\text{H,H}) = 6.8$ Hz, 1H, *iPr CH*), 3.49 (sept, $^3J(\text{H,H}) = 6.8$ Hz, 1H, *iPr CH*), 3.41 (sept, $^3J(\text{H,H}) = 6.8$ Hz, 1H, *iPr CH*), 3.25 (sept, $^3J(\text{H,H}) = 6.8$ Hz, 1H, *iPr CH*), 1.46 (d, $^3J(\text{H,H}) = 6.7$ Hz, 3H, *iPr-CH₃*), 1.40 (d, $^3J(\text{H,H}) = 6.7$

Hz, 3H, *i*Pr-CH₃), 1.21 (d, ³J(H,H) = 6.8 Hz, 3H, *i*Pr-CH₃), 1.09 (d, ³J(H,H) = 6.8 Hz, 3H, *i*Pr-CH₃), 1.04 (d, ³J(H,H) = 6.9 Hz, 3H, *i*Pr-CH₃), 1.02 (d, ³J(H,H) = 6.8 Hz, 3H, *i*Pr-CH₃), 0.91 (d, ³J(H,H) = 6.8 Hz, 3H, *i*Pr-CH₃), 0.64 ppm (d, ³J(H,H) = 6.9 Hz, 3H, *i*Pr-CH₃); ¹³C NMR (100 MHz, C₆D₆, 25 °C): δ = 158.8, 149.6, 147.6, 145.1, 144.7, 142.1, 141.9, 141.0, 132.8, 131.3, 125.0, 124.9, 123.7, 123.4, 122.1, 120.3, 118.2, 111.7, 99.1, 51.6, 29.9, 28.4, 28.3, 27.9, 27.2, 26.2, 25.9, 25.0, 23.8, 22.7, 21.4 ppm; ²⁹Si NMR (79 MHz, C₆D₆, 25 °C): δ = -116.2 ppm; Elemental analysis calcd [%] for C₃₄H₄₃ClN₄Si: C 71.48%, H 7.59%, N 9.81%; found: C 71.23%, H 7.37%, N 9.71%; X-ray: C₃₄H₄₃ClN₄Si, Fw = 571.26, red block, 0.39 × 0.23 × 0.13 mm³, monoclinic, C2/c (no. 15), a = 20.2550(7), b = 9.9597(3), c = 15.6320(4) Å, β = 99.764(2)°, V = 3107.82(15) Å³, Z = 4, D_x = 1.221 g/cm³, μ = 0.19 mm⁻¹. 64810 Reflections were measured at a temperature of 100(2) K up to a resolution of (sin θ/λ)_{max} = 0.78 Å⁻¹. 6268 Reflections were unique [R_{int} = 0.030], of which 5603 were observed [I > 2σ(I)]. Atom C5 was refined with a disorder model corresponding to C-H and CH₂ in a ratio of 1:1. The isopropyl group at C15 was orientationally disordered. Hydrogen atoms were refined with a riding model. 216 Parameters were refined with 61 restraints [distances, angles and displacement parameters of the disordered groups]. R1/wR2 [I > 2σ(I)]: 0.0410 / 0.1067. R1/wR2 [all refl.]: 0.0457 / 0.1094. S = 1.023. Residual electron density between -0.65 and 0.70 e/Å³.

Tri[D^{ipp}IMP]silane (3). To a solution of NEt₃ (1.55 mL, 11.1 mmol) and D^{ipp}IMPH (1.944 g, 7.70 mmol) in THF (12.5 mL) at -78 °C HSiCl₃ (0.25 mL, 2.5 mmol) was added. This mixture was stirred at -78 °C for 45 min, yielding a cloudy, pale yellow mixture, which turned green/grey during stirring for 16 h at room temperature. The mixture was filtered and the solvent was evaporated. The bulk of the product was purified by dissolving the solid residue (1.551 g) in THF (14 mL), filtration, and storage of the dark green solution at -35 °C in the glovebox. Clear colorless crystals had formed after 3 days (583 mg). To obtain a second crop the liquid was separated, concentrated to about two-third the volume and stored at -35 °C again. Three days later a second crop could be isolated (95.5 mg). The crystals were washed with n-hexane (1 mL) and freed of solvent *in vacuo*. White/slightly green crystals were obtained (total: 678 mg, 34%). Crystals suitable for X-ray diffraction analysis were obtained by vapor diffusion of n-hexane (4 mL) into a solution of the crude product (0.5 g) in THF (2 mL). ¹H NMR (400 MHz, C₆D₆, 25 °C): δ = 7.68 (s, 3H, N=C-H), 7.60 (s, 1H, Si-H, ¹J(Si,H)=417 Hz), 6.99 (s, 9H, Ar-H), 6.44 (dd, ³J(H,H) = 1.24 Hz, ³J(H,H) = 3.25 Hz, 3H, pyrrole-H), 6.08 (m, 6H, pyrrole-H), 2.60 (br, 3H, *i*Pr CH), 1.83 (br, 3H, *i*Pr CH), 0.98 (d, ³J(H,H) = 6.9 Hz, 18H, *i*Pr-CH₃), 0.79 (br, 9H, *i*Pr-CH₃), 0.59 ppm (br, 9H, *i*Pr-CH₃); ¹H NMR (400 MHz, C₇D₈, -60 °C): δ = 7.54 (s, 1H, ¹J(Si,H) = 417 Hz, Si-H), 7.43 (s, 3H, N=C-H), 7.14-6.93 (m, 9H, Ar-H), 6.38 (dd, ³J(H,H) = 1.5 Hz, ³J(H,H) = 3.4 Hz, 3H, pyrrole-H), 6.13 (br, 3H, pyrrole-H), 6.03 (t, ³J(H,H) = 3.0 Hz, 3H, pyrrole-H), 2.60 (sept, ³J(H,H) = 6.9 Hz, 3H, *i*Pr CH), 1.64 (sept, ³J(H,H) = 6.9 Hz, 3H, *i*Pr CH), 1.09 (d, ³J(H,H) = 6.9 Hz, 9H, *i*Pr-CH₃), 1.05 (d, ³J(H,H) = 6.9 Hz, 9H, *i*Pr-CH₃), 0.90 (d, ³J(H,H) = 6.9 Hz, 9H, *i*Pr-CH₃), 0.44 ppm (d, ³J(H,H) = 6.9 Hz, 9H, *i*Pr-CH₃); ¹³C NMR (100 MHz, C₇D₈, 25 °C): δ = 152.9, 148.6, 138.6 (br), 136.5, 131.1, 124.5, 123.4, 122.4 (br), 120.9, 113.0, 110.3, 28.3, 27.7, 26.0 (br), 25.0 (br), 23.7, 22.3 ppm (br); ¹³C NMR (100 MHz, C₇D₈, -60 °C): δ = 152.4 (N=C-H), 148.2 (i-Ar), 139.3 (o-Ar), 137.6 (o-Ar), 135.9 (pyr-C), 130.7 (pyr-CH), 124.3 (Ar-CH), 123.3 (Ar-CH), 121.8 (Ar-CH), 120.7 (pyr-CH), 112.7 (pyr-CH), 27.6 (*i*Pr CH), 27.2 (*i*Pr CH), 26.3 (*i*Pr-CH₃), 24.7 (*i*Pr-CH₃), 23.5 (*i*Pr-CH₃), 21.8 ppm (*i*Pr-CH₃); ²⁹Si NMR (79 MHz, C₆D₆, 25 °C): δ = -60.5 ppm (¹J(Si,H) = 417 Hz); IR (ATR): ν̄ = 2355 (Si-H), 1628 cm⁻¹ (C=N); Elemental analysis calcd [%] for C₅₁H₆₄N₆Si: C 77.62%, H 8.17%, N 10.65%; found: C 77.58%, H 8.15%, N 10.65%; X-ray: C₅₁H₆₄N₆Si, Fw = 789.17, colorless block, 0.48 × 0.47 × 0.17 mm³, monoclinic, P2₁/n (no. 14), a = 17.5336(6), b = 13.3186(6), c = 19.7879(6) Å, β = 91.542(2)°, V = 4619.3(3) Å³, Z = 4, D_x = 1.135 g/cm³, μ = 0.09 mm⁻¹. 56581 Reflections were measured at a temperature of 150(2) K up to a resolution of (sin θ/λ)_{max} = 0.65 Å⁻¹. 10604 Reflections were unique [R_{int} = 0.039], of which 8297 were observed [I > 2σ(I)]. One of the isopropyl groups was refined with a disorder model. The Si-H hydrogen atom was refined freely with an isotropic displacement parameter. All other H-atoms were refined with a riding model. 572 Parameters were refined with 203 restraints [distances and angles of the isopropyl groups]. R1/wR2 [I > 2σ(I)]: 0.0397 / 0.0969. R1/wR2 [all refl.]: 0.0556 / 0.1057. S = 1.025. Residual electron density between -0.34 and 0.28 e/Å³.

Di[M^{es}IMP (=L)](M^{es}AMP (=L')) silane (4). To a solution of NEt₃ (1.52 mL, 10.9 mmol) and M^{es}IMPH (1.624 g, 7.69 mmol) in THF (12.5 mL) at -78 °C HSiCl₃ (0.25 mL, 2.5 mmol) was added. This was stirred at -78 °C for 45 min, yielding a cloudy, off-white mixture, which turned yellow/orange during

stirring for 16 h at room temperature. The mixture was filtered and the solvent was evaporated to yield a voluminous foam. The bulk of the product was purified by extracting the solid residue (1.467 g) in THF (11 mL) and storing the resulting orange solution at $-35\text{ }^{\circ}\text{C}$ in the glovebox. After two days no solid material had formed. n-Hexane (11 mL) was carefully layered on top of the clear THF solution and this was stored at r.t. for 3 days, after which orange crystals had formed. The liquid was separated, the crystals washed with n-hexane (1 mL), and dried *in vacuo* (0.361 g, 22%). Crystals suitable for X-ray analysis were obtained by gas phase diffusion of n-hexane into a solution of **4** in a minimal amount of THF. ^1H NMR (400 MHz, C_7D_8 , $25\text{ }^{\circ}\text{C}$): δ = 7.73 (br, 1H, pyrrole-H), 6.90–6.50 (m, 9H, Ar-H & 2 N=C-H & 1 pyrrole-H)*, 6.20 (br, 1H, pyrrole-H), 6.08 (br, 1H, pyrrole-H), 5.93 (br, 1H, pyrrole-H), 5.91 (br, 1H, pyrrole-H), 5.78 (br, 1H, pyrrole-H), 5.62 (br, 1H, pyrrole-H), 5.60 (br, 1H, pyrrole-H), 4.10 (d, $^2J(\text{H,H})$ = 14.3 Hz, 1H, N-CH₂), 4.02 (d, $^2J(\text{H,H})$ = 14.3 Hz, 1H, N-CH₂), 2.38 (s, 3H, Mes-CH₃), 2.30–1.70 ppm (m, 27H, Mes-CH₃); ^1H NMR (400 MHz, C_7D_8 , $-25\text{ }^{\circ}\text{C}$): δ = 7.78 (dd, $J(\text{H,H})$ = 3.4 Hz $J(\text{H,H})$ = 1.7 Hz, 1H, pyrrole-H), 6.85–6.40 (m, 9H, Ar-H & 2 N=C-H & 1 pyrrole-H), 6.14 (t, $J(\text{H,H})$ = 3.0 Hz, 1H, pyrrole-H), 6.07 (s, 1H, pyrrole-H), 6.03 (s, 1H, pyrrole-H), 5.96 (t, $J(\text{H,H})$ = 2.7 Hz, 1H, pyrrole-H), 5.86 (dd, $J(\text{H,H})$ = 1.8 Hz, $J(\text{H,H})$ = 3.8 Hz, 1H, pyrrole-H), 5.68 (dd, $J(\text{H,H})$ = 1.6 Hz, $J(\text{H,H})$ = 2.6 Hz, 1H, pyrrole-H), 5.59 (t, $J(\text{H,H})$ = 3.1 Hz, 2H, pyrrole-H), 4.02 (d, $^2J(\text{H,H})$ = 14.4 Hz, 1H, N-CH₂), 3.89 (d, $^2J(\text{H,H})$ = 14.4 Hz, 1H, N-CH₂), 2.33 (s, 1H, Mes-CH₃), 2.28 (s, 2H, Mes-CH₃), 2.17 (s, 1H, Mes-CH₃), 2.10 (s, 1H, Mes-CH₃), 2.04 (s, 1H, Mes-CH₃), 1.90 (s, 1H, Mes-CH₃), 1.87 (s, 1H, Mes-CH₃), 1.71 ppm (s, 1H, Mes-CH₃); ^{13}C NMR (100 MHz, C_7D_8 , $25\text{ }^{\circ}\text{C}$): δ = 160.4, 156.0, 150.6, 142.4, 141.9, 141.5, 141.4, 138.3, 137.2, 137.1, 135.1, 134.1 (br), 133.7, 133.3 (br), 132.8, 131.3, 130.8, 129.6, 129.5, 129.4, 129.2, 128.8, 128.3, 128.2, 128.1, 127.9, 127.8, 127.2, 121.7, 120.0, 118.0, 115.4, 113.2, 110.8, 100.4, 48.0, 21.1, 21.0, 20.9, 20.9, 20.8, 19.9, 19.3 (br), 19.0, 18.9, 18.8, 18.6 ppm; ^{29}Si NMR (79 MHz, C_6D_6 , $25\text{ }^{\circ}\text{C}$): δ = -120.4 ppm; Elemental analysis calcd (%) for $\text{C}_{42}\text{H}_{46}\text{N}_6\text{Si}$: C 76.09%, H 6.99%, N 12.68%; found: C 75.93%, H 7.05%, N 12.62%; X-ray: $\text{C}_{42}\text{H}_{46}\text{N}_6\text{Si}$, Fw = 662.94, yellow block, $0.59 \times 0.36 \times 0.12\text{ mm}^3$, monoclinic, $\text{P2}_1/\text{n}$ (no. 14), $a = 20.5288(8)$, $b = 9.0717(3)$, $c = 21.4439(5)\text{ \AA}$, $\beta = 115.714(1)^\circ$, $V = 3598.05(19)\text{ \AA}^3$, $Z = 4$, $D_x = 1.224\text{ g/cm}^3$, $\mu = 0.10\text{ mm}^{-1}$. 51677 Reflections were measured at a temperature of $150(2)\text{ K}$ up to a resolution of $(\sin \theta/\lambda)_{\text{max}} = 0.65\text{ \AA}^{-1}$. 8270 Reflections were unique ($R_{\text{int}} = 0.021$), of which 7272 were observed [$I > 2\sigma(I)$]. The hydrogen atoms at the C5x C-H and CH₂ groups were refined freely with isotropic displacement parameters. All other H-atoms were refined with a riding model. 467 Parameters were refined with no restraints. $R1/wR2$ [$I > 2\sigma(I)$]: 0.0357 / 0.0986. $R1/wR2$ [all refl.]: 0.0410 / 0.1025. $S = 1.048$. Residual electron density between -0.32 and 0.30 e/\AA^3 . * determined by HSQC

Reactivity studies

Reaction of DipplIMPH with HSiCl_3 and NEt_3 . NEt_3 (0.41 mL, 3.0 mmol) and DipplIMPH (0.504 g, 1.98 mmol) were dissolved in THF (10 mL). HSiCl_3 (0.21 mL, 1.98 mmol) was added at $-78\text{ }^{\circ}\text{C}$, and the mixture was stirred at $-78\text{ }^{\circ}\text{C}$ for 45 min and at room temperature for 16 h. n-Hexane (30 mL) was added, the mixture was filtered and the residue washed with n-hexane (2 x 10 mL). The filtrate was stored at $-20\text{ }^{\circ}\text{C}$. ^1H NMR shows a mixture of products, including **1b**, **2** and **5**. This mixture could not be purified.

Hydrosilylation of isolated **1b at $70\text{ }^{\circ}\text{C}$.** An NMR sample was prepared by dissolving of crystalline **1b** (12.9 mg, $36.5\text{ }\mu\text{mol}$) and mesitylene (2.9 mg, $24\text{ }\mu\text{mol}$) in C_6D_6 ($\sim 0.5\text{ mL}$). This mixture was monitored by ^1H NMR for 73 h at room temperature. Subsequently, a programmed sequence of ^1H NMR measurements was conducted at $70\text{ }^{\circ}\text{C}$ for 61 h. All spectra were recorded with a relaxation time of 10 s. The ratio of the signal area per H of the compound and the signal area per H of the IS multiplied by the amount of IS gives the amount of compound. The concentration was obtained by dividing this by the approximated 0.5 mL solvent. From this follows that the absolute concentrations have a certain error which is unknown, whereas the relative concentrations are accurate. (Figure 2.4)

Reaction of **1b with DipplIMPLi to generate **6**.** Compounds **1b** (8.2 mg, $23.2\text{ }\mu\text{mol}$) and DipplIMPLi (9.9 mg, $23.4\text{ }\mu\text{mol}$, 39 mass% Et_2O by ^1H NMR) were weighed and dissolved separately, both in C_7D_8 (0.25 mL). A few drops of $[\text{D}_6]\text{THF}$ were needed to dissolve the DipplIMPLi . Combining the solutions at r.t. resulted in a strongly cloudy solution immediately, which was stirred for 3 min prior to filtration into a J-Young NMR tube. NMR measurements were done at $-60\text{ }^{\circ}\text{C}$ and subsequently during

warming at steps of 10 °C. ^1H NMR showed presence of **3** in a **6:3** ratio of approx. 3:1. Spectroscopic data for **6**: ^1H NMR (400 MHz, C_7D_8 , -60°C): δ = 7.91 (s, 1H, N=CH), 7.75 (s, 1H, N=CH), 7.20 (s, 1H, Ar-H), 6.75 (t, $J(\text{H,H})$ = 6.3 Hz, 2H, Ar-H), 6.60 (s, 1H, pyrrole-H), 6.56 (t, $^3J(\text{H,H})$ = 3.8 Hz, 2H, pyrrole-H), 5.93 (dd, $J(\text{H,H})$ = 2.0 Hz, $J(\text{H,H})$ = 3.5 Hz, 1H, pyrrole-H), 5.87 (dd, $J(\text{H,H})$ = 2.0 Hz, $J(\text{H,H})$ = 3.5 Hz, 1H, pyrrole-H), 5.83 (s, $^1J(\text{Si,H})$ = 285 Hz, 1H, Si-H), 3.66 (sept, $^3J(\text{H,H})$ = 6.5 Hz, 1H, *i*Pr CH), 3.01 (sept, $^3J(\text{H,H})$ = 6.5 Hz, 1H, *i*Pr CH), 2.93 (sept, $^3J(\text{H,H})$ = 6.5 Hz, 1H, *i*Pr CH), 2.87 (sept, $^3J(\text{H,H})$ = 6.5 Hz, 1H, *i*Pr CH), 1.50 (d, $^3J(\text{H,H})$ = 6.5 Hz, 3H, *i*Pr-CH₃), 1.20-0.80 ppm (m, 21H, *i*Pr-CH₃); ^1H NMR (400 MHz, C_7D_8 , 25°C): δ = 7.76 (br), 7.21 (br), 7.01 (br), 6.58 (br), 6.44 (br), 5.98 (br), 2.96 ppm (br, *i*Pr CH); ^{29}Si NMR (79 MHz, C_7D_8 , -60°C): δ = -168.5 ppm ($^1J(\text{Si,H})$ = 285 Hz);

Reaction of 2 with HSiCl_3 . A solution of compound **2** (14 mg, 24.3 μmol) in C_6D_6 was introduced into a J-Young NMR tube, HSiCl_3 (2.4 μL , 23.7 μmol) was added and ^1H NMR was measured immediately, showing presence of HSiCl_3 , **2** and a very small amount of **1b** and **5**. The tube was heated in a 70°C oil bath for 2.5 h, showing presence of a decreased amount of HSiCl_3 and a ratio of compound **1b** : **5** : **2** of 21% : 36% : 43%. The tube was heated again in a 70°C oil bath for 20.5 h, showing full consumption of HSiCl_3 and a ratio **1b** : **5** : **2** of 2% : 66% : 32%.

Hydrosilylation of crude 1b at 25°C . An NMR sample was prepared of the non-purified product **1b** in C_6D_6 (~0.5 mL). A sequence of ^1H NMR measurements was conducted at 25°C over 14 days. All spectra were recorded with a relaxation time of 1 s. The ratio of the signal area per H of one of the compounds and the sum of signal area per H of all compounds gives the mole fraction of said compound.

Hydrosilylation of crude 1b at 70°C . An NMR sample was prepared of the non-purified product **1b** in C_6D_6 (~0.5 mL). A programmed sequence of ^1H NMR measurements was conducted at 70°C in 17 h. All spectra were recorded with a relaxation time of 1 s. The ratio of the signal area per H of one of the compounds and the sum of signal area per H of all compounds gives the mole fraction of said compound.

Hydrosilylation of 1b in the presence of Bu_4NCl . Two NMR samples (experiment and control) were prepared by dissolving crystals of **1b** (Exp: 10.1 mg; Control: 11.5 mg), mesitylene (Exp: 2.8 mg; Control: 2.4 mg) and Bu_4NCl (low solubility, Exp: 3 mg; Control: 0 mg) in C_6D_6 (~0.5 mL). The undissolved Bu_4NCl was filtered off. The concentration of Bu_4NCl was determined to be 5-6 mol% vs **1b** (determined by ^1H NMR integration versus the mesitylene internal standard). A sequence of ^1H NMR measurements was conducted at 25°C over 5.5 h (for control) and 18 days (for experiment). All spectra were recorded with a relaxation time of 10 s. The ratio of the signal area per H of the compound and the signal area per H of the IS multiplied by the amount of IS gives the amount of compound. The concentration was obtained by dividing this by the approximated 0.5 mL solvent. From this follows that the absolute concentrations have a certain error which is unknown, whereas the relative concentrations are accurate. The final data point shows a purity of ~ 80% **5**. Spectroscopic data for **5**: ^1H NMR (400 MHz, C_6D_6 , 25°C): δ = 7.14, 7.04 (AB₂, J_{AB} = 7.8 Hz, 3H, Ar-H), 6.77 (ddt, $^3J(\text{H,H})$ = 2.8 Hz, $^4J(\text{H,H})$ = 1.0 Hz, $^5J(\text{H,H})$ = 0.6 Hz, 1H, pyrrole-H5), 6.46 (t, $^3J(\text{H,H})$ = 3.0 Hz, 1H, pyrrole-H4), 6.01 (dq, $^3J(\text{H,H})$ = 3.1 Hz, $^4J(\text{H,H})$ = 1.2 Hz, 1H, pyrrole-H3), 4.22 (dd, $^4J(\text{H,H})$ = 1.4 Hz, $^5J(\text{H,H})$ = 0.7 Hz, 2H, N-CH₂), 3.30 (sept, $^3J(\text{H,H})$ = 6.8 Hz, 2H, *i*Pr CH), 1.20 (d, $^3J(\text{H,H})$ = 6.8 Hz, 6H, *i*Pr-CH₃), 0.99 ppm (d, $^3J(\text{H,H})$ = 6.8 Hz, 6H, *i*Pr-CH₃); ^{29}Si NMR (79 MHz, C_6D_6 , 25°C , $\text{Cr}(\text{acac})_3$); δ = -36.5 ppm.

Hydrosilylation of 1b in the presence of NEt_3 . An NMR sample was prepared by dissolving crystalline **1b** (10.0 mg), mesitylene (2.8 mg), and NEt_3 (2.5 mg) in C_7D_8 (~0.5 mL). A programmed sequence of ^1H NMR measurements was conducted at 70°C over 14.5 h. All spectra were recorded with a relaxation time of 10 s. The ratio of the signal area per H of the compound and the signal area per H of the IS multiplied by the amount of IS gives the amount of compound. The concentration was obtained by dividing this by the approximated 0.5 mL solvent. From this follows that the absolute concentrations have a certain error which is unknown, whereas the relative concentrations are accurate.

Hydrosilylation of 1a at 70°C . An NMR sample was prepared by dissolving **1a** (18.4 mg) and mesitylene (33.6 mg) in C_6D_6 . A sequence of ^1H NMR measurements was conducted at 25°C over 11

days, in between measurements the tube was stored in a 70 °C oil bath. All spectra were recorded with a relaxation time of 10 s. The ratio of the signal area per H of the compound and the signal area per H of the IS multiplied by the amount of IS gives the amount of compound. The concentration was obtained by dividing this by the approximated 0.5 mL solvent. From this follows that the absolute concentrations have a certain error which is unknown, whereas the relative concentrations are accurate.

Stability of 1a and 3 in the presence of Bu₄NCl at 70 °C. Two NMR samples (**1a** and **3**) were prepared by dissolving crystals of the silanes (**1a**: 7.7 mg, **3**: 21.3 mg), mesitylene (for **1a**: 4.3 mg, for **3**: 3.7 mg) and Bu₄NCl (low solubility, for **1a**: 4.5 mg, for **3**: 4.2 mg) in C₆D₆ (~0.5 mL). The undissolved Bu₄NCl was filtered off. The concentration of Bu₄NCl was determined to be ~2 mol% for **1a** and ~4 mol% for **3** (determined by ¹H NMR integration versus the mesitylene internal standard). The NMR tubes were kept at 70 °C for 23 h. ¹H NMR spectra were recorded every hour in the first 7 h and once after a total of 23 h. Both reactions showed no change up to 23 h.

References

- [1] K. Hübler, W. R. Roper, L. J. Wright, *Organometallics* **1997**, *16*, 2730–2735.
- [2] A. Brück, D. Gallego, W. Wang, E. Irran, M. Driess, J. F. Hartwig, *Angew. Chemie Int. Ed.* **2012**, *51*, 11478–11482.
- [3] B. Blom, M. Stözel, M. Driess, *Chem. Eur. J.* **2013**, *19*, 40–62.
- [4] M. Denk, R. Lennon, R. Hayashi, R. West, A. V. Belyakov, H. P. Verne, A. Haaland, M. Wagner, N. Metzler, *J. Am. Chem. Soc.* **1994**, *116*, 2691–2692.
- [5] A. J. Arduengo, R. L. Harlow, M. Kline, *J. Am. Chem. Soc.* **1991**, *113*, 361–363.
- [6] S. Khan, S. S. Sen, D. Kratzert, G. Tavčar, H. W. Roesky, D. Stalke, *Chem. Eur. J.* **2011**, *17*, 4283–4290.
- [7] W. Yang, H. Fu, H. Wang, M. Chen, Y. Ding, H. W. Roesky, A. Jana, *Inorg. Chem.* **2009**, *48*, 5058–5060.
- [8] B. Blom, M. Pohl, G. Tan, D. Gallego, M. Driess, *Organometallics* **2014**, *33*, 5272–5282.
- [9] C.-W. So, H. W. Roesky, J. Magull, R. B. Oswald, *Angew. Chemie Int. Ed.* **2006**, *45*, 3948–3950.
- [10] S. S. Sen, H. W. Roesky, D. Stern, J. Henn, D. Stalke, *J. Am. Chem. Soc.* **2010**, *132*, 1123–1126.
- [11] S. S. Sen, J. Hey, D. Kratzert, H. W. Roesky, D. Stalke, *Organometallics* **2012**, *31*, 435–439.
- [12] F. M. Mück, D. Klotz, J. A. Baus, C. Burschka, R. Tacke, *Chem. Eur. J.* **2014**, *20*, 9620–9626.
- [13] Y. Xiong, S. Yao, M. Driess, *Chem. Eur. J.* **2012**, *18*, 3316–3320.
- [14] G. Tan, B. Blom, D. Gallego, E. Irran, M. Driess, *Chem. Eur. J.* **2014**, *20*, 9400–9408.
- [15] M. Driess, S. Yao, M. Brym, C. van Wüllen, D. Lentz, *J. Am. Chem. Soc.* **2006**, *128*, 9628–9629.
- [16] M. Asay, C. Jones, M. Driess, *Chem. Rev.* **2011**, *111*, 354–396.
- [17] F. Armbruster, I. Fernández, F. Breher, *Dalton Trans.* **2009**, *29*, 5612–5626.
- [18] F. Armbruster, T. Augenstein, P. Oña-Burgos, F. Breher, *Chem. Eur. J.* **2013**, *19*, 17899–17906.
- [19] S. Styra, S. González-Gallardo, F. Armbruster, P. Oña-Burgos, E. Moos, M. Vonderach, P. Weis, O. Hampe, A. Grün, Y. Schmitt, M. Gerhards, F. Menges, M. Gaffga, G. Niedner-Schatteburg, F. Breher, *Chem. Eur. J.* **2013**, *19*, 8436–8446.
- [20] B.-Y. Zheng, X.-J. Jiang, T. Lin, M.-R. Ke, J.-D. Huang, *Dyes Pigm.* **2015**, *112*, 311–316.
- [21] J. Liu, X. Yang, L. Sun, *Chem. Commun.* **2013**, *49*, 11785–11787.
- [22] B. L. Bray, P. H. Mathies, R. Naef, D. R. Solas, T. T. Tidwell, D. R. Artis, J. M. Muchowski, *J. Org. Chem.* **1990**, *55*, 6317–6328.
- [23] M. Xiao, X. Lei, B. Han, M. L. O'Neill, R. M. Pearlstein, R. Ho, H. Chandra, A. Derecskei-Kovacs, *Organoaminosilane Precursors and Methods for Making and Using Same*, **2013**, U.S. Patent 2013129940.
- [24] N. Sakamoto, C. Ikeda, M. Yamamura, T. Nabeshima, *J. Am. Chem. Soc.* **2011**, *133*, 4726–4729.
- [25] D. Gerlach, E. Brendler, T. Heine, J. Wagler, *Organometallics* **2007**, *26*, 234–240.
- [26] D. Gerlach, A. W. Ehlers, K. Lammertsma, J. Wagler, *Z. Naturforsch., B: J. Chem. Sci.* **2009**, *64*, 1571–1579.
- [27] A. Kämpfe, E. Brendler, E. Kroke, J. Wagler, *Chem. Eur. J.* **2014**, *20*, 9409–9418.
- [28] A. Kämpfe, E. Kroke, J. Wagler, *Organometallics* **2014**, *33*, 112–120.
- [29] A. Kämpfe, E. Brendler, E. Kroke, J. Wagler, *Dalton Trans.* **2015**, *44*, 4744–4750.

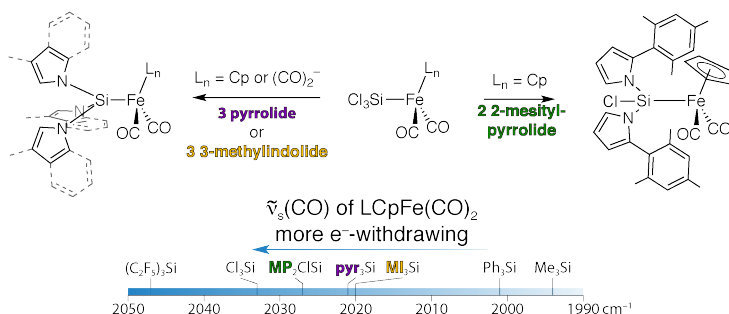
- [30] a) J. R. Pankhurst, T. Cadenbach, D. Betz, C. Finn, J. B. Love, *Dalton Trans.* **2015**, 44, 2066–2070. b) T. Yasumoto, K. Yamamoto, H. Tsurugi, K. Mashima, *Dalton Trans.* **2013**, 42, 9120–9128. c) Q. Wang, L. Xiang, H. Song, G. Zi, *Inorg. Chem.* **2008**, 47, 4319–4328. d) J. Leppin, C. Förster, K. Heinze, *Inorg. Chem.* **2014**, 53, 12416–12427. e) J.-Y. Liu, P. Tao, Y.-X. Wang, Y.-S. Li, *RSC Adv.* **2014**, 4, 19433–19439. f) E. Labisbal, L. Rodríguez, A. Vizoso, M. Alonso, J. Romero, J.-A. García-Vázquez, A. Sousa-Pedrares, A. Sousa, *Z. Anorg. Allg. Chem.* **2005**, 631, 2107–2114. g) K. Mashima, H. Tsurugi, *J. Organomet. Chem.* **2005**, 690, 4414–4423.
- [31] K. P. Bryliakov, E. A. Kravtsov, L. Broomfield, E. P. Talsi, M. Bochmann, *Organometallics* **2007**, 26, 288–293.
- [32] H. Kaneko, H. M. Dietrich, C. Schädle, C. Maichle-Mössmer, H. Tsurugi, K. W. Törnroos, K. Mashima, R. Anwender, *Organometallics* **2013**, 32, 1199–1208.
- [33] H. Hao, S. Bhandari, Y. Ding, H. W. Roesky, J. Magull, H.-G. Schmidt, M. Noltemeyer, C. Cui, *Eur. J. Inorg. Chem.* **2002**, 1060–1065.
- [34] L.-C. Liang, C.-W. Yang, M. Y. Chiang, C.-H. Hung, P.-Y. Lee, *J. Organomet. Chem.* **2003**, 679, 135–142.
- [35] Y. Yang, N. Zhao, H. Zhu, H. W. Roesky, *Organometallics* **2012**, 31, 1958–1964.
- [36] S. Tabthong, T. Nanok, P. Kongsaree, S. Prabpai, P. Hormnirun, *Dalton Trans.* **2014**, 1348–1359.
- [37] S. Pracha, S. Praban, A. Niewpung, G. Kotpisan, P. Kongsaree, S. Saithong, T. Khamnaen, P. Phiriyawirut, S. Charoenchaidet, K. Phomphrai, *Dalton Trans.* **2013**, 42, 15191–15198.
- [38] S. Qiao, W.-A. Ma, Z.-X. Wang, *J. Organomet. Chem.* **2011**, 696, 2746–2753.
- [39] Y. Wei, S. Wang, S. Zhou, Z. Feng, L. Guo, X. Zhu, X. Mu, F. Yao, *Organometallics* **2015**, 34, 1882–1889.
- [40] a) C. E. Anderson, A. S. Batsanov, P. W. Dyer, J. Fawcett, J. A. K. Howard, *Dalton Trans.* **2006**, 5362–5378; b) Vránová, I.; Jambor, R.; Růžička, A.; Hoffmann, A.; Herres-Pawlis, S.; Dostál, L. *Dalton Trans.* **2015**, 44 (1), 395–400.
- [41] K. Lippe, D. Gerlach, E. Kroke, J. Wagler, *Organometallics* **2009**, 28, 621–629.
- [42] M. Novák, L. Dostál, M. Alonso, F. De Proft, A. Růžička, A. Lyčka, R. Jambor, *Chem. Eur. J.* **2014**, 20, 2542–2550.
- [43] E. Kertsus-Banchik, I. Kalikhman, B. Gostevskii, Z. Deutsch, M. Botoshansky, D. Kost, *Organometallics* **2008**, 27, 5285–5294.
- [44] G. W. Fester, J. Eckstein, D. Gerlach, J. Wagler, E. Brendler, E. Kroke, *Inorg. Chem.* **2010**, 49, 2667–2673.
- [45] Y.-S. Li, Y.-R. Li, X.-F. Li, *J. Organomet. Chem.* **2003**, 667, 185–191.
- [46] The free enthalpy of activation at a given temperature was calculated using the following equation:
- $$\Delta G^\ddagger = aT \left[9.972 + \log \left(\frac{T_c}{\Delta \nu} \right) \right] \text{ where } a = 4.575 \cdot 10^{-3} \text{ for kcal/mol}$$
- [47] A. W. Addison, T. N. Rao, J. Reedijk, J. van Rijn, G. C. Verschoor, *J. Chem. Soc., Dalton Trans.* **1984**, 1349–1356.
- [48] IUPAC. Compendium of Chemical Terminology, 2nd ed. [the "Gold Book"]. Compiled by A. D. McNaught and A. Wilkinson. Blackwell Scientific Publications, Oxford (1997). XML on-line corrected version: <http://goldbook.iupac.org> (2006-) created by M. Nic, J. Jirat, B. Kosata; updates compiled by A. Jenkins. ISBN 0-9678550-9-8. doi:10.1351/goldbook.
- [49] E. P. A. Couzijn, J. C. Sloodweg, A. W. Ehlers, K. Lammertsma, *J. Am. Chem. Soc.* **2010**, 132, 18127–18140.
- [50] A. H. J. F. De Keijzer, F. J. J. De Kanter, M. Schakel, V. P. Osinga, G. W. Klumpp, *J. Organomet. Chem.* **1997**, 548, 29–32.
- [51] A. Lends, E. Olszewska, S. Belyakov, N. Erchak, E. Liepinsh, *Heteroat. Chem.* **2015**, 26, 12–28.
- [52] E. P. A. Couzijn, M. Schakel, F. J. J. de Kanter, A. W. Ehlers, M. Lutz, A. L. Spek, K. Lammertsma, *Angew. Chemie Int. Ed.* **2004**, 43, 3440–3442.
- [53] C. Chuit, R. J. P. Corriu, C. Reye, J. C. Young, *Chem. Rev.* **1993**, 93, 1371–1448.
- [54] G. van Koten, J. T. B. H. Jastrzebski, J. G. Noltes, *J. Organomet. Chem.* **1979**, 177, 283–292.

- [55] G. van Koten, J. T. B. H. Jastrzebski, J. G. Noltes, W. M. G. F. Pontenagel, J. Kroon, A. L. Spek, *J. Am. Chem. Soc.* **1978**, *100*, 5021–5028.
- [56] E. L. Muetterties, *J. Am. Chem. Soc.* **1969**, *91*, 4115–4122.
- [57] E. L. Muetterties, *J. Am. Chem. Soc.* **1969**, *91*, 1636–1643.
- [58] H. V. R. Dias, Z. Wang, W. Jin, *Coord. Chem. Rev.* **1998**, *176*, 67–86.
- [59] K. Junold, J. A. Baus, C. Burschka, R. Tacke, *Angew. Chemie Int. Ed.* **2012**, *51*, 7020–7023.
- [60] T. Kaukorat, P. G. Jones, R. Schmutzler, *Chem. Ber.* **1991**, *124*, 1335–1346.
- [61] E. D. Glendening, K. B. J. A. E. Reed, J. E. Carpenter, J. A. Bohmann, C. M. Morales, C. R. Landis, F. Weinhold, *NBO 6.0*, **2013**.
- [62] F. H. Allen, O. Kennard, D. G. Watson, L. Brammer, A. G. Orpen, R. Taylor, *J. Chem. Soc., Perkin Trans. 2* **1987**, S1–S19.
- [63] J. Woning, J. G. Verkade, *Organometallics* **1991**, *10*, 2259–2266.
- [64] M. Yamamura, N. Kano, T. Kawashima, *Tetrahedron Lett.* **2007**, *48*, 4033–4036.
- [65] A. S. Pilcher, P. DeShong, *J. Org. Chem.* **1996**, *61*, 6901–6905.
- [66] G. G. Furin, O. A. Vyazankina, B. A. Gostevsky, N. S. Vyazankin, *Tetrahedron* **1988**, *44*, 2675–2749.
- [67] F. Bitto, K. Kraushaar, U. Böhme, E. Brendler, J. Wagler, E. Kroke, *Eur. J. Inorg. Chem.* **2013**, 2954–2962.
- [68] G. W. Fester, J. Wagler, E. Brendler, E. Kroke, *Eur. J. Inorg. Chem.* **2008**, 5020–5023.
- [69] G. W. Fester, J. Wagler, E. Brendler, U. Böhme, G. Roewer, E. Kroke, *Chem. Eur. J.* **2008**, *14*, 3164–3176.
- [70] F. Bitto, J. Wagler, E. Kroke, *Eur. J. Inorg. Chem.* **2012**, 2402–2408.
- [71] G. W. Fester, J. Wagler, E. Brendler, U. Böhme, D. Gerlach, E. Kroke, *J. Am. Chem. Soc.* **2009**, *131*, 6855–6864.
- [72] K. Hensen, R. Mayr-Stein, T. Stumpf, P. Pickel, M. Bolte, H. Fleischer, *J. Chem. Soc., Dalton Trans.* **2000**, 473–477.
- [73] K. Junold, K. Sinner, J. A. Baus, C. Burschka, C. Fonseca Guerra, F. M. Bickelhaupt, R. Tacke, *Chem. Eur. J.* **2014**, *20*, 16462–16466.
- [74] K. Junold, M. Nutz, J. A. Baus, C. Burschka, C. Fonseca Guerra, F. M. Bickelhaupt, R. Tacke, *Chem. Eur. J.* **2014**, *20*, 9319–9329.
- [75] K. Junold, J. A. Baus, C. Burschka, M. Finze, R. Tacke, *Eur. J. Inorg. Chem.* **2014**, 5099–5102.
- [76] F. M. Mück, K. Junold, J. A. Baus, C. Burschka, R. Tacke, *Eur. J. Inorg. Chem.* **2013**, 5821–5825.
- [77] G. R. Fulmer, A. J. M. Miller, N. H. Sherden, H. E. Gottlieb, A. Nudelman, B. M. Stoltz, J. E. Bercaw, K. I. Goldberg, *Organometallics* **2010**, *29*, 2176–2179.
- [78] D. M. Dawson, D. A. Walker, M. Thornton-Pett, M. Bochmann, *J. Chem. Soc., Dalton Trans.* **2000**, 459–466.
- [79] C. Liu, S. Zhou, S. Wang, L. Zhang, G. Yang, *Dalton Trans.* **2010**, *39*, 8994–8999.
- [80] Gaussian 09, Revision D.01 (**2013**), M. J. Frisch, G. W. Trucks, H. B. Schlegel, G. E. Scuseria, M. A. Robb, J. R. Cheeseman, G. Scalmani, V. Barone, B. Mennucci, G. A. Petersson, H. Nakatsuji, M. Caricato, X. Li, H. P. Hratchian, A. F. Izmaylov, J. Bloino, G. Zheng, J. L. Sonnenberg, M. Hada, M. Ehara, K. Toyota, R. Fukuda, J. Hasegawa, M. Ishida, T. Nakajima, Y. Honda, O. Kitao, H. Nakai, T. Vreven, J. A. Montgomery, Jr., J. E. Peralta, F. Ogliaro, M. Bearpark, J. J. Heyd, E. Brothers, K. N. Kudin, V. N. Staroverov, T. Keith, R. Kobayashi, J. Normand, K. Raghavachari, A. Rendell, J. C. Burant, S. S. Iyengar, J. Tomasi, M. Cossi, N. Rega, J. M. Millam, M. Klene, J. E. Knox, J. B. Cross, V. Bakken, C. Adamo, J. Jaramillo, R. Gomperts, R. E. Stratmann, O. Yazyev, A. J. Austin, R. Cammi, C. Pomelli, J. W. Ochterski, R. L. Martin, K. Morokuma, V. G. Zakrzewski, G. A. Voth, P. Salvador, J. J. Dannenberg, S. Dapprich, A. D. Daniels, O. Farkas, J. B. Foresman, J. V. Ortiz, J. Cioslowski, D. J. Fox, Gaussian, Inc., Wallingford CT.
- [81] A.M.M. Schreurs, X. Xian, L.M.J. Kroon-Batenburg, *J. Appl. Cryst.* **2010**, *43*, 70–82.
- [82] G. M. Sheldrick **2008**, SADABS. Universität Göttingen, Germany.
- [83] G. M. Sheldrick, *Acta Cryst.* **2015**, *A71*, 1–8.
- [84] G. M. Sheldrick, *Acta Cryst.* **2015**, *C71*, 3–8.
- [85] A. L. Spek, *Acta Cryst.* **2009**, *D65*, 148–155.

3

Synthesis of N-heterocycle Substituted Silyl Ligands Within the Coordination Sphere of Iron

N-heterocycle-substituted silyl iron complexes have been synthesized by nucleophilic substitution at an iron-bound trichlorosilyl ligand. The homoleptic (tripyrrolyl)- and tris-(3-methylindolyl)silyl groups were accessed from $(\text{Cl}_3\text{Si})\text{CpFe}(\text{CO})_2$ [Cl_3SiFp] by substitution of chloride for pyrrolide or 3-methylindolide, respectively. Analogously, nucleophilic substitution of Cl for pyrrolide on the anionic Fe(0) synthon $\text{Cl}_3\text{SiFe}(\text{CO})_4^-$ generates the (tripyrrolyl) ligand bound to the iron tetracarbonyl fragment. The bulkier 2-mesitylpyrrolide substitutes a maximum of 2 chlorides on Cl_3SiFp under the same conditions. The tridentate, tri-anionic nucleophile tmim ($\text{tmimH}_3 = \text{tris}(3\text{-methylindol-2-yl})\text{methane}$) proves reluctant to perform the substitution in a straightforward manner, it is however capable of ring-opening and incorporation of THF to form the tris-THF adduct $\text{tmim}(\text{C}_4\text{H}_8\text{O})_3\text{SiFe}(\text{CO})_4^-$. The bidentate, mono-anionic nucleophile 2-(dipp-iminomethyl)pyrrolide [$^{\text{Dipp}}\text{IMP}$, dipp = 2,6-diisopropylphenyl] shows substitution of chloride and addition of a second $^{\text{Dipp}}\text{IMP}$ on the imine backbone. The heterocycle-based silyl ligands were shown to be sterically and electronically tunable, moderately electron-withdrawing ligands. The presented approach to new silyl ligands avoids strongly reducing conditions and potentially reactive hydrosilane intermediates, complementing more common methods.



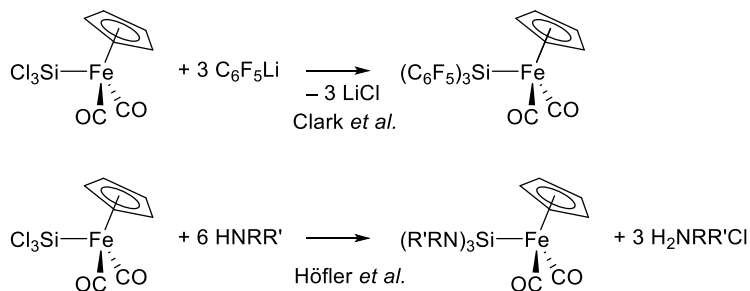
Introduction

Low-valent silicon(II) compounds are attracting considerable attention as strongly donating, tuneable ligands for transition metals.¹ While free silylenes were initially observed as highly reactive intermediates,² the use of nitrogen substituents has given access to a number of persistent silylenes following the first N-heterocyclic silylene (NHSi) reported in 1994 by Denk et al.³ Similarly to N-heterocyclic carbenes (NHC), stable silylenes bind a variety of transition metals.^{4–6} However, owing to the lower electronegativity and larger size of silicon, they conserve a higher Lewis acidity than their carbon-based congeners and they are often stabilized by coordination of a Lewis base, resulting in a 4-coordinate Si(II) center in the metal complex.^{4,7,8} The coordination chemistry of Si(II) ligands being now well established, their use as supporting ligands in catalysis is emerging as a promising area of research^{1,8–11}

In contrast with their neutral congeners, anionic Si(II) ligands (silyl anions or silanides), have seen less use as supporting ligands,^{12–15} even though metal-silyl complexes have been thoroughly studied mainly because of their role as intermediates in catalytic hydrosilylation.^{8,16–18} This presumably arises from the more strongly reducing character of silanides, which suggests that their stability might benefit from electron withdrawing groups. Encouragingly, this approach has allowed for the isolation of free silanides bearing trimethylsilyl and aromatic^{19–23} moieties, and more recently fluoroalkyl²⁴ and pyrazole moieties.²⁵ In this context, the synthesis of silyl-metal species bearing electron-withdrawing N-pyrrolyl or N-indolyl substituents was investigated.

The three classical approaches for the synthesis of silanides are deprotonation of an Si–H bond, nucleophilic cleavage of a Si–Si bond with an alkoxide, and reduction of (1) a silicon-halogen, (2) a disilane or (3) a Si–Ar bond.^{20,23,25} Relatively harsh reaction conditions²⁶ and possible side reactions²⁷ (e.g. substitution at Si by strong bases²⁸) limit the scope of these reactions. Therefore, many compounds containing metal-silicon bonds are not prepared by coordination of a free silanide, but rather by oxidative addition of an Si–H bond to a reduced metal precursor.^{29–31} In particular, the only currently known tris(N-pyrrolyl)silyl complexes have been synthesised by oxidative addition of tris(N-pyrrolyl)silane to Os and Ru.³²

An interesting alternative to these classical routes is substitution at a metal-bound silyl moiety bearing one or more good leaving groups, typically halogens. Following the initial report of nucleophilic substitution of chloride for dimethylamine to obtain *trans*-ClPt(PET₃)₂SiH₂NMe₂,³³ this methodology has been extended to the exchange of Cl on Cp(CO)₂Fe^{II}SiCl₃ (FpSiCl₃) for pentafluorophenyl³⁴ and amido (R⁺RN[–])^{35,36} substituents (Scheme 3.1). It has also been applied to simple silyl group transformations on Ni³⁷ and other group 6–8 transition metals.^{37–44}



Scheme 3.1 Nucleophilic substitution of $-\text{Cl}$ for $-\text{C}_6\text{F}_5$ and $-\text{R}'\text{RN}$ in $(\text{Cl}_3\text{Si})\text{CpFe}(\text{CO})_2$ ^{34,35}

This methodology represents in principle an attractive route to more complex silyl ligands, in part because it avoids the intermediacy of hydrosilanes – which can be subject to undesired rearrangements^{45–51} – and reactive silanides. Here, the synthesis of a range of silyl ligands incorporating pyrrolyl and indolyl substituents by nucleophilic substitution on the Fe-bound SiCl_3 fragment is reported. In particular, it is shown that such substitution reactions are possible on both the neutral Fe(II) complex $\text{Cl}_3\text{Si}-\text{FeCp}(\text{CO})_2$ (**1**) and on the Fe(0) anion $\text{Cl}_3\text{Si}-\text{Fe}(\text{CO})_4^-$ (**2**), the latter being conveniently generated by deprotonation of the corresponding neutral Fe(II) hydride (**3**, Chart 3.1).

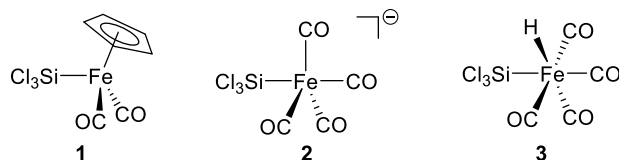


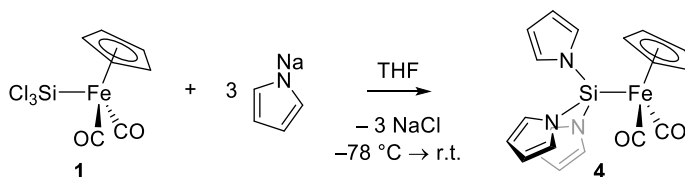
Chart 3.1 Chlorosilyl iron complexes used as precursors for nucleophilic substitution

Results and discussion

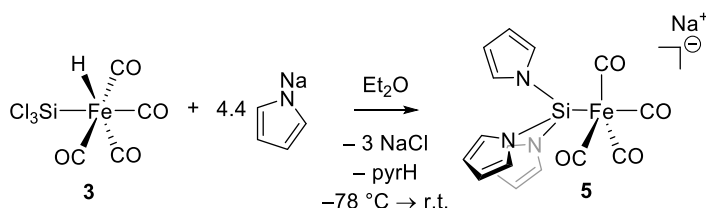
In a first set of experiments, the transformation of the trichlorosilyl ligand into tris-(N-pyrrolyl)silyl was investigated. Complete substitution was achieved on the Fe(II) complex $\text{Cl}_3\text{Si}-\text{FeCp}(\text{CO})_2$ **1**: reaction with 3 equiv sodium pyrrolide produced the trisubstituted complex **4** (Scheme 3.2) resulting in a diagnostic shift of the ^{29}Si NMR resonance from 63.4 to 39.1 ppm. Trisubstitution is evident from the ratio of integrals between the $\text{Pyr}-\text{H}$, and the C_5H_5 ^1H NMR resonances.

In addition, the anionic tris(pyrrolyl)silyl complex Na-5 was accessed by addition of a solution of the hydride complex **3** to 4 equiv sodium pyrrolide in Et_2O at -78°C (Scheme 3.3). Detection of the anionic product by electrospray ionization mass spectrometry (ESI-MS) is straightforward (M^- : $m/z = 393.9943$ a.u., calc'd $m/z = 393.9947$ a.u.), which also provides a convenient way to monitor the reaction. The absence of an Fe–H resonance in the ^1H NMR spectrum indicates that deprotonation has taken place, *i.e.* the fourth equiv of pyrrolide functions as a sacrificial base for deprotonation of **3** to Na-2 . Additionally, the disappearance of the three distinct ^{13}C

NMR resonances around 200 ppm for **3**⁵² and appearance of a single resonance at 217.9 ppm for Na-**5** is consistent with the formation of a fluxional 5-coordinate structure with fast axial-equatorial exchange.^{53–63} The independently synthesized ammonium salt NEt₄-**2**⁵⁴ readily undergoes substitution under the same conditions, showing that nucleophilic substitution is feasible on Cl₃Si bound to Fe(0) and may take place after deprotonation of **3**. From a practical point of view, however, reactions involving NEt₄-**2** are less well-behaved because the counterion is susceptible to Hoffman degradation, *i.e.* 1,2-elimination to give NEt₃, ethylene, and pyrH.



Scheme 3.2 Nucleophilic substitution of chloride for pyrrolide on compound **1**.



Scheme 3.3 Nucleophilic substitution of chloride for pyrrolide on the iron tetracarbonyl complex.

Crystals of Na-**5** suitable for X-ray crystallography were grown by slow diffusion of hexane into a solution of the complex in the presence of benzo-15-crown-5 in THF. The X-ray crystal structure reveals a trigonal bipyramidal (TBP) geometry with the –SiPyr₃ moiety in apical position, as commonly found for analogous phosphine,⁶³ (base stabilised) silylene,^{7,65–84} and silyl^{85–87} iron tetracarbonyl complexes (Figure 3.1). The Si–Fe distance in **5** (2.2576(8) Å) is well in between the extremes, close to the mean for silyl and silylene iron tetracarbonyl complexes (2.1960⁷⁶ < Si–Fe < 2.3630(8),⁸³ <Si–Fe> = 2.2663 Å) and, more generally, of Si–Fe bonds.³⁰ The single precedent of a structurally characterized pyr₃Si-containing complex is Os(SiPyr₃)H(CO)₂(PPh₃)₂·H₂O reported by Hübler et al.³² In this complex, both the N–Si–N angles and the Si–M distance are very similar to those in Na-**5** (see Appendix Table 1). The difference in Si–M distance between the two complexes (0.117 Å) is the same as the difference in covalent radius of iron and osmium (0.12 Å).⁸⁸

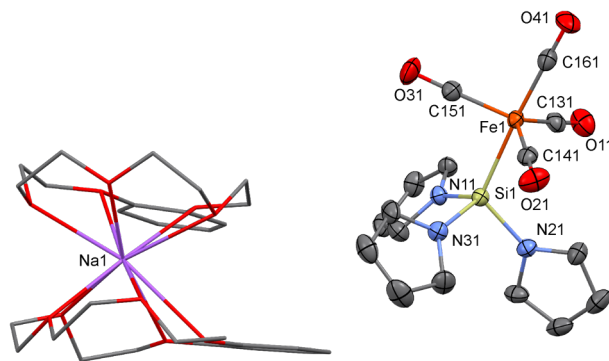


Figure 3.1 Molecular structure of Na-**5** in the crystal. Ellipsoids at 50% probability. Hydrogen atoms were omitted and the counter-ion shown as wireframe for clarity. Selected bond lengths (Å) and angles (°): C151–O31 1.160(4), C161–O41 1.141(4), C131–O11 1.160(4), C141–O21 1.147(4), Fe1–Si1 2.2576(8), Si1–N11 1.771(2), Si1–N21 1.774(2), Si1–N31 1.777(2), N11–Si1–N21 103.2(1), N21–Si1–N31 100.7(1), N31–Si1–N11 99.7(1).

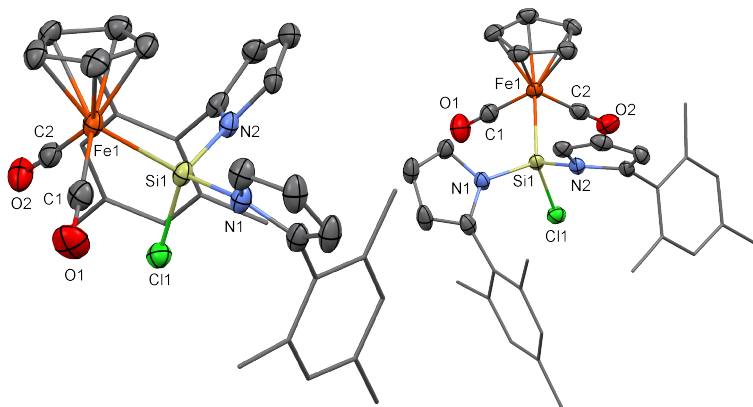
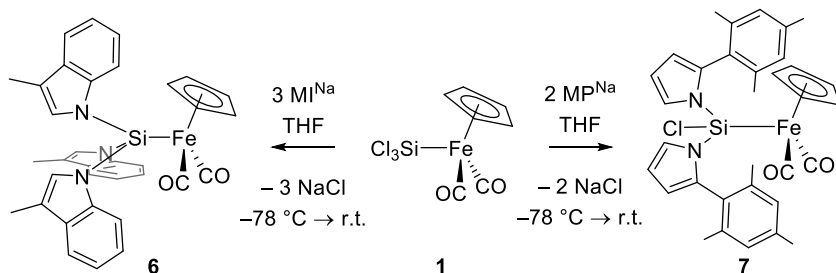


Figure 3.2 Two views of the molecular structure of **7** in the crystal. Ellipsoids at 50% probability. Hydrogen atoms were omitted and mesityl residues shown as wireframe for clarity. Selected bond lengths (Å) and angles (°): C1–O1 1.142(5), C2–O2 1.144(5), Fe1–Si1 2.272(1), Si1–Cl1 2.063(1), Si1–N1 1.787(3), Si1–N2 1.781(3), N1–Si1–Cl1 106.1(1), N1–Si1–N2 103.0(1), N2–Si1–Cl1 105.11(9).

The generality of this substitution for other monodentate heterocycles was investigated. The substitution of chloride for 3-methylindolide (MI) on **1** afforded the trisubstituted **6** (Scheme 3.4), as indicated by a 3:1 ratio of the ^1H NMR resonance integrals of MI with those of the Cp ligand. In contrast, substitution of chloride for the bulkier 2-mesitylpyrrolide (MP) on **1** affords the disubstituted **7** (Scheme 3.4), the structure of which was further confirmed by X-ray crystal structure determination (Figure 3.2). The solid-state structure reveals a piano-stool complex with the silyl ligand as one of the legs. Compared to Na-**5**, the Si–Fe distance is slightly longer ($\Delta d = 0.0144(13)$ Å) and the angle sum of the substituents on silicon is significantly bigger ($314.21(9)$ vs $303.6(17)^\circ$). In solution, compound **7** exhibits three ^1H NMR resonances in a 1:1:1 ratio for the individual methyl-groups on the equivalent mesityl moieties, arising from slow rotation around the $\text{C}_{\text{aryl}}\text{--C}_{\text{pyr}}$ bonds. The energy barriers for

interchanging the methyl groups through rotation around the Si-Fe bond and the C_{aryl}-C_{pyr} bonds were calculated in the gas phase by DFT potential energy surface scan (PES) calculations [see Appendix Figures 3-6].⁸⁹ These calculations show a maximum energy difference of about 8 kcal/mol upon 360° rotation around the Si-Fe bond and of at least 33 kcal/mol upon 180° rotation around either C_{aryl}-C_{pyr} bond. This corroborates the interpretation of the NMR spectrum in terms of a fast rotation around the Si-Fe bond, rendering the mesityl groups equivalent on the NMR time-scale, with magnetically inequivalent methyl groups within a mesityl moiety.



Scheme 3.4 Nucleophilic substitution for 3-methylindole (left) and 2-mesitylpyrrole (right) on **1**.

Table 3.1 ²⁹Si NMR (ppm), IR $\tilde{\nu}(\text{CO})$ (cm⁻¹), crystallographic Si-Fe distance (Å) and the sum of N-Si-N angles (°) of all compounds..

Compound	δ [Si]	$\tilde{\nu}(\text{CO})$	Si-Fe	$\Sigma[\text{N-Si-N}]$
Fp-SiCl₃ (1)	63.4	2033 1985	–	–
(CO)₄Fe-SiCl₃ (2)	67.8	2026 1941 1917	2.233(4)	304.3(6)
Fp-SiPyr₃ (4)	39.1	2021 1970	–	–
(CO)₄Fe-SiPyr₃ (5)	45	2019 1934 1906	2.2576(8)	303.6(2)
Fp-Si(MI)₃ (6)	32.4	2020 1969	–	–
Fp-SiCl(MP)₂ (7)	42.6	2027 1977	2.272(1)	314.2(2)

The series of complexes described herein provides an opportunity to study the effect of substitution on the properties of silyl ligands (Table 3.1). Formal substitution of three chlorides in compound **1** for three pyrrolides in **4** results in a slight shift of the IR bands $\tilde{\nu}_s(\text{CO})$ and $\tilde{\nu}_a(\text{CO})$ to lower energies by 12 and 15 cm⁻¹, respectively, indicating that the pyr₃Si- ligand is slightly more electron donating than the Cl₃Si- analogue. Similarly, the three IR bands associated with CO stretch modes of the Fe(CO)₄ moiety shift slightly from 2026, 1941, and 1917 cm⁻¹ in the Cl₃Si- complex **2** to 2019, 1934, and 1906 cm⁻¹ in the Pyr₃Si- complex **5**. The IR absorptions in the tris-(3-methylindolyl)silyl complex **6** are within 1 cm⁻¹ of those of the tris-pyrrolylsilyl complex **4**, indicating that the net electronegativity of pyr and MI is virtually the same. The $\tilde{\nu}(\text{CO})$ bands of the dipyrrolyl, monochloride complex **7** (2027, 1977 cm⁻¹) are found between those of **1** (2033, 1985 cm⁻¹) and **4** (2021, 1970 cm⁻¹), consistent with intermediate electronic properties between Cl₃Si- and Pyr₃Si-. More generally, the heterocycle silyl ligands in **4**, **6**, and **7** are less donating than Ph₃Si- and Me₃Si- (2001, 1994 cm⁻¹, resp.) and more donating than (C₂F₅)₃Si- and Ph₃P- (2047, 2057 cm⁻¹, resp.) in the corresponding CpFe(CO)₂ complexes (Figure 3.3).

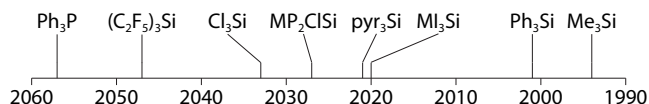


Figure 3.3 Graphical representation of highest $\nu(\text{CO})$ of LCpFe(CO)_2 in cm^{-1} .

As was observed from the effect on $\nu(\text{CO})$, substitution of chloride for pyrrolides increases the overall donor strength of the ligand, which generally arises from a combination of increased σ -basicity and/or decreased π -acidity. Interestingly, the stronger donor Pyr_3Si displays a longer Si-Fe(CO)_4 bond in compound **Na-5** than Cl_3Si in **2** by 0.025 Å. This lengthening indicates a slightly weaker bond, suggesting that π -acidity is important to the Fe–Si bonding in this series of compounds.

The sum of the R–Si–R substituent angles around silicon is found to be less sensitive to the electronegativity of the substituent. Generally speaking, these angles provide a measure for the extent of hybridization of the bonding orbitals: smaller R–Si–R angles indicate more p-character in the Si–R bonding orbitals and consequently more s-character in the Si–M bonding orbital, according to Bent's rule.⁹⁰ In the ideal case, the sum of angles is 328.5° for sp^3 hybridization and 270° for the non-hybridized extreme. The sums of the N–Si–N angles in **Na-5** (303.6(2)°) and **2** (304.3(6)°) are equal within error bounds, but significantly lower than that of the C–Si–C angles in $\text{Me}_3\text{SiFe(CO)}_4^-$ (310.7°),⁸⁷ indicating that electron withdrawing substituents on silicon result in a higher s-character of the σ -bonding orbital. Interestingly, the angles between the substituents on silicon in Fp-based **7** are slightly larger (103–106°) than those in Fe(CO)_4 -based **Na-5** (100–103°), suggesting more p-character in the Si–M bonding orbitals and hence, a less ionic Si–M bond, likely because of the stronger electron-accepting character of the Fe(II) fragment compared to the Fe(0) fragment in **Na-5**.

The ^{29}Si NMR signals in Table 3.1 generally shift towards high field upon substitution of chloride for pyrrolide. Interestingly, the high-field shift observed upon trisubstitution is almost identical on the Fp and Fe(CO)_4 fragments: 24 ppm difference between **1** and **4** vs 23 ppm difference between **2** and **5**. However, the series of Fp complexes (**4**, **6**, **7**) exhibit no straightforward correlation with the donor strength of the ligand: the difference in chemical shift between trisubstituted **4** and disubstituted **7** ($\Delta\delta = 3.5$ ppm) is smaller than that between **4** and the tris-indolyl substituted **6** ($\Delta\delta = 6.7$ ppm), whereas **4** and **6** exhibit indistinguishable donor properties according to $\nu(\text{CO})$. Such non-linearity was also observed by Leis et al.⁶⁹ for a range of HMPA stabilised silylene metal carbonyl complexes ($\text{M} = \text{Fe, Cr, Ru}$; R in $\text{SiR}_2 = t\text{BuO, } t\text{BuS, Me, Cl, 1-AdaO, 2-AdaO, NeopO, TritO, Ph}$). This behaviour has been attributed to a combined influence of diamagnetic and paramagnetic effects on the silicon shift.⁹¹

Overall, the spectroscopic data consistently indicate that pyrrolide and indolide substituents on silicon are electron withdrawing, only slightly less so than chloride,

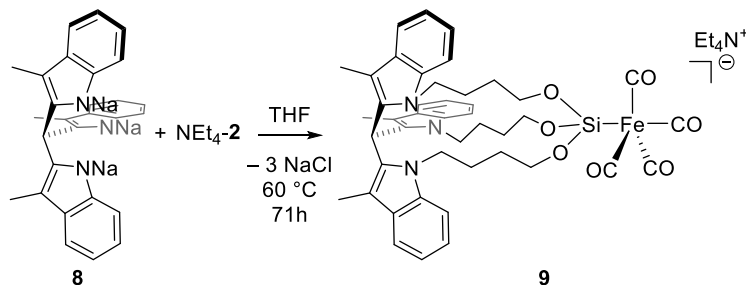
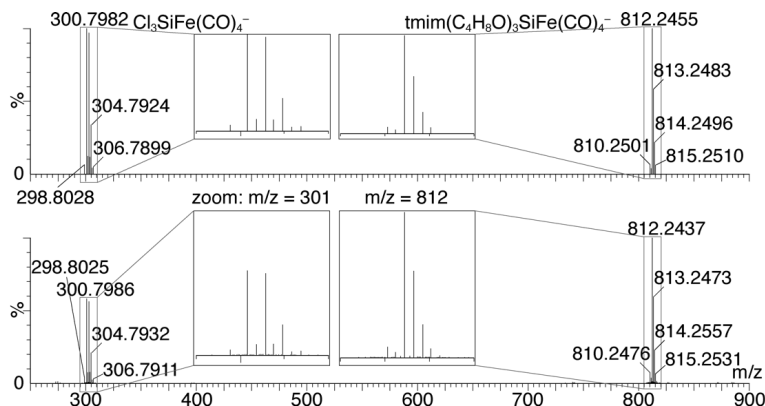
resulting in moderately donating silyl groups. Furthermore, their effect on the electronic properties of the silyl ligand is approximately the same for an anionic Fe(0) and a neutral Fe(II) supporting metal. This suggests that such heterocycles might be used to construct tunable analogues of the SiCl_3 ligand by varying the substitution patterns on the heterocycles.

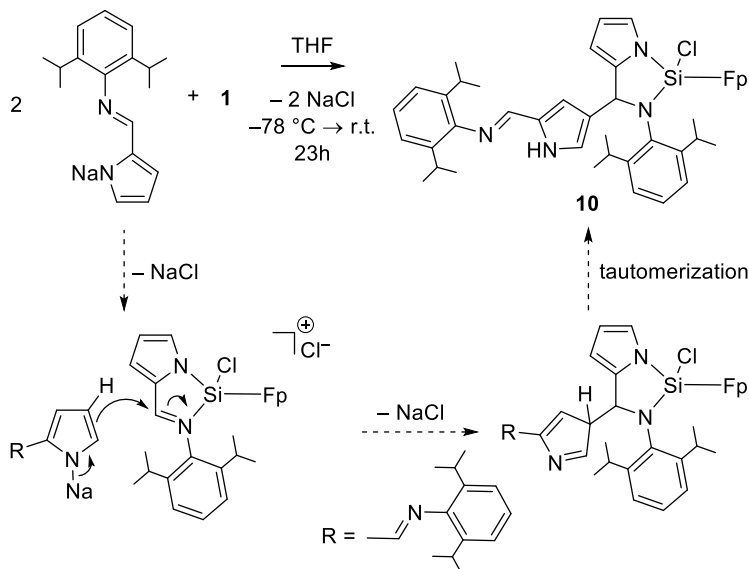
Multidentate N-donors

Having established the substitution at silicon for simple pyrrolide derivatives, the reactivity of multidentate nucleophiles was investigated, starting with the trisodium salt of tris(3-methylindol-2-yl)methane (tmimNa_3 , **8**, Scheme 3.5). The tmim scaffold has previously been shown to form stable phosphine ligands that can be bound to $\text{Fe}(\text{CO})_4$,⁶³ suggesting that a silicon analogue might be accessible. Scaffold tmimH_3 was synthesized according to the literature procedure⁹², followed by deprotonation using NaH. The reaction of **8** with NEt_4 -**2** was initially conducted in THF at 60 °C. Under these conditions, the targeted trisubstitution product could not be detected. In contrast, analysis of the reaction mixture by ESI-MS indicates the presence of an anionic complex incorporating three additional THF molecules at $M^- = 812.2437$ a.u. (Figure 3.4). Interestingly, signals corresponding to the incorporation of one or two THF molecules were not observed, whereas the unsubstituted complex is still present, suggesting that the second and third incorporation of THF are much faster than the first. The corresponding product could unfortunately not be fully isolated, but could be sufficiently enriched to a purity of approx. 70 %, to be analysed by multinuclear NMR (*vide infra*), confirming its identity as the product of triple ring-opening and insertion of THF, compound **9** (Scheme 3.5). In other solvents, the reaction of NEt_4 -**2** and **8** gave unresolved complex mixtures. Additionally, reaction between the neutral precursor **1** and **8** afforded an intractable mixture of products.

The tmim moiety of crude product **9** in CD_3CN gives rise to four resonances in ^1H NMR for the aromatic protons, indicating local 3-fold symmetry (see Appendix Figure 7). Furthermore, the spectrum of the reaction mixture of **9** displays four multiplet signals at $\delta = 3.66$, 3.73, 4.00, and 4.10 ppm which couple in HMQC with two signals in ^{13}C NMR at 44.5 and 61.9 ppm, originating from the diastereotopic protons of N-CH_2 and O-CH_2 . An additional set of three multiplets with a 1:2:1 ratio at $\delta = 1.60$, 1.77, and 2.34 ppm, corresponding to four protons, and coupling with two signals in ^{13}C NMR at 29.1 and 30.7 ppm, originates from the central CH_2 moieties.

We propose that **9** forms through a ring-opening reaction of THF by nucleophilic attack of **8** on the THF α -carbon, presumably preceded by coordination of THF to silicon, making its α -carbon more prone to nucleophilic attack. A related ring opening and incorporation of THF has previously been observed by Okazaki et al.⁹³ in the reaction between $\text{ClSiMe}_2\text{NR}_2$ and the Fp-anion to form $\text{Fp}[\text{CH}_2]_4\text{OSiMe}_2\text{NR}_2$. They explain this by initial coordination of THF to the silane, followed by nucleophilic attack of Fp^- on the α -carbon. Similarly, Dufour et al.⁹⁴ observed ring opening and


$$300.7982 \text{ Cl-SiF}_6(\text{CO})^- \quad \text{tmim}(\text{C}_4\text{H}_9\text{O})\text{-SiF}_6(\text{CO})^- = 812.2$$




Scheme 3.6 Reaction of DippIMP with **1** in THF at $-78^\circ\text{C} \rightarrow \text{r.t.}$, including proposed reaction pathway. $\text{Fp} = \text{Cp}(\text{CO})_2\text{Fe}$.

Finally, the monoanionic bidentate iminopyrrolide substituent DippIMP was investigated as a nucleophile (Scheme 3.6). As the imine functionality in DippIMP is susceptible to intramolecular hydrosilylation, the corresponding hydrosilanes are unsuitable precursors for silyl complexes *via* either deprotonation or oxidative addition.⁴⁷ $\text{DippIMP}^-\text{H}$ was synthesized according to the literature procedure,⁹⁵ followed by deprotonation using NaHMDS. Reaction of either two or three equiv of DippIMPNa with **1** formed the same compound **10**, while reaction of 1 equiv DippIMPNa with **1** afforded a mixture of compounds containing both **1** and **10**. The ^{29}Si NMR resonance of **10** is found at $\delta = 39.4$ ppm, similar to complexes **4**, **6** and **7** (Table 3.1), consistent with substitution at Si taking place. ^1H NMR analysis of **10** indicates that two DippIMP molecules have been incorporated, and that the reaction is more complex than simple disubstitution at silicon. The ^1H NMR spectrum displays five distinct signals for the pyrrole moieties. A COSY spectrum indicates the presence of two distinct pyrrole rings, one with a 3H spin system [$^3J(\text{H},\text{H}) = 2.8$ Hz, $^4J(\text{H},\text{H}) = 1.3$ Hz] and one with a 2H spin system (broad singlets). The weak coupling in the latter suggests at least $^4J(\text{H},\text{H})$ -coupling between them. Moreover, both spin systems are in a 1:1 ratio with the Cp group, indicating the presence of 2 pyrrole moieties for one metal center. Interestingly, the presence of a resonance at $\delta = 9.63$ ppm suggests that the product contains an N–H bond. Finally, a singlet resonance in ^1H NMR at $\delta = 5.75$ ppm accounting for 1H and coupling with an sp^3 -carbon at $\delta = 61.9$ ppm indicates the presence of an $\text{sp}^3\text{-CHN}$ fragment. The data outlined above collectively support the assignment of **10** as the C–C coupled structure depicted in Scheme 3.6. The *i*Pr residues give rise to 3 septets in a 1:1:2 ratio and 5 doublets in 1:1:1:1:4 ratio,

suggesting hindered rotation around the $C_{\text{aryl}}-N_{\text{amine}}$ bond and free rotation around the $C_{\text{aryl}}-N_{\text{imine}}$ bond. In ^{13}C NMR two resonances appear for the carbonyl carbons, which suggests that the substituent is bound to silicon in a bidentate fashion, rendering the silicon atom chiral and hence the carbonyls diastereotopic. The structure inferred from NMR was confirmed by the crystal structure (Figure 3.5). Crystals suitable for X-ray crystallography were grown by slow diffusion of hexane into a THF solution. The N–Si distance is smaller for the former imine (N21–Si) than for the pyrrole substituent (N11–Si), likely due to hyperconjugation of the N21 lone pair into Si, as opposed to N11, where the lone pair is delocalized in the aromatic system. The sum of N–Si–N angles ($304.4(1)^\circ$) is small compared to **7**, due to the 5-membered ring system. As a result, the amount of *s*-character in the Si–Fe bond is higher, resulting in a shorter distance (**10**: 2.2455(8), **7**: 2.272(1) Å).

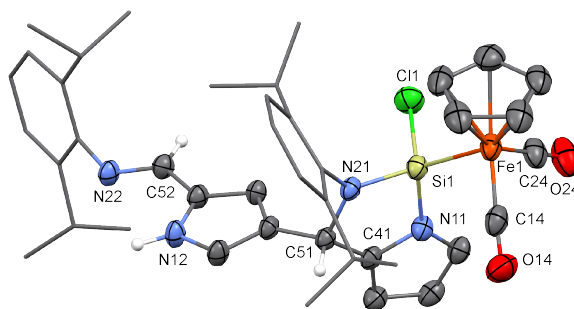


Figure 3.5 Molecular structure of **10** in the crystal. Ellipsoids at 50% probability. Hydrogen atoms and co-crystallised hexane were omitted and diisopropylphenyl residues shown as wireframe for clarity. Selected bond lengths (Å) and angles ($^\circ$): Fe1–Si1 2.2455(8), C14–O14 1.140(4), C24–O24 1.145(4), Si1–Cl1 2.1142(9), Si1–N11 1.761(2), Si1–N21 1.724(2), N21–C51 1.493(3), N22–C52 1.275(3), N21–Si1–N11 91.39(9), N11–Si1–Cl1 102.31(7), N21–Si1–Cl1 110.74(7).

The formation of complex **10** is consistent with initial substitution of two chlorides by one DippIMP , forming an overall cationic complex bearing an iminopyrrolide chlorosilylene ligand (Scheme 3.6). Activation of the imine through coordination to the electron-poor silicon would then facilitate nucleophilic attack of a second DippIMP anion. The preference for the 4-position is likely sterically driven. The formation of **10** is kinetically competitive with that of the intermediate, preventing isolation of the latter.

Conclusions

A series of silyl iron complexes with N-heterocyclic substituents was synthesized by nucleophilic substitution of the chlorides of a metal-bound trichlorosilyl ligand. This method affords homoleptic silyl ligands with unencumbered substituents such as pyrrol-1-yl ($\text{pyr}_3\text{Si-}$) and 3-methylindol-1-yl ($(\text{MI})_3\text{Si-}$), and the heteroleptic silyl ligand $(\text{MP})_2\text{ClSi-}$ with the bulkier 2-mesitylpyrrol-1-yl. The ligands were found to be slightly more electron-donating than $\text{Cl}_3\text{Si-}$, which makes them moderately electron donating and electronically and sterically tunable. Attempts to expand this

methodology to multidentate nucleophiles (tmim, ^{Dipp}IMP) lead to more complex reactivity pathways. The synthesis method described here offers an interesting alternative to common methods of silyl-complex synthesis.

Experimental Section

All reactions involving silicon-containing compounds were conducted under an N₂ atmosphere by using standard glovebox or Schlenk techniques. Diethyl ether, n-hexane, toluene, and acetonitrile were dried with an MBRAUN MB SPS-79 system, degassed by bubbling with N₂ for 30 min, and stored over molecular sieves in a glovebox. THF was distilled from benzophenone/Na, degassed by bubbling with N₂ for 30 min, and stored over molecular sieves in a glovebox. All chemicals were obtained commercially and used as received unless stated otherwise. All NMR chemical shifts are reported relative to TMS with the residual solvent signal as internal standard.⁹⁶ All NMR experiments involving silicon-containing compounds were conducted in J-Young NMR tubes under an N₂ atmosphere. IR spectra were recorded on a Perkin-Elmer Spectrum Two FT-IR spectrometer. ESI-MS measurements were performed on a Waters LCT Premier XE KE317 spectrometer. Elemental analysis was conducted by the Mikroanalytisches Laboratorium Kolbe. Ph₄PCl was dried according to the method described in purification of laboratory chemicals.⁹⁷ The following compounds were synthesized according to literature procedures: Cl₃SiFe(H)(CO)₄ (**3**),^{29,98} NEt₄[Cl₃SiFe(CO)₄] (**2**),⁶⁴ Cl₃SiCpFe(CO)₂ (**1**),^{43,99,100} ^{Dipp}IMPH,⁹⁵ (tmim)₃ (**8**).⁹²

Computational methods

Calculations were performed using Gaussian09, Revision D.01.⁸⁹ All structures were optimized using the TPSS functional with the TZVP basis set. The absence of negative eigenvalues was confirmed for all structures. On the optimized geometries, potential energy surface scans were conducted using the Modredundant method implemented in Gaussian09.

Syntheses

Synthesis of (pyr₃Si)CpFe(CO)₂ (4**).** A pre-cooled THF (1 mL) solution of **1** (39 mg, 0.13 mmol) was added to a pre-cooled THF (4 mL) solution of sodium pyrrolide (33 mg, 0.37 mmol) at -78 °C. The vial was rinsed with THF (1 mL) and the solution added to the mixture, which was allowed to warm to r.t. over 20 h. The solvent was evaporated, toluene (2 mL) was added to the residue, and the solvent was evaporated again to remove most of the residual THF. The mixture was extracted with toluene (2 x 2 mL) and the solvent was removed *in vacuo*. Analytically pure material (44 mg, 0.11 mmol, 87%) was obtained by precipitation from toluene (2 mL) with hexane (12 mL), storage at -35 °C for 20 h and removal of the supernatant. ¹H NMR (400 MHz, C₆D₆, 25 °C) δ = 6.80 [t', ²J(H,H) = 2.0 Hz, ³J(H,H) = 2.0 Hz, 6H, pyrrole-Hα], 6.44 [t', ²J(H,H) = 2.0 Hz, ³J(H,H) = 2.0 Hz, 6H, pyrrole-Hβ], 3.89 ppm [s, 5H]; ¹³C NMR (101 MHz, C₆D₆, 25 °C) δ = 212.4 (CO), 124.5 (pyrrole), 112.4 (pyrrole), 84.6 ppm (Cp); ²⁹Si NMR (79 MHz, C₆D₆, 25 °C) δ = 39.1 ppm; IR (THF): $\tilde{\nu}$ = 2021, 1970 cm⁻¹; Anal. calc'd C₁₉H₁₇FeN₃O₂Si: C 56.59, H 4.25, N 10.42 %; found C 56.57, H 4.29, N 10.37.

Synthesis of [(pyr₃Si)Fe(CO)₄]⁻Na⁺ (5**).** A Et₂O (6 mL) solution of **3** (96 mg, 0.32 mmol) was added dropwise to a pre-cooled suspension of NaPyr (127 mg, 1.44 mmol) in Et₂O (5 mL) at -79 °C, resulting in a pink solution. The mixture was allowed to warm to r.t. and was stirred for another 15 minutes, during which a white precipitate formed. Removal of the precipitate by filtration and concentration *in vacuo* afforded a pink powder (102 mg, 0.26 mmol, 77%). Crystals suitable for X-ray crystallography were grown by slow diffusion of hexane into a concentrated solution of **5** in THF in the presence of benzo-15-crown-5. ¹H NMR (400 MHz, C₆D₆ + C₄H₈O, 25 °C): δ = 7.13 [t', ²J(H,H) = 2.0 Hz, ³J(H,H) = 2.0 Hz, 6H, pyrrole-Hα], 6.36 ppm [t', ²J(H,H) = 2.0 Hz, ³J(H,H) = 2.0 Hz, 6H, pyrrole-Hβ]; ¹³C NMR (101 MHz, C₆D₆ + C₄H₈O, 25 °C) δ = 217.9 (CO), 125.5 (pyrrole), 110.5 ppm (pyrrole); ²⁹Si NMR (79 MHz, C₆D₆ + C₄H₈O, 25 °C) δ = 45.0 ppm; ESI-MS: M⁻: m/z = 393.9943 a.u., calc'd m/z = 393.9947 a.u.; IR (THF): $\tilde{\nu}$ = 2019m, 1934m, 1906s cm⁻¹; The presence of solvation THF in the solid hampered

the determination of anal., which was therefore determined on the crystallized [benzo-15-crown-5]₂Na salt: anal. calc'd C₄₄H₅₂FeN₃NaO₁₄Si: C 55.41, H 5.50, N 4.41 %; found C 55.12, H 5.61, N 4.51 %.

Synthesis of [(MI)₃Si]CpFe(CO)₂ (MI = 3-methylindolyl, **6).** A pre-cooled THF (1 mL) solution of **1** (52 mg, 0.17 mmol) was added to a pre-cooled THF (4 mL) solution of sodium 3-methylindolide [MI^{Na}, 111 mg, 0.500 mmol] at -78 °C. The flask was rinsed with THF (1 mL) and the solution added to the mixture, which was allowed to warm to r.t. and stirred for 20 h. The solvent was evaporated, toluene (2 mL) was added to the residue, and the solvent was evaporated again to remove most of the residual THF. The mixture was extracted with toluene (2 x 2 mL) and the solvent was removed *in vacuo*. Analytically pure material (90 mg, 0.15 mmol, 91%) was obtained by trituration of the solid with hexane (2 mL) and drying *in vacuo*. ¹H NMR (400 MHz, C₆D₆, 25 °C): δ = 7.54 (ddd, ³J(H,H) = 7.8 Hz, ⁴J(H,H) = 1.3 Hz, ⁵J(H,H) = 0.8 Hz, 3H, indole-H7), 7.46 (dt, ³J(H,H) = 8.3 Hz, ⁴J(H,H) = 0.9 Hz, 3H, indole-H4), 7.19 [‘q’, ⁴J(H,H) = 1.0 Hz, 3H, indole-H2), 7.10 (ddd, ³J(H,H) = 7.9 Hz, ³J(H,H) = 7.1 Hz, ⁴J(H,H) = 1.0 Hz, 3H, indole-H6), 6.98 (ddd, ³J(H,H) = 8.4 Hz, ³J(H,H) = 7.1 Hz, ⁴J(H,H) = 1.3 Hz, 3H, indole-H5), 3.79 (s, 5H, Cp), 2.18 ppm (d, ⁴J(H,H) = 1.2 Hz, 9H, CH₃). ¹³C NMR (101 MHz, C₆D₆, 25 °C): δ = 213.5 [CO], 141.0, 133.2, 122.8, 121.1, 119.6, 115.8, 115.1, 84.9 [Cp], 10.0 ppm [CH₃]; ²⁹Si NMR (79 MHz, C₆D₆, 25 °C) δ = 32.4 ppm; IR (THF): $\tilde{\nu}$ = 2020, 1969 cm⁻¹; Anal. calc'd C₃₄H₂₉FeN₃O₂Si: C 68.57, H 4.91, N 7.06 %; found C 68.22, H 5.27, N 6.74 %.

Synthesis of [(MP)₂ClSi]CpFe(CO)₂ (MP = 2-mesitylpyrrolyl, **7).** A pre-cooled THF (1 mL) solution of **1** (72 mg, 0.23 mmol) was added to a pre-cooled THF (4 mL) solution of sodium 2-mesitylpyrrolide [MP^{Na}] (96 mg, 0.46 mmol) at -78 °C, the flask was rinsed with THF (1 mL) and the solution added to the mixture, which was allowed to warm to r.t. over 20h. The solvent was evaporated, toluene (1 mL) was added to the residue, and the solvent was evaporated again to remove most of the residual THF. The mixture was extracted with toluene (2 x 2 mL) and the solvent was removed *in vacuo*. Analytically pure material (85 mg, 0.14 mmol, 60%) was obtained by trituration of the solid with hexane (2x1 mL). Crystals suitable for X-ray crystallography were grown by storing a concentrated solution of **7** in hexane at -35 °C. ¹H NMR (400 MHz, C₆D₆, 25 °C): δ = 6.83 (bs, 2H, Ar-H), 6.78 (dd, ³J(H,H) = 3.0 Hz, ⁴J(H,H) = 1.5 Hz, 2H, pyrrole-H5), 6.75 (s, 2H, Ar-H), 6.46 [‘t’, ³J(H,H) = 3.0 Hz, 2H, pyrrole-H4), 6.20 (dd, ³J(H,H) = 3.0 Hz, ⁴J(H,H) = 1.5 Hz, 2H, pyrrole-H3), 4.00 (s, 5H, Cp), 2.21 (s, 6H, Ar-CH₃), 2.16 (s, 6H, Ar-CH₃), 2.04 ppm (s, 6H, Ar-CH₃); ¹³C NMR (101 MHz, C₆D₆, 25 °C): δ = 212.1 [CO], 140.5, 139.3, 137.8, 137.3, 132.6, 128.5, 127.9, 126.6, 114.7, 111.5, 85.1 [Cp], 21.9 [Ar-CH₃], 21.7 [Ar-CH₃], 21.2 ppm [Ar-CH₃]; ²⁹Si NMR (79 MHz, C₆D₆, 25 °C) δ = 42.6 ppm; IR (THF): $\tilde{\nu}$ = 2027 [CO], 1977 [CO] cm⁻¹; ESI-MS (THF, NEt₄Cl ionizing agent): [M-CO+Cl]⁻: m/z = 615.1183 a.u., calc'd m/z = 615.1090 a.u.

Synthesis of (tmim)Na₃ (Na-8). A solution of **8** (4.95 g, 12.3 mmol) in THF (10 mL) was added to pre-washed (hexane 3 x 5 mL & THF 5 mL) NaH (60% in oil, 2.07 g, 52 mmol) under THF (20 mL) over 15 minutes and stirred for 2.75 h. The excess NaH was removed by filtration and the orange [green luminescent] filtrate was freed of solvent *in vacuo*, yielding a yellow powder (8.46 g, quantitative). Analysis by ¹H NMR showed only (tmim)Na₃ and THF (~30 w%). A titration with HCl (0.1 M in H₂O) on a sample (100.4 mg) in a mixture of THF (4mL) and water (1 mL) was performed to determine the base content, which was consistent with 68.4 w% (tmim)Na₃. This value was used for stoichiometry calculations in subsequent experiments. ¹H NMR (400 MHz, CD₃CN, 25 °C): δ = 7.19 (m, 6H, ArH), 6.62 (m, 6H, ArH), 6.25 (s, 1H, R₃CH), 2.41 ppm (s, 9H, CH₃). ¹³C NMR (101 MHz, CD₃CN, 25 °C): δ = 151.4, 146.0, 132.4, 116.6, 116.2, 115.3, 114.8, 101.8, 37.7 [R₃CH], 10.1 ppm [CH₃].

Synthesis of tmim[C₄H₈O]₃SiFe(CO)₄⁻ Et₄N⁺ (9**).** A solution of Na-**8** (159 mg, 28 w% THF, 0.25 mmol) and **2** (104 mg, 0.240 mmol) in THF (20 mL) was stirred at 60 °C for 72 h. Filtration and evaporation provided 253 mg solid. Precipitation of most of the impurities with Et₂O from THF yielded, after filtration and evaporation of the filtrate, 123 mg material of approx. 70% purity [91.3 μmol, 38%], with minor impurities that could not be identified. ¹H NMR (400 MHz, CD₃CN, 25 °C): δ = 7.45 (d, ³J(H,H) = 8.1 Hz, 3H, indole-H), 7.40 (d, ³J(H,H) = 8.5 Hz, 3H, indole-H), 7.19 [‘t’, ³J(H,H) = 7.7 Hz, 3H, indole-H), 7.06 [‘t’, ³J(H,H) = 7.5 Hz, 3H, indole-H), 6.08 (s, 1H, R₃CH), 4.17 – 4.04 (m, 3H, N-CH₂ or O-CH₂), 4.04 – 3.95 (m, 3H, N-CH₂ or O-CH₂), 3.79 – 3.57 (m, 6H, N-CH₂ or O-CH₂), 3.15 (q, ³J(H,H) = 7.2

Hz, 8H, N(CH₂CH₃)₄), 2.33 (bs, 3H, CH₂), 1.76 (m, 6H, CH₂), 1.61 (m, 3H, CH₂), 1.41 (s, 9H, indole-CH₃), 1.25 – 1.16 ppm (tt, ³J(H,H) = 7.2 Hz, ³J_{HN} = 1.7 Hz, 12H, N(CH₂CH₃)₄); ¹³C NMR (101 MHz, CD₃CN, 25 °C): δ = 220.0 (CO), 136.6 (indole-C), 132.2 (indole-C), 129.8 (indole-C), 122.6 (indole-CH), 119.7 (indole-CH), 119.2 (indole-CH), 111.1 (indole-C), 110.2 (indole-CH), 61.9 (N-CH₂ or O-CH₂), 53.1 (¹J_{CN} = 3.1 Hz, N(CH₂CH₃)₄), 44.5 (N-CH₂ or O-CH₂), 35.9 (R₃CH), 30.7 (CH₂), 29.1 (CH₂), 7.7 (N(CH₂CH₃)₄), 7.1 ppm (indole-CH₃); IR (ATR): $\tilde{\nu}$ = 1998, 1903, 1877, 1866 cm⁻¹.

Synthesis of 2-[(2,6-diisopropylphenyl)iminomethyl]pyrrolide sodium (DippIMP^{Na}). A THF (10 mL) solution of DippIMPH (766 mg, 3.01 mmol) was added to a suspension of NaHMDS (523 mg, 2.85 mmol) in THF (10 mL) and stirred for 30 minutes. The solvent was removed *in vacuo* and the solid washed with hexane (3 x 2 mL) and dried *in vacuo* to yield a white powder (803 mg, 18 w% THF, 2.38 mmol, 84%). ¹H NMR (400 MHz, C₆D₆, 25 °C): δ = 8.07 (d, ⁴J(H,H) = 0.9 Hz, 1H, N=CH), 7.45 ('q', ³J(H,H) = 1.2 Hz, ⁴J(H,H) = 1.2 Hz, ⁴J(H,H) = 1.2 Hz, 1H, pyrrole-H3), 7.19, 7.13 (AB₂ pattern, J_{AB} = 7.84 Hz, 3H, Ar-H), 7.02 (dd, ³J(H,H) = 3.3 Hz, ⁴J(H,H) = 1.2 Hz, 1H, pyrrole-H5), 6.69 (dd, ³J(H,H) = 3.3 Hz, ³J(H,H) = 1.5 Hz, 1H, pyrrole-H4), 3.38 (hept, ³J(H,H) = 6.9 Hz, 2H, *i*Pr-H), 1.22 ppm (d, ³J(H,H) = 6.9 Hz, 12H, *i*Pr-CH₃); ¹³C NMR (101 MHz, C₆D₆ + C₄D₈O, 25 °C): δ = 160.4, 151.7, 140.2, 139.3, 136.3, 123.8, 123.4, 120.9, 111.3, 28.2, 24.4 ppm.

Synthesis of DippIMP-DippAMPSi(CI)CpFe(CO)₂ (L'-LSi(CI)Fp, 10). A pre-cooled THF (0.25 mL) solution of DippIMP^{Na} (28 mg, 79 μmol) was added to a pre-cooled THF (1 mL) solution of **1** (12 mg, 39 μmol) at -78 °C, the flask was rinsed with THF (0.25 mL) and the solution added to the mixture, which was allowed to warm to r.t. over 20 h. Evaporation of the solvent *in vacuo*, trituration with hexane, and drying *in vacuo* yielded the product (10 mg, 13 μmol, 35%) ¹H NMR (400 MHz, C₆D₆ + C₄D₈O, 25 °C) δ = 9.63 (bs, 1H), 7.61 (bs, 1H, N=CH), 7.34 (dd, ³J(H,H) = 2.6, ⁴J(H,H) = 1.0 Hz, 1H, L-pyrrole-H5), 7.13-7.00 (m, 6H, Ar-H), 6.64 ('t', ³J(H,H) = 2.9 Hz, 1H, L-pyrrole-H4), 6.56 (bs, 1H, L'-pyrrole-H), 6.46 (bs, 1H, L'-pyrrole-H), 6.21 (d't', ³J(H,H) = 2.9, ⁴J(H,H) = 1.0 Hz, 1H, L-pyrrole-H3), 5.75 (s, 1H, N-CH), 4.11 (s, 5H, Cp), 3.95 (sept, ³J(H,H) = 6.7 Hz, 1H, L-*i*Pr-H), 3.34 (sept, ³J(H,H) = 6.8 Hz, 1H, L-*i*Pr-H), 3.12 (sept, ³J(H,H) = 6.7 Hz, 2H, L'-*i*Pr-H), 1.38 (d, ³J(H,H) = 6.7 Hz, 3H, L-*i*Pr-CH₃), 1.23 (d, ³J(H,H) = 6.7 Hz, 3H, L-*i*Pr-CH₃), 1.17 ('t', ³J(H,H) = 6.7 Hz, 15H, L-*i*Pr-CH₃ + 4L'-*i*Pr-CH₃), 0.60 ppm (d, ³J(H,H) = 6.7 Hz, 3H, L-*i*Pr-CH₃); ¹³C NMR (101 MHz, C₆D₆ + C₄D₈O, 25 °C) δ = 213.3 (CO), 211.3 (CO), 152.4, 150.9, 149.3, 141.6, 139.2, 138.3, 128.7, 127.3, 125.4, 124.4, 124.2, 123.2, 122.7 (L'-pyrrole-CH), 117.1 (L-pyrrole-C5), 116.8 (L'-pyrrole-CH), 115.8 (L-pyrrole-C4), 104.0 (L-pyrrole-C3), 84.3 (Cp), 61.9 (N-CH), 28.9 (L-*i*Pr-CH), 28.3 (L'-*i*Pr-CH), 28.0 (L-*i*Pr-CH), 27.9 (L-*i*Pr-CH₃), 25.6 (L-*i*Pr-CH₃), 25.1 (L-*i*Pr-CH₃), 23.7 (L'-*i*Pr-CH₃), 23.7 ppm (L'-*i*Pr-CH₃); ²⁹Si NMR (79 MHz, C₆D₆ + C₄D₈O, 25 °C) δ = 39.4 ppm.

References

- [1] Benedek, Z.; Szilvási, T. *RSC Adv.* **2015**, *5*, 5077–5086.
- [2] Skell, P. S.; Goldstein, E. J. *J. Am. Chem. Soc.* **1964**, *86*, 1442–1443.
- [3] Denk, M.; Lennon, R.; Hayashi, R.; West, R.; Belyakov, A. V.; Verne, H. P.; Haaland, A.; Wagner, M.; Metzler, N. *J. Am. Chem. Soc.* **1994**, *116*, 2691–2692.
- [4] Blom, B.; Stoelzel, M.; Driess, M. *Chem. Eur. J.* **2013**, *19*, 40–62.
- [5] Asay, M.; Jones, C.; Driess, M. *Chem. Rev.* **2011**, *111*, 354–396.
- [6] Sen, S. S.; Khan, S.; Samuel, P. P.; Roesky, H. W. *Chem. Sci.* **2012**, *3*, 659–682.
- [7] Zybail, C.; Müller, G. *Angew. Chemie Int. Ed.* **1987**, *26*, 669–670.
- [8] Raouf moghaddam, S.; Zhou, Y. P.; Wang, Y.; Driess, M. *J. Organomet. Chem.* **2016**, *829*, 2–10.
- [9] Zhang, M.; Liu, X.; Shi, C.; Ren, C.; Ding, Y.; Roesky, H. W. *Z. Anorg. Allg. Chem.* **2008**, *634*, 1755–1758.
- [10] Blom, B.; Gallego, D.; Driess, M. *Inorg. Chem. Front.* **2014**, *1*, 134–148.
- [11] Fürstner, A.; Krause, H.; Lehmann, C. W. *Chem. Commun.* **2001**, *80*, 2372–2373.
- [12] Li, H.; Hope-Weeks, L. J.; Krempner, C. *Chem. Commun.* **2011**, *47*, 4117–4119.
- [13] Li, H.; Hung-Low, F.; Krempner, C. *Organometallics* **2012**, *31*, 7117–7124.
- [14] McNerney, B.; Whittlesey, B.; Krempner, C. *Eur. J. Inorg. Chem.* **2011**, *2011*, 1699–1702.

- [15] Styra, S.; González-Gallardo, S.; Armbruster, F.; Oña-Burgos, P.; Moos, E.; Vonderach, M.; Weis, P.; Hampe, O.; Grün, A.; Schmitt, Y.; Gerhards, M.; Menges, F.; Gaffga, M.; Niedner-Schatteburg, G.; Breher, F. *Chem. Eur. J.* **2013**, *19*, 8436–8446.
- [16] Metsänen, T. T.; Gallego, D.; Szilvási, T.; Driess, M.; Oestreich, M. *Chem. Sci.* **2015**, *6*, 7143–7149.
- [17] Vicent, C.; Mas-marza, E.; Sanau, M.; Peris, E. *Organometallics* **2006**, *25*, 3713–3720.
- [18] Roy, A. K.; Taylor, R. B. *J. Am. Chem. Soc.* **2002**, *124*, 9510–9524.
- [19] Sekiguchi, A.; Lee, V. Y.; Nanjo, M. *Coord. Chem. Rev.* **2000**, *210*, 11–45.
- [20] Tamao, K.; Kawachi, A. *Adv. Organomet. Chem.* **1995**, *38*, 1–58.
- [21] Lickiss, P. D.; Smith, C. M. *Coord. Chem. Rev.* **1995**, *145*, 75–124.
- [22] Kleeberg, C.; Cascarano, G.; Giacomazzo, C.; Guagliardi, A.; Nudelmann, A.; Stoltz, B. M.; Bercaw, J. E.; Goldberg, K. I. *Dalton Trans.* **2013**, *42*, 8276–8287.
- [23] Präsang, C.; Scheschkewitz, D. In *Structure and Bonding*; 2013; Vol. 156, pp 1–47.
- [24] Schwarze, N.; Steinhauer, S.; Neumann, B.; Stammler, H.-G.; Hoge, B. *Angew. Chemie Int. Ed.* **2016**, *55*, 16156–16160.
- [25] Armbruster, F.; Fernández, I.; Breher, F. *Dalton Trans.* **2009**, *29*, 5612.
- [26] Korogodsky, G.; Bendikov, M.; Bravo-Zhivotovskii, D.; Apeloig, Y. *Organometallics* **2002**, *21*, 3157–3161.
- [27] Turnblom, E. W.; Boettcher, R. J.; Mislow, K. *J. Am. Chem. Soc.* **1975**, *97*, 1766–1772.
- [28] Becker, B.; Corriu, R. J. P.; Guérin, C.; Henner, B. J. L. *J. Organomet. Chem.* **1989**, *369*, 147–154.
- [29] Graham, W. A. G.; Jetz, W. *Inorg. Chem.* **1971**, *10*, 4–9.
- [30] Corey, J. Y.; Braddock-Wilking, J. *Chem. Rev.* **1999**, *99*, 175–292.
- [31] Corey, J. Y. *Chem. Rev.* **2016**, *116*, 11291–11435.
- [32] Hübler, K.; Roper, W. R.; Wright, L. J. *Organometallics* **1997**, *16*, 2730–2735.
- [33] Bentham, J. E.; Cradock, S.; Ebsworth, E. A. V. *J. Chem. Soc. A* **1971**, 587–593.
- [34] Clark, H. C.; Rake, A. T. *J. Organomet. Chem.* **1974**, *74*, 29–42.
- [35] Höfler, M.; Scheuren, J.; Weber, G. *J. Organomet. Chem.* **1974**, *78*, 347–355.
- [36] Thum, G.; Malisch, W. *J. Organomet. Chem.* **1984**, *264*, C5–C9.
- [37] Choe, S.-B.; Schneider, J. J.; Klabunde, K. J.; Radonovich, L. J.; Ballintine, T. A. *J. Organomet. Chem.* **1989**, *376*, 419–439.
- [38] Albrecht, M.; Kwok, W. H.; Lu, G. L.; Rickard, C. E. F.; Roper, W. R.; Salter, D. M.; Wright, L. J. *Inorg. Chim. Acta* **2005**, *358*, 1407–1419.
- [39] Clark, G. R.; Lu, G.-L.; Rickard, C. E. F.; Roper, W. R.; Wright, L. J. *J. Organomet. Chem.* **2005**, *690*, 3309–3320.
- [40] Hübler, K.; Hunt, P. A.; Maddock, S. M.; Rickard, C. E. F.; Roper, W. R.; Salter, D. M.; Schwerdtfeger, P.; Wright, L. J. *Organometallics* **1997**, *16*, 5076–5083.
- [41] Kwok, W. H.; Lu, G. L.; Rickard, C. E. F.; Roper, W. R.; Wright, L. J. *J. Organomet. Chem.* **2004**, *689*, 2511–2522.
- [42] Freeman, S. T. N.; Lofton, L. L.; Lemke, F. R. *Organometallics* **2002**, *21*, 4776–4784.
- [43] Malisch, W.; Kuhn, M. *Chem. Ber.* **1974**, *107*, 2835–2851.
- [44] Wachtler, U.; Malisch, W.; Kolba, E.; Matreux, J. *J. Organomet. Chem.* **1989**, *363*, C36–C40.
- [45] Kertsus-Banchik, E.; Kalikhman, I.; Gostevskii, B.; Deutsch, Z.; Botoshansky, M.; Kost, D. *Organometallics* **2008**, *27*, 5285–5294.
- [46] Novák, M.; Dostál, L.; Alonso, M.; De Proft, F.; Růžička, A.; Lyčka, A.; Jambor, R. *Chem. Eur. J.* **2014**, *20*, 2542–2550.
- [47] Witteman, L.; Evers, T.; Shu, Z.; Lutz, M.; Klein Gebbink, R. J. M.; Moret, M.-E. *Chem. Eur. J.* **2016**, *22*, 6087–6099.
- [48] Fester, G. W.; Eckstein, J.; Gerlach, D.; Brendler, E.; Kroke, E. *Inorg. Chem.* **2010**, *49*, 2667–2673.
- [49] Lippe, K.; Gerlach, D.; Kroke, E.; Wagler, J. *Organometallics* **2009**, *28*, 621–629.
- [50] Novák, M.; Dostál, L.; Turek, J.; Alonso, M.; De Proft, F.; Růžička, A.; Jambor, R. *Chem. Eur. J.* **2016**, *22*, 5620–5628.
- [51] Novák, M.; Hošnová, H.; Dostál, L.; Glowacki, B.; Jurkschat, K.; Lyčka, A.; Ruzickova, Z.; Jambor, R. *Chem. Eur. J.* **2017**, *23*, 3074–3083.

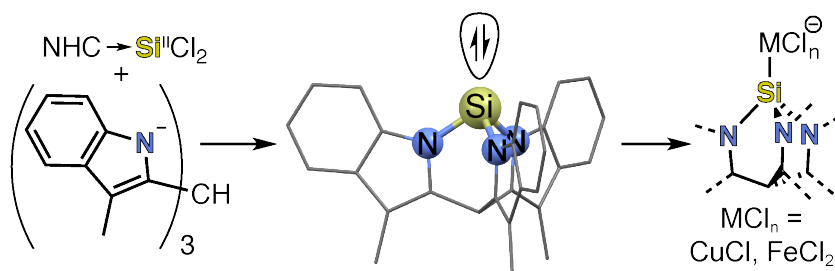
- [52] Connolly, J. W.; Hatlee, M. J.; Cowley, A. H.; Sharp, P. R. *Polyhedron* **1991**, *10*, 841–849.
- [53] Udovich, C. A.; Clark, R. J.; Haas, H. *Inorg. Chem.* **1969**, *8*, 1066–1072.
- [54] Mann, B. E. *J. Chem. Soc., Chem. Commun.* **1971**, 1173–1174.
- [55] Shapley, J. R.; Osborn, J. A. *Acc. Chem. Res.* **1973**, *6*, 305–312.
- [56] Rossi, A. R.; Hoffmann, R. *Inorg. Chem.* **1975**, *14*, 365–374.
- [57] Whitmire, K. H.; Lee, T. R. *J. Organomet. Chem.* **1985**, *282*, 95–106.
- [58] Gansow, O. A.; Burke, A. R.; Vernon, W. D. *J. Am. Chem. Soc.* **1972**, *94*, 2550–2552.
- [59] Cotton, F. A.; Troup, J. M. *J. Am. Chem. Soc.* **1974**, *96*, 3438–3443.
- [60] Jesson, J. P.; Meakin, P. *J. Am. Chem. Soc.* **1973**, *95*, 1344–1346.
- [61] Howell, J. A. S.; Palin, M. G.; McArdle, P.; Cunningham, D.; Goldschmidt, Z.; Gottlieb, H. E.; Hezroni-Langerman, D. *Inorg. Chem.* **1991**, *30*, 4683–4685.
- [62] Howell, J. A. S.; Palin, M. G.; McArdle, P.; Cunningham, D.; Goldschmidt, Z.; Gottlieb, H. E.; Hezroni-Langerman, D. *Inorg. Chem.* **1993**, *32*, 3493–3500.
- [63] Barnard, T. S.; Mason, M. R. *Inorg. Chem.* **2001**, *40*, 5001–5009.
- [64] Graham, W. a. G.; Jetz, W. *Inorg. Chem.* **1971**, *10*, 1647–1653.
- [65] Breit, N. C.; Eisenhut, C.; Inoue, S. *Chem. Commun.* **2016**, *52*, 5523–5526.
- [66] Corey, J. Y.; Chang, L. S.; Corey, E. R. *Organometallics* **1987**, *6*, 1595–1596.
- [67] Chang, L. S.; Corey, J. Y. *Organometallics* **1989**, *8*, 1885–1893.
- [68] Zybilla, C.; Mueller, G. *Organometallics* **1988**, *7*, 1368–1372.
- [69] Leis, C.; Wilkinson, D. L.; Handwerker, H.; Zybilla, C.; Mueller, G. *Organometallics* **1992**, *11*, 514–529.
- [70] Zybilla, C.; Wilkinson, D. L.; Leis, C.; Müller, G. *Angew. Chemie Int. Ed.* **1989**, *28*, 203–205.
- [71] Ghadwal, R. S.; Azhakar, R.; Pröpper, K.; Holstein, J. J.; Dittrich, B.; Roesky, H. W. *Inorg. Chem.* **2011**, *50*, 8502–8508.
- [72] Leis, C.; Zybilla, C.; Lachmann, J.; Müller, G. *Polyhedron* **1991**, *10*, 1163–1171.
- [73] Lang, H.; Weinmann, M.; Frosch, W.; Büchner, M.; Schiemenz, B. *Chem. Commun.* **1996**, *26*, 1299–1300.
- [74] Simons, R. S.; Galat, K. J.; Bradshaw, J. D.; Youngs, W. J.; Tessier, C. A.; Aullón, G.; Alvarez, S. *J. Organomet. Chem.* **2001**, *628*, 241–254.
- [75] Braunstein, P.; Veith, M.; Blin, J.; Huch, V. *Organometallics* **2001**, *20*, 627–633.
- [76] Schmedake, T. A.; Haaf, M.; Paradise, B. J.; Millevolte, A. J.; Powell, D. R.; West, R. J. *Organomet. Chem.* **2001**, *636*, 17–25.
- [77] Weinmann, M.; Rheinwald, G.; Zsolnai, L.; Walter, O.; Büchner, M.; Schiemenz, B.; Huttner, G.; Lang, H. *Organometallics* **1998**, *17*, 3299–3307.
- [78] Lutters, D.; Severin, C.; Schmidtman, M.; Müller, T. *J. Am. Chem. Soc.* **2016**, *138*, 6061–6067.
- [79] Simons, R. S.; Tessier, C. A. *Acta Crystallogr. Sect. C Cryst. Struct. Commun.* **1996**, *52*, 840–842.
- [80] Junold, K.; Baus, J. A.; Burschka, C.; Vent-Schmidt, T.; Riedel, S.; Tacke, R. *Inorg. Chem.* **2013**, *52*, 11593–11599.
- [81] Tacke, R.; Kobelt, C.; Baus, J. A.; Bertermann, R.; Burschka, C. *Dalton Trans.* **2015**, *44*, 14959–14974.
- [82] Blom, B.; Pohl, M.; Tan, G.; Gallego, D.; Driess, M. *Organometallics* **2014**, *33*, 5272–5282.
- [83] Mück, F. M.; Kloß, D.; Baus, J. a; Burschka, C.; Tacke, R. *Chem. Eur. J.* **2014**, *20*, 9620–9626.
- [84] Yang, W.; Fu, H.; Wang, H.; Chen, M.; Ding, Y.; Roesky, H. W.; Jana, A. *Inorg. Chem.* **2009**, *48*, 5058–5060.
- [85] R.S.Simons, C.A.Tessier CCDC 126532: *Experimental Crystal Structure Determination*, **2014**, DOI: 10.5517/cc47npp
- [86] Van An Du, S.O.Baumann, G.N.Stipicic, U.Schubert CCDC 740791: *Experimental Crystal Structure Determination*, **2014**, DOI: 10.5517/ccsvwhy
- [87] H.Pfistner, D.Fenske CCDC 148466: *Experimental Crystal Structure Determination*, **2014**, DOI: 10.5517/cc4zh7t
- [88] Cordero, B.; Gómez, V.; Platero-Prats, A. E.; Revés, M.; Echeverría, J.; Cremades, E.; Barragán, F.; Alvarez, S. *Dalton Trans.* **2008**, No. 21, 2832–2838.
- [89] Gaussion 09, Revision D.01 (**2013**), M. J. Frisch, G. W. Trucks, H. B. Schlegel, G. E. Scuseria, M. A. Robb, J. R. Cheeseman, G. Scalmani, V. Barone, B. Mennucci, G. A. Petersson, H. Nakatsuji, M. Caricato, X. Li, H. P. Hratchian, A. F. Izmaylov, J. Bloino, G. Zheng, J. L. Sonnenberg, M.

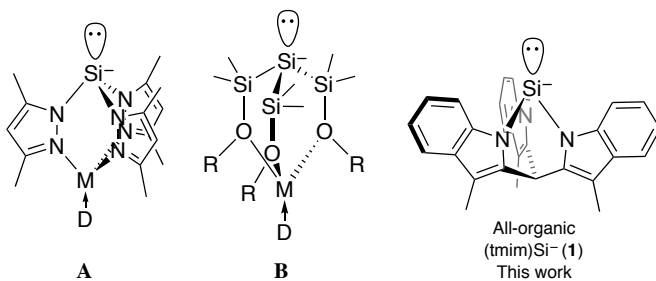
- Hada, M. Ehara, K. Toyota, R. Fukuda, J. Hasegawa, M. Ishida, T. Nakajima, Y. Honda, O. Kitao, H. Nakai, T. Vreven, J. A. Montgomery, Jr., J. E. Peralta, F. Ogliaro, M. Bearpark, J. J. Heyd, E. Brothers, K. N. Kudin, V. N. Staroverov, T. Keith, R. Kobayashi, J. Normand, K. Raghavachari, A. Rendell, J. C. Burant, S. S. Iyengar, J. Tomasi, M. Cossi, N. Rega, J. M. Millam, M. Klene, J. E. Knox, J. B. Cross, V. Bakken, C. Adamo, J. Jaramillo, R. Gomperts, R. E. Stratmann, O. Yazyev, A. J. Austin, R. Cammi, C. Pomelli, J. W. Ochterski, R. L. Martin, K. Morokuma, V. G. Zakrzewski, G. A. Voth, P. Salvador, J. J. Dannenberg, S. Dapprich, A. D. Daniels, O. Farkas, J. B. Foresman, J. V. Ortiz, J. Cioslowski, D. J. Fox, Gaussian, Inc., Wallingford CT.
- [90] Bent, H. A. *Chem. Rev.* **1961**, *61*, 275–311.
- [91] Ernst, C. R.; Spialter, L.; Buell, G. R.; Wilhite, D. L. *J. Am. Chem. Soc.* **1974**, *96*, 5375–5381.
- [92] von Döbeneck, H.; Prietzel, H. *Hoppe-Seyler's Z. Physiol. Chem.* **1955**, *299*, 214–226.
- [93] Okazaki, M.; Iwata, M.; Tobita, H.; Ogino, H. *Dalton Trans.* **2003**, *6*, 1114–1120.
- [94] Dufour, P.; Dartiguenave, M.; Dartiguenave, Y.; Simard, M.; Beauchamp, A. L. *J. Organomet. Chem.* **1998**, *563*, 53–60.
- [95] Li, Y.-S.; Li, Y.-R.; Li, X.-F. *J. Organomet. Chem.* **2003**, *667*, 185–191.
- [96] Fulmer, G. R.; Miller, A. J. M.; Sherden, N. H.; Gottlieb, H. E.; Nudelman, A.; Stoltz, B. M.; Bercaw, J. E.; Goldberg, K. I. *Organometallics* **2010**, *29*, 2176–2179.
- [97] Armarego, W. L. F.; Chai, C. L. L. *Purification of laboratory chemicals*; 2003.
- [98] Krentz, R.; Pomeroy, R. K. *Inorg. Chem.* **1985**, *24*, 2976–2980.
- [99] Ohishi, T.; Shiotani, Y.; Yamashita, M. *J. Org. Chem.* **1994**, *59*, 250–250.
- [100] Malisch, W.; Kuhn, M. *Chem. Ber.* **1974**, *107*, 979–995.

4

A Free Silanide from Nucleophilic Substitution at Silicon(II)

The free silanide derived from tris(3-methylindol-2-yl)methane $[(\text{tmim})\text{Si}^-]$ was synthesized through nucleophilic substitution on the Si(II) precursor $\text{Idipp} \rightarrow \text{SiCl}_2$ ($\text{Idipp} = 2,3\text{-dihydro-1,3-bis[2,6-diisopropylphenyl]-1H-imidazol-2-ylidene}$). This approach circumvents the need for strained tetrahedral silane synthetic intermediates. The $[\text{tmim}]\text{Si}^-$ anion affords a series of metal silanides by direct complexation to the base metal salts CuCl and FeCl_2 . In CH_3CN , anionic $[\text{tmim}]\text{SiCuCl}^-$ dissociates into $[\text{tmim}]\text{Cu}(\text{NCCH}_3)_3$. Anionic $[(\text{tmim})\text{SiFeCl}_2]^-$ is a rare example of a high spin silyl iron complex. Computational investigations show that the ligand cone-angle (194.6°) of $[\text{tmim}]\text{Si}^-$ resembles that of $\text{P}(o\text{-tol})_3$ ($194(6)^\circ$), and its electron-donating properties are close to those of PMe_3 .

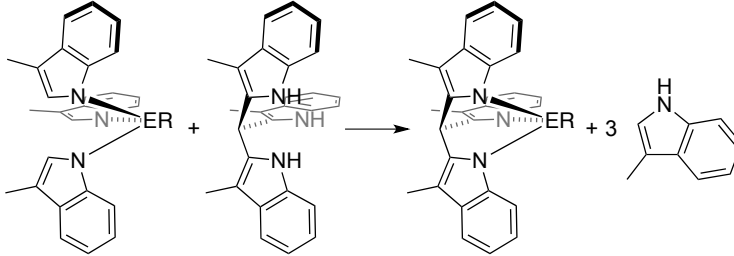




Results and Discussion

The tmim scaffold had previously been used to prepare the stable phosphine (tmim)P,⁹ which is isoelectronic to **1**, suggesting that the latter should not suffer from excessive strain. However, unsuccessful initial attempts to synthesize tetrahedral Si(IV) precursors to **1** such as (tmim)SiCl and (tmim)SiH prompted the execution of detailed strain-enthalpy calculations.¹⁰ To this end, the enthalpy of the homodesmotic reactions depicted in Table 4.1 was calculated at the TPSS/TZVP level, which provides an estimate of the strain of the corresponding cage compound. As expected, the experimentally accessible (tmim)P displays a very small strain of +1.2 kcal/mol. The targeted Si⁻ analogue **1** affords an even slightly negative reaction enthalpy [−1.6 kcal/mol], suggesting that it may be stable. In contrast, the strain is significantly higher for the tetrahedral silanes ($\Delta H_{R=H}$ = 13.1 kcal/mol and $\Delta H_{R=Cl}$ = 14.4 kcal/mol, respectively). This difference can be understood using orbital hybridization. In compliance with Bent's Rule,¹¹ compounds featuring a lone pair on the central element will use hybrid orbitals with high *p*-character to form bonds with the nitrogen atoms, which allows for the smaller N–Si–N angles favored by the cage structure. These calculations motivated the search for a synthetic route to the targeted Si⁻ compound **1** that would not involve tetrahedral Si(IV) intermediates.

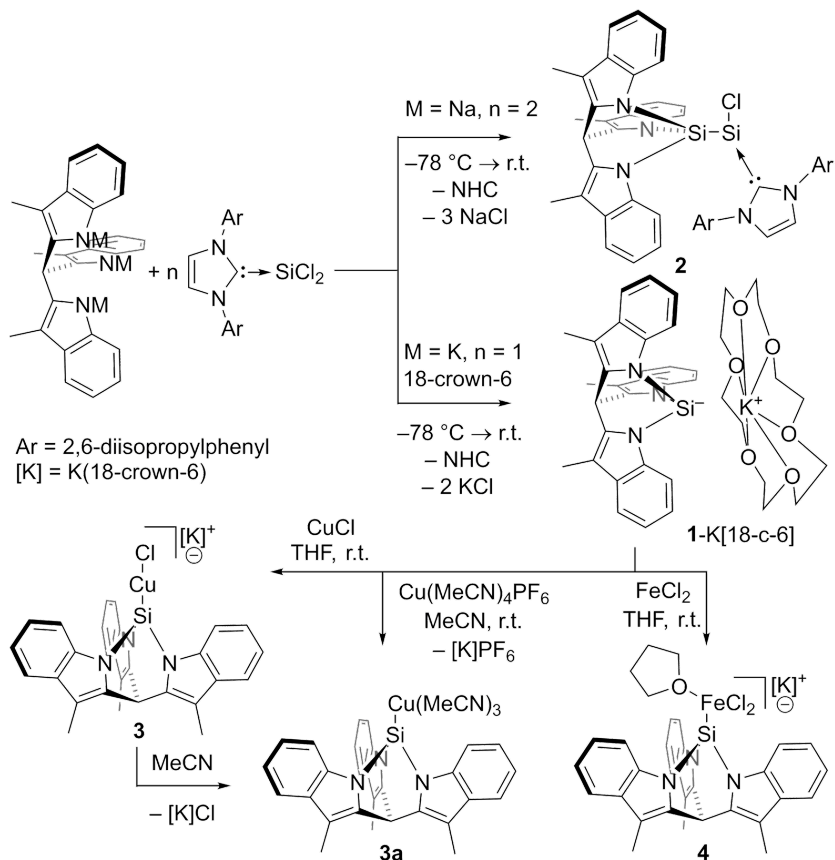
Table 4.1 Homodesmotic reactions calculated for ER = SiCl, SiH, P, Si⁻. Reaction enthalpies and N–E–N angles of the ER-containing entities.



ER =	$\Delta H/\text{kcal}\cdot\text{mol}^{-1}$	Angle/° open	Angle/° cage
SiCl	14.4	109.2	101.7
SiH	13.1	109.0	100.6
P	1.2	99.9	94.3
Si ⁻	−1.6	95.8	89.9

Therefore, the idea that a silanide could be synthesized by direct substitution at Si(II) was investigated. Recently developed Idipp→SiCl₂ (Idipp = 2,3-dihydro-1,3-bis(2,6-diisopropylphenyl)-1H-imidazol-2-ylidene) was chosen because it has been shown to act as a convenient Si(II) synthon.^{12a,b} In particular, substitution of Cl for group 15 elements has afforded phosphasilenyliidene [Si=PR],^{12c} arylamino silylene,^{12d} and diamido silylene^{12e} structures. A first substitution attempt with the trisodium salt (tmim)Na₃ in THF afforded a complex mixture, from which the silyl-silylene **2** [(tmim)Si–Si[Cl]←Idipp] could be identified as a component by an X-ray crystal structure (Figure 4.1, Scheme 4.1). The observation of **2** suggests that nucleophilic

attack of **1** on a second equiv of $\text{Idipp} \rightarrow \text{SiCl}_2$ is kinetically competitive with the reaction of tmim^- with $\text{Idipp} \rightarrow \text{SiCl}_2$ to form **1**. Enhancing the nucleophilicity of the tmim^{3-} trianion to favour the first substitution reaction by using its tripotassium salt and one equiv of 18-crown-6 gratifyingly allowed clean substitution of both chlorides of $\text{Idipp} \rightarrow \text{SiCl}_2$ to afford **1-K[18-c-6]** in 55% yield.



Scheme 4.1 Synthesis and complexation reactions of **1**.

A single set of ^1H NMR resonances for **1-K[18-c-6]** in the aromatic region indicates C_3 symmetry, consistent with a bicyclo[2.2.2]octane topology. In MeCN solution, **1-K[18-c-6]** exists as solvent-separated ion pair as evidenced by distinct diffusion coefficients for the anion and cation measured by DOSY NMR.¹³ Accordingly, the ^{29}Si NMR shows a resonance at -48.1 ppm, which is in good agreement with the DFT calculated value of $\delta = -46.6$ ppm for the free silanide anion. Moreover, it is close to the observed shift for **A** [-38.6 , $M = \text{Mo}$, see Chart 4.1]^{1e} and significantly different from the electronically distinct **B** [-194.7 ppm, $M = \text{K}$, $R = \text{C}_2\text{H}_5\text{OMe}$, see Chart 4.1].^{6b} Crystals suitable for X-ray diffraction were grown from a concentrated acetonitrile solution at -35°C . The structure shows an ion pair with at most a weak interaction

between the ions by the large Si–K distance [3.8807(6) Å, Figure 4.1]. Reported distances for contact ion pairs of Si[–] K⁺[18-c-6]^{4a,b,14} range from 3.2911(16)^{14a} to 3.9413(18) Å,^{14b} featuring silanide **1** at the large distance part of that spectrum, exceeded only by the cyclosilyl dianion reported by Fischer et al.^{14b} The bicyclo[2.2.2]octane core possesses N–Si–N angles of 90.30(6)–91.14(4)°, consistent with a strong *p*-character of the bonding orbitals and in agreement with the DFT-predicted angles [*vide supra*].

Table 4.2 Computational $\tilde{\nu}(\text{CO})$ of Si(III) ligands in LCpIrCO.

L		$\tilde{\nu}(\text{CO})/\text{cm}^{-1}$	
Si[MI] ₃ ^a		II	
Si[Pz] ₃ Li (A)		IV	
Si(C ₂ F ₅) ₃		III	
PMe ₃		I	
Si(tmim) (1)		V	
VI			

^aSi[3-methylindol-2-yl]₃

The properties of **1** as a ligand were first investigated computationally. Regarding the steric properties of the ligand, the Tolman cone angle was determined to be 194.6°, which is the same as that of P(*o*-tol)₃ [194(6)°].¹⁵ The frontier orbitals of **1** are localized on the aromatic system, with the lone pair on silicon occupying the HOMO-4 at an energy of 9.6 kcal/mol below the HOMO. The *in-silico* analogue of the Tolman electronic parameter (CEP) was determined for a range of NHCs and phosphines in LCpIrCO.¹⁶ Typical values are $\tilde{\nu}(\text{CO}) = 2115$ for PF₃, 2049 for PPh₃, 2039 for 1,3-bis(methyl)-4,5-dihydroimidazol-2-ylidene, 2033 for 1,3-bis(methyl)imidazol-2-ylidene, and 2028 cm^{–1} for P^{*i*}Bu₃. The CEP was also determined for a range of Si(III) ligands (Table 4.2).^{1f} The calculated vibrational frequency puts ligand **1** ($\tilde{\nu}(\text{CO}) = 2038$ cm^{–1}) at the weak donor extreme of the list of silanide ligands, just beyond Si(C₂F₅)₃ ($\tilde{\nu}(\text{CO}) = 2034$ cm^{–1}) and ligand Li-**A** ($\tilde{\nu}(\text{CO}) = 2024$ cm^{–1}). The electronic properties of **1** can be best compared to PMe₃ ($\tilde{\nu}(\text{CO}) = 2037$ cm^{–1}). Interestingly, the non-strained tris[3-methylindol-N-yl]silyl ligand [Si(MI)₃] with $\tilde{\nu}(\text{CO}) = 2021$ cm^{–1} is a stronger donor than **1**, illustrating the stabilizing effect of the cage structure on the silicon-centered lone pair.

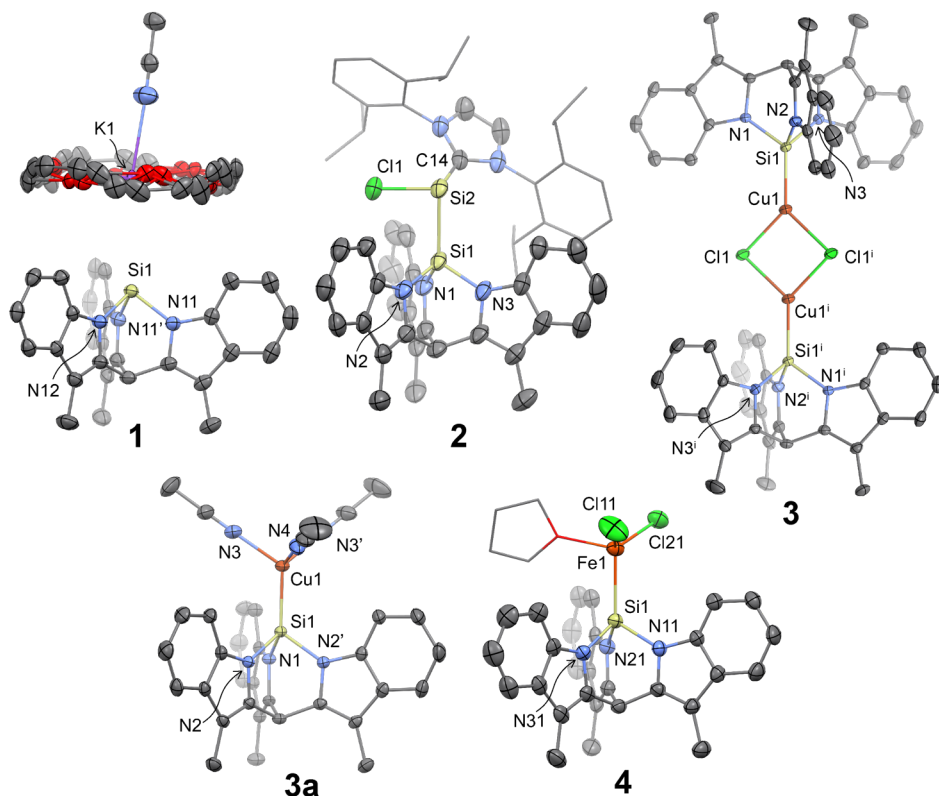


Figure 4.1 Molecular structure in the crystal of **1-K[18-c-6]**, **2**, **3**, **3a**, and **4**. Ellipsoids are drawn at 50% probability. For clarity, hydrogen atoms, $K^+[18-c-6]$ and co-crystallized solvent are omitted where necessary, and only the core atoms are plotted in **2**, **3**, **3a**, and **4**. The crown-ether in **1-K[18-c-6]** is disordered on a mirror plane. The unit cell of **4** contains 2 independent molecules of which one is shown. Symmetry code $' = x, 1-y, z$ (for **1-K[18-c-6]**) and $x, -y, z$ (for **3a**) and $i = -x, -y, -z$. Selected bond distances (Å) and angles (°): **1-K[18-c-6]**: Si1–K1 3.8807(6), N11–Si1 1.8421(10), N12–Si1 1.8405(14), N11–Si1–N11' 90.30(6), N11–Si1–N12 91.14(4), **2**: Si1–Si2 2.3732(11), C14–Si2 1.967(3), N1–Si1 1.769(3), N2–Si1 1.783(3), N3–Si1 1.770(3), N1–Si1–N2 96.25(12), N2–Si1–N3 95.61(13), N3–Si1–N1 99.29(12), **3**: Si1–Cu1 2.1905(9), N1–Si1 1.799(2), N2–Si1 1.805(3), N3–Si1 1.798(3), N1–Si1–N2 93.62(11), N2–Si1–N3 93.41(12), N3–Si1–N1 93.74(11), **3a**: Si1–Cu1 2.2106(7), N1–Si1 1.805(2), N2–Si1 1.8069(15), N1–Si1–N2 93.30(7), N2–Si1–N2' 92.14(10), **4**: molecule 1: Si1–Fe1 2.4482(12), N11–Si1 1.789(3), N21–Si1 1.808(3), N31–Si1 1.806(3), N11–Si1–N21 94.05(16), N21–Si1–N31 94.55(15), N31–Si1–N11 94.28(15), molecule 2: Si5–Fe2 2.4589(12), N12–Si5 1.792(3), N22–Si5 1.801(3), N32–Si5 1.810(3), N12–Si5–N22 92.54(15), N22–Si5–N32 94.49(15), N32–Si5–N12 94.80(15).

The ability of **1** to act as a ligand for transition metals was demonstrated with copper(I) and iron(II) chlorides (Scheme 4.1). First, complexation of **1** to $Cu(I)Cl$ in THF produces the poorly soluble chlorocuprate **3**. The ^{29}Si NMR resonance could not be observed, which is likely due to the large quadrupole moment of the adjacent copper atom.¹⁷ The monomeric nature of chlorocuprate **3** was confirmed by ESI-MS (THF, $C_{28}H_{22}N_3SiCuCl^- = 526.0345$ a.u.) and by DOSY NMR from a similar diffusion coefficient for **3** and the neutral monomer **3a** in CD_2Cl_2 (*vide infra*). Interestingly, the X-ray crystal structure of **3** displays a centrosymmetric dimer with a Cu_2Cl_2 diamond

core. This is the first report of a silanide-supported Cu_2X_2 -dimer.^{1e,18-20} The Cu–Si distance (2.1905(9) Å) is marginally shorter than that reported for the monomeric silyl chloro cuprate based on ligand **A** (Chart 4.1, 2.197(2) Å)^{1e} and hence the shortest reported for copper silanides, presumably because of the large Si *s*-character of the bonding orbital.²¹

In acetonitrile solution, complex **3** dissociates to the neutral trisacetonitrile copper silyl complex **3a** by elimination of $\text{K}[18\text{-c-}6]\text{Cl}$, as was established by comparison of ^1H NMR data from an authentic sample of **3a** synthesized from **1**- $\text{K}[18\text{-c-}6]$ and $\text{Cu}(\text{MeCN})_4\text{PF}_6$. An X-ray crystal structure of **3a** reveals that formal substitution of Cl for MeCN (**3** \rightarrow **3a**) causes a slight lengthening of the Cu–Si bond ($\Delta d = 0.020(1)$ Å).

Finally, complexation of **1** to $\text{Fe}(\text{II})\text{Cl}_2$ in THF afforded the anionic dichloroferrate complex **4**. The ^1H NMR spectrum features one set of 6 paramagnetically shifted resonances in addition to that of the $\text{K}^+[18\text{-c-}6]$ counterion, suggesting retention of local C_3 symmetry. The solid-state structure of **4** contains two independent molecules in the unit cell. The structure confirms the anionic nature of the complex, displaying Si–Fe distances of 2.4482(12) Å and 2.4589(12) Å. Only one high-spin $\text{Fe}(\text{II})$ complex of a monodentate silylene is known, which forms at low temperatures.²² High spin, monodentate silyl iron complexes have been reported for simple SiR_3 silyls ($\text{R} = \text{H}$, alkyl, aryl, SiMe_3),²³ but **4** is the first nitrogen supported silyl complex of this kind.

Interestingly, the geometry around silicon is sensitive to coordination. In the ideal case, the sum of angles is 328.5° for sp^3 hybridization and 270° for the non-hybridized extreme. The N–Si–N angle sum increases from $272.58(10)^\circ$ in uncoordinated **1** to $278.75(14)^\circ$ in **3a**, $280.8(2)^\circ$ in **3**, and $282.9(3)/281.8(3)^\circ$ in **4**, which can be explained by an increasing *p*-character of the lone pair upon binding to a Lewis acid and a consequent decrease in the *p*-character of the Si–N bonding orbitals. This is confirmed by NBO analysis²⁴ of **1**, **3a**, **3**, and **4**: the *s*-character of the silicon Natural Hybrid Orbital (NHO) corresponding to the lone pair in **1** and forming the M–Si bond in the complexes decreases from 62.8% in **1** to 57.4% for **3a**, 59.3% for **3**, and 58.9% for **4**.

Conclusions

In summary, nucleophilic substitution on the neutral $\text{Si}(\text{II})$ compound $\text{Idipp} \rightarrow \text{SiCl}_2$ afforded a free silanide (**1**) derived from tris(3-methylindol-2-yl)methane (tmim). This approach avoids the intermediacy of strained tetrahedral silane intermediates and may find further applications in silanide synthesis. The ability of **1** to act as a ligand in metal complexes was demonstrated: coordination to $\text{Cu}(\text{I})$ afforded the dimeric silyl cuprate $[(\text{tmim})\text{SiCu}(\mu\text{-Cl})_2]^{2-}$, featuring the shortest known silyl copper distance, and its neutral acetonitrile-solvated analogue $(\text{tmim})\text{SiCu}(\text{NCMe})_3$. Complexation to FeCl_2 gave the corresponding ferrate $[(\text{tmim})\text{SiFeCl}_2(\text{THF})]^-$, a rare example of a high

spin silyl iron complex. The ability of $(\text{tmim})\text{Si}^-$ to act as a ligand for metal complexes warrants further studies towards catalytic activity of these complexes.

Experimental Section

All reactions involving air-sensitive compounds were conducted under and N_2 atmosphere by using standard glovebox or Schlenk techniques. Acetonitrile and n-hexane were dried with an MBRAUN MB SPS-79 system, THF and DCM were distilled from benzophenone/Na or CaH_2 , respectively, HMDSO was not pre-dried. All solvents were degassed by bubbling with N_2 for 30 min, and stored over molecular sieves in a glovebox. Deuterated acetonitrile, THF, and DCM were degassed by four freeze-pump-thaw cycles and stored over molecular sieves in a glovebox. Skatole, KH 30 w% in mineral oil, 2,6-diisopropylaniline, HSiCl_3 , KOtBu ($\geq 97\%$), FeCl_2 , $\text{Cu}(\text{MeCN})_4\text{PF}_6$ were purchased from Sigma-Aldrich. Triethyl orthoformate, glyoxal 40 w%, TMSCl , paraformaldehyde, 18-crown-6, CuCl were purchased from Acros. All commercially obtained chemicals were used as received, except for 18-crown-6 and CuCl . Drying of 18-crown-6 was done according to literature.²⁵ From CuCl , copper oxides and hydroxides were removed with hydrochloric acid as described in literature and the resulting solid was azeotropically dried with acetonitrile until $\nu(\text{C}\equiv\text{N})$ in IR disappeared.²⁶ All NMR measurements were performed on a Varian VNMRs400 or Varian MRF400 spectrometer, shifts are reported relative to TMS with the residual solvent signal as internal standard.²⁷ All DOSY spectra were recorded with a gradient pulse duration of 2 ms and a gradient delay of 30 ms. All NMR experiments involving air-sensitive compounds were conducted in J-Young NMR tubes under an N_2 atmosphere. IR spectra were recorded on a Perkin-Elmer Spectrum Two FT-IR spectrometer. ESI-MS measurements were performed on a Waters LCT Premier XE KE317 spectrometer. Elemental analysis was conducted by Medac Ltd.. The compounds $(\text{tmim})\text{H}_3$,²⁸ Idipp ,^{29–31} Idipp-SiCl_2 ,³² were prepared according to reported procedures. Idipp-SiCl_2 contained $\sim 10\%$ of unidentified Idipp -containing impurities after purification.

Computational methods

Calculations were performed using Gaussian09, Revision D.01.¹⁰ All structures were optimized using the TPSS functional with the TZVP basis set (Mo: SDD incl. ECP), except for the LCplRCO complexes. The absence of negative eigenvalues was confirmed for all structures. On the optimized geometries, NMR calculations were conducted as single point with the TPSS functional and IGLO-III basis set (Li: def2TZVP; Mo: SDD incl. ECP) with inclusion of a solvent model (SCRF = Acetonitrile). The ^{29}Si shifts are reported relative to TMS, calculated using the same method. The method was benchmarked with the known silanides **A** $\text{Li}^+(\text{Pz})_3\text{Si}^-$ ($\delta_{\text{calc}} = -36.3$, $\delta_{\text{exp}} = -35.0$ ppm) and $(\text{CO})_3\text{Mo}(\text{Pz})_3\text{Si}^-$ ($\delta_{\text{calc}} = -37.3$, $\delta_{\text{exp}} = -38.6$ ppm).^{1e,6c} In accordance with Gusev et al.,¹⁶ the CEP calculations were performed using the MPW1PW91 functional with the basis sets SDD (associated with ECP) for Ir (and Mo) and 6-311+G(d,p) for all other atoms. Tight geometry optimizations and the ultrafine integration grid (int=ultrafine) were employed for all Ir-complexes. NBO-analysis was done with the NBO6 program,²⁴ the amount of s-character for **4** was obtained by averaging over α and β spin.

X-ray crystal structure determinations

$(\text{tmim})\text{Si}^- \text{K}[18\text{-crown-6}]^+ [1\text{-K}[18\text{-c-6}]]$. $[\text{C}_{14}\text{H}_{27}\text{KNO}_6][\text{C}_{28}\text{H}_{22}\text{N}_3\text{Si}] \cdot \text{CH}_3\text{CN}$, Fw = 814.09, colourless block, $0.36 \times 0.32 \times 0.31$ mm³, monoclinic, C2/m (no. 12), $a = 24.8529(8)$, $b = 14.0712(6)$, $c = 12.6649(6)$ Å, $\beta = 100.339(2)^\circ$, $V = 4357.1(3)$ Å³, $Z = 4$, $D_x = 1.241$ g/cm³, $\mu = 0.20$ mm⁻¹. 101617 Reflections were measured on a Bruker Kappa ApexII diffractometer with sealed tube and Triumph monochromator ($\lambda = 0.71073$ Å) at a temperature of 150(2) K up to a resolution of $(\sin \theta/\lambda)_{\text{max}} = 0.65$ Å⁻¹. The crystal appeared to be broken in two fragments. Consequently, two orientation matrices were used for the integration with the Eval15 software³³ and the reflection data were stored in the HKLF5 format.³⁸ A multiscan absorption correction and scaling was performed with TWINABS³⁴ (correction range 0.69–0.75). 5285 Reflections were unique ($R_{\text{int}} = 0.025$), of which 4759 were observed [$I > 2\sigma(I)$]. The structure was solved with Patterson superposition methods using SHELXT.³⁵

Least-squares refinement was performed with SHELXL-2014³⁶ against F^2 of all reflections. Non-hydrogen atoms were refined freely with anisotropic displacement parameters. The crown ether and the non-coordinated acetonitrile were refined with a disorder model. Hydrogen atoms of the cation were located in difference Fourier maps and all other hydrogen atoms were introduced in calculated positions. All hydrogen atoms were refined with a riding model. 383 Parameters were refined with 300 restraints (distances, angles and displacement parameters of the disordered groups). $R1/wR2$ [$I > 2\sigma(I)$]: 0.0319 / 0.0898. $R1/wR2$ [all refl.]: 0.0358 / 0.0927. $S = 1.023$. Batch scale factor BASF = 0.3652(13). Residual electron density between -0.24 and 0.38 e/Å³. Geometry calculations and checking for higher symmetry was performed with the PLATON program.³⁷

[tmim]Si-Si[Cl]←ldipp (2). C₅₅H₅₈ClN₅Si₂ + disordered solvent, Fw = 880.69^[*], orange block, 0.45 × 0.32 × 0.12 mm³, monoclinic, P2₁/c (no. 14), $a = 11.2805(5)$, $b = 22.6490(13)$, $c = 22.1298(13)$ Å, $\beta = 91.097(2)^\circ$, $V = 5652.9(5)$ Å³, $Z = 4$, $D_x = 1.035$ g/cm³^[*], $\mu = 0.15$ mm⁻¹^[*]. 68885 Reflections were measured on a Bruker Kappa ApexII diffractometer with sealed tube and Triumph monochromator ($\lambda = 0.71073$ Å) at a temperature of 150(2) K up to a resolution of $[\sin \theta/\lambda]_{\max} = 0.61$ Å⁻¹. The crystal appeared to be broken in many fragments. Only the orientation matrix of the major component was used for the integration with the Eval15 software³³. A multiscan absorption correction and scaling was performed with SADABS³⁴ (correction range 0.62-0.75). 10538 Reflections were unique ($R_{\text{int}} = 0.065$), of which 6886 were observed [$I > 2\sigma(I)$]. The structure was solved with Patterson superposition methods using SHELXT.³⁵ Least-squares refinement was performed with SHELXL-2014³⁶ against F^2 of all reflections. The crystal structure contains large voids (1356 Å³ / unit cell) filled with severely disordered THF solvent molecules. Their contribution to the structure factors was secured by back-Fourier transformation using the SQUEEZE algorithm³⁹ resulting in 325 electrons / unit cell. Non-hydrogen atoms were refined freely with anisotropic displacement parameters. Hydrogen atoms were introduced in calculated positions and refined with a riding model. 579 Parameters were refined with no restraints. $R1/wR2$ [$I > 2\sigma(I)$]: 0.0631 / 0.1740. $R1/wR2$ [all refl.]: 0.0961 / 0.1966. $S = 1.036$. Residual electron density between -0.42 and 0.49 e/Å³. Geometry calculations and checking for higher symmetry was performed with the PLATON program.³⁷ [*] Derived values do not contain the contribution of the disordered THF solvent molecules.

Dimer of [tmim]SiCuCl⁻ K[18-crown-6]⁺ (3). [C₁₂H₂₄KO₆]₂[C₅₆H₄₄Cl₂Cu₂N₆Si₂] · 4.5CH₂Cl₂, Fw = 2044.12, colourless block, 0.26 × 0.10 × 0.08 mm³, triclinic, $P \overline{1}$ (no. 2), $a = 11.3775(4)$, $b = 12.8622(5)$, $c = 19.0019(7)$ Å, $\alpha = 106.992(1)$, $\beta = 91.818(2)$, $\gamma = 114.690(2)^\circ$, $V = 2378.09(15)$ Å³, $Z = 1$, $D_x = 1.427$ g/cm³, $\mu = 0.93$ mm⁻¹. 42675 Reflections were measured on a Bruker Kappa ApexII diffractometer with sealed tube and Triumph monochromator ($\lambda = 0.71073$ Å) at a temperature of 150(2) K up to a resolution of $[\sin \theta/\lambda]_{\max} = 0.65$ Å⁻¹. The X-ray intensities were integrated with the Eval15 software³³. A multiscan absorption correction and scaling was performed with SADABS³⁴ (correction range 0.65-0.75). 10915 Reflections were unique ($R_{\text{int}} = 0.059$), of which 6898 were observed [$I > 2\sigma(I)$]. The structure was solved with Patterson superposition methods using SHELXT.³⁵ Least-squares refinement was performed with SHELXL-2016³⁶ against F^2 of all reflections. Diffuse electron density at the inversion center at 0,1/2,0 was modeled as disordered CH₂Cl₂ with partial occupancy. Non-hydrogen atoms were refined freely with anisotropic displacement parameters. Hydrogen atoms were introduced in calculated positions and refined with a riding model. 562 Parameters were refined with 45 restraints (distances, angles and displacement parameters of the dichloromethane molecules). $R1/wR2$ [$I > 2\sigma(I)$]: 0.0508 / 0.1138. $R1/wR2$ [all refl.]: 0.0997 / 0.1321. $S = 1.041$. Residual electron density between -0.73 and 1.07 e/Å³. Geometry calculations and checking for higher symmetry was performed with the PLATON program.³⁷

[tmim]SiFeCl₂⁻ K[18-crown-6]⁺ (4). [C₂₀H₄₀KO₆][C₃₂H₃₀Cl₂FeN₃OSi], Fw = 1075.05, colourless block, 0.36 × 0.16 × 0.08 mm³, triclinic, $P \overline{1}$ (no. 2), $a = 13.9803(9)$, $b = 20.5521(11)$, $c = 22.1248(11)$ Å, $\alpha = 64.722(3)$, $\beta = 75.222(2)$, $\gamma = 76.287(2)^\circ$, $V = 5498.1(5)$ Å³, $Z = 4$, $D_x = 1.299$ g/cm³, $\mu = 0.52$ mm⁻¹. 98856 Reflections were measured on a Bruker Kappa ApexII diffractometer with sealed tube and Triumph monochromator ($\lambda = 0.71073$ Å) at a temperature of 150(2) K up to a resolution of $[\sin \theta/\lambda]_{\max} = 0.59$ Å⁻¹. The X-ray intensities were integrated with the Eval15 software³³. A multiscan absorption correction and scaling was performed with SADABS³⁴ (correction range 0.54-0.75). 19386

Reflections were unique ($R_{\text{int}} = 0.062$), of which 12712 were observed [$I > 2\sigma(I)$]. The structure was solved with Direct Methods using SHELXS-97.⁴⁰ Least-squares refinement was performed with SHELXL-2016³⁶ against F^2 of all reflections. Non-hydrogen atoms were refined freely with anisotropic displacement parameters. Two of potassium coordinated THF molecules were refined with a disorder model. Hydrogen atoms were introduced in calculated positions and refined with a riding model. 1323 Parameters were refined with 579 restraints (distances, angles and displacement parameters of the THF molecules). $R1/wR2$ [$I > 2\sigma(I)$]: 0.0635 / 0.1635. $R1/wR2$ [all refl.]: 0.1045 / 0.1903. $S = 1.020$. Residual electron density between -0.55 and $1.69 \text{ e}/\text{\AA}^3$. Geometry calculations and checking for higher symmetry was performed with the PLATON program.³⁷

(tmim)SiCu(NCCH₃)₃ (3a). $\text{C}_{34}\text{H}_{31}\text{CuN}_6\text{Si} \cdot 3.5\text{CH}_3\text{CN}$, $\text{Fw} = 758.96$, colourless block, $0.14 \times 0.13 \times 0.11 \text{ mm}^3$, monoclinic, $I2/m$ (no. 12), $a = 14.3323(7)$, $b = 13.9735(6)$, $c = 20.1085(10) \text{ \AA}$, $\beta = 98.613(2)^\circ$, $V = 3981.8(3) \text{ \AA}^3$, $Z = 4$, $D_x = 1.266 \text{ g/cm}^3$, $\mu = 0.62 \text{ mm}^{-1}$. 43775 Reflections were measured on a Bruker Kappa ApexII diffractometer with sealed tube and Triumph monochromator ($\lambda = 0.71073 \text{ \AA}$) at a temperature of 150(2) K up to a resolution of $[\sin \theta/\lambda]_{\text{max}} = 0.65 \text{ \AA}^{-1}$. The X-ray intensities were integrated with the Eval15 software³³. A multiscan absorption correction and scaling was performed with SADABS³⁴ (correction range 0.69-0.75). 4766 Reflections were unique ($R_{\text{int}} = 0.049$), of which 3684 were observed [$I > 2\sigma(I)$]. The structure was solved with Patterson superposition methods using SHELXT.³⁵ Least-squares refinement was performed with SHELXL-2017³⁶ against F^2 of all reflections. Non-hydrogen atoms were refined freely with anisotropic displacement parameters. The non-coordinated acetonitrile molecules were refined with a disorder model. Hydrogen atoms were introduced in calculated positions and refined with a riding model. 293 Parameters were refined with 99 restraints (distances, angles and displacement parameters of the acetonitrile molecules). $R1/wR2$ [$I > 2\sigma(I)$]: 0.0376 / 0.0869. $R1/wR2$ [all refl.]: 0.0568 / 0.0950. $S = 1.051$. Residual electron density between -0.26 and $0.38 \text{ e}/\text{\AA}^3$. Geometry calculations and checking for higher symmetry was performed with the PLATON program.³⁷

Syntheses

Synthesis of (tmim)Na₃. A solution of (tmim)H₃ (4.95 g, 12.3 mmol) in THF (10 mL) was added to pre-washed (hexane 3 x 5 mL & THF 5 mL) NaH (60% in oil, 2.07 g, 52 mmol) under THF (20 mL) over 15 minutes and stirred for 2.75h. The excess NaH was removed by filtration and the orange (green luminescent) filtrate was freed of solvent *in vacuo*, yielding a yellow powder (8.46 g, quantitative). Analysis by ¹H NMR showed only (tmim)Na₃ and THF (~30 w%). A titration with HCl (0.10 M in H₂O) on a sample (100.4 mg) in a mixture of THF (4mL) and water (1 mL) was performed to determine the base content, which was consistent with 68.4 w% (tmim)Na₃. ¹H NMR (400 MHz, CD₃CN, 25 °C): $\delta = 7.19$ (m, 6H, ArH), 6.62 (m, 6H, ArH), 6.25 (s, 1H, R₃CH), 2.41 ppm (s, 9H, CH₃). ¹³C NMR (101 MHz, CD₃CN, 25 °C): $\delta = 151.4, 146.0, 132.4, 116.6, 116.2, 115.3, 114.8, 101.8, 37.7$ (R₃CH), 10.1 ppm (CH₃).

Reaction of (tmim)Na₃ with Idipp-SiCl₂. A -79 °C solution of Idipp-SiCl₂ (57.6 mg, 0.118 mmol) in THF (2 mL) was added to a pre-cooled solution of (tmim)Na₃ (75.0 mg, 27 w% THF, 0.117 mmol) in THF (3 mL). The mixture was stirred at r.t. for 16h. Filtration and removal of the solvent *in vacuo* afforded 116.7 mg of a complex mixture containing at least (tmim)Na₃, Idipp and Idipp-SiCl₂. This mixture was redissolved in THF (4 mL) and stirred for another 16h. Crystals suitable for x-ray crystallography were grown from this solution by vapor diffusion with hexane.

Synthesis of (tmim)K₃. A solution of (tmim)H₃ (2.00 g, 4.96 mmol) in THF (10 mL) was added to pre-washed (hexane 3 x 5 mL) KH (2.36 g, 30 w% in oil, 18 mmol) under THF (2 mL) and stirred for 1.75h. The excess KH was removed by filtration and the orange solution, which exhibits green luminescence, was freed of solvent *in vacuo*, yielding a yellow powder (3.08 g, 4.76 mmol, 96%). A titration with HCl (0.01 M in H₂O) on a sample (duplo; 11.1 mg & 13.6 mg) in a mixture of THF (4mL) and water (1 mL) was performed to determine the content (tmim)K₃ (81.2±1.5 w%). ¹H NMR (400 MHz, CD₃CN + C₆H₆O 1:1, 25 °C): $\delta = 7.23$ (d, ³J(H,H) = 7.8 Hz, 1H, indole-H7), 7.18 (d, ³J(H,H) = 7.9 Hz, 1H, indole-H4), 6.67 (ddd, ³J(H,H) = 8.0 Hz, ³J(H,H) = 6.7 Hz, ⁴J(H,H) = 1.4 Hz, 1H, indole-H5), 6.60 (ddd, ³J(H,H) = 7.8 Hz, ³J(H,H) = 6.7 Hz, ⁴J(H,H) = 1.2 Hz, 1H, indole-H6), 6.17 (s, 1H, R₃CH), 2.24 ppm

[s, 3H, CH₃]; ¹³C NMR (101 MHz, CD₃CN + C₄H₈O 1:1, 25 °C): δ = 153.2, 146.2, 132.1, 116.5, 116.4, 115.3, 114.2, 101.1, 39.1, 10.0 ppm.

Synthesis of (tmim)Si⁺ K[18-crown-6]⁺ (1-K[18-c-6]). A -79 °C solution of Idipp-SiCl₂ (700.6 mg, 90% purity, 1.293 mmol) in THF (15 mL) was added to a pre-cooled yellow suspension with green luminescence of (tmim)K₃ (674.5 mg, 10 w% THF, 1.172 mmol) and 18-crown-6 (310.1 mg, 1.173 mmol) in THF (45 mL) and stirred for 30 min. Upon warming to r.t. over 30 min the suspension became less turbid, less luminescent, and darker orange. From this moment, immediate work-up is necessary to prevent formation of by-products. Following filtration and evaporation the solid was suspended in THF (10 mL) and precipitated and washed with hexane (30 mL + 10 mL). The orange solid was washed with acetonitrile (16 mL in 4 portions) and the remaining white powder was extracted in acetonitrile (120 mL), leaving a small amount of unidentified white residue. Evaporation of the filtrate yielded a white solid (468.9 mg, 0.641 mmol, 55%). Crystals suitable for X-ray crystallography were grown from a concentrated acetonitrile solution at -35 °C. ¹H NMR (400 MHz, CD₃CN, 25 °C): δ = 7.71 (d, ³J(H,H) = 8.1 Hz, ⁴J(H,H) = 1.0 Hz, ⁵J(H,H) = 1.0 Hz, 3H, indole-H7), 7.30 (ddd, ³J(H,H) = 7.7 Hz, ⁴J(H,H) = 1.3 Hz, ⁵J(H,H) = 0.8 Hz, 3H, indole-H4), 6.95 (ddd, ³J(H,H) = 8.2 Hz, ³J(H,H) = 7.0 Hz, ⁴J(H,H) = 1.3 Hz, 3H, indole-H6), 6.85 (ddd, ³J(H,H) = 7.9 Hz, ³J(H,H) = 7.0 Hz, ⁴J(H,H) = 1.1 Hz, 3H, indole-H5), 5.92 (s, 1H, R₃CH), 3.54 (s, 34H, K[18-crown-6]⁺), 2.40 ppm (s, 9H, CH₃); ¹³C NMR (101 MHz, CD₃CN, 25 °C): δ = 142.2, 141.8, 131.2, 120.5, 118.7, 118.2, 112.1, 104.3, 70.9, 33.8, 8.7 ppm; ²⁹Si NMR (79 MHz, C₄H₈O, 25 °C): δ = -48.1 ppm; DOSY NMR (400 MHz, CD₃CN, 25 °C): D = 12.5 [(tmim)Si⁺], 14.7 [K[18-crown-6]⁺] × 10⁻¹⁸ m²/s; Elemental analysis calcd (%) for C₄₀H₄₈N₃O₆SiK: C 65.63, H 6.33, N 5.74; found: C 64.90, H 6.19, N 6.41.

Synthesis of (tmim)SiCuCl⁺ K[18-crown-6]⁺ (3). THF (2 mL) was added to a solid mixture of 1-K[18-c-6] (31.4 mg, 0.0429 mmol) and CuCl (4.3 mg, 0.043 mmol) and stirred for 30 minutes. The resulting grey suspension was filtered, washed with THF (3 × 1 mL) and the grey solid extracted in DCM (5 × 1 mL). Drying *in vacuo* afforded complex **3** as a white powder (31.2 mg, 0.0375 mmol, 87.4%). Crystals suitable for X-ray crystallography were grown by vapor diffusion of Et₂O into a concentrated solution of **3** in DCM at room temperature. ¹H NMR (400 MHz, CD₂Cl₂, 25 °C): δ = 7.97 (d, ³J(H,H) = 8.1 Hz, 3H, indole-H7), 7.36 (d, ³J(H,H) = 7.7 Hz, 3H, indole-H4), 7.06 (t, ³J(H,H) = 7.6 Hz, 3H, indole-H6), 6.94 (t, ³J(H,H) = 7.4 Hz, 3H, indole-H5), 5.92 (s, 1H, R₃CH), 3.31 ppm (s, 26H, K[18-crown-6]⁺), 2.40 (s, 9H, CH₃); ¹³C NMR (101 MHz, CD₂Cl₂, 25 °C) δ = 140.4, 140.0, 131.0, 120.9, 118.6, 112.6, 105.7, 70.3, 33.0, 8.7 ppm; ²⁹Si NMR could not be measured due to large quadrupole moment of the adjacent copper atom (Q_{exp}[⁶³Cu] = -21.1(4) e fm², Q_{exp}[⁶⁵Cu] = -19.5(4) e fm²); ⁴¹ DOSY NMR (400 MHz, CD₂Cl₂, 25 °C): D = 9.3 [(tmim)SiCuCl⁺], 9.9 [K[18-crown-6]⁺] × 10⁻¹⁸ m²/s; ESI-MS⁻ C₂₈H₂₂N₃SiCuCl⁺ m/z calc = 526.0568; found = 526.0645.

Generation of (tmim)SiCu(NCCH₃)₃ in solution from **3 (3a).** A solid sample (~10 mg, ~12 μmol) of **3** was dissolved in CD₃CN (~0.5 mL). ¹H NMR (400 MHz, CD₃CN, 25 °C): δ = 7.95 (d, ³J(H,H) = 8.2 Hz, 3H, indole-H7), 7.35 (d, ³J(H,H) = 7.8 Hz, 3H, indole-H4), 7.04 (br t, 3H, indole-H6), 6.94 (t, ³J(H,H) = 7.4 Hz, 3H, indole-H5), 6.00 (s, 1H, R₃CH), 3.54 (s, 27H, K[18-crown-6]⁺), 2.40 ppm (s, 9H, CH₃).

Note: solubility of KCl in CH₃CN in pure acetonitrile and acetonitrile containing 0.15 M 18-crown-6 at 25 °C was reported by Liotta et al.⁴² Pure: 2.43·10⁻⁴; 0.15 M 18-crown-6: 5.55·10⁻² mol/L = 28 μmol/0.5 mL. That means that ratio K[18-c-6]⁺:18-c-6 = 1:3. Present solution is ~10 mg/0.5 mL = 12 μmol/0.5 mL CD₃CN, which is well within solubility.

Synthesis of (tmim)SiCu(NCCH₃)₃ from Cu(NCCH₃)₄PF₆ (3a). A solution of Cu(NCCH₃)₄PF₆ (15.2 mg, 0.0408 mmol) in CH₃CN (1 mL) was added to a suspension of 1-K[18-c-6] (30.1 mg, 0.0411 mmol) in CH₃CN (1 mL), and the remaining Cu(NCCH₃)₄PF₆ solution was transferred using CH₃CN (1 mL). The suspension immediately dissolved fully and produced a coarse, white and a fine, brown precipitate within 5 minutes. Agitation and decantation of the liquid provided clean white solid, which was dried *in vacuo* (8.4 mg, 0.0137 mmol, 33%), more crops could be obtained by precipitation from the mother liquor. Crystals suitable for X-ray crystallography were grown by storing a concentrated CH₃CN solution at -35 °C for 16 h. ¹H NMR (400 MHz, CD₂Cl₂, 25 °C) δ = 7.75 (d, ³J(H,H) = 8.1 Hz, 3H, indole-H7), 7.39 (d, ³J(H,H) = 7.7 Hz, 3H, indole-H4), 7.06 (t, ³J(H,H) = 7.5 Hz, 3H, indole-H6), 6.97 (t, ³J(H,H) = 7.4 Hz, 3H, indole-H5), 5.93 (s, 1H, R₃CH), 2.41 (s, 9H, CH₃), 2.14 ppm (s, 9H, CH₃CN). ¹H

NMR (400 MHz, CD₃CN, 25 °C) δ = 7.96 (‘dt’, ³J(H,H) = 8.2 Hz, ⁴J(H,H) = 0.9 Hz, ⁵J(H,H) = 0.9 Hz, 3H, indole-*H*7), 7.34 (‘dt’, ³J(H,H) = 7.9 Hz, ⁴J(H,H) = 1.0 Hz, ⁵J(H,H) = 1.0 Hz, 3H, indole-*H*4), 7.04 (ddd, ³J(H,H) = 8.2 Hz, ³J(H,H) = 7.0 Hz, ⁴J(H,H) = 1.3 Hz, 3H, indole-*H*6), 6.93 (ddd, ³J(H,H) = 8.0 Hz, ³J(H,H) = 7.0 Hz, ⁴J(H,H) = 1.1 Hz, 3H, indole-*H*5), 5.97 (s, 1H, R₃CH), 2.39 (s, 9H, CH₃), 1.96 ppm (s, CH₃CN); ¹³C NMR (101 MHz, CD₂Cl₂, 25 °C) δ = 140.2, 139.9, 131.2, 120.5, 118.9, 118.5, 111.7, 106.3, 33.0, 8.7, 2.4 ppm; DOSY NMR (400 MHz, CD₂Cl₂, 25 °C): D = 9.5 × 10⁻¹⁸ m²/s; No satisfactory elemental analysis could be obtained because of the MeCN solvation.

Synthesis of [tmim]SiFeCl₂⁻ K[18-crown-6]⁺ (4). A suspension of 1-K[18-c-6] (70.1 mg, 0.0958 mmol) in THF (4 mL) was added to a suspension of FeCl₂ (12.1 mg, 0.0955 mmol) in THF (2 mL). Over 60 min the solution became almost clear yellow. The mixture was filtered, concentrated to 2 mL and Et₂O was added until nucleation was observed. At room temperature, over 30 minutes a microcrystalline solid appeared, after which the solution was stored at -35 °C for 16 h, filtration, washing with THF (0.2 mL, -35 °C) and extracting in THF (3 × 0.5 mL) afforded a pale yellow/green solid after removal of the solvent in vacuo (48.1 mg, 19 w% THF, 0.0499 mmol, 52%). Crystals suitable for X-ray crystallography were grown by vapor diffusion of HMDSO into a THF solution. ¹H NMR (400 MHz, C₆D₆O, 25 °C) δ = 26.97 (br s, 3H*, Indole-H), 9.96 (br s, 3H*, Indole-H), 8.66 (br s, 3H*, Indole-H), 6.99 (br s, 3H*, Indole-H), 4.36 (br s, 1H*, R₃CH), 4.08 (br s, 26H*, K+[18-crown-6]), 3.61 (br s, 10H*, THF), 1.73 (br s, 10H*, THF), 1.33 ppm (br s, 9H*, CH₃); ¹³C NMR (101 MHz, C₆D₆O, 25 °C) δ = 149.0 (Indole-C), 145.2 (Indole-C), 137.6 (Indole-C), 134.5 (Indole-CH), 128.0 (Indole-CH), 126.5, 116.9 (Indole-CH), 76.2 (K+[18-crown-6]), 56.8 (R₃CH), 32.1 ppm (CH₃). *integrals obtained by peak deconvolution. No satisfactory elemental analysis could be obtained due to the high reactivity of 4.

References

- [1] a) Wang, W.; Inoue, S.; Irran, E.; Driess, M. *Angew. Chemie Int. Ed.* **2012**, *51*, 3691–3694. b) Wiberg, N. *Coord. Chem. Rev.* **1997**, *163*, 217–252. c) Lerner, H. *Coord. Chem. Rev.* **2005**, *249*, 781–798. d) Li, J.; Merkel, S.; Henn, J.; Meindl, K.; Döring, A.; Roesky, H. W.; Ghadwal, R. S.; Stalke, D. *Inorg. Chem.* **2010**, *49*, 775–777. e) Styra, S.; González-Gallardo, S.; Armbruster, F.; Oña-Burgos, P.; Moos, E.; Vonderach, M.; Weis, P.; Hampe, O.; Grün, A.; Schmitt, Y.; Gerhards, M.; Menges, F.; Gaffga, M.; Niedner-Schatteburg, G.; Breher, F. *Chem. Eur. J.* **2013**, *19*, 8436–8446. f) Benedek, Z.; Szilvási, T. *RSC Adv.* **2015**, *5*, 5077–5086.
- [2] a) Fürstner, A.; Krause, H.; Lehmann, C. W. *Chem. Commun.* **2001**, *80*, 2372–2373. b) Gallego, D.; Brück, A.; Irran, E.; Meier, F.; Kaupp, M.; Driess, M.; Hartwig, J. F. *J. Am. Chem. Soc.* **2013**, *135*, 15617–15626. c) Wang, W.; Inoue, S.; Enthaler, S.; Driess, M. *Angew. Chemie Int. Ed.* **2012**, *51*, 6167–6171. d) Metsänen, T. T.; Gallego, D.; Szilvási, T.; Driess, M.; Oestreich, M. *Chem. Sci.* **2015**, *6*, 7143–7149. e) Gallego, D.; Inoue, S.; Blom, B.; Driess, M. *Organometallics* **2014**, *33*, 6885–6897. f) Zhang, M.; Liu, X.; Shi, C.; Ren, C.; Ding, Y.; Roesky, H. W. *Z. Anorg. Allg. Chem.* **2008**, *634*, 1755–1758. g) Brück, A.; Gallego, D.; Wang, W.; Irran, E.; Driess, M.; Hartwig, J. F. *Angew. Chemie Int. Ed.* **2012**, *51*, 11478–11482. h) Blom, B.; Enthaler, S.; Inoue, S.; Irran, E.; Driess, M. *J. Am. Chem. Soc.* **2013**, *135*, 6703–6713.
- [3] a) Simon, M.; Breher, F. *Dalton Trans.* **2017**, *46*, 7976–7997. b) Okazaki, M.; Ohshitanai, S.; Iwata, M.; Tobita, H.; Ogino, H. *Coord. Chem. Rev.* **2002**, *226*, 167–178.
- [4] a) Ichinohe, M.; Toyoshima, M.; Kinjo, R.; Sekiguchi, A. *J. Am. Chem. Soc.* **2003**, *125*, 13328–13329. b) Jenkins, D. M.; Teng, W.; Englich, U.; Stone, D.; Ruhlandt-Senge, K. *Organometallics* **2001**, *20*, 4600–4606. c) Abersfelder, K.; Scheschkewitz, D. *J. Am. Chem. Soc.* **2008**, *130*, 4114–4121. d) Ichinohe, M.; Kinjo, R.; Sekiguchi, A. *Organometallics* **2003**, *22*, 4621–4623. e) Molev, G.; Tumanskii, B.; Sheberla, D.; Botoshansky, M.; Bravo-Zhivotovskii, D.; Apeloig, Y. *J. Am. Chem. Soc.* **2009**, *131*, 11698–11700. f) Nakamoto, M.; Fukawa, T.; Lee, Y. Y.; Sekiguchi, A. *J. Am. Chem. Soc.* **2002**, *124*, 15160–15161.
- [5] Scheschkewitz, D.; Hofmann, M.; Ghaffari, A.; Amseis, P.; Präsang, C.; Mesbah, W.; Geiseler, G.; Massa, W.; Berndt, A. *J. Organomet. Chem.* **2002**, *646*, 262–270.
- [6] a) Hitchcock, P. B.; Lappert, M. F.; Layh, M. *Chem. Commun.* **1998**, 2179–2180. b) Li, H.; Hope-Weeks, L. J.; Krempner, C. *Chem. Commun.* **2011**, *47*, 4117–4119. c) Armbruster, F.;

- Fernández, I.; Breher, F. *Dalton Trans.* **2009**, 29, 5612. d) Mashin, E.; Kratish, Y.; Kaushansky, A.; Bravo-Zhivotovskii, D.; Apeloig, Y. *Struct. Chem.* **2017**, 28, 537–544.
- [7] Schwarze, N.; Steinhauer, S.; Neumann, B.; Stammeler, H.-G.; Hoge, B. *Angew. Chemie Int. Ed.* **2016**, 55, 16156–16160.
- [8] Krempner, C.; Chisholm, M. H.; Gallucci, J. *Angew. Chemie Int. Ed.* **2008**, 47, 410–413.
- [9] Barnard, T. S.; Mason, M. R. *Inorg. Chem.* **2001**, 40, 5001–5009.
- [10] Gaussian 09, Revision D.01, M. J. Frisch, G. W. Trucks, H. B. Schlegel, G. E. Scuseria, M. A. Robb, J. R. Cheeseman, G. Scalmani, V. Barone, B. Mennucci, G. A. Petersson, H. Nakatsuji, M. Caricato, X. Li, H. P. Hratchian, A. F. Izmaylov, J. Bloino, G. Zheng, J. L. Sonnenberg, M. Hada, M. Ehara, K. Toyota, R. Fukuda, J. Hasegawa, M. Ishida, T. Nakajima, Y. Honda, O. Kitao, H. Nakai, T. Vreven, J. A. Montgomery, Jr., J. E. Peralta, F. Ogliaro, M. Bearpark, J. J. Heyd, E. Brothers, K. N. Kudin, V. N. Staroverov, T. Keith, R. Kobayashi, J. Normand, K. Raghavachari, A. Rendell, J. C. Burant, S. S. Iyengar, J. Tomasi, M. Cossi, N. Rega, J. M. Millam, M. Klene, J. E. Knox, J. B. Cross, V. Bakken, C. Adamo, J. Jaramillo, R. Gomperts, R. E. Stratmann, O. Yazyev, A. J. Austin, R. Cammi, C. Pomelli, J. W. Ochterski, R. L. Martin, K. Morokuma, V. G. Zakrzewski, G. A. Voth, P. Salvador, J. J. Dannenberg, S. Dapprich, A. D. Daniels, O. Farkas, J. B. Foresman, J. V. Ortiz, J. Cioslowski, and D. J. Fox, Gaussian, Inc., Wallingford CT, **2013**.
- [11] Bent, H. A. *Chem. Rev.* **1961**, 61, 275–311.
- [12] a) Ghadwal, R. S.; Roesky, H. W.; Merkel, S.; Henn, J.; Stalke, D. *Angew. Chemie Int. Ed.* **2009**, 48, 5683–5686. b) Ghadwal, R. S.; Azhakar, R.; Roesky, H. W. *Acc. Chem. Res.* **2013**, 46, 444–456. c) Geiß, D.; Arz, M. I.; Straßmann, M.; Schnakenburg, G.; Filippou, A. C. *Angew. Chemie Int. Ed.* **2015**, 54, 2739–2744. d) Al-Rafia, S. M. I.; McDonald, R.; Ferguson, M. J.; Rivard, E. *Chem. Eur. J.* **2012**, 18, 13810–13820. e) Hadlington, T. J.; Abdalla, J. A. B.; Tirfoin, R.; Aldridge, S.; Jones, C.; Nagase, S.; Power, P. P.; Mountford, P.; Aldridge, S. *Chem. Commun.* **2016**, 52, 1717–1720.
- [13] Pregosin, P. S. *Magn. Reson. Chem.* **2017**, 55, 405–413.
- [14] a) Klapötke, T. M.; Vasisht, S. K.; Fischer, G.; Mayer, P. *J. Organomet. Chem.* **2010**, 695, 667–672. b) Fischer, R.; Konopa, T.; Baumgartner, J.; Marschner, C. *Organometallics* **2004**, 23, 1899–1907. c) Wallner, A.; Hlina, J.; Konopa, T.; Wagner, H.; Baumgartner, J.; Marschner, C.; Flörke, U. *Organometallics* **2010**, 29, 2660–2675.
- [15] Tolman, C. A. *J. Am. Chem. Soc.* **1970**, 92, 2956–2965.
- [16] Gusev, D. G. *Organometallics* **2009**, 28, 763–770.
- [17] Vingerhoets, P.; Flanagan, K. T.; Avgoulea, M.; Billowes, J.; Bissell, M. L.; Blaum, K.; Brown, B. A.; Cheal, B.; De Rydt, M.; Forest, D. H.; Geppert, C.; Honma, M.; Kowalska, M.; Krämer, J.; Krieger, A.; Mané, E.; Neugart, R.; Neyens, G.; Nörtershäuser, W.; Otsuka, T.; Schug, M.; Stroke, H. H.; Tungate, G.; Yordanov, D. T. *Phys. Rev. C* **2010**, 82, 64311.
- [18] a) Khan, S.; Ahirwar, S. K.; Pal, S.; Parvin, N.; Kathewad, N. *Organometallics* **2015**, 34, 5401–5406. b) Parvin, N.; Dasgupta, R.; Pal, S.; Sen, S. S.; Khan, S. *Dalton Trans.* **2017**, 46, 6528–6532.
- [19] Farwell, J. D.; Hitchcock, P. B.; Lappert, M. F.; Protchenko, A. V. *J. Organomet. Chem.* **2007**, 692, 4953–4961.
- [20] Heine, A.; Stalke, D. *Angew. Chemie Int. Ed.* **1993**, 32, 121–122.
- [21] a) Troadec, T.; Prades, A.; Rodriguez, R.; Mirgalet, R.; Baceiredo, A.; Saffon-Merceron, N.; Branchadell, V.; Kato, T. *Inorg. Chem.* **2016**, 55, 8234–8240. b) Tan, G.; Blom, B.; Gallego, D.; Driess, M. *Organometallics* **2014**, 33, 363–369.
- [22] Hänninen, M. M.; Pal, K.; Day, B. M.; Pugh, T.; Layfield, R. A. *Dalton Trans.* **2016**, 45, 11301–11305.
- [23] a) Roddick, D. M.; Tilley, T. D.; Rheingold, A. L.; Geib, S. J. *J. Am. Chem. Soc.* **1987**, 109, 945–946. b) Kim, Y. O.; Goff, H. M. *J. Am. Chem. Soc.* **1988**, 110, 8706–8707. c) Heyn, R. H.; Tilley, T. D. *Inorg. Chim. Acta* **2002**, 341, 91–98. d) Turculet, L.; Feldman, J. D.; Tilley, T. D. *Organometallics* **2003**, 22, 4627–4629. e) Hatanaka, T.; Ohki, Y.; Tatsumi, K. *Eur. J. Inorg. Chem.* **2013**, 2013, 3966–3971.
- [24] Glendening, E. D.; J, K. B.; Reed, A. E.; Carpenter, J. E.; Bohmann, J. A.; Morales, C. M.; Landis, C. R.; Weinhold, F. *NBO 6.0*; **2013**.
- [25] Gokel, G. W.; Cram, D. J. *J. Org. Chem.* **1974**, 39, 2445–2446.

- [26] Armarego, W. L. F.; Chai, C. L. L. *Purification of laboratory chemicals*; **2003**.
- [27] Fulmer, G. R.; Miller, A. J. M.; Sherden, N. H.; Gottlieb, H. E.; Nudelman, A.; Stoltz, B. M.; Bercaw, J. E.; Goldberg, K. I. *Organometallics* **2010**, *29*, 2176–2179.
- [28] von Döbeneck, H.; Prietzel, H. *Hoppe-Seyler's Z. Physiol. Chem.* **1955**, *299*, 214–226.
- [29] Jafarpour, L.; Stevens, E. D.; Nolan, S. P. *J. Organomet. Chem.* **2000**, *606*, 49–54.
- [30] Hintermann, L. *Beilstein J. Org. Chem.* **2007**, *3*, 2–6.
- [31] Pompeo, M.; Froese, R. D. J.; Hadei, N.; Organ, M. G. *Angew. Chemie Int. Ed.* **2012**, *51*, 11354–11357.
- [32] Ghadwal, R. S.; Roesky, H. W.; Merkel, S.; Henn, J.; Stalke, D. *Angew. Chemie Int. Ed.* **2009**, *48*, 5683–5686.
- [33] A. M. M. Schreurs, X. Xian, L. M. J. Kroon-Batenburg, *J. Appl. Cryst.* **2010**, *43*, 70–82.
- [34] G. M. Sheldrick **2014**, SADABS and TWINABS. Universität Göttingen, Germany.
- [35] G. M. Sheldrick. *Acta Cryst.* **2015**, *A71*, 3–8.
- [36] G. M. Sheldrick. *Acta Cryst.* **2015**, *C71*, 3–8.
- [37] A. L. Spek, *Acta Cryst.* **2009**, *D65*, 148–155.
- [38] R. Herbst-Irmer, G. M. Sheldrick, *Acta Cryst.* **1998**, *B54*, 443–449.
- [39] A. L. Spek. *Acta Cryst.* **2015**, *C71*, 9–18.
- [40] G. M. Sheldrick, *Acta Cryst.* **2008**, *A64*, 112–122.
- [41] Vingerhoets, P.; Flanagan, K. T.; Avgoulea, M.; Billowes, J.; Bissell, M. L.; Blaum, K.; Brown, B. A.; Cheal, B.; De Rydt, M.; Forest, D. H.; Geppert, C.; Honma, M.; Kowalska, M.; Krämer, J.; Krieger, A.; Mané, E.; Neugart, R.; Neyens, G.; Nörtershäuser, W.; Otsuka, T.; Schug, M.; Stroke, H. H.; Tungate, G.; Yordanov, D. T. *Phys. Rev. C* **2010**, *82*, 64311.
- [42] Liotta, C. *Phase Transfer Catalysis: Principles and Techniques*; Elsevier Science, **2012**.

5

Synthesis and Complexation of a Free Germanide bearing a tridentate N-heterocyclic substituent

The tris-heterocycle germanide $(\text{tmim})\text{Ge}^-$ (**1**) ($\text{tmimH}_3 = \text{tris}[3\text{-methylindol-2-yl)]\text{methane}$) was synthesized by nucleophilic substitution for the tmim^{3-} trianion on $\text{GeCl}_2\cdot\text{dioxane}$. Complexation of the germanide to CuCl resulted in the dimeric chlorocuprate $[(\text{tmim})\text{GeCu}(\mu\text{-Cl})]_2^{2-}$, which is prone to dissociation in MeCN to form the neutral, solvated germylcopper $(\text{tmim})\text{Ge}(\text{NCMe})_3$. The reaction of **1** with $\text{Fe}_2(\text{CO})_9$ afforded the germyl iron tetracarbonyl $[(\text{tmim})\text{GeFe}(\text{CO})_4]^-$. Analysis of the $\tilde{\nu}(\text{CO})$ vibrations in this complex indicates that the combined electron donating and accepting properties of **1** are found in between those of $(\text{tmim})\text{P}$ and $(\text{tmim})\text{Si}^-$. In contrast to $(\text{tmim})\text{Si}^-$, $(\text{tmim})\text{Ge}^-$ is reluctant to coordinate to FeCl_2 , likely because of its softer Lewis base character. Key structural features of the ligands and complexes reflect changes in their electronic properties. In particular, the N–Ge–N angles increase upon coordination to a metal fragment, suggesting increasing hybridization of the Ge s- and p-orbitals. These findings will be useful in further understanding low-valent heavier group 14 complexes in organometallic chemistry.

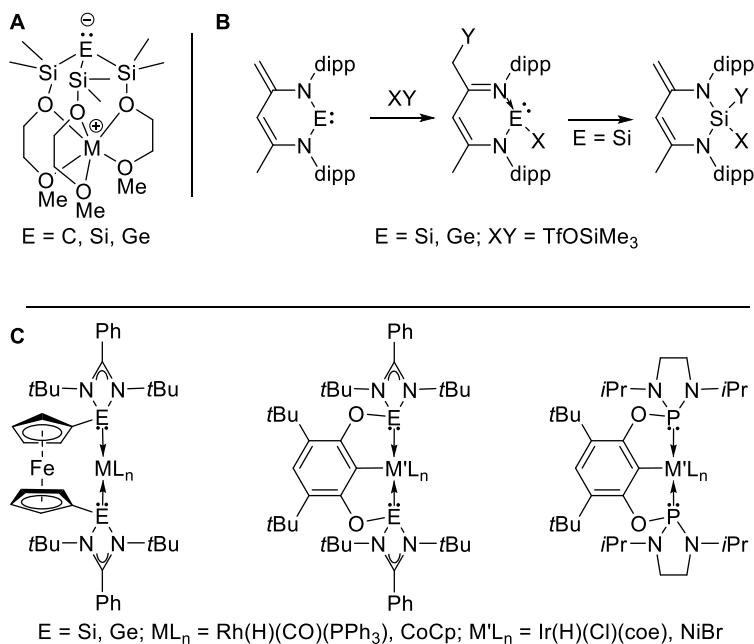
Introduction

Ligands based on the heavier analogues of carbenes have received considerable interest in recent years.^{1–3} The major part of known Si(II) and Ge(II) species are base-stabilised silylenes or germylenes, *i.e.* compounds featuring two anionic and at least one donating, neutral substituent. Such compounds can serve as ligands for a broad range of transition metals and some – mainly silylenes – have found application in catalysis.^{4–11} Ge(II) compounds are generally less reducing than their Si(II) counterparts and hence more easily accessible, largely because Ge(II) precursors such as GeCl_2 -dioxane are readily available.

Because of their similar covalent radii (Si: 1.11(2) and Ge: 1.20(4) Å),¹² Si(II) and Ge(II) often give rise to similar structures and parallel reactivity, but instructive differences are known. For example, Aquino *et al.* investigated the electronic properties, *e.g.* Brønsted acidity, of zwitterionic, silyl-substituted methanides, silanides, and germanides ($\text{R}_3\text{E(II)}$ anions), showing that basicity decreases down group 14 (Scheme 5.1, A).¹³ They also note that the methanides are markedly different from the silanides and germanides, both structurally and electronically, mainly due to significant hyperconjugation of the lone pair into the adjacent silyl groups. The decreased basicity also translates in increased stability of E(II) compounds going down group 14. For example, the mere existence of compounds of type X_2E (X = halo, $\text{N}(\text{SiMe}_3)_2$) for E = Ge(II), Sn(II) illustrates this difference, as the Si(II) homologues decompose well below ambient temperature. The stability of these germylenes and stannylene is due to the increasing energy separation of the central atom's s- and p-orbitals, descending group 14.^{14–18}

Another illustrative example is the addition of small molecules over the β -diketiminato silylene or germylene (Scheme 5.1, B). Despite their structural resemblance, the silylene showed a thermodynamic preference for 1,1-addition and formal oxidation of Si(II) to Si(IV), whereas in the germylene 1,4-addition was preferred, transforming the diamido-germylene centre in a base-stabilised amido(triflate)germylene.^{19–21} Finally, the catalytic activity of homologous silylene and germylene complexes has been compared. In hydroformylation catalysis, a rhodium complex of a ferrocene-bridged disilylene ligand (Scheme 5.1, C) proved to be much more active than its germylene analogue.²² This difference was attributed to the enhanced σ -donor strength of the silylene. The same trend was observed in the cyclotrimerization reaction of phenylacetylene catalysed by the analogous CoCp complex.⁶ The decreased reactivity of the germylene complex is in this case attributed to a stronger coordination of Ge to Co, hampering the creation of an active site. Interestingly, in the C–H borylation of arenes catalysed by an iridium SiCSi pincer complex featuring two silylene donor moieties (Scheme 5.1, C) the yield was only slightly higher compared to the germylene (90% and 80%), but significantly

higher compared to the related phosphine complex (64%).¹⁰ The increased reactivity of the Si and Ge complexes is thought to arise from stronger σ -donor properties compared to P. Complexes of these ligands with NiBr showed similar reactivity for the silylene and phosphine in a Sonogashira coupling. Interestingly, the germylene complex showed an increased yield from 40% to 53% compared to the silylene complex.⁵



Scheme 5.1 A; study of electronic nature of the anions.¹³ B; distinct small molecule activation.^{19–21} C; silylene and germylene catalysts.^{5,6,10,22}

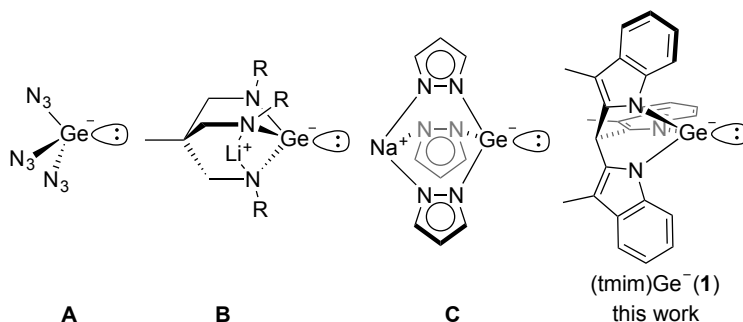


Chart 5.1 Naked tri-nitrogen substituted germanides.

In chapter 4 of this thesis, the synthesis and coordination chemistry of an unusual Si(II) anion supported by the tmim scaffold (tmimH₃ = tris(3-methylindol-2-yl)methane) by substitution on an Si(III) precursor is reported.²³ The introduction of electron-withdrawing groups to delocalize the negative charge and the tight cage

structure are thought to enhance the stability of the anion by lowering the energy of the lone pair. To gain understanding on the influence of this cage design on ligand properties, the analogous germanide **1** (Chart 5.1) was investigated. All-nitrogen substituted germanides similar to **1** have received some attention, examples including triazidogermanide **A**, bicyclo triamidogermanide **B**, and the zwitterionic tripyrazolyl germanide **C** (Chart 5.1).^{24–30} Their coordination chemistry is scarce and structurally characterized complexes are limited to a tungsten(II) complex derived from structure **A**, a gold(I) complex derived from structure **B**, and iron(III) complexes of a tetradentate triphosphinogermeryl ligand.^{24–26} In this chapter, the synthesis of compound **1** and its complexation to soft Lewis-acidic metal fragments (CuCl , $\text{Cu}(\text{NCMe})_3$, and $\text{Fe}(\text{CO})_4$) is reported. In contrast to the silanide, coordination to the harder Lewis acid FeCl_2 results in at most a weak interaction with a small association constant in solution. The properties of **1** as a ligand are compared with those of the anionic $\text{Si}(\text{III})$ and the neutral $\text{P}(\text{III})$ analogues, showing that its donor ability is situated between those. Analysis of the N–E–N angles, N–E, and E–M distances provides insight in the electronic nature of the ligands.

Results and discussion

The substituent $(\text{tmim})\text{H}_3$ was synthesised and deprotonated according to published procedures.^{23,31} Subsequently, the germanide **1** was synthesised by nucleophilic substitution of chloride for the *tmim* tri-anion on GeCl_2 -dioxane (Scheme 5.2), which is commonly used to synthesize germanides.^{24–29,32,33} The germanide was obtained either as its sodium salt **1-Na** or as its potassium salt **1-K**. The synthesis of **1-Na** requires an excess of GeCl_2 -dioxane to reach completion, which is tentatively attributed to formation of insoluble NaGeCl_3 . In contrast, a stoichiometric amount of GeCl_2 -dioxane was sufficient for the synthesis of **1-K**. Therefore, the potassium salt **1-K** was used for complexation studies.

A single set of ^1H resonances in the aromatic region indicates that **1** possesses threefold-symmetry, as expected for a bicyclo[2.2.2]octane topology. The presence of **1** was detected by ESI-MS as the molecular anion (M^- = measured: 474.1085 a.u., calc'd: 474.1031 a.u.). Crystals of **1** suitable for X-ray crystallography were grown by storing a concentrated sample of **1-Na** in THF at -35°C for two days. The molecular structure shows the presence of a free tricoordinate germanide with a solvated sodium counter ion (Figure 5.1). The N–Ge–N angles provide a crude measure for the extent of hybridization of the Ge valence orbitals (s,p).³⁴ Ideally, the sum of angles is 270° in non-hybridized and 328.5° in sp^3 hybridized systems. The sum of the N–Ge–N angles ($263.5(3)^\circ$) suggests negligible hybridization of the Ge valence orbitals, with the lone pair located in the s-orbital. Angles close to 90° are commonly found in germanides, also in the absence of a cage structure enforcing them as for example in compound **A** (Chart 5.1).^{27,28,35–37} This is a consequence of the generally low propensity of heavier elements to undergo orbital hybridization, *i.e.* the inert pair effect.^{14–18}

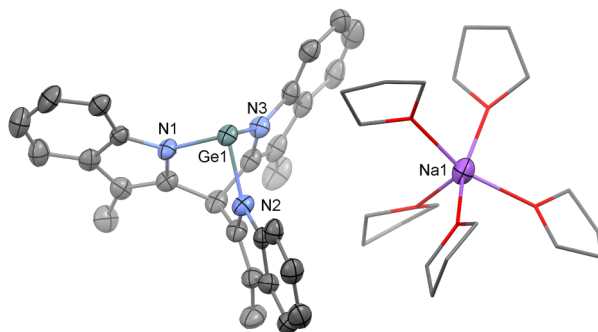
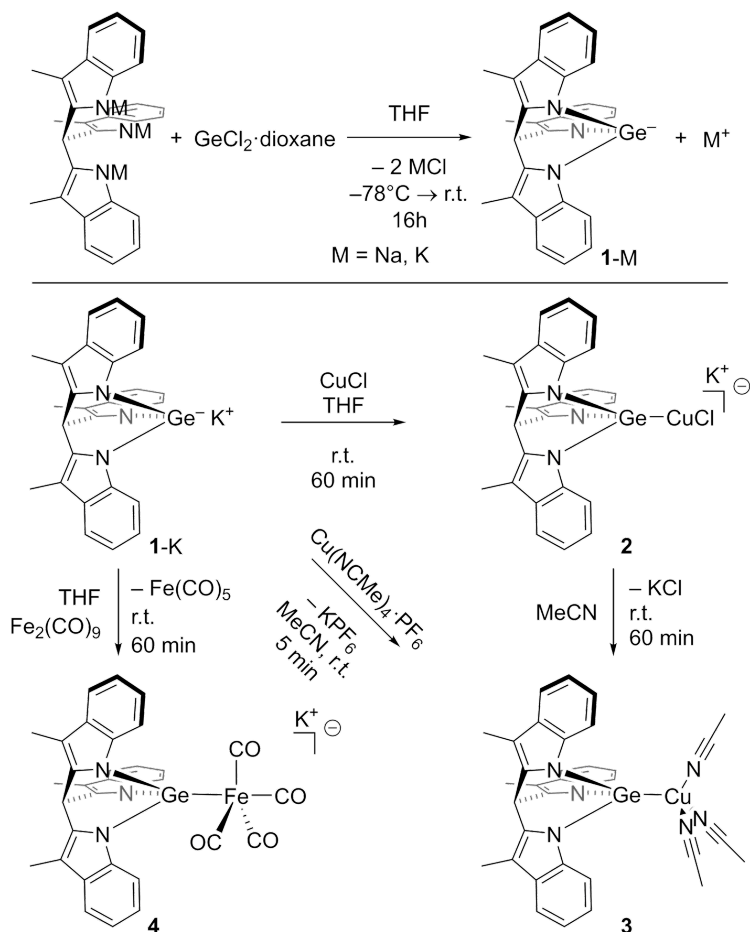


Figure 5.1 Molecular structure of **1**-Na in the crystal. Ellipsoids are drawn at the 50% probability level. Hydrogen atoms are omitted for clarity. Selected bond distances [Å] and angles [°]: N1–Ge1 1.956(5), N2–Ge1 1.970(4), N3–Ge1 1.971(5), N1–Ge1–N2 88.0(2), N2–Ge1–N3 88.1(2), N1–Ge1–N3 87.5(2).

The coordination chemistry of the synthesised germanide was investigated with 1st row transition metal salts (Scheme 5.2). Germanide **1**-K was complexed to one equiv of CuCl in THF at ambient temperature to form the chloro cuprate **2**. A single set of ¹H resonances in the aromatic region shows retention of threefold symmetry. In solution, the chloro cuprate exists as a monomer as was evidenced by the identical diffusion coefficients observed in DOSY NMR for **1** and **2** in C₆D₆O. Crystals suitable for X-ray crystallography were grown from a concentrated THF solution at –35 °C. In the solid-state, complex **2** exists as two distinct dimers with a Cu₂Cl₂ diamond core, similar to the (tmim)Si chloro cuprate.²³ Unlike the silicon analogue, the structure of **2** is slightly bent: the Cl–Cu–Cl planes within a molecule form an angle of 21°. The sum of the N–Ge–N angles in the two distinct ligands of the two individual molecules is: unit 1: 273.0(6)° and 272.7(6)°; unit 2: 272.7(6)° and 272.4(6)°. This suggests a slight rehybridization in the direction of sp³ compared to the free germanide **1**, for which the sum of the N–Ge–N angles is 263.5(3)°. Compound **2** constitutes only the second structurally characterized example of a germyl cuprate, next to bis(triphenylgermyl)copper as reported by Orlov et al.³⁸ Diamond core dimeric structures [Cu₂X₂; X = C₆F₅, I] related to **2** were previously observed for germylene complexes bearing nacnac- and aminotroponimate ligands.^{39–41} This diamond core is generally planar; it is bent only in a Cu₂l₂ complex bearing a bidentate digermylene ligand, forcing the bent geometry.⁴² This suggests that crystal packing effects are responsible for the bent structure observed in complex **2**. The Ge–Cu bond length of 2.2590(19) Å in **2** is remarkably short, shorter distances being found only in germylene complexes of copper nacnac.⁴³



Scheme 5.2 Synthesis of **1-M** by nucleophilic substitution of Cl for tmim in $\text{GeCl}_2 \cdot \text{dioxane}$ and synthesis of transition metal complexes **2-4**.

Similar to the silicon analogue, the chloride in anionic cuprate **2** can be displaced by acetonitrile to form a neutral copper germanide. A saturated solution of **2** in acetonitrile produces crystals within 16 h [Figure 5.2]. The solid-state structure of **3** shows a monomeric, tris-acetonitrile complex. This complex is one of few neutral monodentate germyl copper complexes.^{44–47} The Ge–Cu distance in **3** [Ge1–Cu1 2.2922(5) Å] is the shortest observed for such complexes.^{44,45} To determine whether the chlorocuprate dissociates in acetonitrile and THF solution, an authentic sample of neutral **3** was synthesised by complexation of **1-K** to $\text{Cu}(\text{MeCN})_4 \cdot \text{PF}_6$. The ^1H NMR spectrum of the resulting complex is identical to that of **2** in CD_3CN , whereas a significant difference can be seen in the chemical shift of the indole-H7 between both samples in THF (7.62, 7.94 ppm for **3** and **2**, resp.). This suggests that complex **2** exists as a molecular chlorocuprate in THF but dissociates to the neutral complex **3** in acetonitrile.

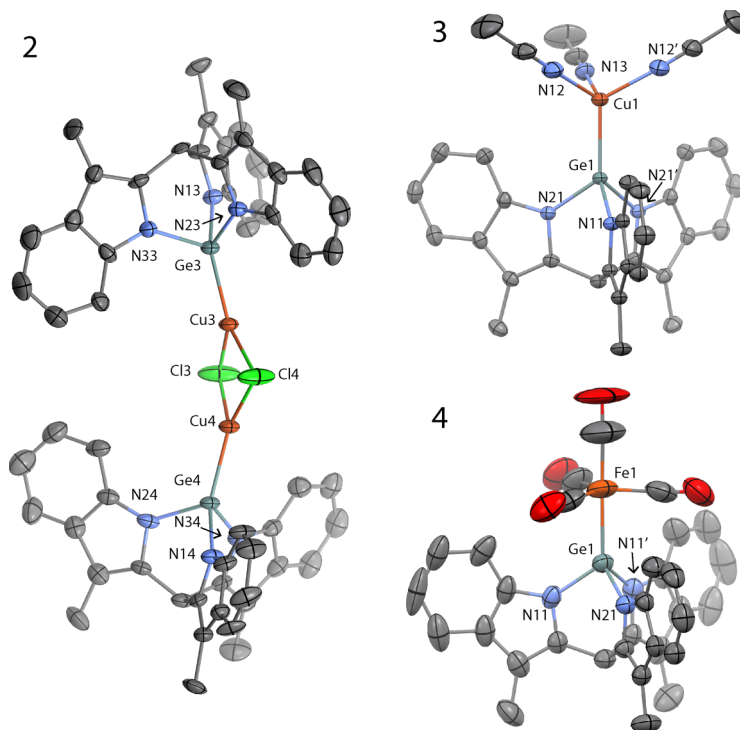
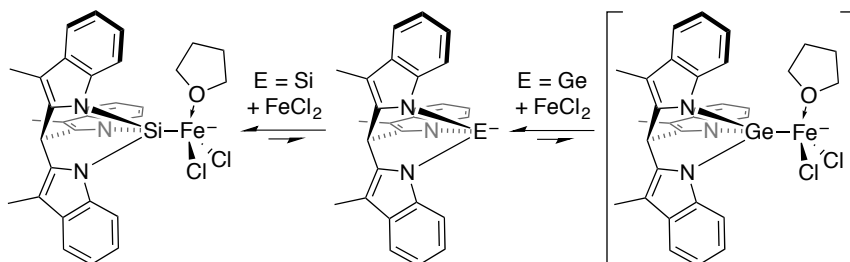


Figure 5.2 Molecular structure of the di-anion of **2**, neutral **3**, and the anion of **4** in the crystal. Ellipsoids are drawn at the 50% probability level. Hydrogen atoms, THF solvated potassium cations, and co-crystallized MeCN are omitted for clarity. Accented atom labels arise from mirror symmetry. The asymmetric unit of **2** contains 2 distinct molecules of which one is shown. Selected bond distances [Å] and angles [°]: **2**: Unit 1: Ge1–Cu1 2.2590(19), Ge2–Cu2 2.2560(19), Ge1–N11 1.899(7), Ge1–N21 1.898(8), Ge1–N31 1.905(7), Ge2–N12 1.911(8), Ge2–N22 1.907(7), Ge2–N32 1.917(8), N11–Ge1–N21 90.3(3), N21–Ge1–N31 91.4(4), N31–Ge1–N11 91.3(3), N12–Ge2–N22 90.6(4), N22–Ge2–N32 91.2(4), N32–Ge2–N12 90.8(3), angle between planes Cl1–Cu1–Cl2 and Cl1–Cu2–Cl2: 20.59. Unit 2: Ge3–Cu3 2.2613(17), Ge4–Cu4 2.2604(17), Ge3–N13 1.907(8), Ge3–N23 1.902(10), Ge3–N33 1.901(8), Ge4–N14 1.909(8), Ge4–N24 1.917(10), Ge4–N34 1.900(10), N13–Ge3–N23 90.6(4), N23–Ge3–N33 91.4(4), N33–Ge3–N13 90.6(3), N14–Ge4–N24 90.3(4), N24–Ge4–N34 91.9(4), N34–Ge4–N14 90.1(4), angle between planes Cl3–Cu3–Cl4 and Cl3–Cu4–Cl4: 21.24; **3**: Ge1–Cu1 2.2922(5), Ge1–N11 1.9110(16), Ge1–N21 1.9161(12), N11–Ge1–N21 90.20(5), N21–Ge1–N21' 88.69(5); **4**: Ge1–Fe1 2.2979(19), Ge1–N11 1.890(5), Ge1–N21 1.903(6), N11–Ge1–N21 92.61(17), N11–Ge1–N11' 92.4(2).

The synthesis of an $\text{Fe}(\text{CO})_4$ derivative of compound **1** is of interest as a way to investigate its electronic properties as a ligand. Reaction of **1**-K with $\text{Fe}_2(\text{CO})_9$ in THF at room temperature afforded very cleanly the $\text{Fe}(\text{CO})_4$ complex **4** (Figure 5.2) with loss of $\text{Fe}(\text{CO})_5$. Retention of the threefold-symmetry is indicated by a single set of ^1H NMR resonances in the aromatic region. Crystals suitable for X-ray crystallography were grown by diffusion of hexane into a concentrated THF solution of **4**. The structure is very similar to that of the neutral phosphine analogue $(\text{tmim})\text{PFe}(\text{CO})_4$ reported by Barnard and Mason.⁴⁸ The distinct axial and equatorial CO resonances of **4** in ^{13}C NMR were observed in a 1:3 ratio at $-40\text{ }^\circ\text{C}$ ($\delta = 222.57, 212.16\text{ ppm}$) and 1 coalesced resonance at $70\text{ }^\circ\text{C}$ ($\delta = 215.54\text{ ppm}$). One broad resonance at room

temperature ($\delta = 215.05$ ppm, FWHM = 125 Hz) suggests that this is above the coalescence temperature. In $(\text{tmim})\text{PFe}(\text{CO})_4$, similar fluxional behaviour was ascribed to hindered axial-equatorial exchange of the carbonyl ligands caused by steric repulsion of the indole rings on the carbonyls in the square pyramidal intermediate of plausible Berry pseudorotation⁴⁹ as well as turnstile rotation.⁴⁸ For the phosphine complex the coalescence temperature is estimated to be 97 °C, albeit not observed.⁵⁰ The lower coalescence temperature for the germanium analogue suggests a lower energy barrier for the carbonyl exchange, which can be ascribed to the longer Ge-Fe bond with respect to the P-Fe bond, reducing steric congestion around the iron centre.

Whereas copper chloride and iron carbonyl give well defined complexes with germanide **1**, it binds only weakly to FeCl_2 (Scheme 5.3). In the ^1H NMR of an equimolar solution of **1**-K and FeCl_2 in THF the indole-H7 peak broadens (FWHM, from 2.8 to 40 Hz) and shifts 0.50 ppm to low-field (Figure 5.3). Concomitantly, the R_3CH signal shifts 0.13 ppm to high-field. This is in contrast with $(\text{tmim})\text{Si}^-$,²³ which binds to FeCl_2 to form $(\text{tmim})\text{SiFeCl}_2\cdot\text{THF}$, causing a low-field shift of 20 ppm for the indole-H7 and a high-field shift of 1.5 ppm for the R_3CH signal. The weaker affinity of **1** for FeCl_2 with respect to $(\text{tmim})\text{Si}^-$ can be understood in terms of Hard and Soft Acids and Bases (HSAB), the germanide being a softer Lewis base than the silanide.



Scheme 5.3 coordination of the silanide and germanide ligands to iron dichloride.

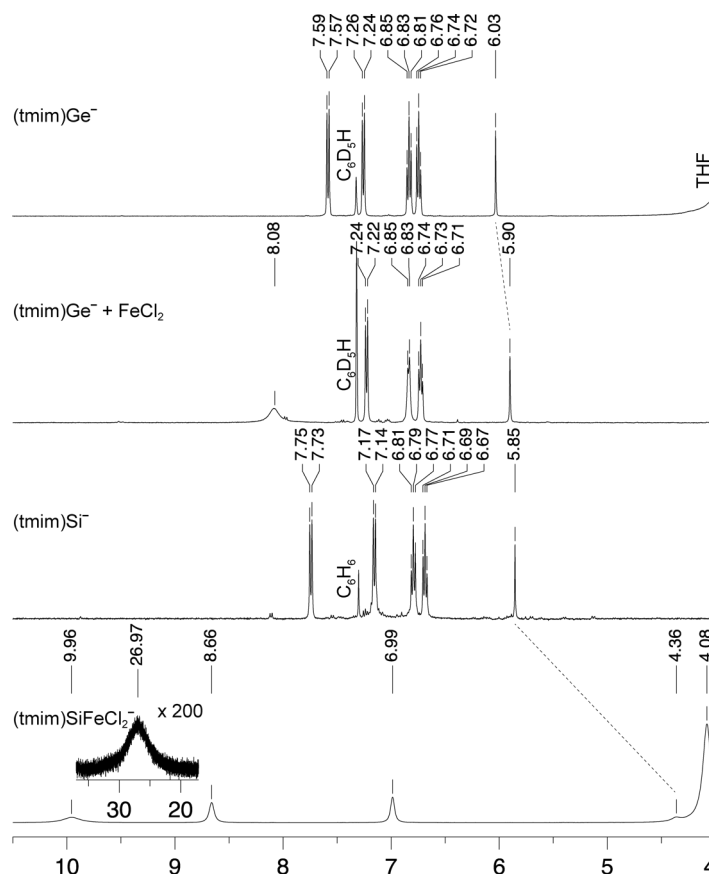


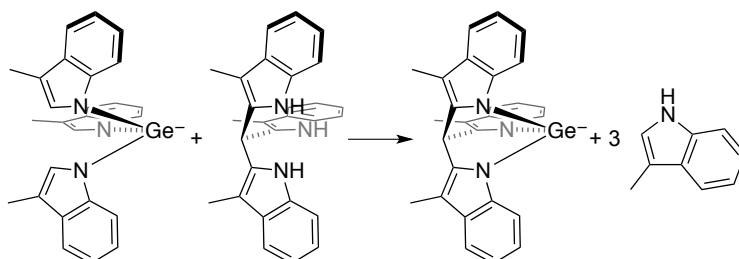
Figure 5.3 ^1H NMR spectra of $(\text{tmim})\text{E}^-$ compounds [$\text{E} = \text{Ge}, \text{Si}, \text{SiFeCl}_2$] and an equimolar mixture of 1-K and FeCl_2 in $\text{THF}-d_8 + \text{C}_6\text{D}_6$ [Ge] or $\text{THF}-d_8$ [Si].

The series of Ge compounds described herein, provide a rare opportunity to compare side by side the properties of isostructural ligands featuring three different central elements, namely P(III),^{48,50} Si(II),²³ and Ge(II). Key geometrical and spectroscopic parameters are collected in Table 5.1. In the solid state, the anions $(\text{tmim})\text{Ge}^-$ and $(\text{tmim})\text{Si}^-$ possess rather acute N–E–N angles [$\Sigma(\text{N–Si–N}) = 272.58(9)^\circ$, $\Sigma(\text{N–Ge–N}) = 263.5(3)^\circ$], with respect to the phosphine analogue [$\Sigma(\text{N–P–N}) = 285.30(12)^\circ$, Table 5.1].^{48,50} The more acute angles in $(\text{tmim})\text{Ge}^-$ compared to $(\text{tmim})\text{Si}^-$ likely arise from the larger atomic radius of germanium, because the through-space $\text{N}\cdots\text{CH}\cdots\text{N}$ angles are larger in $(\text{tmim})\text{Ge}^-$, indicating that the tmim scaffold needs to open up to accommodate the larger Ge^- anion. This is also reflected in the N–E distances being larger in $(\text{tmim})\text{Ge}^-$. Despite this, the strain energy (Chapter 4) was calculated to be very low [$\Delta H = -1.0$ kcal/mol, Scheme 5.4]. The difference in N–E–N angles between Si and P is likely a combined effect of the slightly larger P-radius and the absence of a negative charge on phosphorus, *i.e.* less repulsion for the anionic indole moieties.

Table 5.1 Sum of angles, distances and $\tilde{\nu}(\text{CO})$ in tmimE compounds (E = P, Si⁻, Ge⁻) and their complexes.

E =	P	Si ⁻	Ge ⁻
tmimE			
$\Sigma \text{N-E-N} / ^\circ$	285.30(12)	272.58(9)	263.5(3)
$\langle \text{N-E} \rangle / \text{\AA}$	1.7084(8)	1.8416(6)	1.966(3)
$\langle \text{N}\cdots\text{CH}\cdots\text{N} \rangle / ^\circ$	62.3	64.7	67.5
[(tmimE)Cu($\mu\text{-Cl}$)]₂²⁻			
$\text{Cu-E} / \text{\AA}$	-	2.1906(10)	2.2590(19)
$\Sigma \text{N-E-N} / ^\circ$	-	280.8(2)	272.6(3)
$\langle \text{N-E} \rangle / \text{\AA}$	-	1.8010(17)	1.906(2)
(tmimE)Cu(NCMe)₃			
$\text{Cu-E} / \text{\AA}$	-	2.2106(8)	2.2922(5)
$\Sigma \text{N-E-N} / ^\circ$	-	278.73(12)	269.10(9)
$\langle \text{N-E} \rangle / \text{\AA}$	-	1.8063(10)	1.9144(8)
(tmimE)Fe(CO)₄			
$\text{Fe-E} / \text{\AA}$	2.1539(5)	-	2.2979(19)
$\Sigma \text{N-E-N} / ^\circ$	292.56(12)	-	277.6(3)
$\langle \text{N-E} \rangle / \text{\AA}$	1.7085(8)	-	1.894(3)
$\tilde{\nu}(\text{CO}) / \text{cm}^{-1}$ exp	2076 2006 1977	2029 ^[a] - 1920	2037 1954 1933
$\tilde{\nu}(\text{CO}) / \text{cm}^{-1}$ calc	2074 2012 1990	2026 1956 1939	2032 1961 1948

^[a] Tentative assignment from a spectrum measured on a mixture of components.

**Scheme 5.4** Homodesmotic reaction used for strain calculations.

The solid-state structures of the complexes presented herein correlate with changes in orbital hybridization at the central atom. Upon complexation, the N-E-N angles increase in all ligands, which can be explained by an increasing *p*-character of the lone pair upon binding to a Lewis acid and a consequent decrease in the *p*-character of the E-N bonding orbitals. This is in agreement with Bent's rule:³⁴ increased electronegativity of a substituent (from a lone pair to a metal fragment) results in increased *p*-character of the bonding orbitals. The E-N distances decrease upon complexation for both tmimSi and **1**, but the E-N distances in tmimP remain unchanged within the error bounds upon complexation to Fe(CO)₄. This difference can be interpreted as a consequence of the stronger electron-donor character of the anionic ligands as compared with (tmim)P, which results in a higher degree of charge transfer upon complexation, causing a shortening of the N-E bonds as the electron density at the central element is depleted.

In the cuprates of tmimGe and tmimSi the E–Cu distances are very short and mutually similar ($\Delta d(\text{E–Cu}) = 0.0686(13) \text{ \AA}$), taking into account the difference in covalent radii ($0.09(4) \text{ \AA}$).¹² The metal fragment in the acetonitrile complexes is somewhat less e^- -withdrawing as is reflected in tightening of the N–E–N angles and a slight increase in E–N distance from LCuCl^- to $\text{LCu}(\text{NCMe})_3$, correlating with slightly longer Cu–E bonds. This can be taken to indicate that the increase in coordination number in the acetonitrile complex outweighs the loss of the more electron-rich, anionic chloride ligand.

For comparison with **4**, complexation of $[\text{tmim}]\text{Si}^-$ to $\text{Fe}(\text{CO})_4$ was investigated. It affords a mixture of 2 major components of which one is tentatively assigned to $[(\text{tmimSi})\text{Fe}(\text{CO})_4]^-$ on the basis of ESI-MS and IR (in combination with DFT-calculated $\tilde{\nu}(\text{CO})$, Table 5.1). Isolation of the silyl iron complex was unsuccessful. The vibrational frequency of the carbonyls in $(\text{tmim})\text{EFe}(\text{CO})_4$ (E = Si^- , Ge^- , P; Table 5.1) indicates that the silanide is the strongest electron donor, the germanide is somewhat weaker and the phosphine is a significantly weaker donor.

Conclusions

The free germanide tmimGe^- (**1**, $(\text{tmim})\text{H}_3 = \text{tris}(3\text{-methylindol-2-yl})\text{methane}$) was synthesised through nucleophilic substitution on $\text{GeCl}_2 \cdot \text{dioxane}$ by the trianion tmim^{3-} . Germanide **1** was shown to coordinate to Cu(I) and Fe(0) fragments, affording the chloro cuprate $[(\text{tmim})\text{GeCuCl}]^-$ and the iron carbonyl complex $[(\text{tmim})\text{GeFe}(\text{CO})_4]^-$. The chloro cuprate was shown to dissociate in acetonitrile to give the neutral acetonitrile solvated complex $(\text{tmim})\text{GeCu}(\text{NCMe})_3$. Contrasting with the reactivity of the analogous silanide, coordination of **1** to FeCl_2 results in at most a weak interaction. With the existence of the analogous tmimP and tmimSi^- , and complexes thereof, a rare opportunity arose of comparing the properties of isostructural ligands featuring different central elements, namely P(III), Si(II), and Ge(II). The relative electron donor strength was interrogated from the observed $\tilde{\nu}(\text{CO})$ in IR spectroscopy, showing that the donor strength follows the trend $\text{P} < \text{Ge} < \text{Si}$. Analysis of the N–E–N angles, N–E, and E–M distances provides insight in the electronic nature of the ligands, suggesting increased hybridization of the Ge s- and p-orbitals upon complexation to a metal fragment. The findings presented here contribute to the understanding of low-valent heavier group 14 ligands and their complexes and may provide important insights necessary for further development of this promising class of ligands.

Experimental Section

All reactions involving air-sensitive compounds were conducted under an N_2 atmosphere by using standard glovebox or Schlenk techniques. Acetonitrile and n-hexane were dried with an MBRAUN MB SPS-79 system, THF was distilled from benzophenone/Na. All solvents were degassed by bubbling with N_2 for 30 min, and stored over molecular sieves in a glovebox. Deuterated acetonitrile and THF were degassed by four freeze-pump-thaw cycles and stored over molecular sieves in a glovebox. Skatole, NaH (60 wt% in mineral oil), KH (30 wt% in mineral oil), $FeCl_2$ were purchased from Sigma-Aldrich. Triethyl orthoformate, $Fe_2(CO)_9$, CuCl were purchased from Acros. $GeCl_2$ -dioxane was purchased from ABCR. All commercially obtained chemicals were used as received, except for CuCl. From CuCl, copper oxides and hydroxides were removed with hydrochloric acid as described in literature and the resulting solid was azeotropically dried with acetonitrile until $\nu(C\equiv N)$ in IR disappeared.⁵¹ All NMR measurements were performed on a Varian VNMR400 or Varian MRF400 spectrometer, shifts are reported relative to TMS with the residual solvent signal as internal standard.⁵² All NMR experiments involving air-sensitive compounds were conducted in J-Young NMR tubes under an N_2 atmosphere. IR spectra were recorded on a Perkin-Elmer Spectrum Two FT-IR spectrometer. ESI-MS measurements were performed on a Waters LCT Premier XE KE317 spectrometer. Elemental analysis was conducted by the Mikroanalytisches Laboratorium Kolbe (**3,4**) or Medac Ltd. (**2**). The compounds $(tmim)H_3$,³¹ $(tmim)Na_3$,²³ $(tmim)K_3$,²³ were prepared according to reported procedures.

Computational methods

Calculations were performed using Gaussian09, Revision D.01.⁵³ The absence of negative eigenvalues was confirmed for all structures. All structures were optimized using the TPSS functional with the TZVP basis set.

Syntheses

Synthesis of $(tmim)GeNa$ (1-Na**).** Solutions of $(tmim)Na_3$ (501 mg, 27 w% THF, 0.78 mmol) in THF (10 mL) and $GeCl_2$ -dioxane (337 mg, 1.46 mmol) in THF (6 mL) were cooled to $-79^\circ C$. The $GeCl_2$ -dioxane solution was added to the $tmim$ solution, resulting in a suspension. This was allowed to warm to r.t. over 16 h. Filtration and removal of the solvent, followed by recrystallization from THF at $-35^\circ C$ and drying *in vacuo* afforded a yellow powder (190 mg, 34 w% THF, 0.405 mmol, 32%). 1H NMR (400 MHz, CD_3CN , $25^\circ C$) δ = 7.56 (dt, $^3J(H,H)$ = 8.3 Hz, $^4J(H,H)$ = 0.8 Hz, $^5J(H,H)$ = 0.8 Hz, 3H, Indole-H7), 7.32 (dt, $^3J(H,H)$ = 7.8 Hz, $^4J(H,H)$ = 1.1 Hz, $^5J(H,H)$ = 1.1 Hz, 3H, Indole-H4), 6.92 (ddd, $^3J(H,H)$ = 8.1 Hz, $^3J(H,H)$ = 7.0 Hz, $^4J(H,H)$ = 1.3 Hz, 3H, Indole-H6), 6.83 (ddd, $^3J(H,H)$ = 7.9 Hz, $^3J(H,H)$ = 7.0 Hz, $^4J(H,H)$ = 1.1 Hz, 3H, Indole-H5), 6.01 (s, 1H, R_3CH), 2.43 ppm (s, 9H, CH_3). ^{13}C NMR (101 MHz, CD_3CN , $25^\circ C$) δ = 141.9 (2x ^{Ar}qC), 131.2 (^{Ar}qC), 119.9 (^{Ar}CH), 118.6 (^{Ar}CH), 117.7 (^{Ar}CH), 112.2 (^{Ar}CH), 103.4 (^{Ar}qC), 34.2 (R_3CH), 8.9 ppm (CH_3).

Synthesis of $(tmim)GeK$ (1-K**).** A solution of $GeCl_2$ -dioxane (203 mg, 0.875 mmol) in THF (6 mL) was added over 20 minutes to an orange, green luminescent solution of $(tmim)K_3$ (500 mg, 10 w% THF, 0.869 mmol) in THF (15 mL) and stirred overnight. The resulting yellow suspension was diluted to 40 mL and centrifuged for 10 minutes at 2000 rpm. The decanted supernatant was concentrated to 6 mL, during which precipitation occurred. Decanting and washing with THF (4 x 0.5 mL) yielded a white microcrystalline powder (297 mg). Repetitive storing of the combined THF fractions at $-35^\circ C$ for 16h, decanting and washing with cold THF yielded 2 more crops (m_{total} = 506 mg, 37 w% THF, 0.62 mmol, 71%). 1H NMR (400 MHz, CD_3CN , $25^\circ C$) δ = 7.58 (dt, $^3J(H,H)$ = 8.1 Hz, $^4J(H,H)$ = 0.9 Hz, $^5J(H,H)$ = 0.9 Hz, 3H, Indole-H7), 7.34 (dt, $^3J(H,H)$ = 7.8 Hz, $^4J(H,H)$ = 1.0 Hz, $^5J(H,H)$ = 1.0 Hz, 3H, Indole-H4), 6.94 (ddd, $^3J(H,H)$ = 8.1 Hz, $^3J(H,H)$ = 6.9 Hz, $^4J(H,H)$ = 1.3 Hz, 3H, Indole-H6), 6.85 (ddd, $^3J(H,H)$ = 7.9 Hz, $^3J(H,H)$ = 7.0 Hz, $^4J(H,H)$ = 1.1 Hz, 3H, Indole-H5), 6.03 (s, 1H, R_3CH), 2.46 ppm (s, 9H, CH_3). 1H NMR (400 MHz, $C_6H_8O + C_6D_6$, $25^\circ C$) δ = 7.54 (d, $^3J(H,H)$ = 8.0 Hz, 3H, Indole-H7), 7.21 (d, $^3J(H,H)$ = 7.7 Hz, 3H, Indole-H4), 6.79 (t, $^3J(H,H)$ = 7.5 Hz, 3H, Indole-H6), 6.70 (t, $^3J(H,H)$ = 7.3 Hz, 3H, Indole-H5), 5.99 (s, 1H, R_3CH), 2.41 ppm (s, 9H, CH_3). ^{13}C NMR (101 MHz, CD_3CN , $25^\circ C$) δ = 142.0 (C),

141.9 [C_a], 131.2 [C_e], 120.0 [C_i], 118.6 [C_g], 117.7 [C_h], 112.2 [C_j], 103.4 [C_c], 34.2 [C_b], 8.9 ppm [C_d]. DOSY NMR (400 MHz, C₄D₈O, 25 °C): D = 7×10^{-18} m²/s; Satisfactory elemental analysis could not be obtained, likely due to THF solvation.

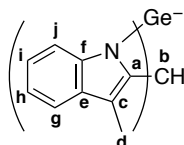


Chart 5.2 Assignment in [tmim]Ge⁻ (**1**)

Synthesis of [tmim]GeCuClK (2**).** To the combined solids **1**-K (30 mg, 40 w% THF, 35 μmol) and CuCl (3.5 mg, 35 μmol) was added THF (2 mL) and the suspension was stirred for 60 min, during which the amount of solid increased. The resulting suspension was freed of solvent *in vacuo*, affording a white powder (29 mg, 27 w% THF, 35 μmol, 99%). ¹H NMR (400 MHz, C₄D₈O, 25 °C) δ = 7.96 (d, ³J(H,H) = 8.1 Hz, 3H, Indole-H7), 7.26 (d, ³J(H,H) = 7.7 Hz, 3H, Indole-H4), 6.90 (t, ³J(H,H) = 7.5 Hz, 3H, Indole-H6), 6.77 (t, ³J(H,H) = 7.4 Hz, 3H, Indole-H5), 6.05 (s, 1H, R₃CH), 2.43 ppm (s, 9H, CH₃). ¹³C NMR (101 MHz, C₄D₈O, 25 °C) δ = 140.5 [ArqC], 139.8 [ArqC], 130.6 [ArqC], 118.9 [ArCH], 117.3 [ArCH], 116.8 [ArCH], 111.5 [ArCH], 102.8 [ArqC], 32.7 (R₃CH), 7.8 ppm (CH₃); DOSY NMR (400 MHz, C₄D₈O, 25 °C): D = 7×10^{-18} m²/s; ESI-MS C₂₈H₂₂N₃ClGeCu⁺: exp: 572.0092, sim: 572.0009 a.u.; Elemental analysis calcd (%) for C₂₈H₂₂N₃ClGeKCu: C 55.03, H 3.63, N 6.87; found: C 53.85, H 4.42, N 6.45.

Synthesis of [tmim]GeCu(MeCN)₃ (3**) from **2**.** A solution of **2** (~10 mg) in CD₃CN (0.4 mL) was allowed to stand for 16 h, during which crystals of **3** grew. ¹H NMR (400 MHz, CD₃CN, 25 °C) δ = 7.78 (d, ³J(H,H) = 8.1 Hz, 3H, Indole-H7), 7.34 (ddd, ³J(H,H) = 7.7 Hz, ⁴J(H,H) = 1.3 Hz, ⁵J(H,H) = 0.7 Hz, 3H, Indole-H4), 6.94 (t, ³J(H,H) = 7.5 Hz, 3H, Indole-H6), 6.87 (ddd, ³J(H,H) = 7.9 Hz, ³J(H,H) = 6.9 Hz, ⁴J(H,H) = 1.1 Hz, 3H, Indole-H5), 6.04 (s, 1H, R₃CH), 2.42 ppm (s, 9H, CH₃); ¹³C NMR (101 MHz, CD₃CN, 25 °C) δ = 141.4 [ArqC], 140.8 [ArqC], 131.1 [ArqC], 120.7 [ArCH], 118.9 [ArCH], 118.5 [ArCH], 112.5 [ArCH], 104.7 [ArqC], 33.6 (R₃CH), 8.7 ppm (CH₃).

Synthesis of [tmim]GeCu(MeCN)₃ (3**) from Cu(MeCN)₄PF₆.** A solution of **1**-K (32 mg, 38 w% THF, 39 μmol) in acetonitrile (0.5 mL) was added to a solution of Cu(MeCN)₄PF₆ (14 mg, 39 μmol) in acetonitrile (0.5 mL), the vial was rinsed with acetonitrile (2 x 0.5 mL) and the solution was added to the mixture. Within 5 minutes a white solid precipitated. After 3 hours, the mixture was filtered and the white residue washed with acetonitrile (2 x 0.5 mL) and freed of solvent *in vacuo*. (21 mg, 32 μmol, 83%). ¹H NMR (400 MHz, C₄H₈O + C₆D₆, 25 °C) δ = 7.62 (d, ³J(H,H) = 8.0 Hz, 3H, Indole-H7), 7.28 (d*, Indole-H4), 6.86 (t, ³J(H,H) = 7.5 Hz, 3H, Indole-H6), 6.79 (t, ³J(H,H) = 7.3 Hz, 3H, Indole-H5), 6.04 (s, 1H, R₃CH), 2.42 ppm (s, 9H, CH₃). *doublet overlaps with C₆D₅H. ¹H NMR (400 MHz, CD₃CN, 25 °C) δ = 7.77 (d, ³J(H,H) = 8.1 Hz, 3H, Indole-H7), 7.34 (d, ³J(H,H) = 7.7 Hz, 3H, Indole-H4), 6.94 (t, ³J(H,H) = 7.5 Hz, 3H, Indole-H6), 6.87 (t, ³J(H,H) = 7.3 Hz, 3H, Indole-H5), 6.04 (s, 1H, R₃CH), 2.42 ppm (s, 9H, CH₃). ¹³C NMR (101 MHz, CD₃CN, 25 °C) δ = 141.4 [ArqC], 140.8 [ArqC], 131.1 [ArqC], 120.7 [ArCH], 118.9 [ArCH], 118.5 [ArCH], 112.4 [ArCH], 104.7 [ArqC], 33.6 (R₃CH), 8.7 ppm (CH₃). Elemental analysis calcd (%) for C₃₄H₃₁N₆GeCu: C 61.89, H 4.74, N 12.74; found: C 61.28, H 4.94, N 12.24.

Synthesis of [tmim]GeFe(CO)₄K (4**).** A solution of **1**-K (122 mg, 62 w% THF, 0.15 mmol) in THF (13 mL) was added to an orange suspension of Fe₂(CO)₉ (54 mg, 147 μmol) in THF (5 mL) and stirred for 30 min. The solution was freed of solvent *in vacuo* to a burgundy solid, which was dissolved in THF (1.5 mL) and cooled to -35 °C, cold hexane (15 mL) was added and after 16h at -35 °C the suspension was filtered and the white solid dried *in vacuo* (105 mg, 15 w% THF, 0.13 mmol, 88%). ¹H NMR (400 MHz, CD₃CN, 70 °C) δ = 8.00 (d, ³J(H,H) = 8.2 Hz, 3H), 7.41 (d, ³J(H,H) = 7.8 Hz, 3H), 7.04 (ddd, ³J(H,H) = 8.3 Hz, ³J(H,H) = 6.8 Hz, ⁴J(H,H) = 1.5 Hz, 3H), 6.96 (t, ³J(H,H) = 7.4 Hz, 3H), 6.17 (s, 1H), 2.49 ppm (s, 8H). ¹H NMR (400 MHz, CD₃CN, 25 °C) δ = 7.96 (dt, ³J(H,H) = 8.3 Hz, ⁴J(H,H) = 0.9 Hz, 3H, Indole-H7), 7.40 (ddd, ³J(H,H) = 7.8 Hz, ⁴J(H,H) = 1.3 Hz, ⁵J(H,H) = 0.7 Hz, 3H, Indole-H4), 7.04 (ddd, ³J(H,H) = 8.3 Hz, ³J(H,H) = 7.0 Hz, ⁴J(H,H) = 1.3 Hz, 3H, Indole-H6), 6.95 (ddd, ³J(H,H) = 7.9 Hz, ³J(H,H) = 7.0 Hz, ⁴J(H,H) = 1.1 Hz, 3H, Indole-H5), 6.15 (s, 1H), 2.46 ppm (s, 9H). ¹H NMR (400 MHz, CD₃CN, -

40 °C) δ = 7.94 (dt, $^3J(\text{H,H})$ = 8.3 Hz, $^4J(\text{H,H})$ = 0.9 Hz, 3H), 7.40 (ddd, $^3J(\text{H,H})$ = 7.8 Hz, $^4J(\text{H,H})$ = 1.3 Hz, $^5J(\text{H,H})$ = 0.7 Hz, 3H), 7.04 (ddd, $^3J(\text{H,H})$ = 8.3 Hz, $^3J(\text{H,H})$ = 7.0 Hz, $^4J(\text{H,H})$ = 1.3 Hz, 3H), 6.95 (ddd, $^3J(\text{H,H})$ = 7.9 Hz, $^3J(\text{H,H})$ = 7.0 Hz, $^4J(\text{H,H})$ = 1.1 Hz, 3H), 6.15 (s, 1H), 2.45 ppm (s, 9H). ^{13}C NMR (101 MHz, CD_3CN , -40 °C): δ = 222.6 ($^{\text{ax}}\text{CO}$), 212.2 ($^{\text{eq}}\text{CO}$), 140.3 ($^{\text{Ar}}\text{qC}$), 139.0 ($^{\text{Ar}}\text{qC}$), 130.4 ($^{\text{Ar}}\text{qC}$), 121.3 ($^{\text{Ar}}\text{CH}$), 119.0 (2 $^{\text{Ar}}\text{CH}$), 112.2 ($^{\text{Ar}}\text{CH}$), 105.6 ($^{\text{Ar}}\text{qC}$), 32.4 (R_3CH), 8.4 ppm (CH_3). ^{13}C NMR (101 MHz, CD_3CN , 25 °C): δ = 215.1 (FWHM = 125 Hz, CO), 141.0 ($^{\text{Ar}}\text{qC}$), 139.9 ($^{\text{Ar}}\text{qC}$), 131.2 ($^{\text{Ar}}\text{qC}$), 121.5 ($^{\text{Ar}}\text{CH}$), 119.3 ($^{\text{Ar}}\text{CH}$), 119.2 ($^{\text{Ar}}\text{CH}$), 112.9 ($^{\text{Ar}}\text{CH}$), 105.6 ($^{\text{Ar}}\text{qC}$), 33.1 (R_3CH), 8.6 ppm (CH_3). ^{13}C NMR (101 MHz, CD_3CN , 70 °C): δ = 215.5 (CO), 141.6 ($^{\text{Ar}}\text{qC}$), 140.5 ($^{\text{Ar}}\text{qC}$), 131.8 ($^{\text{Ar}}\text{qC}$), 121.6 ($^{\text{Ar}}\text{CH}$), 119.5 ($^{\text{Ar}}\text{CH}$), 119.4 ($^{\text{Ar}}\text{CH}$), 113.3 ($^{\text{Ar}}\text{CH}$), 105.7 ($^{\text{Ar}}\text{qC}$), 33.7 (R_3CH), 8.8 ppm (CH_3); ESI-MS $\text{C}_{32}\text{H}_{22}\text{O}_4\text{GeN}_3\text{Fe}^-$: exp: 642.0437, sim: 642.0180 a.u.; IR (THF): $\tilde{\nu}$ = 2037, 1954, 1933 cm^{-1} ; Elemental analysis calcd [%] for $\text{C}_{44}\text{H}_{46}\text{N}_3\text{O}_{10}\text{GeFeK}$: C 56.96, H 4.91, N 4.45; found: C 56.92, H 4.78, N 4.05.

Interaction between 1 and FeCl_2 . The combined solids 1-K (30 mg, 40 w% THF, 35 μmol) and FeCl_2 (4.6 mg, 36 μmol) were dissolved in THF (2 mL) and stirred for 60 min. ^1H NMR [400 MHz, $\text{C}_6\text{D}_6\text{O} + \text{C}_6\text{D}_6$, 25 °C] δ^* = 8.08 (br s, 3H), 7.23 (d, $^3J(\text{H,H})$ = 7.6 Hz, 3H), 6.83 (br d, $^3J(\text{H,H})$ = 6.8 Hz, 3H), 6.73 (t, $^3J(\text{H,H})$ = 7.1 Hz, 3H), 5.90 (s, 1H), 2.40 ppm (s, 9H). * relative to $\text{C}_6\text{D}_5\text{H}$ in THF (7.32 ppm).

References

- [1] Benedek, Z.; Szilvási, T. *Organometallics* **2017**, *36*, 1591–1600.
- [2] Benedek, Z.; Szilvási, T. *RSC Adv.* **2015**, *5*, 5077–5086.
- [3] Kilian, M.; Wadepohl, H.; Gade, L. H. *Organometallics* **2008**, *27*, 524–533.
- [4] Fürstner, A.; Krause, H.; Lehmann, C. W. *Chem. Commun.* **2001**, *80*, 2372–2373.
- [5] Gallego, D.; Brück, A.; Irran, E.; Meier, F.; Kaupp, M.; Driess, M.; Hartwig, J. F. *J. Am. Chem. Soc.* **2013**, *135*, 15617–15626.
- [6] Wang, W.; Inoue, S.; Enthaler, S.; Driess, M. *Angew. Chemie Int. Ed.* **2012**, *51*, 6167–6171.
- [7] Metsänen, T. T.; Gallego, D.; Szilvási, T.; Driess, M.; Oestreich, M. *Chem. Sci.* **2015**, *6*, 7143–7149.
- [8] Gallego, D.; Inoue, S.; Blom, B.; Driess, M. *Organometallics* **2014**, *33*, 6885–6897.
- [9] Zhang, M.; Liu, X.; Shi, C.; Ren, C.; Ding, Y.; Roesky, H. W. *Z. Anorg. Allg. Chem.* **2008**, *634*, 1755–1758.
- [10] Brück, A.; Gallego, D.; Wang, W.; Irran, E.; Driess, M.; Hartwig, J. F. *Angew. Chemie Int. Ed.* **2012**, *51*, 11478–11482.
- [11] Blom, B.; Enthaler, S.; Inoue, S.; Irran, E.; Driess, M. *J. Am. Chem. Soc.* **2013**, *135*, 6703–6713.
- [12] Cordero, B.; Gómez, V.; Platero-Prats, A. E.; Revés, M.; Echeverría, J.; Cremades, E.; Barragán, F.; Alvarez, S. *Dalton Trans.* **2008**, No. 21, 2832–2838.
- [13] Li, H.; Aquino, A. J. A.; Cordes, D. B.; Hase, W. L.; Krempner, C. *Chem. Sci.* **2017**, *8*, 1316–1328.
- [14] Lee, G.; West, R.; Mu, T. *J. Am. Chem. Soc. Commun.* **2003**, *125*, 8114–8115.
- [15] Levason, W.; Reid, G.; Zhang, W. *Coord. Chem. Rev.* **2011**, *255*, 1319–1341.
- [16] Al-Rafia, S. M. I.; McDonald, R.; Ferguson, M. J.; Rivard, E. *Chem. Eur. J.* **2012**, *18*, 13810–13820.
- [17] Protchenko, A. V.; Birjukumar, K. H.; Dange, D.; Schwarz, A. D.; Vidovic, D.; Jones, C.; Kaltsoyannis, N.; Mountford, P.; Aldridge, S. *J. Am. Chem. Soc.* **2012**, *134*, 6500–6503.
- [18] Lui, M. W.; Merten, C.; Ferguson, M. J.; McDonald, R.; Xu, Y.; Rivard, E. *Inorg. Chem.* **2015**, *54*, 2040–2049.
- [19] Driess, M.; Yao, S.; Brym, M.; van Wüllen, C.; Lentz, D. *J. Am. Chem. Soc.* **2006**, *128*, 9628–9629.
- [20] Yao, S.; Xiong, Y.; Driess, M. *Organometallics* **2011**, *30*, 1748–1767.
- [21] Meltzer, A.; Inoue, S.; Präsang, C.; Driess, M. *J. Am. Chem. Soc.* **2010**, *132*, 3038–3046.
- [22] Schmidt, M.; Blom, B.; Szilvási, T.; Schomäcker, R.; Driess, M. *Eur. J. Inorg. Chem.* **2017**, *2017*, 1284–1291.
- [23] See Chapter 4.
- [24] Filippou, A. C.; Steck, R.; Kociok-Köhn, G. *J. Chem. Soc. Dalton Trans.* **1999**, No. 14, 2267–2268.
- [25] Contel, M.; Hellmann, K. W.; Gade, L. H.; Scowen, I. J.; McPartlin, M.; Laguna, M. *Inorg. Chem.* **1996**, *35*, 3713–3715.

- [26] Coste, S. C.; Vlaisavljevich, B.; Freedman, D. E. *Inorg. Chem.* **2017**, *56*, 8195–8202.
- [27] Peerless, B.; Keane, T.; Meijer, A. J. H. M.; Portius, P. *Chem. Commun.* **2015**, *51*, 7435–7438.
- [28] Steiner, A.; Stalke, D. *J. Chem. Soc., Chem. Commun.* **1993**, No. 22, 1702–1704.
- [29] Veith, M.; Schütt, O.; Huch, V. *Angew. Chemie Int. Ed.* **2000**, *39*, 601–604.
- [30] Fernández, I.; Oña-Burgos, P.; Armbruster, F.; Krummenacher, I.; Breher, F. *Chem. Commun.* **2009**, *1*, 2586.
- [31] von Döbeneck, H.; Prietzel, H. *Hoppe-Seyler's Z. Physiol. Chem.* **1955**, *299*, 214–226.
- [32] Steiner, A.; Stalke, D. *Inorg. Chem.* **1995**, *34*, 4846–4853.
- [33] Filippou, A. C.; Johannes G. Winter; Gabriele Kociok-Köhn; Carsten Troll, A.; Hinz, I. *Organometallics* **1999**, *18*, 2649–2659.
- [34] Bent, H. A. *Chem. Rev.* **1961**, *61*, 275–311.
- [35] Khrustalev, V. N.; Antipin, M. Y.; Zemlyansky, N. N.; Borisova, I. V.; Ustynyuk, Y. A.; Lunin, V. V.; Izod, K. *Appl. Organomet. Chem.* **2005**, *19*, 360–362.
- [36] Nogai, S.; Schriewer, A.; Schmidbaur, H. *Dalton Trans.* **2003**, No. 16, 3165.
- [37] Kersting, B.; Krebs, B. *Inorg. Chem.* **1994**, *33*, 3886–3892.
- [38] Orlov, N. A.; Bochkarev, L. N.; Nikitinsky, A. V.; Zhiitsov, S. F.; Zakharov, L. N.; Fukin, G. K.; Ya. Khorshev, S. *J. Organomet. Chem.* **1997**, *547*, 65–69.
- [39] Zhao, N.; Zhang, J.; Yang, Y.; Zhu, H.; Li, Y.; Fu, G. *Inorg. Chem.* **2012**, *51*, 8710–8718.
- [40] Ferro, L.; Hitchcock, P. B.; Coles, M. P.; Fulton, J. R. *Inorg. Chem.* **2012**, *51*, 1544–1551.
- [41] Yadav, D.; Siwatch, R. K.; Sinhababu, S.; Nagendran, S. *Inorg. Chem.* **2014**, *53*, 600–606.
- [42] Yadav, D.; Kumar Siwatch, R.; Sinhababu, S.; Karwasara, S.; Singh, D.; Rajaraman, G.; Nagendran, S. *Inorg. Chem.* **2015**, *54*, 11067–11076.
- [43] York, J. T.; Young, V. G.; Tolman, W. B. *Inorg. Chem.* **2006**, *45*, 4191–4198.
- [44] Hlina, J.; Arp, H.; Walewska, M.; Flörke, U.; Zangger, K.; Marschner, C.; Baumgartner, J. *Organometallics* **2014**, *33*, 7069–7077.
- [45] Orlov, N. a; Bochkarev, L. N.; Nikitinsky, A. V; Kropotova, V. Y.; N. Zakharov, L.; Fukin, G. K.; Khorshev, S. Y. *J. Organomet. Chem.* **1998**, *560*, 21–25.
- [46] Piers, E.; Lemieux, R. E. D. *Organometallics* **1995**, *14*, 5011–5012.
- [47] Glockling, F.; Hooton, K. A. *J. Chem. Soc.* **1962**, 2658.
- [48] Barnard, T. S.; Mason, M. R. *Inorg. Chem.* **2001**, *40*, 5001–5009.
- [49] Couzijn, E. P. A.; Slootweg, J. C.; Ehlers, A. W.; Lammertsma, K. *J. Am. Chem. Soc.* **2010**, *132*, 18127–18140.
- [50] Barnard, T. S.; Mason, M. R. *Organometallics* **2001**, *20*, 206–214.
- [51] Armarego, W. L. F.; Chai, C. L. L. *Purification of laboratory chemicals*; 2003.
- [52] Fulmer, G. R.; Miller, A. J. M.; Sherden, N. H.; Gottlieb, H. E.; Nudelman, A.; Stoltz, B. M.; Bercaw, J. E.; Goldberg, K. I. *Organometallics* **2010**, *29*, 2176–2179.
- [53] Gaussian 09, Revision D.01, M. J. Frisch, G. W. Trucks, H. B. Schlegel, G. E. Scuseria, M. A. Robb, J. R. Cheeseman, G. Scalmani, V. Barone, B. Mennucci, G. A. Petersson, H. Nakatsuji, M. Caricato, X. Li, H. P. Hratchian, A. F. Izmaylov, J. Bloino, G. Zheng, J. L. Sonnenberg, M. Hada, M. Ehara, K. Toyota, R. Fukuda, J. Hasegawa, M. Ishida, T. Nakajima, Y. Honda, O. Kitao, H. Nakai, T. Vreven, J. A. Montgomery, Jr., J. E. Peralta, F. Ogliaro, M. Bearpark, J. J. Heyd, E. Brothers, K. N. Kudin, V. N. Staroverov, T. Keith, R. Kobayashi, J. Normand, K. Raghavachari, A. Rendell, J. C. Burant, S. S. Iyengar, J. Tomasi, M. Cossi, N. Rega, J. M. Millam, M. Klene, J. E. Knox, J. B. Cross, V. Bakken, C. Adamo, J. Jaramillo, R. Gomperts, R. E. Stratmann, O. Yazyev, A. J. Austin, R. Cammi, C. Pomelli, J. W. Ochterski, R. L. Martin, K. Morokuma, V. G. Zakrzewski, G. A. Voth, P. A. Salvador, J. J. Dannenberg, S. Dapprich, A. D. Daniels, O. Farkas, J. B. Foresman, J. V. Ortiz, J. Cioslowski, and D. J. Fox, Gaussian, Inc., Wallingford CT, **2013**.

Appendix

Spectroscopic data accompanying chapter 2

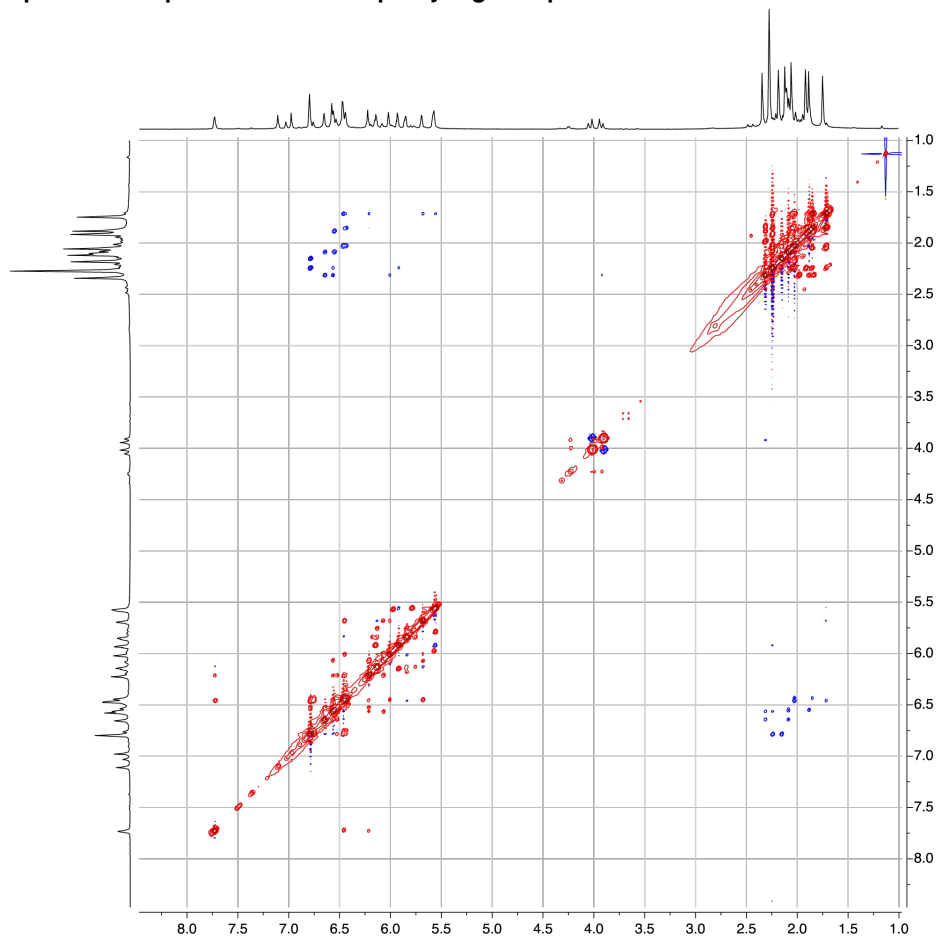


Figure 1 EXSY (red)/NOESY (blue) NMR spectrum of $[\text{MesIMP}]_2[\text{MesAMP}]\text{Si}$ (**4**) in C_7D_8 at $-10\text{ }^\circ\text{C}$.

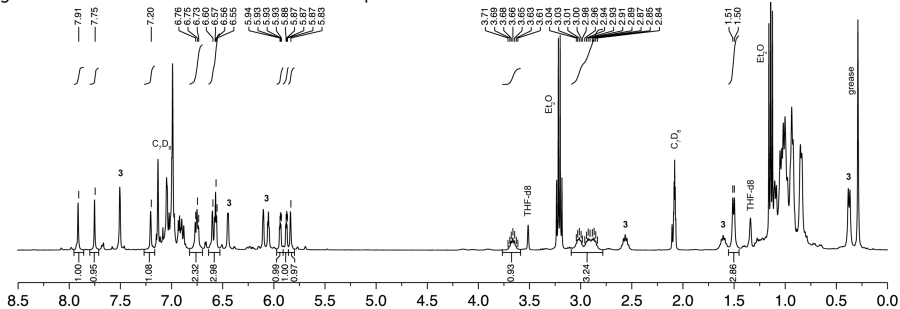


Figure 2 ^1H NMR spectrum of $[\text{DippIMP}]_2\text{SiHCl}$ (**6**) in C_7D_8 (+ THF-d_8) at $-60\text{ }^\circ\text{C}$, polluted with $[\text{DippIMP}]_3\text{SiH}$.

Computational and spectroscopic data accompanying chapter 3

Table 1 Selected bond distances and angles for $\text{pyr}_3\text{SiFe}(\text{CO})_4^-$ (**5**), $\text{Cl}_3\text{SiFe}(\text{CO})_4^-$ (**2**), and the related $\text{pyr}_3\text{PFe}(\text{CO})_4$ and $\text{pyr}_3\text{SiOsXL}_4$.

$\text{\AA}/^\circ$	$\text{Pyr}_3\text{SiFe}(\text{CO})_4^-$	$\text{Cl}_3\text{SiFe}(\text{CO})_4^-$ ^a	$\text{Pyr}_3\text{PFe}(\text{CO})_4$ ¹	$\text{Pyr}_3\text{SiOsXL}_4$ ²
E(1)–M(1)	2.2576(8)	2.233(4)	2.1661(7)	2.375(2)
E(1)–N(1)	1.771(2)	2.080(8)	1.688(2)	1.788(7)
E(1)–N(2)	1.774(2)	2.087(3)	1.698(2)	1.787(7)
E(1)–N(3)	1.777(2)	2.092(3)	1.691(2)	1.770(7)
$\Sigma r_{\text{cov}}[\text{E}, \text{M}]^{[3]}$	2.43(4)		2.39(4)	2.55(4)
$\Sigma r_{\text{cov}}[\text{E}, \text{N}]^{[3]}$	1.82(2)		1.78(3)	1.82(2)
N(1)–E(1)–N(2)	103.22(10)	101.23(13)	101.38(11)	99.5(3)
N(2)–E(1)–N(3)	100.70(10)	100.99(1)	100.55(10)	100.3(3)
N(3)–E(1)–N(1)	99.68(10)	102.05(63)	102.05(12)	101.1(3)
$\Sigma(\text{N}–\text{Si}–\text{N})$	303.60(17)	304.3(6)	304.0(2)	300.9(5)

^aaverage and standard error of 2 reports.^{3,4}

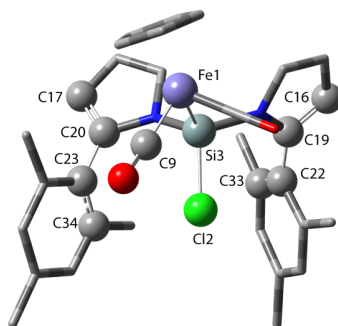


Figure 3 *In-silico* optimized geometry of MP_2ClSiFp (**7**). Atoms used to define dihedral angles are shown in ball-and-stick.

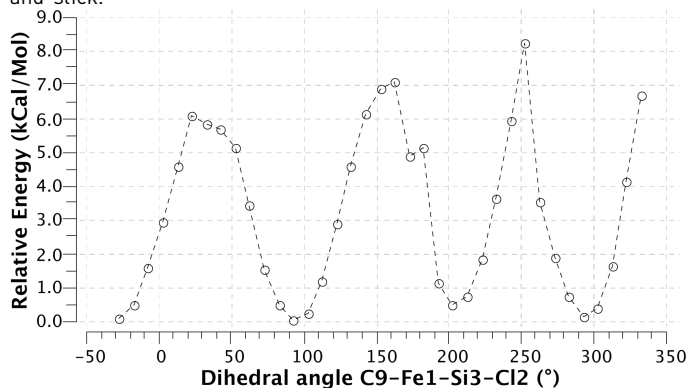
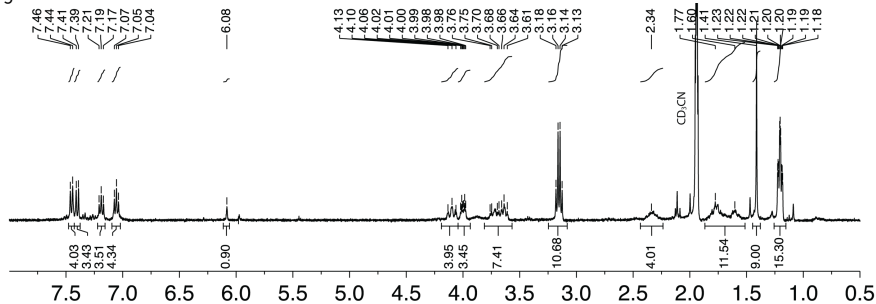
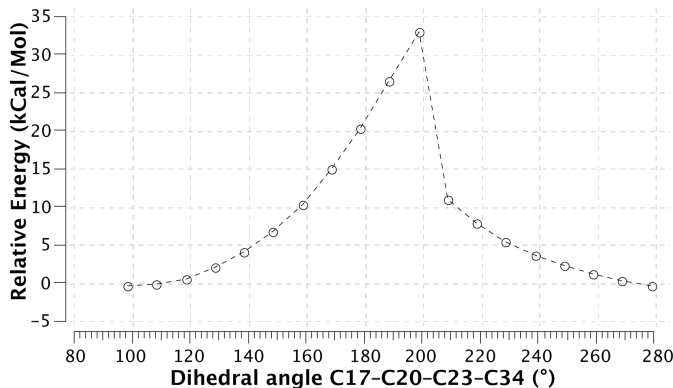
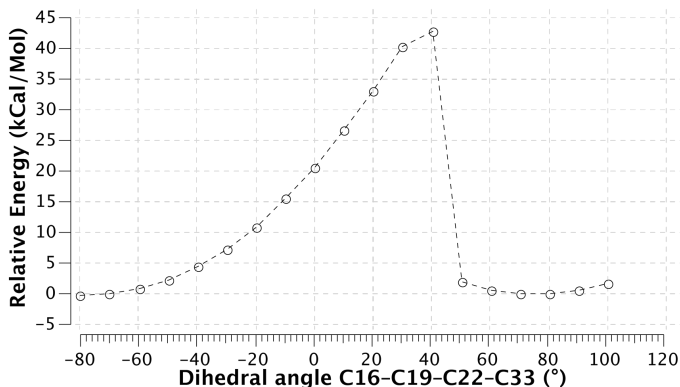


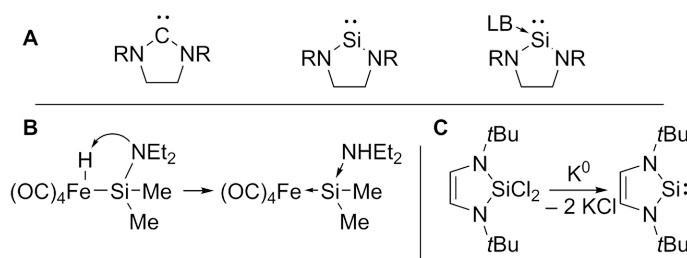
Figure 4 Relaxed PES scan of rotation around the Fe–Si bond in MP_2ClSiFp (**7**). Labels defined in Figure 3.



- [1] Barnard, T. S.; Mason, M. R. *Inorg. Chem.* **2001**, 40 (19), 5001–5009.
 [2] Hübler, K.; Roper, W. R.; Wright, L. J. *Organometallics* **1997**, 16 (12), 2730–2735.
 [3] Van An Du, S.O.Baumann, G.N.Stipicic, U.Schubert CCDC 740791: *Experimental Crystal Structure Determination*, **2014**, DOI: 10.5517/ccsvvhy
 [4] R.S.Simons, C.A.Tessier CCDC 126532: *Experimental Crystal Structure Determination*, **2014**, DOI: 10.5517/cc47npp

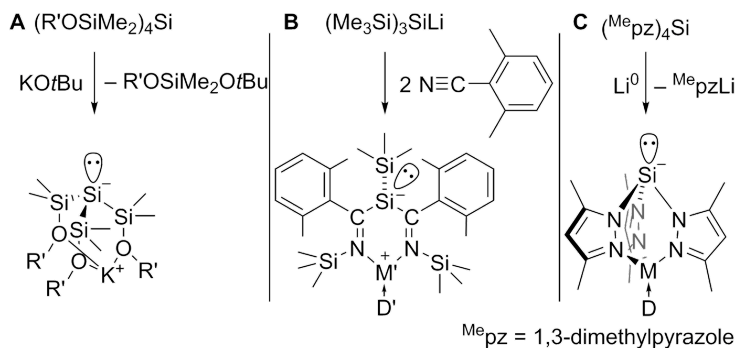
Summary and Outlook

Low-valent silicon(II) compounds have recently emerged as a promising class of strong donor ligands for transition metals, with potential applications in homogeneous catalysis. N-heterocyclic silylenes (NHSis, Scheme 1A) are the heavier analogues of the widely-used N-heterocyclic carbenes (NHCs). Due to less effective stabilization from the adjacent nitrogen atom, NHSis are intrinsically more reactive than NHCs, and often benefit from stabilization with a Lewis-base. The heavier group 14 analogues (Ge(II)-Pb(II)) are increasingly more stable due to the increasing energy difference between the s- and p-orbital, stabilizing the s^2 configuration.



Scheme 1 General structure of NHCs, NHSis, and base-stabilised silylenes (A), first metal-bound (B) and metal-free (C) silylenes.

The evolution of silylenes started with the isolation as base stabilized, metal-bound species in 1977 (Scheme 1B), synthesized by oxidative addition of R_3Si-H followed by proton transfer to an Si-bound diethylamine. In this silylene, the reactive lone-pair is stabilised by the Lewis-acidic metal and the empty p-orbital by interaction with the lone pair of the amine. Decades later, kinetic stabilization allowed for isolation of the first free NHSi by reduction of the corresponding dichlorosilane (Scheme 1C). In this silylene, the steric bulk provides kinetic shielding to the reactive Si(II) centre. With the synthesis of free silylenes established, direct complexation became an attractive method to access silylene complexes. Investigations in the catalytic activity of these complexes has revealed that silylenes are strong σ -donors and are also able to participate in catalysis by cooperatively activating a substrate. Silylene ligands have been employed in a wide variety of catalytic reactions, *e.g.* hydrosilylation, amide reduction, alkyne cyclotrimerisation, arene borylation, aryl halide amination and hydroformylation. Additionally, catalytic C-C cross-coupling reactions are well-represented with examples of Suzuki, Heck, Kumada, Negishi and Sonogashira reactions. Silylenes have shown to be promising alternatives to widely used ligands such as NHCs and phosphines.



Scheme 2 Synthesis of zwitterionic silanides.

A potentially interesting class of Si(III) ligands are anionic silanides (R_3Si^-), which are formally isoelectronic to phosphines and base-stabilized silylenes. Since phosphines are being widely applied as monodentate ligands in homogeneous catalysis, one could expect monodentate silyl ligands to find similar applications as stronger donor analogues. However, the Si–M bond has been shown to be often highly reactive: transition-metal complexes of silanides are often intermediates in catalytic hydrosilylation, where they are usually formed by oxidative addition of a hydrosilane. The reactivity of the Si–M bond can be tamed by incorporation into multidentate architectures or by steric protection (e.g. $t\text{Bu}_3\text{Si}^-$ or $(\text{Me}_3\text{Si})_3\text{Si}^-$). Recent studies have shown that naked silanides can be stabilized in zwitterionic structures, in which the cation is located away from the anionic centre, bound by pendant donor groups (Scheme 2). When these donor groups are electron-withdrawing N-heterocycles such as pyrazoles, they confer additional stability to the Si(III) center by induction, even with only moderate steric protection (Scheme 2C).

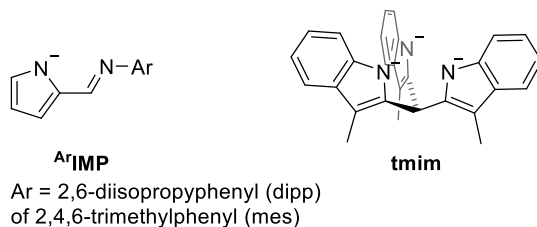


Chart 1 N-heterocycle based substituents covered in this thesis.

In this thesis, the use of pyrrole-derived N-heterocycles to stabilize Si(III) compounds, in particular silanides, was investigated. Two general architectures have been studied: the mono-anionic, bidentate iminopyrrole dippIMP ($\text{dippIMP} = 2\text{-(N-[2,6-diisopropylphenyl]iminomethyl)pyrrole}$) and the tri-anionic, tridentate tmim ($\text{tmimH}_3 = \text{tris[3-methylindol-2-yl]methane}$) (Chart 1).

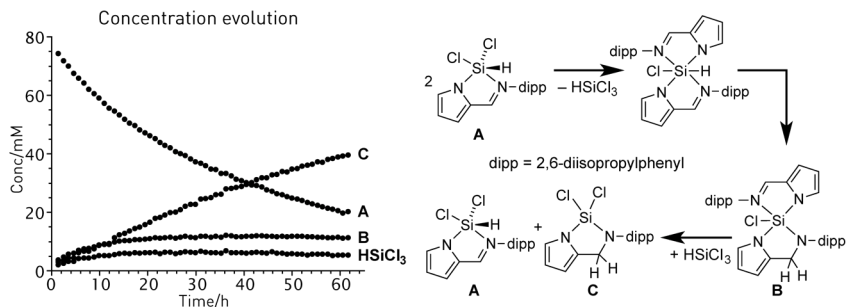


Figure 1 Concentration in time of silanes observed in ¹H NMR. Proposed reaction pathway for hydrosilylation of [dippIMP]SiCl₂H.

In **chapter 2** the synthesis of hydrosilanes as potential precursors for subsequent silylene or silanide synthesis was investigated. Hydrosilanes bearing the dippIMP substituent were synthesized. Somewhat surprisingly, these silanes undergo an intra-molecular hydrosilylation reaction of the imine forming the bidentate 2-(N-(2,6-diisopropylphenyl)aminomethylene)pyrrolide [dippAMP] substituent, hampering their use as Si(III) precursors. However, this system proved to be well suited to investigate this apparently catalyst-free hydrosilylation reaction. In particular, steric effects play a critical role: full substitution of Cl₃SiH by dippIMP afforded the stable hydrosilane [dippIMP]₃SiH, while the slightly less bulky mesIMP [2-(N-(2,4,6-methylphenyl)iminomethyl)pyrrolide] afforded the hydrosilylated [mesIMP]₂[mesAMP]Si. Detailed studies on the reaction of the monosubstituted [dippIMP]SiCl₂H revealed distinct reaction steps allowing for the proposal of a reaction pathway involving a redistribution of substituents (Figure 1). Additionally, the presence of chloride ions in the form of Bu₄NCl was found to accelerate the reaction.

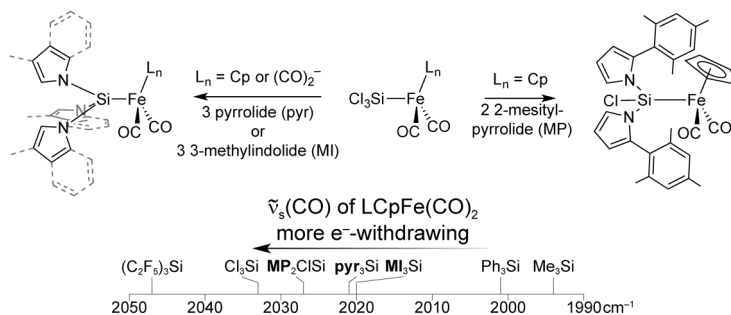
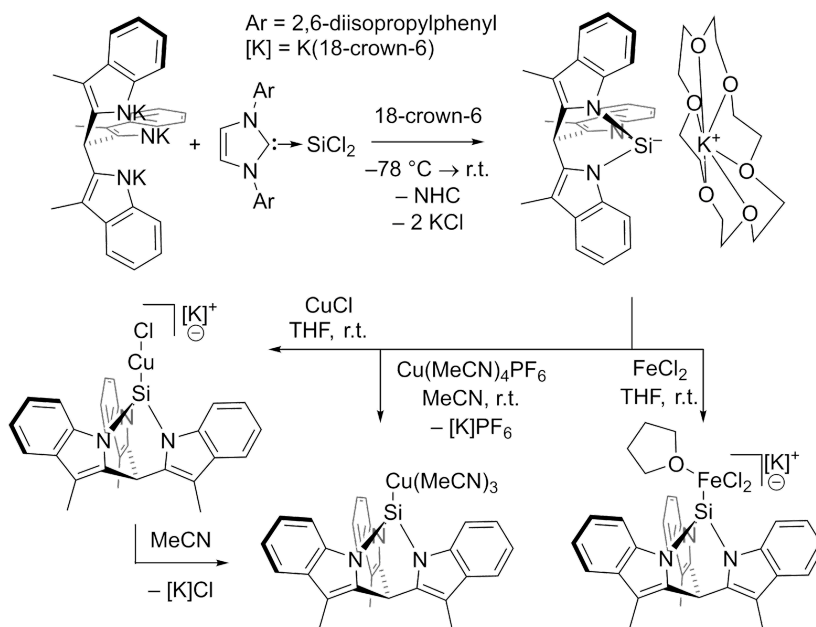


Figure 2 Top: nucleophilic substitution of Cl for N-heterocycles pyrrole, 3-methylindole, and 2-mesitylpyrrole. Bottom: vibrational modes of LCpFe(CO)₂ in relation to selected ligands (Me₃Si, Ph₃Si, Cl₃Si and (C₂F₅)₃Si).

To avoid the undesired hydride transfer reaction, a synthesis method for metal-silyls that does not require hydrosilanes as a synthetic intermediate is desirable. In **chapter 3** a method was investigated in which the silicon atom was first bound to iron as an -SiCl₃ ligand, followed by chloride substitution at silicon to form the ligand within the coordination sphere of the metal. Inspired by the previously reported

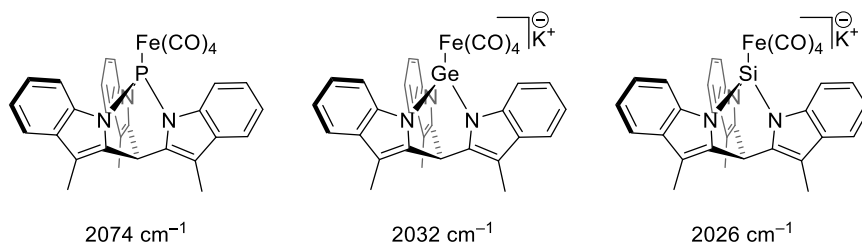
substitution of Cl for C_6F_5 and NR_2 on $Cl_3SiCpFe(CO)_2$, substitution for N-heterocycles was performed. The neutral Fe(II) compound $[Cl_3Si]CpFe(CO)_2$ (Cl_3SiFp) was subjected to chloride substitution using the sodium salts of pyrrole (pyr), 3-methylindole (MI), and 2-mesitylpyrrole (MP) (Figure 2). In this way, the homoleptic pyr_3Si^- and $(MI)_3Si^-$, and the heteroleptic $(MP)_2ClSi^-$ groups were accessed. The same method afforded the pyr_3Si^- ligand from the anionic Fe(0) precursor $Cl_3Si-Fe(CO)_4^-$. Attempted substitution for the tridentate tmim on $Cl_3Si-Fe(CO)_4^-$ and bidentate, monoanionic ^{dipp}IMP on Cl_3SiFp gave rise to unexpected complex reactions. The electron-donating properties of the silyl ligands bearing pyr, MI and MP were assessed by IR spectroscopy. These ligands are classified as rather weakly electron-donating within silyl ligands, reinforcing the idea that the electron-withdrawing nature of pyrroles can be used to stabilize reduced silicon compounds. However, the reluctance of tmim to react with the $Cl_3Si-Fe(CO)_4$ group led us to seek an alternative route, which is described in in **chapter 4**.



Scheme 3 Synthesis and complexation reactions of the silanide $(tmim)Si^-$ with $CuCl$ and $FeCl_2$.

In **chapter 4**, the tmim moiety was used to access a free silanide. This silanide was found difficult to access through the corresponding tetrahedral silanes $(tmim)SiH$ and $(tmim)SiCl$ intermediates. Calculations of the corresponding strain enthalpy suggest that the bicyclic structures $(tmim)SiH$ and $(tmim)SiCl$ are significantly strained while the target $(tmim)Si^-$ is not, akin to the previously known phosphorus analogue $(tmim)P$. Avoiding the aforementioned strained tetrahedral intermediates, $(tmim)Si^-$ was synthesized through nucleophilic substitution for tmim on the Si(III) precursor $Idipp \rightarrow SiCl_2$ ($Idipp = 2,3\text{-dihydro-1,3-bis}(2,6\text{-diisopropylphenyl})\text{-1H-}$

imidazol-2-ylidene) [Scheme 3]. The ability of the novel silanide $(\text{tmim})\text{Si}^-$ to ligate transition metals was demonstrated: it affords a series of metal silanides by direct complexation to the base-metal salts CuCl and FeCl_2 [Scheme 3]. In CH_3CN , the anionic $(\text{tmim})\text{SiCuCl}^-$ dissociates into the neutral, solvated copper silanide $(\text{tmim})\text{SiCu}(\text{NCCH}_3)_3$. The anionic $[(\text{tmim})\text{SiFeCl}_2(\text{THF})]^-$ is a rare example of a high spin silyl-iron complex. Computational investigations show that the combined σ -donating and π -accepting properties of $[(\text{tmim})\text{Si}^-]$ are close to those of PMe_3 and that the cone angle (194.6°) is the same as that of $\text{P}(\text{o-tol})_3$ ($194(6)^\circ$). Interestingly, the acute N–Si–N angles in the cage structure decrease the electron donating capacity of the ligand with respect to the “open” tris[3-methylindol-1-yl]silyl ligand. The described substitution on a Si(II) precursor offers an interesting alternative method for the synthesis of free silanides and is anticipated to find more applications in this field in the future.



Scheme 4 complexes $(\text{tmim})\text{EFe}(\text{CO})_4$ ($\text{E} = \text{P}, \text{Ge}^-, \text{Si}^-$) and the highest energy $\tilde{\nu}(\text{CO})$ in IR.

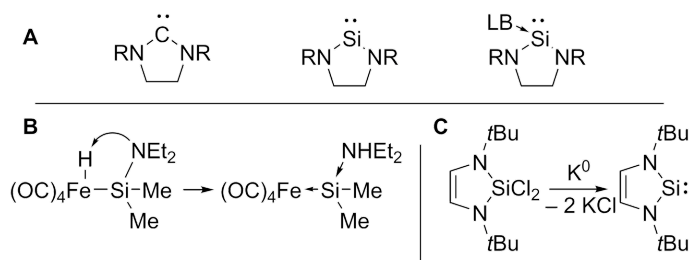
The accessibility of both $(\text{tmim})\text{Si}$ and $(\text{tmim})\text{P}$ offers an opportunity to compare the properties of isostructural ligands with different central elements. In **chapter 5**, this series was further expanded with the synthesis of the corresponding germanide by nucleophilic substitution for tmim on GeCl_2 -dioxane. Similar to the analogous silanide, complexation of the germanide $(\text{tmim})\text{Ge}^-$ to CuCl resulted in a germyl chloro cuprate, which also underwent dissociation in MeCN to the neutral trisacetonitrile germyl copper complex. In contrast to $(\text{tmim})\text{Si}^-$, $(\text{tmim})\text{Ge}^-$ is reluctant to coordinate to FeCl_2 to form the germyl dichloro iron complex, likely because of the softer Lewis base character of $(\text{tmim})\text{Ge}^-$. The reaction of $(\text{tmim})\text{GeK}$ as well as $(\text{tmim})\text{SiK}[18\text{-c-}6]$ with $\text{Fe}_2(\text{CO})_9$ afforded the germyl and silyl iron tetracarbonyl, akin to their phosphine analogue $(\text{tmim})\text{PFe}(\text{CO})_4$ [Scheme 4]. The electron donating properties of $(\text{tmim})\text{Ge}^-$ were shown to be in between those of $(\text{tmim})\text{P}$ and $(\text{tmim})\text{Si}^-$. The N–Ge–N angles in the solid-state structures of $(\text{tmim})\text{Ge}^-$ and its complexes increase upon complexation, suggesting increased hybridisation of the Ge s- and p-orbitals.

The knowledge obtained from this work is anticipated to further aid in the controlled synthesis of N-substituted silanes, silyl ligands, and silanides. Nucleophilic substitution on a metal-bound silyl ligand and the SiCl_2 synthon $\text{Idipp} \rightarrow \text{SiCl}_2$ offer interesting alternatives to established methods for the synthesis of silyl-metal

complexes and free silanides, potentially allowing for the formation of structures that would otherwise be difficult to access. The properties of the unusual free silanide $(\text{tmim})\text{Si}^-$ will warrant further investigation. In particular, the large strain calculated for $(\text{tmim})\text{SiH}$ compared to $(\text{tmim})\text{Si}^-$ would make the former an unusually acidic hydrosilane. The low-coordinate metal complexes obtained with $(\text{tmim})\text{Si}^-$ are also envisaged to be convenient Si-M synthons by, for example, substitution of the acetonitrile ligands in $(\text{tmim})\text{SiCu}(\text{NCCH}_3)_3$. Additionally, the isolation of the low-coordinate silyl iron chloride complex warrants research into its use in C-C cross coupling catalysis. Another interesting line of research could be electronic and steric tuning of the silanide ligand. Addition of electron withdrawing groups on the indole moieties may allow for inductive stabilization of the Si^- site. Addition of directed bulk will increase the steric demand of the ligand. Overall, the findings in this thesis contribute to the understanding of heavier group-14 analogues of carbenes and carbanions and promise to be instrumental for further development of this promising class of ligands.

Samenvatting en Vooruitblik

Laagvalente silicium(II)-verbindingen zijn recent onder de aandacht gekomen als een veelbelovende klasse van sterke donorliganden voor overgangsmetalen, met potentiële toepassingen in de homogene katalyse. N-heterocyclische silylenen [NHSi's, Figuur 1A] zijn de zwaardere analogen van de veel gebruikte N-heterocyclische carbenen [NHC's]. Vanwege de minder effectieve stabilisatie van het silyleen door de aangrenzende stikstofatomen zijn NHSi's reactiever dan NHC's en worden ze vaak gestabiliseerd door een Lewis-base (LB). De zwaardere groep 14-analogen van Si [Ge(II)-Pb(II)] worden steeds stabielere als gevolg van het toenemende energieverschil tussen het s- en p-orbitaal, waardoor de s²-configuratie wordt gestabiliseerd.

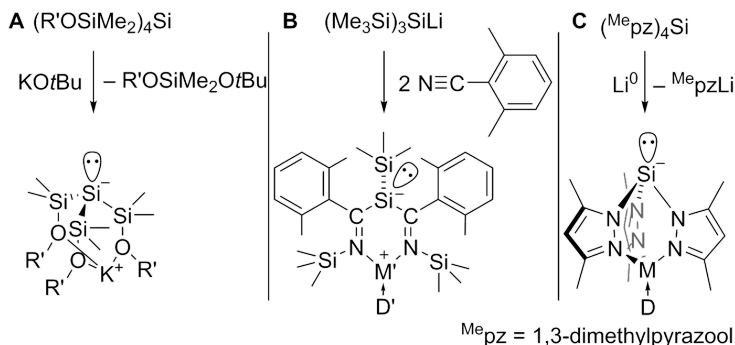


Figuur 1 Algemene structuur van NHC's, NHSi's en Lewis-base-gestabiliseerde silylenen (A), vroege voorbeelden van metaal-gebonden (B) en metaal-vrije (C) silylenen.

De ontwikkeling van silylenen begon met hun isolatie als base-gestabiliseerde, metaal-gebonden verbinding in 1977 (Figuur 1B). Deze werden gesynthetiseerd door oxidatieve additie van R₃Si-H aan Fe(CO)₅ gevolgd door protonoverdracht naar een Si-gebonden diethylamine. In dit silyleen wordt het reactieve vrije-elektronenpaar gestabiliseerd door het Lewis-zure metaal. Het lege p-orbitaal wordt door interactie met het vrije elektronenpaar van het amine gestabiliseerd. Decennia later werd de isolatie van het eerste vrije NHSi mogelijk door middel van kinetische stabilisatie. De synthese werd uitgevoerd door reductie van het analoge dichloorsilaan (Figuur 1C). In dit silyleen zorgt de sterische hindering voor kinetische afscherming van het reactieve Si(II) centrum. Doordat de syntheseroute van vrije silylenen hiermee bekend was, werd directe complexering een aantrekkelijke methode voor de synthese van silyleencomplexen.

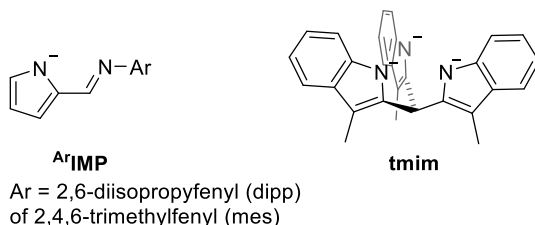
Onderzoek naar de katalytische activiteit van deze complexen heeft in het verleden aangetoond dat silylenen sterke σ-donoren zijn en in staat zijn om aan katalyse deel te nemen door coöperatief een substraat te activeren. Silyleenliganden zijn al toegepast in een grote verscheidenheid van katalytische reacties, waaronder hydrosilylering, amide-reductie, alkyn-cyclotrimerisatie, areen-borylering, arylhalide-aminering en hydroformylering. Daarnaast worden ze veel gebruikt in katalytische C-C koppelingsreacties zoals Suzuki, Heck, Kumada, Negishi en

Sonogashira reacties. Silylenen bleken daarin veelbelovende alternatieven voor veel gebruikte liganden zoals NHC's en fosfines.



Figuur 2 Synthese van zwitterionische silaniden.

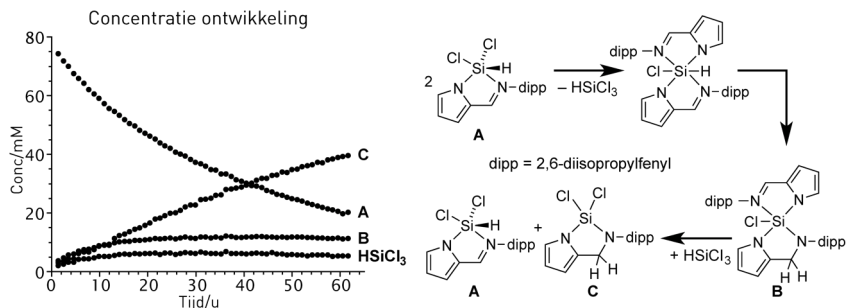
Een interessante klasse van Si(III)-liganden zijn anionische silaniden (R_3Si^-), die formeel iso-elektronisch zijn met fosfines en base-gestabiliseerde silylenen. Omdat fosfines op grote schaal worden toegepast als monodentate liganden in homogene katalyse, zou men kunnen verwachten dat monodentate silylliganden (metaal gebonden silaniden) vergelijkbare toepassingen vinden als sterkere donoranalogen. Het is echter aangetoond dat de Si-M-binding vaak zeer reactief is. Overgangsmetaalcomplexen van silaniden zijn vaak tussenproducten bij katalytische hydrosilylering, waar ze meestal worden gevormd door oxidatieve additie van een hydrosilaan aan een gereduceerd metaalfragment. De reactiviteit van de Si-M-binding kan worden getemperd door de silaniden in te bouwen in multidentate structuren of door sterische bescherming van de Si-M-binding (bijvoorbeeld tBu_3Si^- of $(Me_3Si)_3Si^-$). Recente studies hebben aangetoond dat vrije silaniden kunnen worden gestabiliseerd in zwitterionische structuren, waarin het kationische centrum zich op afstand van het anionische centrum bevindt (Figuur 2A en B). Wanneer deze donorgroepen elektronenzuigende N-heterocycli zijn, zoals pyrazolen, verlenen ze op inductieve wijze extra stabiliteit aan het Si(III) centrum, zelfs met slechts matige sterische bescherming (Figuur 2C).



Figuur 3 Substituenten gebaseerd op N-heterocyclische verbindingen zoals beschreven in dit proefschrift.

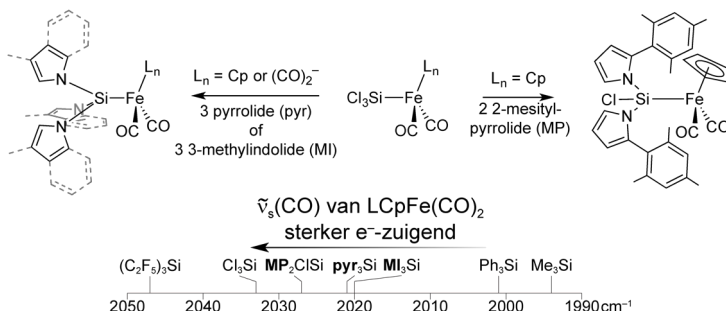
In dit proefschrift staat het gebruik van N-heterocyclische verbindingen afgeleid van pyrrool beschreven voor het stabiliseren van Si(II)-verbindingen, in het bijzonder

silaniden. Twee algemene structuren worden beschreven: het monoanionische, bidentate iminopyrrool dipp|MP ($\text{dipp|MPH} = 2\text{-[N-(2,6-diisopropylfenyl)iminomethyl]pyrrool}$) en het tri-anionische, tridentate tmim ($\text{tmimH}_3 = \text{tris-[3-methylindol-2-yl]methaan}$) (Figuur 3).



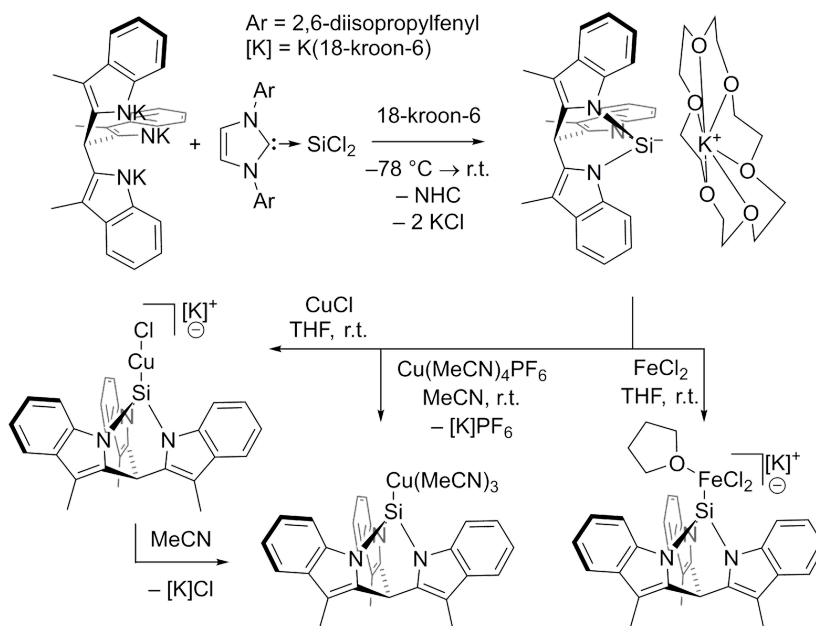
Figuur 4 Concentratieverloop in de tijd van silanen in de intramoleculaire hydrosilylering van $[\text{dipp}] \text{Mg} \text{SiCl}_2 \text{H}$ (^1H NMR) en voorgestelde reactiepad.

In hoofdstuk 2 wordt de synthese van hydrosilanen als potentiële uitgangsstoffen voor latere silyleen- of silanidesynthesen beschreven, met name van hydrosilanen die het ^{di}ppIMP-substituent dragen. Enigszins verrassend ondergaan deze silanen een intramoleculaire hydrosilyleringsreactie van het imine. Dit resulteert in de vorming van het bidentate 2-(N-(2,6-diisopropylfenyl)aminomethyleen)pyrrolide (^{di}ppAMP) substituent, hetgeen hun gebruik als Si(III)-synthons belemmert (Figuur 4). Dit systeem bleek echter goed geschikt om deze schijnbaar niet-gecatalyseerde hydrosilyleringsreactie te onderzoeken. Sterische effecten spelen een kritieke rol in deze reactie: volledige substitutie van Cl₃SiH met ^{di}ppIMP levert het stabiele hydrosilaan (^{di}ppIMP)₃SiH op, terwijl het iets minder sterisch gehinderde ^{mes}IMP [2-(N-(2,4,6-methylfenyl)iminomethyl)pyrrolide] het gehydrosilyleerde silaan (^{mes}IMP)₂(^{mes}AMP)Si geeft. Gedetailleerde studies naar de reactie van het monogesubstitueerde (^{di}ppIMP)SiCl₂H onthulden verschillende reactiestappen die het mogelijk maken een reactieroute voor te stellen (Figuur 4). Bovendien blijkt de aanwezigheid van chloride-ionen in de vorm van Bu₄NCl de reactie te versnellen.



Figuur 5 Boven: nucleofiele substitutie van Cl^- voor N-heterocyclische pyrrool, 3-methylindool en 2-mesitylpyrrool. Onder: vibrationele CO-modi van LCpFe(CO)_2 in relatie tot geselecteerde Si-liganden.

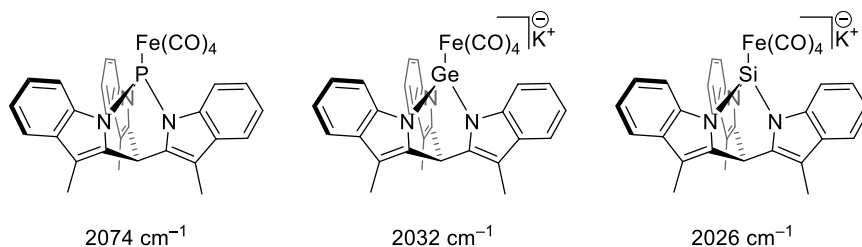
Om de ongewenste hydride-overdrachtsreactie te vermijden, is een synthesemethode voor silylmetaalcomplexen wenselijk waarbij geen hydrosilanen als intermediair betrokken zijn. In hoofdstuk 3 wordt een methode beschreven waarbij het siliciumatoom eerst wordt gebonden als een SiCl_3 -ligand, gevolgd door chloride-substitutie op silicium. Op deze manier wordt het silylligand gevormd binnen de coördinatieschil van het metaal. Geïnspireerd door de eerder gerapporteerde substitutie van Cl voor C_6F_5 of NR_2 op $\text{Cl}_3\text{SiCpFe}(\text{CO})_2$, werd substitutie voor N-heterocyclus uitgevoerd. De chlorides in de neutrale Fe(III)-verbinding $[\text{Cl}_3\text{SiCpFe}(\text{CO})_2]$ ($[\text{Cl}_3\text{SiFp}]$) zijn gesubstitueerd door pyrrool (pyr), 3-methylindool (MI) en 2-mesitylpyrrool (MP) door reactie met de overeenkomstige natriumzouten (Figuur 5). Op deze manier zijn de homoleptische pyr_3Si^- en $(\text{MI})_3\text{Si}^-$, en de heteroleptische $(\text{MP})_2\text{ClSi}$ -liganden verkregen. Via dezelfde werkwijze is het analoge $(\text{pyr}_3\text{Si})\text{-Fe}(\text{CO})_4^-$ complex verkregen via de anionische Fe(0)-precursor $\text{Cl}_3\text{Si-Fe}(\text{CO})_4^-$. De elektronendonerende eigenschappen van de ijzergebonden silylliganden werden bestudeerd met IR-spectroscopie. Deze liganden zijn geclassificeerd als vrij zwak elektronendonerend voor silylliganden, wat het idee versterkt dat de elektronenzuigende aard van pyrrolen kan worden gebruikt om gereduceerde siliciumverbindingen te stabiliseren.



Figuur 6 Synthese- en complexatiereacties van het silanide $[\text{tmim}]\text{Si}^-$ met CuCl en FeCl_2 .

De substitutiereacties beschreven in hoofdstuk 3 bleken niet te werken met de $\text{di}^{\text{pp}}\text{IMP}$ en tmim groepen. In hoofdstuk 4 is de tmim -groep daarom gebruikt om toegang te verkrijgen tot een vrij silanide. Dit silanide blijkt moeilijk toegankelijk via de overeenkomstige 4-omringde $(\text{tmim})\text{SiH}$ en $(\text{tmim})\text{SiCl}$ silanen als

tussenproducten. Berekeningen aan de bicyclische structuren $(\text{tmim})\text{SiH}$ en $(\text{tmim})\text{SiCl}$ laten zien dat deze een aanzienlijke ringspanningsenthalpie hebben. Het silanide $(\text{tmim})\text{Si}^-$ heeft echter een beperkte ringspanningsenthalpie, vergelijkbaar met het reeds bekende fosforanaloog $(\text{tmim})\text{P}$. Om de hiervoor genoemde gespannen tetraëdrische tussenproducten te vermijden werd $(\text{tmim})\text{Si}^-$ gesynthetiseerd door nucleofiele substitutie van chloride voor tmim op de Si(III) -precursor $\text{Idipp} \rightarrow \text{SiCl}_2$ (Idipp = 2,3-dihydro-1,3-bis(2,6-diisopropylfenyl)-1H-imidazol-2-ylideen) (Figuur 6). Vervolgens werd de coördinatiechemie van het nieuwe silanide $(\text{tmim})\text{Si}^-$ met overgangsmetalen bestudeerd; dit leverde een reeks metaalsilaniden op door directe complexering aan CuCl en FeCl_2 (Figuur 6). In CH_3CN dissocieert het anionische $(\text{tmim})\text{SiCuCl}^-$ tot het neutrale, gesolvateerde kopersilanide $(\text{tmim})\text{SiCu}(\text{NCCH}_3)_3$. Het anionische $[(\text{tmim})\text{SiFeCl}_2(\text{THF})]^-$ is een uniek voorbeeld van een silylijzercomplex met hoge-spin elektronenconfiguratie. Theoretisch onderzoek toont aan dat de gecombineerde σ -donerende en π -accepterende eigenschappen van $[(\text{tmim})\text{Si}^-]$ dicht bij die van PMe_3 liggen, hetgeen erg zwak donerend is voor silylliganden. Interessant is dat de kleine N-Si-N-hoeken in de kooiconstructie de elektronendonerende capaciteit van het ligand verlagen ten opzichte van het "open" tris (3-methylnol-1-yl)silylligand. De beschreven substitutie op een Si(II) -precursor biedt een interessante alternatieve methode voor de synthese van vrije silaniden.



Figuur 7 complexen $(\text{tmim})\text{EFe}(\text{CO})_4$ ($\text{E} = \text{P}, \text{Ge}^-, \text{Si}^-$) en de hoogste energie $\tilde{\nu}(\text{CO})$ in IR.

De toegankelijkheid van zowel $(\text{tmim})\text{Si}$ als $(\text{tmim})\text{P}$ biedt de mogelijkheid om de eigenschappen van isostructurele liganden te vergelijken met verschillende centrale elementen. In hoofdstuk 5 wordt deze reeks verder uitgebreid met de synthese van het overeenkomstige germanide door nucleofiele substitutie van chloride voor tmim op GeCl_2 -dioxaan. Vergelijkbaar met het analoge silanide resulteert de complexering van het germanide $(\text{tmim})\text{Ge}^-$ aan CuCl in een germylchlorocupraat. Ook deze verbinding ondergaat dissociatie in MeCN tot het neutrale trisacetonitril-germylkopercomplex. In tegenstelling tot $(\text{tmim})\text{Si}^-$, coördineert $(\text{tmim})\text{Ge}^-$ niet gemakkelijk aan FeCl_2 om het germyldichloorijzercomplex te vormen, waarschijnlijk is dit het gevolg van het zachtere Lewis-basekarakter van $(\text{tmim})\text{Ge}^-$. De reactie van $(\text{tmim})\text{GeK}$ evenals $(\text{tmim})\text{SiK}$ [18-kroon-6] met $\text{Fe}_2(\text{CO})_9$ levert de germyl- en silyl-ijsertetracarbonyl complexen op, vergelijkbaar met hun fosfine-analoog $(\text{tmim})\text{PFe}(\text{CO})_4$ (Figuur 7). De elektrondonerende eigenschappen van $(\text{tmim})\text{Ge}^-$

blijken tussen die van $(\text{tmim})\text{P}$ en $(\text{tmim})\text{Si}$ te liggen. Kristalstructuren tonen aan dat de N-Ge-N-hoeken in $(\text{tmim})\text{Ge}^-$ toe nemen na complexering aan een metaal, hetgeen een verhoogde hybridisatie van de Ge s- en p-orbitalen suggereert.

Verwacht wordt dat het onderzoek dat in dit proefschrift staat beschreven zal bijdragen aan de gecontroleerde synthese van N-gesubstitueerde silanen, silylliganden en silaniden. Nucleofiele substitutie op een, aan een metaal gebonden, silylligand en de SiCl_2 -synthon $\text{Idipp} \rightarrow \text{SiCl}_2$ bieden interessante alternatieven voor bestaande methoden voor de synthese van silyl-metaalcomplexen en vrije silaniden. Mogelijk bieden ze alternatieven voor de vorming van structuren die anders moeilijk toegankelijk zouden zijn. De eigenschappen van het ongebruikelijke vrije silanide $(\text{tmim})\text{Si}^-$ rechtvaardigen verder onderzoek. In het bijzonder zou de grote ringspanning, berekend voor $(\text{tmim})\text{SiH}$, in vergelijking met $(\text{tmim})\text{Si}^-$, het hydrosilaan een ongebruikelijk zuur kunnen maken. Daarnaast lijken de metaalcomplexen verkregen met $(\text{tmim})\text{Si}^-$ geschikte Si-M-synthons door, bijvoorbeeld, substitutie van de acetonitrilliganden in $(\text{tmim})\text{SiCu}(\text{NCCH}_3)_3$. Bovendien rechtvaardigt de isolatie van het silylijzerchloridecomplex onderzoek naar het gebruik ervan als katalysator in C-C koppelingsreacties. Een andere interessante onderzoekslijn zou elektronische en sterische variatie van het silanide-ligand kunnen zijn. Toevoeging van elektronenzuigende groepen aan de indoolgroepen kan inductieve stabilisatie van het Si-anion mogelijk maken. Toevoeging van gerichte bulk zal de sterische invloed van het ligand verhogen. Over het algemeen dragen de bevindingen in dit proefschrift bij tot het begrip van zwaardere groep-14-analogen van carbenen en carbanionen en lijken ze de verdere ontwikkeling van deze veelbelovende klasse van liganden mogelijk te maken.

Dankwoord

Een onderzoek van meer dan vier jaar kun en wil je niet alleen doen. De mensen waarmee ik heb samengewerkt hebben ieder mijn onderzoek in meer of mindere mate gevormd. Net die kleine tip gegeven, dat artikel onder mijn neus geschoven, soms uitgebreide metingen gedaan, op die manier een methode uitgelegd, mijn onderzoek heb ik uitgevoerd met jullie sturing. Daarbuiten is er een aantal mensen dat altijd geïnteresseerd was en me steunde als ik dat nodig had.

Marc-Etienne, I was one of your first PhD students. I have always greatly appreciated that you are very approachable and were always available for advice or a discussion. We share our love for chemistry and whisky, albeit both in slightly different ways. You were always happy to be drawn out of your office to the lab, you'll never completely abandon the hands-on work. You never allowed me to call myself stupid: I've had occasions where I messed up something, you invariably replied "it's not stupid, these things happen". Always patient, I feel like you've corrected a great deal of repetitive mistakes in the last run. Out of all people you have undoubtedly contributed the most, from directional advice to corrections of my sometimes fairly Dutch and always concise style of writing. I hope you will be able to guide a large number of PhD students in the future as personal and passionate as you've guided me.

Bert, ik waardeerde jouw input uit werkbijeenkomsten en group-meetings zeer. Heel erg bedankt dat je ondanks je drukke schema mijn mentor wilt zijn voor mijn huidige baan als docent. Je zet je enorm in voor de vakgroep en het departement, dit resulteert zich in de voorbereiding die de groep sinds recent ondergaat. Leo, Berth-Jan, Matthias, Gerard, Adri, bedankt voor alle adviezen als reacties op presentaties, posters op (internationale) congressen, en mailtjes met kristalstructuren.

Bij de analyse van de grote hoeveelheid NMR data en puzzels die ik heb geproduceerd kon ik altijd rekenen op jouw hulp, Johann. Regelmatig werd je zo (aanstekelijk) enthousiast dat je de meest exotische metingen ging uitvoeren, allerlei multinucleaire of 2D technieken met de gekste afkortingen. Zo heb je pogingen gedaan om chloor en aluminium te meten en kwamen we erachter waarom dat een niche is. Henk, ook jij stond altijd voor iedereen klaar. Vanaf het moment dat je met pensioen ging hebben we nog vaak gewenst dat je weer even terug was, in het lab en aan de koffietafel. Bedankt voor de gezellige tijd en natuurlijk je hulp met de ESI-MS. Jord, ik heb het fijn gevonden met je samen te werken, ondanks onze verschillende levensfasen zijn onze visies en ambities vergelijkbaar. Ik had het leuk gevonden als ik bij Synaffix weer je collega had kunnen zijn. Richard, bedankt voor het bijstaan van iedereen bij OCC. Thomas, je spontaniteit, grote behulpzaamheid en praktisch denken maken je een grote aanwinst voor de groep. We hadden het ook regelmatig over whisky, maar die asbakken waar jij en Marc-Etienne van houden kan ik nog

steeds niet goed wegstrijken. Milka, ondanks dat je door werk overspoeld wordt ben je iedereen altijd 2 stappen voor, deels omdat mensen soms gewoon 2 stappen achterlopen. Bij iedereen zorg jij ervoor dat alles op rolletjes blijft lopen en zij zich ten volle kunnen concentreren op het onderzoek. Ik heb genoten van de gezellige koffie- en lunchpauzes met jullie allemaal.

Martin, ik heb veel van je geleerd als ik weer eens met een al-dan-niet kristal naar je toe kwam. Ik vond het altijd leuk om mee te kijken tot het moment dat de uren durende meting gestart werd. Uiteindelijk hebben 16 structuren mijn proefschrift gehaald, je hebt er vele malen meer voor mij opgelost. Mijn eureka-moment kwam met een mailtje van jou, waarin de structuur van het silanide van hoofdstuk 4 nog ingepakt zat in een .zip!

Emily! Op de vraag of je mijn paranimf wilde zijn reageerde je heel enthousiast, waardoor ik wist dat ik een goede keuze had gemaakt. Ik ben blij dat je me bijstaat op dit voor mij belangrijke moment. Je bent altijd vrolijk en behulpzaam, goede eigenschappen voor een paranimf. Ik vind het knap hoe snel je het Nederlands weer hebt opgepakt en dat je je best doet deze taal te blijven praten, ook als het onderwerp ingewikkeld wordt.

Sharon, jij bent de enige die echt weet hoe het voor mij is geweest. Ik ben je ontzettend dankbaar voor al je hulp en steun die je zelfs kon opbrengen als ik lastig was (vanochtend nog). Zonder jou denk ik niet dat ik het tot hier gered had. We hebben veelal dezelfde visie, maar ik leer ook veel van jouw creatievere kijk op de wereld, zo vullen we elkaar aan. Ik prijs me heel gelukkig met zo'n slimme en lieve, soms een beetje gekke en vooral vrolijke rots in de branding. Ik ben blij dat je ook aan mijn zijde wilt staan tijdens de verdediging.

Serhii, I'm happy that I could work with such a creative and driven researcher. You were always keen to help with suggestions or practicalities. Having your research close to mine helped us both a great deal. All the best with the rest of your project! Emma, een hele tijd mijn buurtje, we konden altijd elkaar om advies vragen als we ergens niet uitkwamen of mee zaten. Ik voelde me vereerd toen je me vroeg je paranimf te zijn! We moeten wel de dinertjes met zijn vieren voortzetten, vanaf nu heb ik weer alle tijd. Bas, heerlijk recht-door-zee, door jou begrijp ik wat een "ongezouten" mening is, heel verfrissend. Manuel, voor jou mag het ook wel in het Nederlands, hè? De vakgroep werd een heel stuk minder filosofisch met jouw vertrek. Ik kon altijd genieten van jouw diepe gesprekken en grote algemene kennis. Suresh, Yuxing, Alessio, Peter, Maria, Jimmy, Jing, Eduard, and Pradip I've enjoyed working with you. Stefan, we zijn nu beiden docent, door onze gesprekken en jouw enthousiasme merkte ik dat ikzelf ook graag het onderwijs in wilde, dank je! Jacco, heel veel geluk met je start-up! Charl, buurman tijdens de laatste loodjes en kamergenoot tijdens conferenties. Succes met schrijven, je komt er zeker doorheen! Martine, van Master- naar PhD-student, succes! Dide, ongeveer 10 jaar geleden

leerden wij elkaar kennen, al die tijd hebben we hetzelfde pad gevolgd qua opleiding. Jij wilt graag door in het academisch onderzoek, wat ik heb verlaten. Ik bewonder je ambitie om in die richting door te gaan. Je wens is dat meer vrouwen hetzelfde doen en dat zo de academische top minder masculien wordt, ik hoop dat je als inspiratie gaat dienen.

Natuurlijk wil ik de studenten bedanken die hebben meegewerkt aan de onderdelen van mijn onderzoek. Helaas heeft niet alles deze thesis gehaald, wat in geen geval te wijten is aan de studenten. Mijn enige master student, Laurens, jouw extraverte karakter gaf de vakgroep een vrolijke twist. Jouw bipyrrrol systemen leken veelbelovend, maar gedroegen zich helaas niet zoals wij wilden. Stella, jouw eerste luchtvrrije synthese was al meteen spectaculair goed: 92% opbrengst en spat zuiver, ik weet niet of ik je nog geëvenaard heb met deze reactie. Verder was je altijd heel gedreven en vastberaden om de resultaten te begrijpen, met een beetje puzzelen kwam je er ook altijd achter. Desmond, onvermoeibaar, zelfs met 6% opbrengst en een moeilijke zuivering ging je steeds vrolijk het lab weer op. Cody, je was zeer enthousiast en nieuwsgierig, samen met Oscar heb je het onderzoek gedaan voor hoofdstuk 5. Elsemiek, ik vond het leuk om een meer praktisch georiënteerde HBO student te kunnen begeleiden, omdat ikzelf ook ooit zo was. Je was veelal vrolijk en hebt een mooi eindresultaat behaald. Tim Evers and Shu Zhan, the both of you have established a base on which I could start off with the silicon-ligands research, thank you for this. There is of course a multitude of students that I didn't get the opportunity to supervise in the lab. Your out-of-the-box thinking have undoubtedly helped me as well. Therefore I also want to thank Laura, Cecilia, Bart, Richt, Maxime, Joost, Dirk-Jan, Hidde, Thom, Marc, Yuri, Daniël, Roel, Yoni, Laurens, Kirsten, Elena, Rohald, Raoul, Sam and all the other students that once helped shaping the OCC group.

Kevin en Mariëtte, de gezellige etentjes en dagjes uit hebben mij veel rust geboden. Ik vind het altijd leuk als jullie er zijn. Laten we dit voortzetten!

Bij alle klussen en logistiek heb ik ook altijd kunnen rekenen op Manon en Erwin. Met Manon als fotograaf van de grote dag verwacht ik hele mooie foto's. Ik voel me altijd erg welkom bij jullie beiden.

Karin en Frans, zo noem ik jullie eigenlijk nooit. Opnieuw: Mam en pap, jullie waren en zijn altijd heel erg geïnteresseerd in wat ik deed, soms draafde ik wat door in mijn uitleg en werd het lastig om nog bij te blijven, maar jullie deden altijd je best. Ik ben jullie heel erg dankbaar dat jullie altijd voor mij klaar staan waar jullie kunnen. Ik zie veel van jullie in mij terug, van Karin de voldoening die ze krijgt van onderwijzen en van Frans het praktisch creatieve, problemen oplossen en klussen. Luc, broeder, ik ben trots op je dat je zo goed aan de weg timmert. Helaas, door onze agenda's hebben we niet heel veel tijd voor elkaar. Maar ik weet dat als het nodig is je alles voor me zou laten vallen.

Curriculum Vitae

Léon Witteman was born on November 9, 1989 in Nieuwegein, the Netherlands.

After completing high school at the HAVO level in 2007 he started his chemistry training at the University of Applied Sciences in Utrecht by following the Organic Chemistry track. This track included two internships, for which in 2009/2010 Léon did research at Schering-Plough, optimising a continuous flow Moffatt-Swern oxidation on kg-scale. The second internship, in the Condensed Matter and Interfaces group of Utrecht University, focussed on the luminescent properties of Sm^{3+} in a CsCdBr_3 lattice and the possibility for upconversion of NIR light (Prof. Dr. A Meijerink). Graduation in 2011 was followed by the Master Nanomaterials: Chemistry and Physics at Utrecht University, which he completed in 2013 with a Master's thesis on the cation exchange in zinc selenide colloidal quantum dots (Dr. C. de Mello-Donega).

Hereafter, Léon started as a PhD student in the Organic Chemistry and Catalysis group under the supervision of Dr. M.-E. Moret and Prof. Dr. R.J.M. Klein Gebbink. The research project, the results of which are described in this thesis, focussed on development of Si(II) ligands bearing N-heterocycles for base metal catalysis. This work was presented in parts at national and international conferences including NCCC 2014, 2015, 2016 and OMCOS 2015.



List of Publications

A Free Silanide from Nucleophilic Substitution at Silicon(II). Witteman, L., Evers, T., Lutz, M., Moret, M.-E. Submitted (Chapter 4 of this thesis)

Formation of exceptionally weak C–C bonds by metal-templated pinacol coupling. Folkertsma, E.; Benthem, S.H.; Witteman, L.; van Slagmaat, C.A.M.R.; Lutz, M.; Klein Gebbink, R.J.M.; Moret, M.-E. *Dalton Trans.* **2017**, 46 (19).

Hydrosilylation in Aryliminopyrrolide-Substituted Silanes. Witteman, L.; Evers, T.; Shu, Z.; Lutz, M.; Klein Gebbink, R.J.M.; Moret, M.-E. *Chem. Eur. J.* **2016**, 22 (17), 6087–6099. (Chapter 2 of this thesis)

Spectroscopic Characterization of a Monomeric, Cyclopentadienyl-Based Rhenium(V) Dioxo Complex. Raju, S.; Jastrzebski, J.T.B.H.; Lutz, M.; Witteman, L.; Dethlefsen, J.R.; Fristrup, P.; Moret, M.-E.; Klein-Gebbink, R.J.M. *Inorg. Chem.* **2015**, 54 (22), 11031–11036.

Tailoring ZnSe–CdSe Colloidal Quantum Dots via Cation Exchange: From Core/Shell to Alloy Nanocrystals. Groeneveld, E.; Witteman, L.; Lefferts, M.; Ke, X.; Bals, S.; Van Tendeloo, G.; de Mello-Donaga, C. *ACS Nano* **2013**, 7 (9), 7913–7930.